BIOZENTRUM
Universität Basel

Assembly and Regulation of the Type III Secretion System of *Yersinia enterocolitica*

Inauguraldissertation

zur Erlangung der Würde eines Doktors der Philosophie
vorgelegt der
Philosophisch-Naturwissenschaftlichen Fakultät der Universität Basel

von

Andreas Diepold
aus Ulm/Donau, Deutschland

Basel, 2010

creative commons

Namensnennung-Keine kommerzielle Nutzung-Keine Bearbeitung 2.5 Schweiz

---

Sie dürfen:

das Werk vervielfältigen, verbreiten und öffentlich zugänglich machen

Zu den folgenden Bedingungen:

Namensnennung. Sie müssen den Namen des Autors/Rechteinhabers in der von ihm festgelegten Weise nennen (wodurch aber nicht der Eindruck entstehen darf, Sie oder die Nutzung des Werkes durch Sie würden entlohnt).

Keine kommerzielle Nutzung. Dieses Werk darf nicht für kommerzielle Zwecke verwendet werden.

Keine Bearbeitung. Dieses Werk darf nicht bearbeitet oder in anderer Weise verändert werden.

- Im Falle einer Verbreitung müssen Sie anderen die Lizenzbedingungen, unter welche dieses Werk fällt, mitteilen. Am Einfachsten ist es, einen Link auf diese Seite einzubinden.
- Jede der vorgenannten Bedingungen kann aufgehoben werden, sofern Sie die Einwilligung des Rechteinhabers dazu erhalten.
- Diese Lizenz lässt die Urheberpersönlichkeitsrechte unberührt.

Quelle: http://creativecommons.org/licenses/by-nc-nd/2.5/ch/ Datum: 3.4.2009

Table of Contents

Chapter 1

Introduction

1.1. Type III secretion

1.1.1. Structure and function of the type III secretion system

Bacteria that live in contact with eukaryotic hosts, whether as symbionts or as pathogens, have often evolved mechanisms to manipulate host cell behavior to their benefit. Various Gram-negative bacterial species employ a type III secretion (T3S) system that allows the translocation of effector proteins into host cells (Cornelis and Wolf-Watz, 1997; Galán and Collmer, 1999) (Figure 1.1). The targets and biochemical activities of these effectors widely vary within and between organisms. Frequently, cellular signaling pathways are manipulated or the host cytoskeleton is modulated (Tampakaki *et al.*, 2004; Mota and Cornelis, 2005).

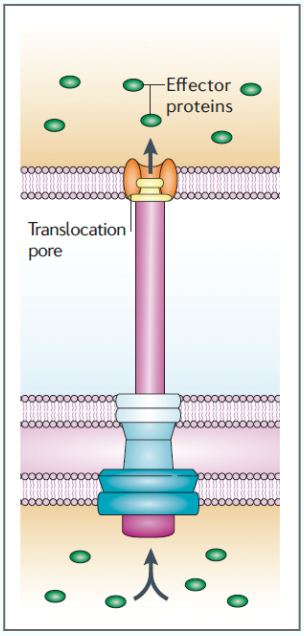

Figure 1.1: Function of the bacterial type III secretion system (Cornelis, 2006)**.**

The injectisome is a large protein complex that spans both bacterial membranes with ring-shaped structures (blue) and contains cytosolic components (pink) as well as an extracellular hollow needle (rose). It is formed by the bacterium in the host, usually induced by temperature. Upon contact with a host cell, a translocation pore (orange) is assembled at the needle tip (yellow) within the host cell membrane. The effector proteins (green) are then translocated into the host cytoplasm.

The T3S machinery, termed injectisome, can directly translocate effector proteins from the bacterial cytosol into the host cytoplasm. It shares this feature with the Type IV and Type VI secretion systems (T4S, T6S, respectively; Figure 1.2). The overall structure of the T3S system is related to the T4S system (Cascales and Christie, 2003). Both involve a cytosolic ATPase, a core complex spanning both bacterial membranes (Kubori *et al.*, 1998; Chandran *et al.*, 2009; Fronzes *et al.*, 2009b), and an extracellular appendix. However, at least the extracellular filament of the T4S system seems to assemble in a more transient way (Fronzes *et al.*, 2009a; Sivanesan *et al.*, 2010). In its outer membrane (OM) part, the T3S also displays

strong homology to the secretin of type II secretion systems (D'Enfert and Pugsley, 1989) (Figure 1.2).

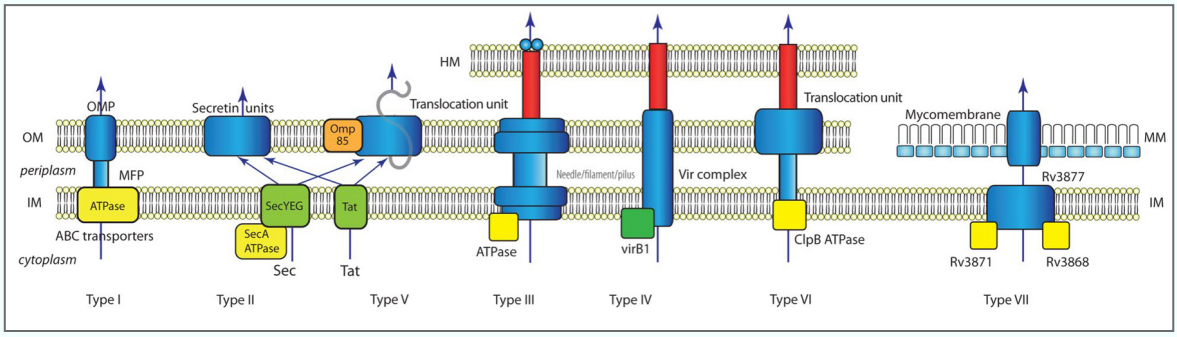

Figure 1.2: Comparison of known bacterial secretion systems (Tseng *et al.*, 2009)**.**

This simplified view shows the basic features of each secretion system. HM, Host membrane; OM, Bacterial outer membrane; IM, Bacterial inner membrane; MM, Mycomembrane; MFP, Membrane fusion protein. Structural proteins are shown in blue, ATPases and chaperones in yellow, extracellular domains in red, additional factors in green or orange.

When type III secretion systems were first analyzed in detail, the most striking observation was their close relationship to the bacterial flagellum (Fields *et al.*, 1994; Woestyn *et al.*, 1994; Van Gijsegem *et al.*, 1995). This became even more evident when the first partial structure of an injectisome, the needle complex (NC)[1] of *Salmonella enterica* SPI-1, was visualized by electron microscopy (EM) (Kubori *et al.*, 1998). The homology centers on the so-called basal body spanning both bacterial membranes, whereas the flagellum possesses additional proteins such as the motor / stator proteins for rotation, and the extracellular filament (Figure 1.3 a, b).

The phylogenetic relationship between the flagellum and the injectisome is a matter of debate. While it seems evident that motility was beneficial for bacteria long before the advent of eukaryotic hosts that would have rendered translocation systems beneficial, phylogenetic studies suggest that both systems share a common ancestor, and have since evolved differently from each other (Gophna *et al.*, 2003).

A notable difference between various pathogenic T3S systems is the nature of the extracellular appendices (Cornelis and Van Gijsegem, 2000). Most injectisomes build a

[1] Needle complex (NC): The part of an injectisome that can be purified and visualized in some bacteria. This part includes the needle and the transmembrane rings, but not the IM export machinery or the cytosolic components, like the ATPase or the C ring.

needle-like structure with a length between 40 and 80 nm (Cornelis, 2006) (Figure 1.3 b). As adaptation to their host cells, the injectisomes of enteropathogenic *Escherichia coli* (EPEC) contain a long filament on top of this needle, which is built by another protein (Knutton *et al.*, 1998; Daniell *et al.*, 2001) (Figure 1.3 c). Likewise, plant pathogens express a protein forming a pilus with a length up to several µm to be able to penetrate the host cell wall (Roine *et al.*, 1997; Jin and He, 2001) (Figure 1.3 d).

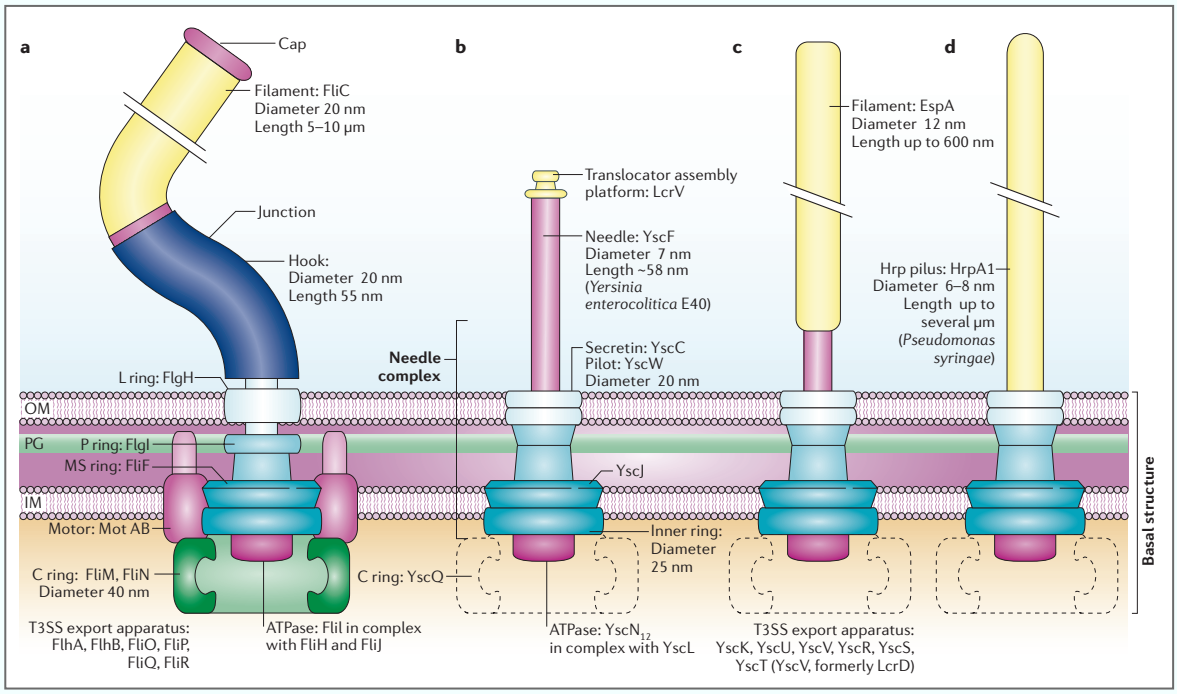

Figure 1.3: Structure of the flagellum and injectisomes from different subfamilies (Cornelis, 2006)**.**

Schematic representation of the flagellum **(a)**, the Ysc injectisome **(b)**, the EPEC injectisome **(c)**, and the injectisome from plant pathogens **(d)**. The putative structure of the C ring, that could not yet be visualized in an injectisome, is represented in a dashed line.

Based on protein homologies, T3S systems can be classified into different subfamilies (Cornelis, 2006). The Ysc system studied in this work is present in *Yersinia* spp., some *Pseudomonas* spp., and *Aeromonas* spp. Other well-studied systems are the injectisomes from *Salmonella* spp. SPI-1[2] and *Shigella flexneri* ("SPI-1-like"), and the injectisomes from EPEC, EHEC and *Salmonella* SPI-2 ("SPI-2-like"). Plant pathogens can possess two types of T3S systems (Hrp1 and Hrp2).

[2] *Salmonella* spp. harbor two *Salmonella* pathogenicity islands (SPIs) each encoding a type III secretion system. SPI-1 is required for invasion, whereas systemic infections and intracellular accumulation of *Salmonella* depend on the function of SPI-2 (Hansen-Wester and Hensel, 2001).

While effector proteins are diverse and highly adapted to the specific lifestyle of the bacterium, the export apparatus itself is conserved among species (Cornelis, 2006), especially within the basal body. This part of the injectisome is thought to consist of at least nine different highly conserved proteins (YscC, J, N, Q, R, S, T, U, V in *Yersinia*) and three less-conserved proteins (YscD, K, L in *Yersinia*). Table I shows an overview of these proteins and their homologues in other organisms and the flagellum.

Flagellum	**Injectisomes**				
	Yersinia Ysc	*S. enterica* SPI-1	*S. flexneri*	Plant pathogens	Function and location
-	YscC	InvG	MxiD	HrcC	Secretin Outer membrane
FliG	*YscD*	*PrgH*	*MxiG*	*HrcD*	*MS ring* *Inner membrane*
FliF	YscJ	PrgK	MxiJ	HrcJ	MS ring, lipoprotein Inner membrane
-	*YscK*	*OrgA*	*MxiK*	*HrpD*	*Interacts with ATPase and putative C ring; cytosolic*
FliH	*YscL*	*OrgB*	*MxiN*	*HrpE*	*Putative negative regulator of ATPase; cytosolic*
FliI	YscN	InvC/SpaL	Spa47	HrcN	ATPase Cytosolic
FliN+FliM	YscQ	InvK/SpaO	Spa33	HrcQ ($HrcQ_A$ + $HrcQ_B$)	Putative C-ring Cytosolic
FliP	YscR	InvL/SpaP	Spa24	HrcR	Export apparatus Inner membrane
(FliQ)	YscS	SpaQ	Spa9	HrcS	Export apparatus Inner membrane
FliR	YscT	InvN/SpaR	Spa29	HrcT	Export apparatus Inner membrane
FlhB	YscU	SpaS	Spa40	HrcU	Export apparatus* Inner membrane
FlhA	YscV**	InvA	MxiA	HrcV	Export apparatus Inner membrane

*: involved in substrate specificity switching
**: initially described as LcrD

Table I: Conserved homologues in the flagellum and different injectisomes subfamilies.

Names of the injectisome components are given for *Yersinia* spp., *S. enterica* Typhimurium SPI-1, *Shigella* spp., and plant pathogens (adapted from Cornelis (2006), includes data from Deane *et al.* (2010)). Less conserved proteins are designated in italics.

After the first visualization of a needle complex in *Salmonella* (Kubori *et al.*, 1998), additional structures of NCs from *Shigella* (Tamano *et al.*, 2000; Blocker *et al.*, 2001) and EPEC (Daniell *et al.*, 2001; Sekiya *et al.*, 2001) were solved, and resolution could be increased by cryo-EM techniques and averaging (Marlovits *et al.*, 2004; Marlovits *et al.*, 2006; Sani *et al.*, 2006; Hodgkinson *et al.*, 2009). In recent years, the availability of crystal structures of various T3S component domains (Yip *et al.*, 2005; Zarivach *et al.*, 2007; Zarivach *et al.*, 2008; Spreter *et al.*, 2009; Wiesand *et al.*, 2009) has allowed to dock several of these structures into medium-resolution electron density maps obtained by EM, such that now parts of the system have been described at molecular resolution (Moraes *et al.*, 2008; Spreter *et al.*, 2009; Schraidt *et al.*, 2010) (Figure 1.4).

Most of this progress has been based on the purification of needle complexes. However, essential parts of the injectisome are missing from this structure, because they are either transiently connected with the needle complex or are lost during the purification procedure. For this reason, there is a bias in knowledge towards the structural components of the injectisome. In contrast, comparably little is known about assembly, function, and regulation of the cytosolic and non-structural proteins, such as the ATPase, the proposed C ring and the export machinery.

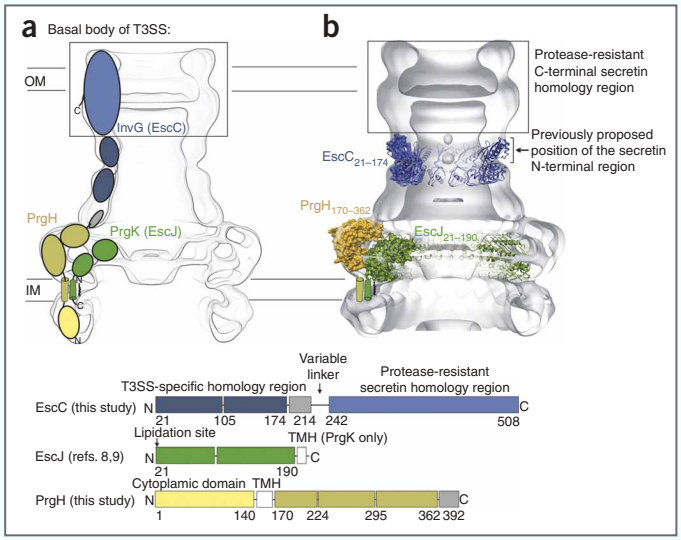

Figure 1.4: Modeling of protein crystal structure data into an overall shape generated by EM averaging (Spreter *et al.*, 2009)**.**

a Representation of the membrane-spanning part of the T3S basal body and its components. **b** Crystal structures of basal body components and their proposed localization within the basal body. The displayed crystal structures have been derived from different organisms (EscC and EscJ from EPEC, PrgH from *Salmonella* SPI-1). The electron density map was generated in *Salmonella* SPI-1.

1.1.2. Components of the injectisome

The injectisome requires more than twenty proteins to assemble, about fifteen of which are thought to be part of the functional protein complex. In *Yersinia*, all T3S genes are located on a large virulence plasmid, called pYV in *Y. enterocolitica* (Figure 1.5). The following chapter gives a brief overview of the conserved components of the injectisome, depicted in Figure 1.6. All of these are essential for the translocation of effectors. The protein names are given for *Yersinia* (see Table I for homologues).

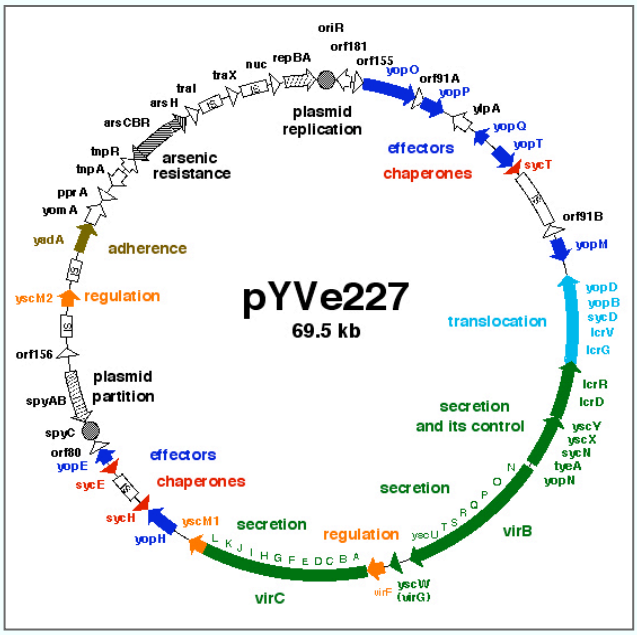

Figure 1.5: Genetic map of the pYVe227 plasmid of *Y. enterocolitica* W22703.

This virulence plasmid is closely related to pYVe40, which was mainly used in this study. The genes are coloured according to the part of the apparatus they encode. Genes in green encode the Ysc secretion machinery and its control; genes in light blue encode the translocation machinery; genes in dark blue encode the effector proteins; genes in red encode chaperones; genes in orange are involved in regulation of gene expression; the gene in brown encodes an adhesin; genes in gray encode arsenic resistance proteins.

YscV is labelled with its former name LcrD. Taken from "Pathogenicity Islands and Other Mobile Virulence Elements", ASM Press (1999).

Needle

The extracellular needle is generated by helical polymerization of a small protein (YscF) (Cordes *et al.*, 2003; Deane *et al.*, 2006). The needle is terminated by a tip (LcrV, which most likely forms a pentamer) (Müller *et al.*, 2005; Broz *et al.*, 2007), which is proposed to act as a scaffold for a hydrophobic pore (YopB and YopD) permeating the host membrane (Håkansson *et al.*, 1996; Blocker *et al.*, 1999). The length of the needle is regulated by a protein (YscP) that has been proposed to act as a molecular ruler, as its size linearly correlates with needle length (Journet *et al.*, 2003; Cornelis *et al.*, 2006; Wagner *et al.*, 2009).

Membrane rings

The basal body contains two membrane-spanning ring structures. The OM ring consists of a 12-14mer of a protein from the secretin family (YscC) (Koster *et al.*, 1997; Kubori *et al.*, 1998; Blocker *et al.*, 2001; Spreter *et al.*, 2009). Its polymerization and integration into the OM is assisted by a pilotin (YscW) (Koster *et al.*, 1997; Burghout *et al.*, 2004a). The so-called MS ring in the inner membrane (IM) is formed of 20-24 copies of a lipoprotein (YscJ) (Kimbrough and Miller, 2000; Crepin *et al.*, 2005; Yip *et al.*, 2005; Silva-Herzog *et al.*, 2008), which interacts with a bitopic protein (YscD) (Kimbrough and Miller, 2000) proposed to connect the two rings through its periplasmic domain (Spreter *et al.*, 2009).

IM export machinery

In addition to the MS ring, the IM contains five proteins YscR, S, T, U, and V, which are highly conserved essential components of the injectisome. All five proteins span the inner membrane with multiple transmembrane helices (Allaoui *et al.*, 1994; Fields *et al.*, 1994; Ghosh, 2004; Berger *et al.*, 2010), as has also been shown for their flagellar counterparts, FliP, FliQ, FliR, FlhB, and FlhA (Ohnishi *et al.*, 1997; Minamino and Macnab, 2000). Based on their topology and localization, and because interactions were observed between these proteins, as well as to the MS ring component and the ATPase (Minamino and Macnab, 2000; McMurry *et al.*, 2004), YscR, S, T, U, V have been termed “export apparatus” or “IM export machinery” (Cornelis, 2006). YscR, S, and T consist mainly of TM helices, whereas YscU and YscV both contain a large soluble C-terminal domain (Plano *et al.*, 1991; Allaoui *et al.*, 1994).

Despite the great importance that has been attributed to these proteins, very little is known about their localization, stoichiometry, or function in the injectisome. Only for YscU, a function in the recognition of export substrates could be shown (Sorg *et al.*, 2007).

All five proteins were proposed to be located within a membrane patch inside the MS ring, where they are thought to select substrates and to control the access to the translocation channel (Aizawa, 2001; Tampakaki *et al.*, 2004). Taking into account the predicted number of transmembrane helices of each protein, the inside diameter of the model of the MS ring (6 nm; Yip *et al.*, 2005), and an estimated transmembrane helix average diameter of 1.2 nm (Althage *et al.*, 2004), one copy of each protein would just about fit into this position.

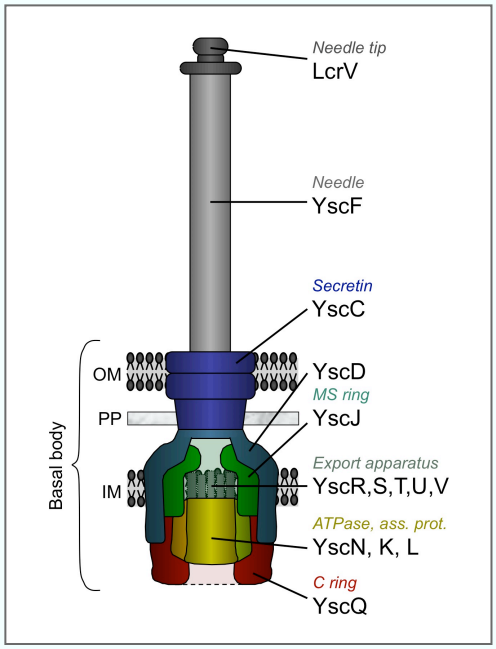

Figure 1.6: Schematic representation of the *Y. enterocolitica* injectisome (modified from Diepold *et al.* (2010))

The tip structure is derived from Müller *et al.* (2005); the global structure of YscC, D, J is based on data from Spreter *et al.* (2009); position and overall shape of the IM proteins and the cytoplasmic components are derived from homology to the flagellar structures and functional data presented in this work. OM, Outer membrane; PP, Periplasm; IM, Inner membrane.

Cytosolic components

There are four essential cytosolic components that are thought to be part of the injectisome structure: An ATPase (YscN), two adjacent proteins (YscK and YscL), and a homologue of the flagellar C ring component (YscQ). All four proteins have been shown to interact (Jackson and Plano, 2000). The *P. syringae* ATPase HrcN is activated upon oligomerization and forms hexamers as well as dodecamers (Woestyn *et al.*, 1994; Pozidis *et al.*, 2003; Müller *et al.*, 2006). The obvious idea about the function of the ATPase is that is energizes the transport. However, the observed substrate export rates (up to a thousand molecules per minute) (Schlumberger *et al.*, 2005) would be too high for the low measured ATPase activity (Chevance and Hughes, 2008). In addition, in the flagellum it has been shown that export is not completely dependent on the ATPase, but on the proton-motive force (PMF) (Minamino and Namba, 2008; Paul *et al.*, 2008). The role of the PMF has also been demonstrated for the injectisome (Wilharm *et al.*, 2004). Therefore, the main function of the ATPase might rather be to detach chaperones and unfold export substrates (Akeda and Galán, 2005). While YscL might act as a negative regulator of the ATPase (Blaylock *et al.*, 2006; Pallen *et al.*, 2006), as has been shown for its flagellar homologue FliH (Minamino and Macnab, 2000; González-Pedrajo *et al.*, 2002), the role of YscK and YscQ is unclear. Although the function of the flagellar C ring in reversal of the rotation direction (Driks and DeRosier, 1990; Khan *et al.*, 1992) is obsolete in the injectisome, the homologue of YscQ has been shown to localize to the proximal side of the injectisome in *Shigella* (Morita-Ishihara *et al.*, 2005).

1.1.3. Regulation of the type III secretion system

Regulation of type III secretion is mainly exerted on two levels: formation of the injectisome, which is a relatively slow process, and secretion of effectors, which occurs very rapidly once it is triggered (Schlumberger *et al.*, 2005). Both steps can be induced separately *in vitro*, and there is strong evidence that they occur discretely *in vivo* as well. However, the molecular signals leading to the events *in vivo* are only beginning to be characterized.

Formation of the injectisome is generally induced when the temperature reaches the body temperature of the host. In *Yersinia* and *Shigella*, expression of the injectisome proteins is turned on at 37°C (Skurnik *et al.*, 1984; Michiels *et al.*, 1991; Lambert de Rouvroit *et al.*, 1992; Hoe and Goguen, 1993; Durand *et al.*, 2000).[3] This is achieved through the temperature-dependent expression of the main transcription factor VirF, and through the dissociation of the chromosomal histone-like protein YmoA, which blocks transcription of the injectisome genes at lower temperatures, from the DNA (Michiels *et al.*, 1991; Lambert de Rouvroit *et al.*, 1992) (Figure 1.7).

Once the injectisome is built, it is ready for the export of effectors. However, no undirected secretion of effector proteins into the surrounding medium occurs *in vivo*. Translocation of effectors only occurs into host cells, after contact to those cells has been established (Rosqvist *et al.*, 1994; Sory *et al.*, 1995). *In vitro*, secretion into the supernatant can be induced, even in the absence of host cells, by chelation of Ca^{2+} ions (in the case of *Yersinia* and *Pseudomonas*) or addition of Congo red (in *Shigella*) (Cornelis, 2006). Whether these conditions mimic host cell contact or are artefacts could not be determined so far. Cisz *et al.* (2008) showed that in *P. aeruginosa*, calcium addition in previously secretion-permissive medium blocked only the secretion of effectors, but not of translocators, pointing out that the regulation of secretion is more complex than thought previously. Effector translocation *in vivo* can also be controlled by microaerobic conditions in *S. flexneri* and EHEC (Marteyn *et al.*, 2010; Schüller and Phillips, 2010) and by the pH value of the surrounding vacuole in *S. enterica* SPI-2 (Yu *et al.*, 2010). These examples show that the translocation of effectors is likely to be controlled differently between species, according to the lifestyle of the respective bacterium.

[3] In *Salmonella*, expression of SPI-1 T3S genes seems to be influenced stronger by factors like pH, osmolarity and oxygen levels (Ibarra *et al.*, 2010) and has been shown to change over time (Bumann, 2002), which is conceivably benefitial for the subsequent steps of invasion and intracellular survival.

At least five proteins (YopN, SycN, TyeA, YscB, LcrG) are required for the control of effector secretion in *Yersinia*. Deletion of any of these protein leads to a "Ca^{2+} blind" phenotype with effector secretion under normally secretion-non-permissive conditions (Yother and Goguen, 1985; Forsberg and Wolf-Watz, 1988). A complex involving at least four of these proteins (Ferracci *et al.*, 2005) is thought to act as a "plug" at the cytoplasmic side of the injectisome (Figure 1.7). The *Shigella* YopN homologue MxiC has been shown to interact with the ATPase Spa47 (Botteaux *et al.*, 2009), suggesting a pathway through which the effect of this plug is exerted. Based on the crystal structure of the *Shigella* needle subunit MxiH and various mutants displaying defects in host sensing, a model has been devised where host sensing at the needle tip is transmitted to the secretion apparatus and the plug via changes in the helical architecture of the needle (Deane *et al.*, 2006).

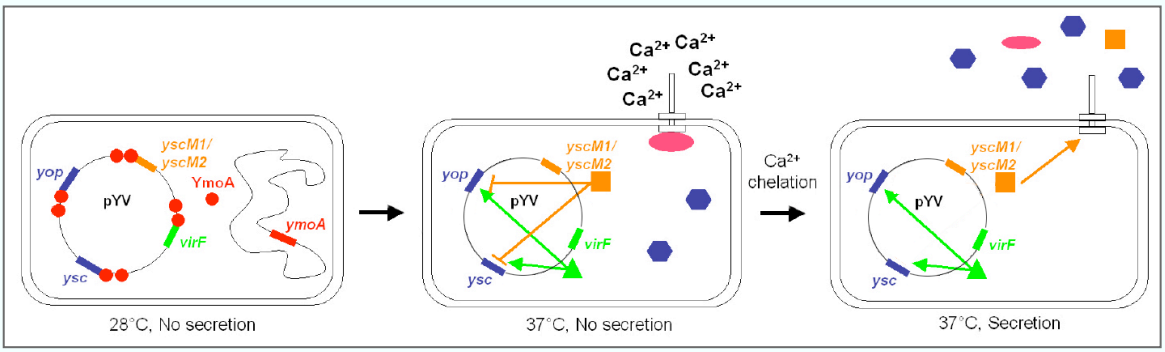

Figure 1.7: Simplified schematic view of type III secretion regulation in *Yersinia enterocolitica* (adapted from Müller (2004))

At 28°, the histone-like protein YmoA blocks the promoter regions of the T3S genes (*virF*, *yop* and *ysc*). At 37°, YmoA dissociates, and VirF, the main transcription factor of T3S gene expression, triggers transcription of the *yop* and *ysc* genes. However, transcription remains partially downregulated by YscM1/M2. Secretion is blocked by the presence of Ca^{2+} in the medium through the action of the secretion plug (pink). As soon as Ca^{2+} is chelated or host cell contact is established, the secretion plug is released and YscM1/M2 are secreted, along with the effectors, which allows VirF to fully activate *yop* and *ysc* gene expression. pYV, *Yersinia* virulence plasmid; *yop*, effector protein genes; *ysc*, injectisome component genes.

Beyond these "on-off" type mechanisms, there are further layers of regulation. In *Yersinia*, it has been shown that chelation of calcium ions in the medium at 37°C not only allows secretion, but also leads to an increase in the synthesis of effector and translocator proteins (Stainier *et al.*, 1998) as well as in the synthesis of machinery proteins (Allaoui *et al.*, 1995b). The effect of the extracellular calcium concentration on the production of needles was reported to be even more pronounced (Müller *et al.*, 2005). This effect is based on the action of two proteins, YscM1 and YscM2 (Stainier *et al.*, 1998). Both of these proteins

downregulate transcription of the T3S genes (Figure 1.7). Once conditions are secretion-permissive, they are exported, which leads to an increased expression of injectisome components and effectors. While it is clear that transcription levels are influenced by the extracellular calcium level, the scale of the effect strongly differs between reports (Allaoui *et al.*, 1995b; Stainier *et al.*, 1998; Müller *et al.*, 2005). So far, no quantitative comparison of the effect of the calcium concentration on different events has been performed.

Another type of regulation is provided by the feedback inhibition of secretion by effectors, once a cell has been infected by a bacterium. Cisz *et al.* (2008) showed that the presence of ExoS, the *P. aeruginosa* homologue of YopE, in a host cell suppresses translocation of effectors into this cell by subsequently attaching bacteria. A similar role could be exerted by YopH, an effector highly similar to the negative regulators YscM1/M2 in *Y. enterocolitica* (Stainier *et al.*, 1998).

The increased availability of reporter constructs and imaging techniques that allow to follow the events during infection of host cells are likely to lead to new insights into events during *in vivo* infection and its regulation that could not be assayed or discriminated *in vitro* before.

1.2. Assembly of bacterial transmembrane protein complexes

1.2.1. Challenges in the purification and characterization of transmembrane complexes

Bacteria harbor a variety of transmembrane protein complexes. They function, among other things, in attachment (such as fimbrae and adhesins), movement (flagella), or transport across membranes (secretion systems, see Figure 1.2). In general, it is assumed that the intermolecular forces that predominate in membrane complexes greatly differ from those governing soluble protein complexes (Helms, 2002). Association of membrane proteins can be caused by affinity between transmembrane helices (reviewed in Schneider *et al.* (2007); Figure 1.8 A) or by the entropically favorable decrease in lipid order around the proteins in a complex (Morrow *et al.*, 1985; Figure 1.8 B). Of course, complex formation of membrane proteins can also be caused by motifs outside of the transmembrane helices, as was proposed for the "ring-building motif" in type III secretion systems (Spreter *et al.*, 2009).

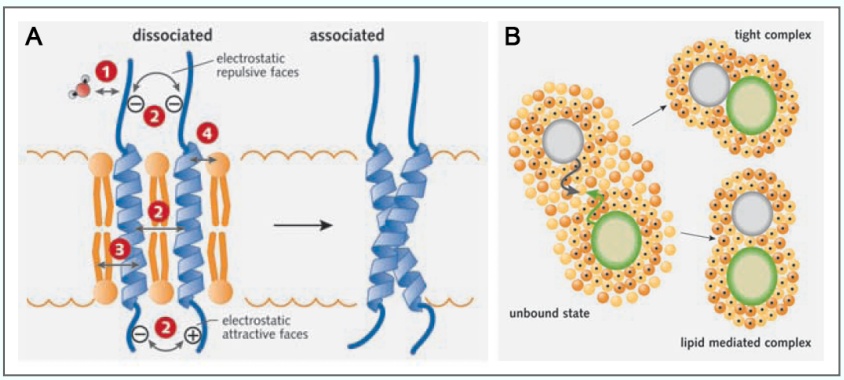

Figure 1.8: Forces in the formation of membrane complexes (adapted from Helms (2002)).

A: Illustration of the forces that may lead to the association of transmembrane helices. 1 represents protein:water, 2 protein:protein, 3 protein:bilayer core and 4 protein:bilayer interface interactions. Proteins are shown in blue, lipid molecules in orange and water molecules in red and gray. **B**: Decrease in the amount of ordered lipids during the assembly of a membrane protein complex. The lipids in the first and second layers around the proteins are assumed to be entropically confined and are marked by black dots (76 when gray and green proteins are separated, and only 56 and 62 in the 'tight' or 'lipid-mediated' complexes).

It is a particularity of the two-dimensional space to which proteins in membrane complexes are restrained, that the integration of proteins into the complex is very demanding. This especially applies to closed membrane rings, as in the injectisome. Proteins enclosed by such a ring have to be integrated either before ring closure, or by a special integration mechanism.

At the moment, our understanding of forces that govern the assembly of protein complexes within membranes remains limited, mostly due to the lack of defined structures. Purification of large transmembrane complexes is notoriously difficult. On one side, the complex has to be extracted from the membrane, and in some cases from the peptidoglycan layer, which requires destabilization of the bacterial membrane and the use of detergent; on the other side, the complex should remain intact and not lose any components, which calls for very gentle conditions. The ensuing difficulties are illustrated by the fact that, although 15-30% of all ORFs in different species are predicted to encode transmembrane proteins (Kashino, 2003) and membrane protein-containing complexes are crucial to maintain cell signaling, metabolism and other central functions, comparatively few membrane protein complexes have been purified and characterized in detail. The task becomes even more difficult when the assembly of a transmembrane complex is examined. In this case, the purification ideally does not rely on physicochemical properties of the complex, such as its size (a criterion otherwise often used to purify large complexes), as this would likely exclude early intermediates. Instead, a component thought to be the nucleation core of the complex or integrated early can be fused to an affinity tag. While it involves the alteration of a protein, the advantage of this method is that it allows to apply relatively gentle purification procedures that are largely independent of the assembly state of the complex.

In many cases, a tandem-affinity purification (TAP) tag strategy is used for the purification of protein complexes. The TAP tag originally consists of the Calmodulin Binding Peptide (CBP), a TEV protease cleavage site, and Protein A (Rigaut *et al.*, 1999). In other studies, different combinations of affinity tags, like a combination of FLAG and His tag, proved to result in higher yields (Yang *et al.*, 2006). The TAP approach has even been used for genome-wide protein complex screens in yeast (Gavin *et al.*, 2002; Gavin *et al.*, 2006). While membrane protein complexes were excluded in the first analysis, they were purified with a modified protocol and analyzed in the follow-up study. 340 out of 628 tagged membrane proteins could be purified, a ratio similar to the one in soluble proteins. However, the overview of all purified complexes shows that protein complexes are still significantly underrepresented (Gavin *et al.*, 2006), pointing out the difficulties in copurification.

A completely different approach to study the assembly of transmembrane complexes is the utilization of fluorescent fusion proteins. The main advantage of this approach is the possibility to trace assembly *in vivo* in real time without the need of lengthy, and possibly complex-disrupting, purification procedures. A major disadvantage is the need to fluorescently label several components to get a high resolution in the order of assembly. Furthermore, all of the following requirements have to be fulfilled to be able to use this

technique: (i) The labeled protein has to be present in multiple copies within the complex to be detectable, (ii) the protein complex needs to have a specific distribution within the cell that differs from the distribution of the free component (unless more sophisticated diffusion-based methods such as fluorescence correlation or cross-correlation spectroscopy are applied), (iii) the used fluorescent tag must not impede the formation of the complex, (iv) the microscope must have a sufficient resolution and especially a high sensitivity to visualize and resolve the assembled proteins. As most fluorescent proteins have a size of 25-30 kDa (Shaner *et al.*, 2005), and smaller alternatives, such as tetracysteine tags (Adams *et al.*, 2002; Andresen *et al.*, 2004), require additional manipulation (Enninga *et al.*, 2005) and may also disturb the function of the protein (own unpublished observations), a test for the formation and/or functionality of the protein complex harboring the fusion protein is essential in this approach.

If all requirements are met, the analysis of fluorescent fusion proteins can yield valuable insights into the *in vivo* assembly of bacterial membrane complexes, as shown by two recent studies (Lybarger *et al.*, 2009; Minamino *et al.*, 2009).

1.2.2. Assembly of the bacterial flagellum

Along with the ribosome, the bacterial flagellum is one of the most complex prokaryotic nanomachines. The assembly of this transmembrane complex has been studied for thirty years, and has been extensively reviewed (Aizawa, 1996; Aldridge and Hughes, 2002; Macnab, 2003; Macnab, 2004; Apel and Surette, 2008; Chevance and Hughes, 2008; Minamino *et al.*, 2008).

A landmark paper in the study of flagellar assembly was published in 1992, when Kubori *et al.* examined the formation of flagellar precursors in a wide array of deletion mutants. They found that overall, assembly of the flagellum starts at the IM and proceeds sequentially to more distal structures. The first detected structure was the MS ring, which did not require any other structural protein than its component FliF. In various deletion strains, different precursors of the hook-basal body[4] could be visualized, which allowed to establish an approximate pathway for flagellar assembly (Kubori *et al.*, 1992).

Further studies, mainly based on heterologous overexpression of proteins, helped to elaborate details of the assembly pathway: Immediately after assembly of the MS ring, the C ring /

[4] Hook-basal bodies (HBB): The secretion machinery of the flagellum, without rotor/stator proteins and the extracellular flagellin appendix, expressed by the class 2 operons (see Figure 1.10).

switch complex, consisting of FliG, FliM, and FliN, can be formed (Kubori *et al.*, 1997; Lux *et al.*, 2000; Macnab, 2003) (Figure 1.9A)[5]. For the next observable steps, integration of the eight proteins FlhA, FlhB, FliH, FliI, FliO, FliP, FliQ, and FliR, proposed to form an export apparatus, has to occur. Whether in wild-type conditions, these proteins require the MS ring and the C ring for their assembly, could not be determined so far, which leaves the possibility that assembly of the export apparatus is an independent event (Macnab, 2003; McMurry *et al.*, 2004).

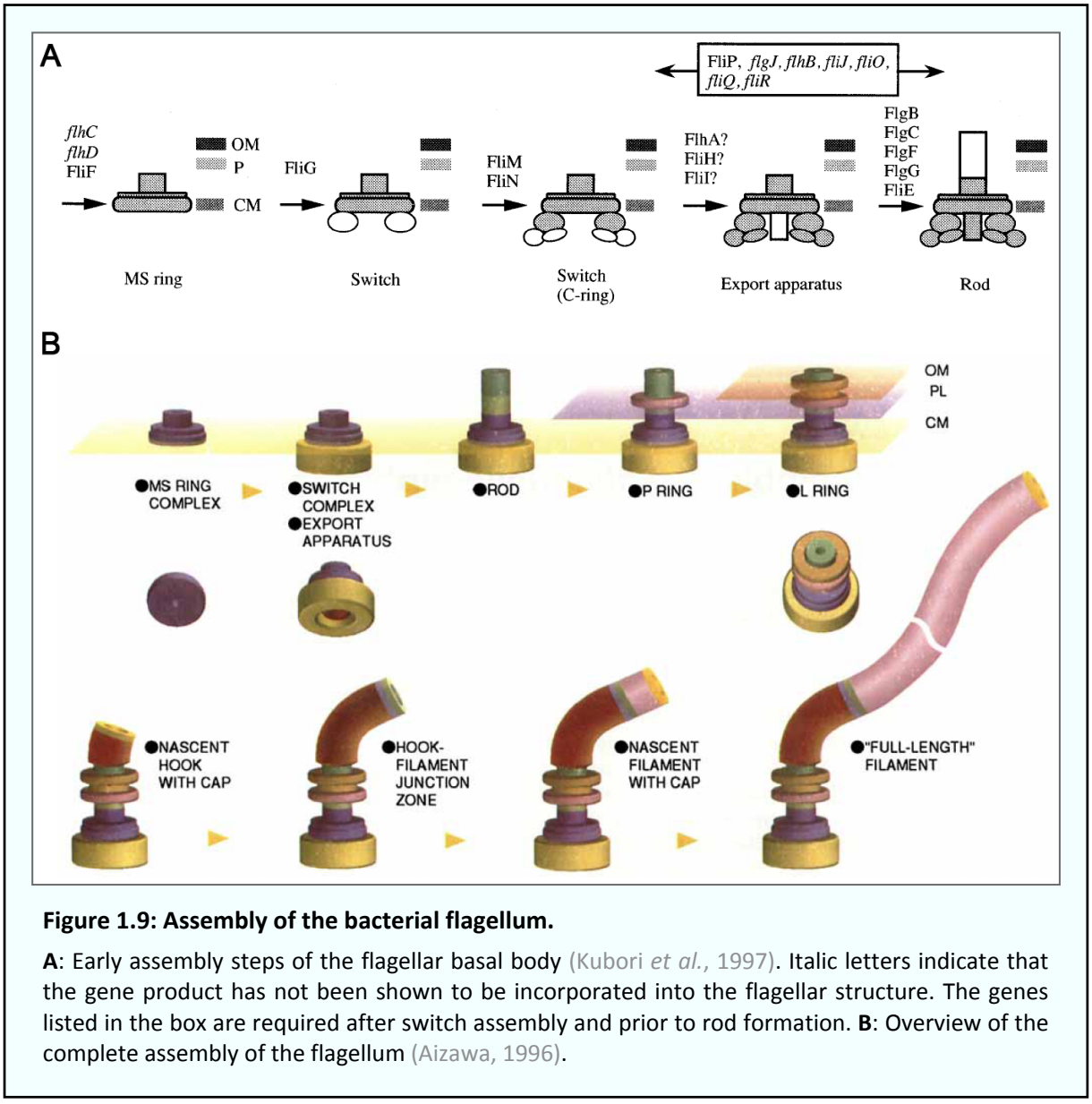

Figure 1.9: Assembly of the bacterial flagellum.

A: Early assembly steps of the flagellar basal body (Kubori *et al.*, 1997). Italic letters indicate that the gene product has not been shown to be incorporated into the flagellar structure. The genes listed in the box are required after switch assembly and prior to rod formation. **B**: Overview of the complete assembly of the flagellum (Aizawa, 1996).

[5] The flagellar C ring is essential not only for the switching of the rotation direction, but also for the export of distal components (Macnab, 2003). However, two recent reports showed that in C ring mutants, the export can be partially restored by overexpression of the ATPase (Konishi *et al.*, 2009) or the master regulator (Erhardt and Hughes, 2010).

Afterwards, the flagellum grows outwards, subsequently forming the rod, the P and L rings in the peptidoglycan layer and in the OM, respectively, the hook, and the filament. The polymerization of the extracellular components is guided by specific cap proteins (Ikeda *et al.*, 1985; Yonekura *et al.*, 2000). An overview of the complete assembly pathway is depicted in Figure 1.9B.

The protein assembly order is, in a simpler way, mirrored in the order of expression of the flagellar genes. Genetic studies in *E. coli* (Komeda, 1986; Kutsukake *et al.*, 1990; Chilcott and Hughes, 2000) showed that the 14 flagella operons are arranged in a regulatory cascade of three classes: The single class 1 operon flhDC controls expression of the class 2 operons, which encode for hook-basal body components (shown red in Figure 1.10) and the transcriptional activator for the class 3 operons. Transcription of the class 3 operons does not occur before completion of hook-basal bodies and leads to the expression of the rotor/stator proteins and the flagellin filament, as well as the linked chemotaxis system (shown blue in Figure 1.10).

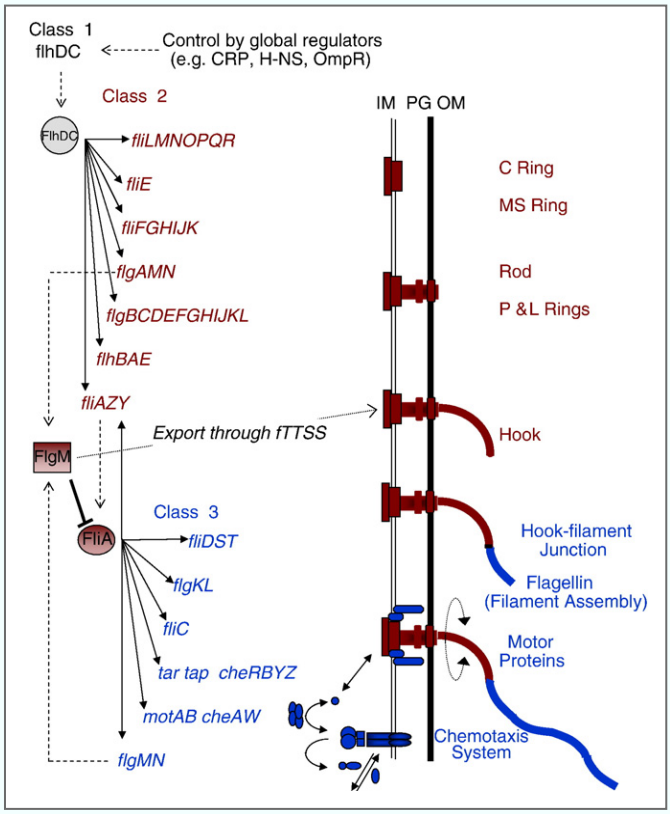

Figure 1.10: Temporal order of gene expression and assembly of the flagellum (Apel and Surette, 2008).

The operons for the flagella systems are expressed in a defined temporal order (left side, top to bottom). Class 2 and 3 operons and proteins are marked in red and blue, respectively. The class 3 sigma-factor FliA is inhibited by the anti-sigma factor FlgM until FlgM is exported by a functional T3S system.

1.2.3. Assembly of the type III secretion injectisome

The assembly of the injectisome has not been studied as intensely as the assembly of the flagellum. Transcriptional control of the operons of the injectisome is simpler compared to the flagellum. As the virulence T3S systems have only one transcription factor (class 1) and no homologues of the proteins encoded in the class 3 operons in the flagellum, all injectisome components are encoded in operons corresponding to the flagellar class 2, and transcription is expected to occur simultaneously. A more detailed analysis is performed in chapter 4.2.

Most studies on the assembly of the injectisome were performed in *Salmonella* SPI-1 (*Yersinia* homologues are given in brackets). When the *Salmonella* MS ring components PrgH and PrgK (YscD and YscJ) were overexpressed in *E. coli*, stable ring structures could be observed (Kimbrough and Miller, 2000). This suggested that injectisome assembly is initiated at the IM, like it is the case for the flagellum (Kimbrough and Miller, 2002). Next, the MS ring would, through an unknown mechanism, assemble with the secretin ring (YscC) in the OM, which has been shown in *Yersinia* to be a stable structure as well, in the presence of its pilotin (YscW) (Koster *et al.*, 1997; Burghout *et al.*, 2004a; Burghout *et al.*, 2004b). As all further cytosolic and IM components of the injectisome (YscK, L, N, Q, R, S, T, U, V in *Yersinia*) are required for export of the needle subunit, which is the next observable event, their assembly order could not be assigned. After needle assembly is finished, the substrate specificity of the export machinery is switched (Agrain *et al.*, 2005), and the system is ready for effector secretion (Figure 1.11).

Sukhan *et al.* (2001) showed that InvG (YscC), PrgH (YscD), and PrgK (YscJ) were required to form the "needle base" corresponding to both transmembrane rings. While they could purify low amounts of assembled InvG from the membrane in mutants lacking any of the two other proteins, PrgH multimers were found in low amounts in the InvG mutant strain, but not in a PrgK mutant, and the detection of PrgK multimers required the presence of both other membrane-ring forming proteins. Again, the order of the later steps could not be assessed, and an assembly pathway similar to the one depicted in Figure 1.11 was proposed.

An additional study was performed in EPEC (Ogino *et al.*, 2006). As in the other organisms, the three proteins forming the transmembrane rings, EscC, D, J (YscC, D, J, respectively) were required for assembly of the T3S apparatus. This study further showed by pull-down experiments that EscC directly interacts with EscD and the needle subunit EscF, while EscJ could only be shown to interact with EscF.

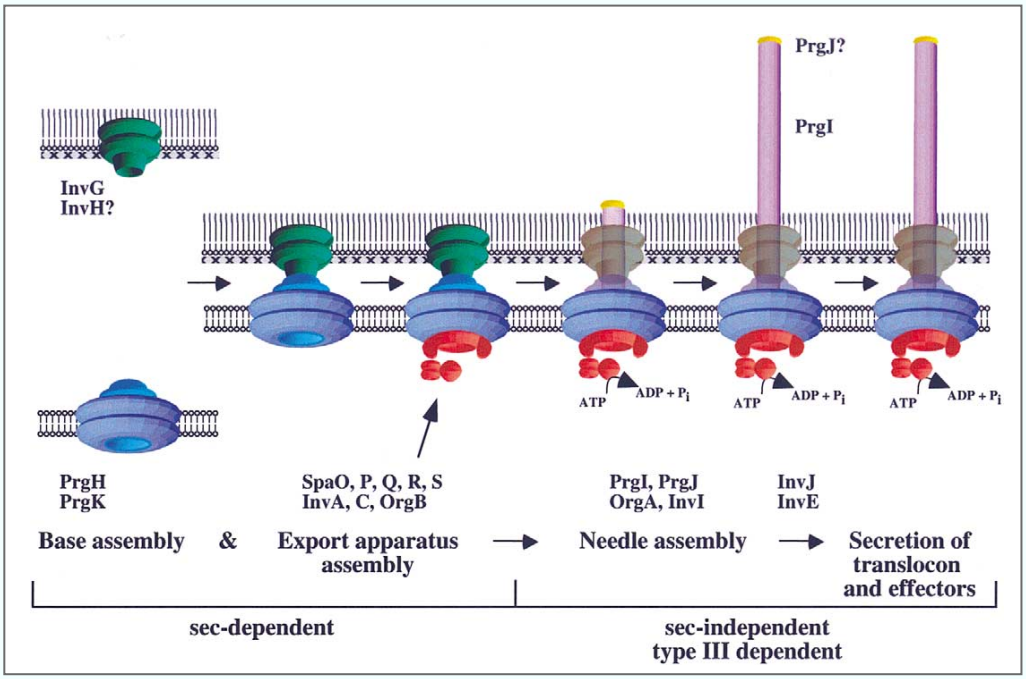

Figure 1.11: Assembly model for the *Salmonella* SPI-1 injectisome (Kimbrough and Miller, 2002).

During the sec-dependent phase, the base components PrgH/PrgK and InvG are exported and self-assemble in the membranes. At some point during this phase the export apparatus (depicted in red) becomes associated with the base, making it competent for secretion of type III-dependent substrates. The type III-dependent phase begins with the secretion and assembly of needle components (PrgI, PrgJ). Following completion of the needle, the specificity of the secretion apparatus is switched to secrete translocators and effectors.

These studies are further reviewed by Cornelis (2006), and Enninga and Rosenshine (2009). The main obstacle in all presented analyses is the low number of distinguishable intermediate structures which does not allow to track any event before the formation of the "needle base" and between this event and the completion of the needle. An approach based on fluorescently labeled proteins, which has the potential to overcome these problems, has not been applied prior to this work.

Chapter 2

Aim of the thesis

The formation of the type III secretion injectisome involves the assembly of about fifteen different, mostly multimeric proteins into a structure spanning both bacterial membranes. This assembly is likely to occur in an ordered fashion, but due to the lack of observable intermediate structures, little is known about the sequence of events. Our aim was to shed light on this process by using a novel approach. Through the creation of functional fluorescent fusion proteins that cover the major subcomplexes of the injectisome, and the analysis of their localization in strains lacking other type III secretion components, we sought to determine the requirements for the assembly of the respective proteins.

In combination with co-immunoprecipitation experiments, this approach permits to determine the assembly order and kinetics of the *Yersinia* injectisome in much more detail than previous studies. Further, it is not restricted to the components of the needle complex, but also allows, for the first time, the observation of dynamic properties of the cytosolic components of the injectisome *in vivo*.

Chapter 3

Assembly of the *Yersinia* type III secretion injectisome

The following chapter is an excerpt from the manuscript "Deciphering the assembly of the *Yersinia* type III secretion injectisome", published in April 2010 in The EMBO Journal **29**(11), pp. 1928-1940, that has been adapted in style and figure numeration for inclusion in this thesis. It contains the abstract, results, supplementary information, and discussion from the manuscript, and is followed by an additional "extended discussion" chapter including new data that we generated or were published by other groups after the submission of this manuscript.

Material and methods used in the manuscript are included in the corresponding chapter (chapter 6). The original published paper in its final print layout is attached in the appendix (chapter 7.7).

Authors' contributions

I contributed to the manuscript in conceiving the study, designing and generating bacterial strains and plasmids (strains and plasmids labeled pAD...), performing experiments, analyzing data, creating all figures and supplementary information and writing the paper.

Marlise Amstutz contributed in designing and generating bacterial strains and plasmids (constructs involving YscC, labeled pMA...), and in performing and analyzing experiments (especially in fluorescence microscopy and immunofluorescence).

Sören Abel contributed in generation and analysis of fluorescence microscopy images.

Isabel Sorg contributed in generation of strains (labeled pISO...) and antibodies.

3.1. Abstract

The assembly of the *Yersinia enterocolitica* type III secretion injectisome was investigated by grafting fluorescent proteins onto several components, YscC (outer-membrane (OM) ring), YscD (forms the inner-membrane (IM) ring together with YscJ), YscN (ATPase), and YscQ (putative C ring). The recombinant injectisomes were functional and appeared as fluorescent spots at the cell periphery. Epistasis experiments with the hybrid alleles in an array of injectisome mutants revealed a novel outside-in assembly order: whereas YscC formed spots in the absence of any other structural protein, formation of YscD foci required YscC, but not YscJ. We therefore propose that the assembly starts with YscC and proceeds through the connector YscD to YscJ, which was further corroborated by co-immunoprecipitation experiments. Completion of the membrane rings allowed the subsequent assembly of cytosolic components. YscN and YscQ attached synchronously, requiring each other, the interacting proteins YscK and YscL, but no further injectisome component for their assembly. These results show that assembly is initiated by the formation of the OM ring and progresses inwards to the IM ring and, finally, to a large cytosolic complex.

3.2. Various substructures of the *Yersinia* injectisome including the C ring can be monitored using functional fluorescent fusion proteins

To visualize the injectisome and its subunits, the wild-type alleles of *yscC*, *yscD*, and *yscQ* on the virulence plasmid of *Y. enterocolitica* MRS40 were replaced by hybrid genes encoding the fluorescent proteins YscC–mCherry, EGFP–YscD, and EGFP–YscQ. Further, a non-polar complete deletion of *yscN* was constructed and complemented *in trans* with a plasmid encoding EGFP–YscN. The fusion proteins were expressed at near wild-type levels; no proteolytic release of the fluorophore was detected (Supplementary Figure 1)[6].

To test the functionality of the fusion proteins, the pattern of proteins secreted into the supernatant in secretion-permissive medium (BHI-Ox) was analyzed 3 h after induction of the system. YscC–mCherry, EGFP–YscN, and EGFP–YscQ were fully functional, whereas the strain expressing EGFP–YscD secreted a lower amount of effector proteins (Figure 3.1 B). All fusion proteins allowed the formation of needles, which could be visualized by transmission electron microscopy (data not shown).

The localization of the hybrid proteins was analyzed by fluorescence microscopy. Three hours after induction of synthesis of the injectisome, fluorescent spots were observed at the cell periphery for all labeled proteins (Figure 3.1 A). The formation of these spots was independent of the Ca^{2+} concentration in the medium, showing that their appearance was not directly linked to the secretion of Yop proteins by the T3S system (Figure 3.1 A).

To ascertain that the membrane spots correspond to assembled basal bodies, we constructed a strain expressing both YscC–mCherry and EGFP–YscQ, and monitored the localization of the green fluorescence from EGFP–YscQ and the red fluorescence from YscC–mCherry. As visible in Figure 3.1 C, the green and red spots largely colocalized, with small deviations because of chromatic aberrations of the microscope. We thus assumed that the fluorescent spots correspond to assembled basal bodies. In a minority of cells, a polarily localized YscC–mCherry spot without EGFP–YscQ equivalent could be observed in addition to the colocalizing spots. We assumed that these polar spots consist of misassembled YscC–mCherry proteins. Colocalization of spots was also observed for EGFP–YscD and EGFP–YscN with YscC–mCherry (data not shown). To test for colocalization of the needle with the

[6] Supplementary figures are directly following the discussion, chapter 3.9.

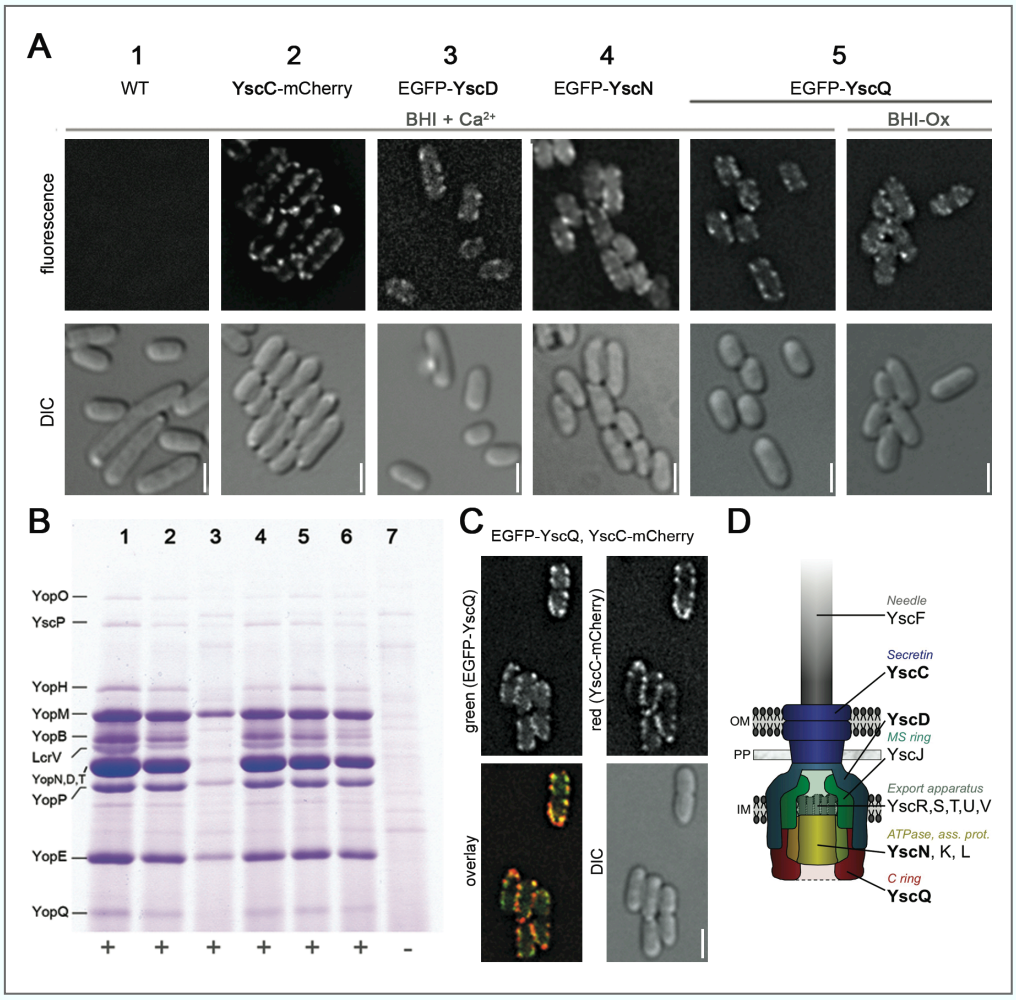

Figure 3.1: Fluorescently labelled Ysc proteins are functional and allow visualization of the injectisome.

(A) Fluorescence deconvolution microscopy showing the formation of fluorescent spots at the bacterial membrane of *Y. enterocolitica* bacteria grown in secretion-non-permissive (BHI+Ca^{2+}) and secretion-permissive medium (BHI-Ox): 1—MRS40 [wild type], 2—MA4005 [YscC–mCherry], 3—AD4050 [EGFP–YscD], 4—AD4136(pAD182) [ΔYscN+pBAD–*egfp–yscN*], 5—AD4016 [EGFP–YscQ]. All fusion proteins except for EGFP–YscN are encoded under their native promoter on the pYV virulence plasmid. Upper lane: mCherry fluorescence for strain 2, EGFP fluorescence for other strains; lower lane: corresponding DIC picture. All fluorescence pictures were taken 3 h after the induction of the T3S system by temperature shift to 37°C. Scale bars: 2 µm. **(B)** Analysis of the Yop proteins secreted in secretion-permissive conditions. The tagged strains are fully functional for effector secretion, except for the strain expressing EGFP–YscD (lane 3), which shows reduced secretion. Culture supernatants were separated on a 12% SDS–PAGE gel and stained with Coomassie Brilliant Blue. Strains as listed in (A), 6—MAAD4006 [EGFP–YscQ, YscC–mCherry], 7—AD4051 [ΔYscD, negative control]. Bottom line: Needle formation (+/−) in the tested strains (data not shown). **(C)** Fluorescence microscopy showing the colocalization of EGFP–YscQ with YscC–mCherry in MAAD4006 bacteria. Fluorescent pictures were obtained as described in (A). **(D)** Model of the *Yersinia* Ysc injectisome. Fluorescently labelled proteins are shown in bold print.

basal body components, bacteria producing EGFP–YscQ were analyzed by immunofluorescence with purified antibodies directed against the needle subunit. Overlays of the resulting pictures with the EGFP–YscQ fluorescence revealed that the majority of spots for YscF and YscQ colocalized (Supplementary Figure 2). A fraction of YscQ spots did not correspond to YscF spots. Most likely, the needles of these basal bodies were detached during the immunofluorescence procedure. We conclude from all these experiments that the fluorescent spots correspond to functional injectisomes.

3.3. Assembly of the injectisome starts from the secretin ring in the OM and proceeds inwards through stepwise assembly of YscD and YscJ

As earlier work has shown that secretins can insert in the OM provided they are assisted by their pilotin (Burghout *et al.*, 2004a; Guilvout *et al.*, 2006), the fluorescent YscC–mCherry and its pilotin YscW were expressed *in trans* in *Y. enterocolitica* MRS40(pMA8)(pRS6), in the absence of the pYV virulence plasmid encoding the T3S components. YscC–mCherry localized in membrane spots (Figure 3.2 A), as observed before for PulD, the secretin involved in a type II secretion pathway (Buddelmeijer *et al.*, 2009). These data thus confirm earlier results showing that YscC only requires its pilotin for assembly in the OM (Burghout *et al.*, 2004a). In the absence of YscW, the majority of YscC–mCherry clustered in spots at the bacterial pole (Supplementary Figure 3). This phenotype was clearly distinguishable from the membrane spot formation in the presence of YscW, and confirmed the function of YscW in proper localization and oligomerization of YscC (Burghout *et al.*, 2004a).

Not surprisingly, mutants lacking any of the structural ring proteins YscC, YscD, or YscJ failed to assemble the cytosolic injectisome components YscN and YscQ (Table II), showing that establishment of the membrane-spanning structure formed by YscC, YscD, and YscJ is at the beginning of injectisome formation. To test for the assembly order of these proteins, we combined the *egfp–yscD* allele on the pYV plasmid with non-polar deletions in *yscC* and *yscJ*. While the absence of YscC clearly abolished the formation of EGFP–YscD spots at the bacterial membrane, the absence of YscJ did not affect this assembly (Figure 3.2 B). This implies that YscC assembles first, followed by YscD, and finally YscJ.

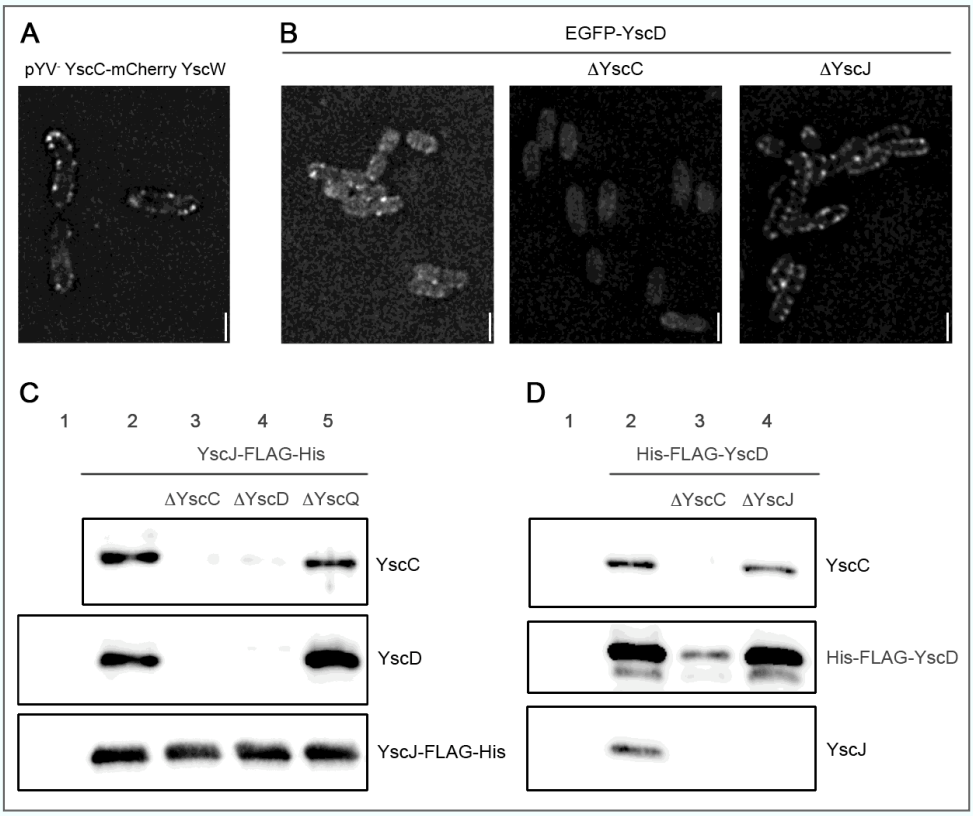

Figure 3.2: YscC assembly only requires its pilotin; YscD assembly requires the presence of YscC, but not of YscJ. Copurification of the three structural ring proteins suggests the stepwise assembly order YscC–YscD–YscJ.

(A) Fluorescence microscopy showing the formation of secretin spots [YscC–mCherry] at the bacterial membrane in a strain lacking the virulence plasmid pYV, after in trans expression of YscC–mCherry and YscW (plasmids pMA8, pRS6) for 3 h at 37°C. Scale bars: 2 µm. **(B)** Fluorescence microscopy showing the formation of YscD spots at the bacterial membrane in strains AD4050 [EGFP–YscD], MAAD4018 [EGFP–YscD, ΔYscC], and AD4080 [EGFP–YscD, ΔYscJ]. YscD remains cytosolic in the absence of YscC, whereas it assembles in membrane spots in the absence of YscJ. **(C)** Analysis of the copurification of YscC and YscD after affinity purification of YscJ. Deletion of either YscC or YscD abolishes the copurification of the respective other protein with YscJ-FLAG-His. Bacteria were incubated for 3 h at 37°C, spheroplasted, and lysed. Proteins were purified by FLAG affinity, separated on 4–12% gradient SDS–PAGE, and analyzed by immunoblot with the respective anti-YscC, -YscD, or -YscJ antibodies. All strains were ΔYadA to facilitate cell lysis: 1—LJM4029 [WT], 2—AD4054 [YscJ-FLAG-His], 3—AD4109 [YscJ-FLAG-His, ΔYscC], 4—AD4110 [YscJ-FLAG-His, ΔYscD], 5—AD4112 [YscJ-FLAG-His, ΔYscQ]. **(D)** Analysis of the copurification of YscC and YscJ after affinity purification of YscD. Whereas deletion of YscC abolishes copurification of YscJ with His-FLAG-YscD, YscJ is not required for the interaction between YscC and YscD. Samples were obtained as described for (C). All strains were ΔYadA to facilitate cell lysis: 1—LJM4029 [WT], 2—AD4055 [His-FLAG-YscD], 3—ADMA4101 [His-FLAG-YscD, ΔYscC], 4—AD4089 [His-FLAG-YscD, ΔYscJ].

To confirm this order of assembly, we performed co-immunoprecipitation assays using strains in which the wild-type alleles of *yscD* or *yscJ* on the virulence plasmid were replaced by *his-flag-yscD* or *yscJ-flag-his*, respectively. The affinity tagged proteins were functional for

effector secretion (data not shown) and hence assumed to assemble in the same way as wild type. They were further combined with non-polar deletions in *yscC*, *yscD*, or *yscJ*. In each of the strains, the adhesin YadA was removed to facilitate cell lysis. Synthesis of the injectisome in these strains was induced under secretion-non-permissive conditions. Mild crosslinking was performed, spheroplasts were created, and the bacteria were lysed by the addition of detergent (see Material and methods). Afterwards, a one-step affinity purification was performed, and the (co-)purification of YscC, YscD, and YscJ was tested. YscJ-FLAG-His copurified YscC and YscD from complete injectisomes, and removal of YscQ, a protein thought to act further downstream in the assembly process, did not affect this copurification. In contrast, removal of YscC prevented copurification of YscD with YscJ-FLAG-His, and removal of YscD prevented copurification of YscC (Figure 3.2 C). Likewise, His-FLAG-YscD copurified YscC and YscJ from complete injectisomes. However, although removal of YscC prevented copurification of YscJ with His-FLAG-YscD, removal of YscJ still allowed the copurification of YscC (Figure 3.2 D). The amount of purified His-FLAG-YscD was reduced in the absence of YscC, most likely as a consequence of decreased cellular YscD levels, either because of its mislocalization in the absence of YscC or because of a lower expression level. Taken together, these data indicate (i) that the insertion of the secretin ring in the OM is required for the subsequent association of YscD and YscJ and (ii) that YscD makes the link between YscC and YscJ. Hence, the OM ring is the first ring of the injectisome to be assembled. This assembly step is followed by the attachment of YscD, which then allows the completion of the MS ring by YscJ.

3.4. The C ring only assembles in the presence of the membrane rings, YscN, YscK, and YscL

To determine at which stage the C ring forms during the assembly process, we combined the *egfp–yscQ* allele with an array of deletions in most injectisome genes (Table II; chapter 7.3 for details of strains). Deletion of any of the membrane ring proteins (YscC, YscD, or YscJ) completely abolished the formation of membrane spots and led to an increased diffuse cytoplasmic fluorescence (Figure 3.3). This indicates that the C ring forms after the YscCDJ ring structure. Removal of the ATPase YscN or any of its two interacting proteins YscK and YscL (Jackson and Plano, 2000; Blaylock *et al.*, 2006) also fully prevented C ring formation (Figure 3.3), indicating that assembly of the C ring additionally requires YscN as well as YscK and YscL.

Protein missing	Family/Function	Localization	YscC- mCherry fluorescence	EGFP- YscD fluorescence	EGFP- YscN fluorescence	EGFP- YscQ fluorescence
all (pYV⁻)			+ (pMA8 + pRS6)	*n.d.*	*n.d.*	*n.d.*
YscC	Secretin ring	OM		- (MAAD4018)	- (ADMA4156)	- (ADMA4151)
YscD	MS ring	IM	*n.d.*		*n.d.*	- (AD4052)
YscJ	MS ring	IM	+ (ADMA4082)	+ (AD4080)	- (AD4139)	- (ADMA4082)
YscN	ATPase	cytoplasmic, IM-associated	+ (ADMA4137)	*n.d.*		- (AD4104)
YscK	ATPase-associated	cytoplasmic, IM-associated	*n.d.*	*n.d.*	- (AD22840)	- (AD22723)
YscL	ATPase-associated	cytoplasmic, IM-associated	*n.d.*	*n.d.*	- (AD4141)	- (AD4039)
YscQ	C ring	cytoplasmic, IM-associated	+ (MA4007)	+ (AD4061)	- (AD4142)	
YscR	Export machinery	IM	*n.d.*	*n.d.*	*n.d.*	+ (AD4032)
YscS	Export machinery	IM	*n.d.*	*n.d.*	*n.d.*	+ (AD4034)
YscT	Export machinery	IM	*n.d.*	*n.d.*	*n.d.*	+ (AD4036)
YscU	Export machinery, *1)*	IM	*n.d.*	*n.d.*	*n.d.*	+ (AD4026)
YscV(LcrD)	Export machinery	IM	+ (MA4011)	*n.d.*	*n.d.*	+ (AD4038)
YscRSTUV	Export machinery	IM	*n.d.*	*n.d.*	+ (AD4143)	+ (AD4108)
YscF	Needle subunit	extracellular	+ (MA4015)	*n.d.*	+ (AD4157)	+ (AD4020)
LcrV	Needle tip	extracellular	*n.d.*	*n.d.*	*n.d.*	+ (AD4042)
YscH	unknown	exported	*n.d.*	*n.d.*	*n.d.*	+ (AD22769)
YscI	unknown, *2)*	exported	*n.d.*	*n.d.*	*n.d.*	+ (AD4022)
YscO	unknown	exported	*n.d.*	*n.d.*	*n.d.*	+ (AD4024)
YscX	unknown	exported	*n.d.*	*n.d.*	*n.d.*	+ (AD4027)
YscY	Chaperone of YscX	cytoplasmic	*n.d.*	*n.d.*	*n.d.*	+ (AD4040)
YopN	Ca^{2+} plug	cytoplasmic, IM-associated	*n.d.*	*n.d.*	*n.d.*	+ (AD4043)
LcrG	Ca^{2+} plug	cytoplasmic, IM-associated	*n.d.*	*n.d.*	*n.d.*	+ (AD4041)

1) Substrate specificity switch; 2) Proposed inner rod

Table II: Formation of fluorescent spots in various injectisome mutants

The formation of fluorescent spots was checked for YscC-mCherry, EGFP-YscD, EGFP-YscN, and EGFP-YscQ in combination with deletions of different proteins. + : Spot formation at the bacterial membrane; - : Diffuse cytosolic fluorescence. The corresponding strains are given in brackets (see Chapter 7.3 for strain details). n.d.: not determined.

Removal of individual proteins YscR, S, T, U, or V from the export apparatus as well as a complete deletion of all these proteins did not completely abolish the formation of the C ring. However, in the absence of YscR, YscS, or YscV, the number of spots was reduced, indicating that these proteins are either beneficial (but not absolutely required) for C ring formation, or have a stabilizing effect on fully assembled injectisomes.

As expected from the fact that YscF, YscI, YscO, YscX, and YopN are substrate proteins exported by the injectisome itself, their absence also did not prevent the formation of the C ring. Likewise, deletion of LcrG, a regulatory protein (Nilles *et al.*, 1997; Torruellas *et al.*, 2005), had no effect on assembly of the C ring (Figure 3.3; see Table II for additional strains).

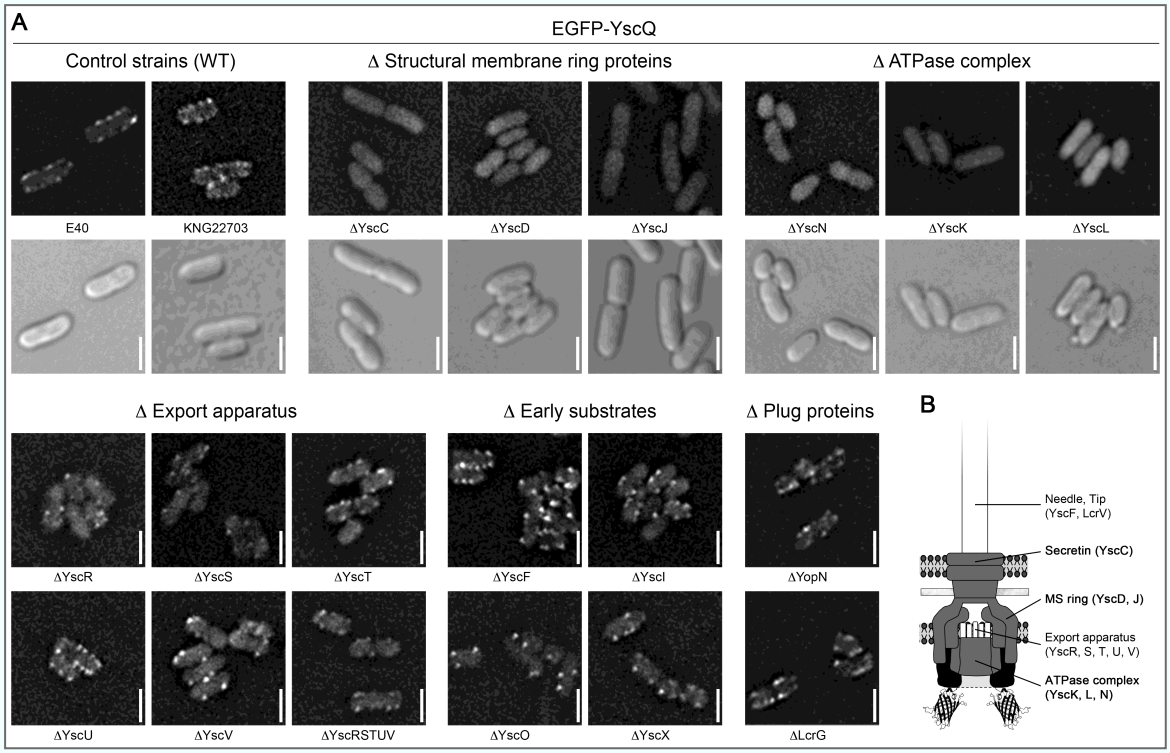

Figure 3.3: C ring formation requires both transmembrane rings and the ATPase complex, but not the export apparatus or any secreted substrate.

(A) Fluorescence microscopy pictures of bacteria expressing EGFP–YscQ combined with deletions of different genes. Micrographs were taken 3 h after induction of the T3S system. (For the control strains and the strains with deletions in the proteins required for C ring formation—upper lane: EGFP fluorescence, lower lane: corresponding DIC picture). Scale bars: 2 µm. **(B)** Schematic representation of the injectisome showing the components required (bold, dark) and not required (normal, light) for C ring formation. For information about the used strains, refer to Table II.

3.5. ATPase assembly not only requires the presence of the YscCDJ platform, but also needs YscK, YscL, and YscQ

Finally, assembly of the ATPase YscN was tested. As replacement of the wild-type allele on the virulence plasmid by a gene encoding a fluorescent fusion protein decreased the expression of downstream genes in the virB operon, whereas a complete deletion of *yscN* was non-polar (Figure 3.1 B), *egfp–yscN* was cloned in a pBAD vector and used to complement *in trans* double deletions in *yscN* and several other genes. Induction of synthesis of EGFP–YscN with 0.05% arabinose led to YscN protein levels similar to the native level (Supplementary Figure 1), and to effector secretion at wild-type levels (data not shown). As shown in Figure 4, YscN assembly required the presence of YscC (secretin), YscJ (MS ring), YscK and YscL (two proteins known to interact with the ATPase), and YscQ (the C ring). In contrast, even the complete deletion of the IM export proteins YscR, S, T, U, V still allowed formation of YscN spots, albeit again in a reduced number (Figure 3.4).

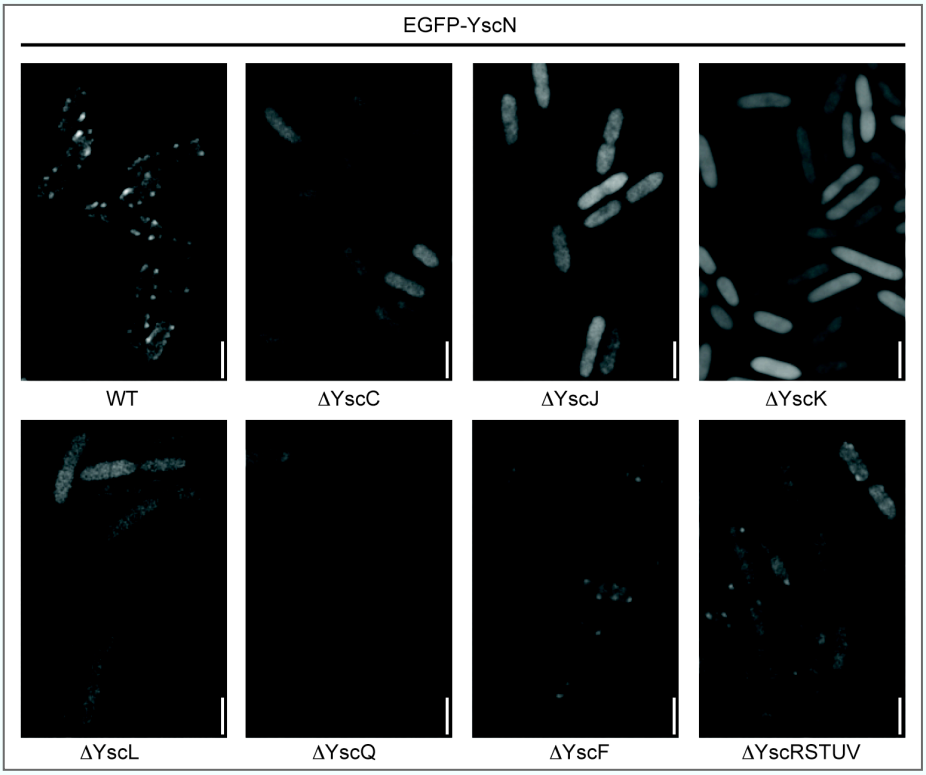

Figure 3.4: The assembly of the ATPase requires both transmembrane rings, YscK, YscL, and YscQ, but not the export apparatus.

Fluorescence microscopy pictures of YscN null mutants complemented with EGFP–YscN combined with deletions of different genes. Wild-type protein levels were established by EGFP–YscN induction with 0.05% arabinose. Micrographs were taken 3 h after induction of EGFP–YscN and the T3S system. Scale bars: 2 µm. For information about the used strains, refer to Table II.

These data suggest that the cytosolic components of the injectisome form a single large ATPase–C ring complex, requiring all of its components YscK, L, N, Q to assemble.

In agreement with the essential function of YscQ for the ATPase assembly, we did not observe any needle formation in strains that lack YscQ, but overexpress YscN, in contrast to recent results obtained with the flagellum (Konishi *et al.*, 2009) (data not shown).

3.6. ATPase activity of YscN is not required for the assembly of the ATPase–C ring complex at the injectisome

To determine whether assembly of the C ring requires YscN for its ATPase activity or as a structural component, a deletion of *yscN* in an *egfp–yscQ* background was examined. As expected, the resulting strain secreted neither Yops nor the ruler and needle subunits. Secretion could be complemented in trans by a wild-type *yscN* allele, but not by an *yscN* allele encoding $YscN_{K175E}$ altered in the Walker box (Figure 3.5 B, C).

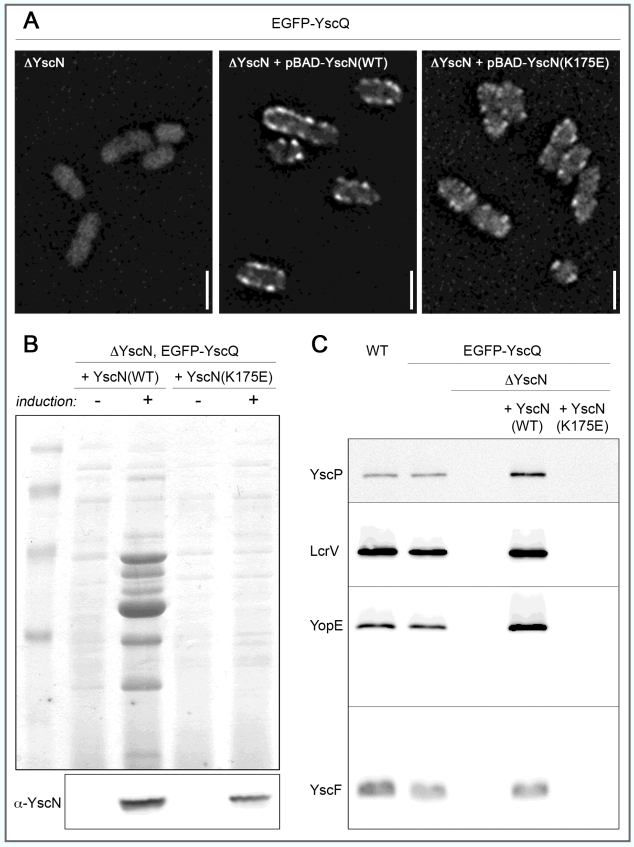

Figure 3.5: The structure, but not the ATPase activity of YscN, is required for the formation of the C ring.

(A) Fluorescence microscopy showing the formation of C ring spots in AD4104 [EGFP–YscQ, ΔYscN], complemented with plasmids encoding wild-type YscN or the catalytically inactive YscN(K175E), 3 h after induction of the type III secretion system. Scale bars: 2 µm. **(B)** Upper part: Analysis of Yop protein secretion in strain AD4104 complemented with wild type, or catalytically inactive YscN. Expression of YscN was either not induced (–) or induced with 0.05% arabinose (+). Culture supernatants were separated on a 12% SDS–PAGE gel and stained with Coomassie Brilliant Blue. Lower part: Expression of YscN in the corresponding strains. Cell pellets were separated on a 12% SDS–PAGE gel and analyzed by immunoblot with anti-YscN antibodies. **(C)** Export of different classes of substrates in strains expressing EGFP–YscQ, and the different YscN variants. Culture supernatants were separated on a 15% SDS–PAGE gel and analyzed by immunoblot with the respective antibodies.

Interestingly, however, although $YscN_{K175E}$ was not functional, it did restore the formation of the C ring spots (Figure 3.5 A), implying that the YscN requirement for the formation of the ATPase–C ring complex is exclusively structural.

3.7. After assembly of the ATPase–C ring complex, needle formation and effector secretion take place rapidly

The kinetics of C ring formation in a strain expressing EGFP–YscQ was followed in a time-course experiment. Pictures were taken every 20 min up to 2 h after induction of the ysc-yop regulon (Cornelis *et al.*, 1989) in a Ca^{2+}-depleted medium. Weak diffuse cytoplasmic fluorescence could be observed 20 and 40 min after the temperature shift, suggesting that synthesis of YscQ was turned on directly after the shift, and that EGFP folds rapidly in the

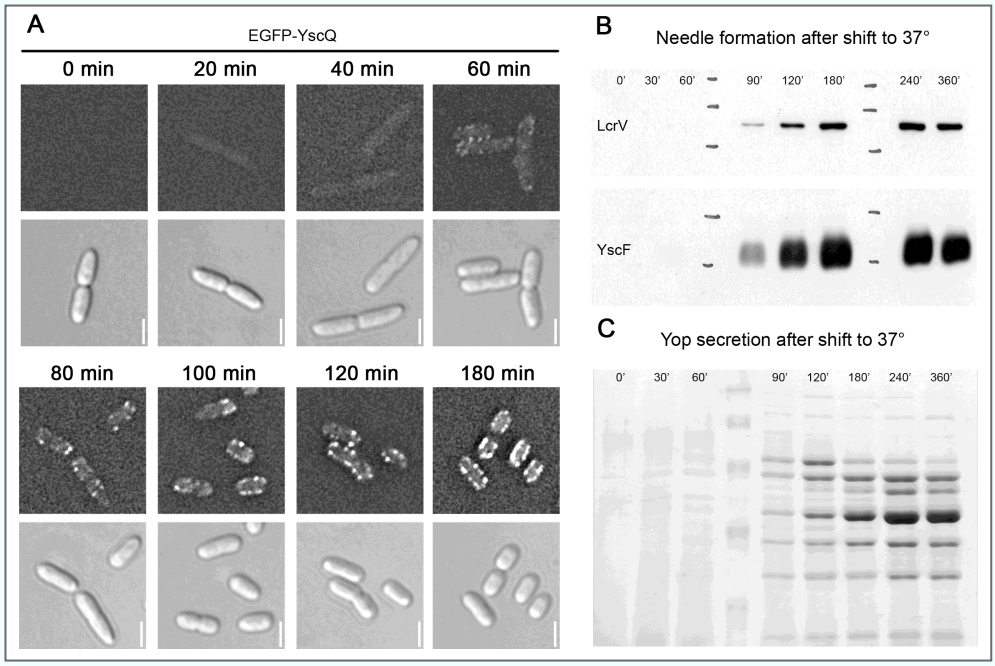

Figure 3.6: Formation of the C ring occurs about 60 min after induction of the T3S system. It directly precedes needle formation and effector secretion.

(A) Fluorescence microscopy showing the formation of C ring spots [EGFP–YscQ] in strain AD4016 at various time points after induction of the synthesis of the T3S system by temperature shift to 37°C (upper lane: EGFP fluorescence; lower lane: corresponding DIC picture). Scale bars: 2 µm. **(B)** Time course of needle formation in wild-type strain MRS40. Needle formation was monitored by SDS–PAGE analysis of purified needles. The needle pellet was separated on a 15% gel and analyzed by immunoblot with anti-LcrV and anti-YscF antibodies, respectively. **(C)** Time course of Yop protein secretion by wild-type strain MRS40. Culture supernatants were separated on a 12% SDS–PAGE gel and stained with Coomassie Brilliant Blue. All time-course experiments were performed in secretion-permissive conditions (Ca^{2+}-depleted medium).

Yersinia cytosol (Figure 3.6 A). The rapid synthesis of YscQ was also confirmed by immunoblotting (data not shown). The first membrane spots could, however, only be observed 60 min after induction. Although the fluorescence intensity of single spots seemed to increase over time, the number of spots stayed roughly constant up to 3 h after induction (Figure 3.6 A). Interestingly, the timeframe of appearance of the C ring was approximately the same as the timeframe of appearance of the needles (Figure 3.6 B) and secretion of the effector proteins (Figure 3.6 C), suggesting that needle formation and effector secretion occur within a short time after establishment of the ATPase–C ring complex. A model of injectisome assembly that incorporates the above mentioned results is depicted in Figure 3.7.

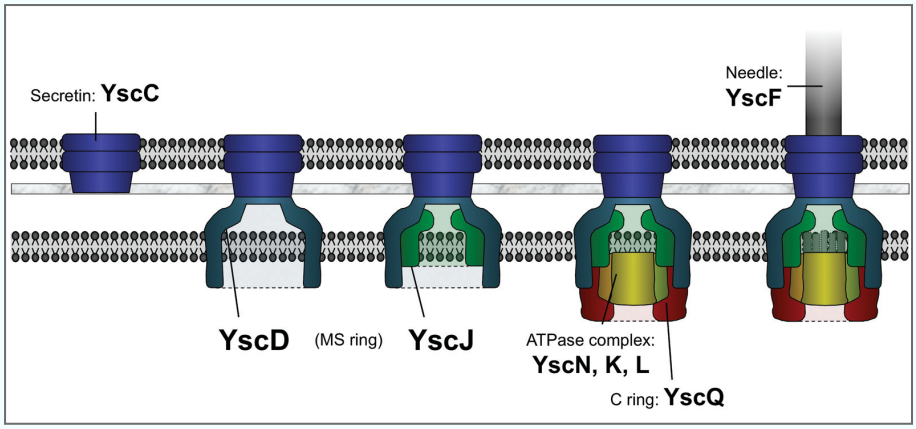

Figure 3.7: Model of assembly of the *Yersinia* injectisome.

Formation of the injectisome is initiated by formation of the secretin ring in the outer membrane. Next, YscD attaches to YscC, which allows the subsequent completion of the MS ring by attachment of YscJ. After the formation of the membrane ring structures, the ATPase–C ring complex, consisting of YscN, K, L, and Q assembles at the cytoplasmic side of the injectisome. The exact time point of the integration of the IM proteins YscR, S, T, U, and V is unclear. Afterwards, the needle consisting of YscF and LcrV can be assembled. Bold font denotes protein names, normal font denotes functional subunits. The global structure of YscC, D, J is derived from Spreter *et al.* (2009).

3.8. Discussion

The assembly of the T3S injectisome is a complex process that engages >20 different proteins, and results in the formation of a nanomachine spanning both bacterial membranes and protruding outside the bacterium. So far, little is known about this process. On the basis of the observation that heterologously overexpressed *S. enterica* MS ring components PrgH and PrgK form large rings in the absence of any other T3S component, a model was proposed (Kimbrough and Miller, 2002) in which the IM ring assembles first, and then fuses with the secretin ring in the OM. This model suggests the same general assembly scheme as the one that has been proposed for the flagellum (Kubori *et al.*, 1997; Macnab, 2003), but does not explain how the two membrane rings find each other. The subsequent steps of assembly could not be examined so far.

To gain better insight into the assembly process and the functional relations between the proteins, we constructed strains in which a number of injectisome constituents were fused to fluorescent proteins. To minimize artefacts because of non-native expression levels or timing of the fusion proteins, we replaced the wild-type allele on the pYV virulence plasmid by the hybrid allele in the case of *yscC*, *yscD*, and *yscQ*. The hybrid *yscN* was plasmid borne, but it was expressed at wild-type level.

All recombinant injectisomes were functional, and in all cases, fluorescent spots appeared at the bacterial membrane, distributed all over the bacterial body. Colocalization of the fluorophores confirmed that the fluorescent spots correspond to injectisomes. The brightness of the spots likely results from the multimeric nature of the tagged proteins, although at this stage, one cannot conclude that each spot corresponds to only one injectisome. A fluorescence quantification based on external standards, presently in progress, will address this question.

We observed that the membrane ring-forming proteins YscC, YscD, and YscJ are required for assembly of any cytosolic structure. Importantly, by monitoring the formation of YscC–mCherry and EGFP–YscD spots, we observed that YscC assembles independently of YscD and YscJ and that YscD assembles independently of YscJ, but not of YscC. Co-immunoprecipitation assays confirmed that YscJ requires YscD to become attached to YscC. All this implies that the assembly of the injectisome is initiated by formation of the secretin ring in the OM and proceeds inwards through stepwise assembly of YscD and YscJ. These data contradict the earlier report that PrgH and PrgK, the *Salmonella* homologues of YscD

and YscJ, can form a ring alone (Kimbrough and Miller, 2000). The discrepancy might result from the fact that the earlier study was based on heterologously overexpressed proteins, whereas this study is based on functional proteins produced in their natural environment at native expression levels. These data are also at odd with the report indicating that MxiD and MxiJ, the *Shigella* homologues of YscC and YscJ, interact even in the absence of the connector (Schuch and Maurelli, 2001). However, this interaction was observed in the absence of the pilot protein. In this case, the majority of secretin proteins are mislocalized to the IM (Koster *et al.*, 1997), which might lead to non-native interaction with MxiJ. Interestingly, it was shown recently that the assembly of two ring-forming IM components of the *Vibrio cholerae* type II secretion complex also depends on the presence of the OM secretin (Lybarger *et al.*, 2009), suggesting conservation or convergent evolution of the formation process in these two prokaryotic export systems. Taken together, our results show that the order of assembly of the OM and IM rings differs between the injectisome and the flagellum. We do not see any obvious reason for this, but this observation indicates that the two nanomachines differ more than is often thought. The flagellum is indeed significantly more complex than the injectisome because it rotates, which implies not only a motor but also bushings in the peptidoglycan and the OM. The P and L rings, having this function, are precisely replaced by a very stable secretin ring in the injectisome. This basic structural difference might explain the different order of assembly of the two nanomachines.

The outside-in assembly order consistently shown by co-immunoprecipitation and fluorescence microscopy further implies that YscD is the connector between the two membrane rings, which is coherent with recent crystal structure and modeling data (Spreter *et al.*, 2009). Our biochemical data allow to assess the recent models to integrate the crystal structures of the membrane ring proteins into the overall shape generated by electron microscopy averaging of purified injectisomes (Hodgkinson *et al.*, 2009; Spreter *et al.*, 2009). The electron density between the membranes would be generated by YscD. This in turn places YscJ in the IM, as proposed by manual fits (Moraes *et al.*, 2008; Hodgkinson *et al.*, 2009; Spreter *et al.*, 2009), but not by the best automated fit (Hodgkinson *et al.*, 2009).

After assembly of the OM and IM membrane rings, cytosolic components can assemble onto the structure. The observation that the proposed C ring component YscQ assembles in membrane spots colocalizing with the other components shows that the C ring is an integral component of the injectisome, confirming an assumption so far mainly based on immunogold-labeling experiments (Morita-Ishihara *et al.*, 2005). Our data indicate that a

large cytosolic complex consisting of the ATPase YscN, the two interacting proteins YscK and YscL, and the C ring component YscQ is formed, requiring all of its components, but not the ATPase activity of YscN for assembly. This differs again from the situation in the flagellum. There, FliM, FliN, and FliG (together forming the C ring) appear in significant amount in the membrane fraction in the presence of FliF (MS ring), but in the absence of FliI (ATPase) or FliH (homologue to YscL). This suggests that the flagellar C ring forms in the absence of the ATPase complex (Kubori *et al.*, 1997), in agreement with the observation that it forms on overexpression of FliM, FliN, and FliG together with FliF (Lux *et al.*, 2000; Young *et al.*, 2003). Although the heterologous overexpression of the proteins in these studies might account for the different observations, these results can also be the consequence of functional differences between the two nanomachines. As the constraint of rotation and spatial separation of the C ring and ATPase does not exist for the injectisome, the apparatus could be optimized for secretion. A tighter contact between the ATPase complex and the C ring might be a consequence of this optimization. The fact that we could not overcome the requirement of YscQ for secretion by overexpression of the ATPase is consistent with the essential function of YscQ for assembly of the complete ATPase–C ring complex.

Our results are also in perfect agreement with earlier results showing interactions between YscK, YscL, YscN, and YscQ (Jackson and Plano, 2000). However, the hypothesis that YscQ recruits the ATPase should be revised: YscK, L, N, and Q would rather assemble in one step. The proposed function of YscL as a negative regulator of ATPase activity (Blaylock *et al.*, 2006) as well as its direct interaction with YscN and YscQ (Jackson and Plano, 2000) is consistent with the presence of YscL in this complex. Less is known about the function of YscK. As it interacts with YscQ, but not with YscN and weakly at the most with YscL (Jackson and Plano, 2000; Blaylock *et al.*, 2006), it might act at the interface of the ATPase–C ring complex.

Formation and assembly of the ATPase–C ring complex did not depend on any of the five proteins forming the export apparatus, even though the number of membrane spots was reduced when YscR, YscS, YscV, or the five proteins YscRSTUV were missing. This implies that a YscKLNQ complex docks onto the IM ring rather than onto the export apparatus, which agrees with the observations made with the flagellum (Kubori *et al.*, 1997). As currently, little is known about stoichiometry, localization, and function of the export apparatus, its function in the assembly process remains unclear.

In conclusion, this work shows that the assembly of the injectisome starts with the formation of the stable secretin ring in the OM, and proceeds inwards through discrete attachment steps of YscD and YscJ at the IM. Afterwards, the components of the cytosolic ATPase–C ring complex assemble at the cytosolic side of the injectisome in one step, which allows the subsequent fast steps leading to needle formation and effector secretion.

3.9. Supplementary Figures

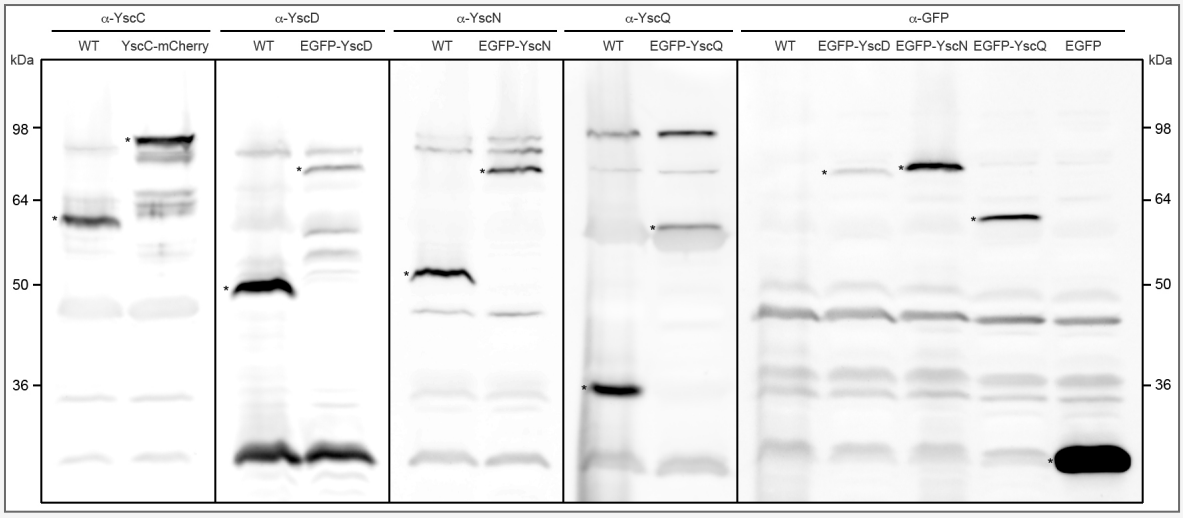

Supplementary Figure 1: Stability of the fluorescent fusion proteins

Total cells incubated for 3 hours at 37° in non-secretion-permissive conditions were separated on a 12% SDS-PAGE gel and subsequently analyzed by immunoblot with the specific antibodies, and with a anti-GFP antibody (polyclonal rabbit, Torrey Pines Biolabs, Houston, TX, USA). WT: MRS40; YscC-mCherry: MA4005; EGFP-YscD: AD4050; EGFP-YscN (ΔYscN + pBAD-*egfp-yscN*): AD4136(pAD182); EGFP-YscQ: AD4016; EGFP (pBAD-*egfp*): MRS40(pISO101). All fusion proteins except for EGFP-YscN are encoded under their native promoter on the pYV virulence plasmid (see Material and Methods for details).

The theoretical expected molecular weight for the wild-type and fluorescent fusion protein, respectively, are: YscC: 67.2 kDa / 97.1 kDa; YscD: 46.8 kDa / 75.9 kDa; YscN: 47.8 kDa / 77.5 kDa; YscQ: 34.4 kDa / 62.8 kDa; EGFP: 26.9 kDa. The corresponding bands are marked by asterisks.

YscC-mCherry could not be detected by the GFP antibody.

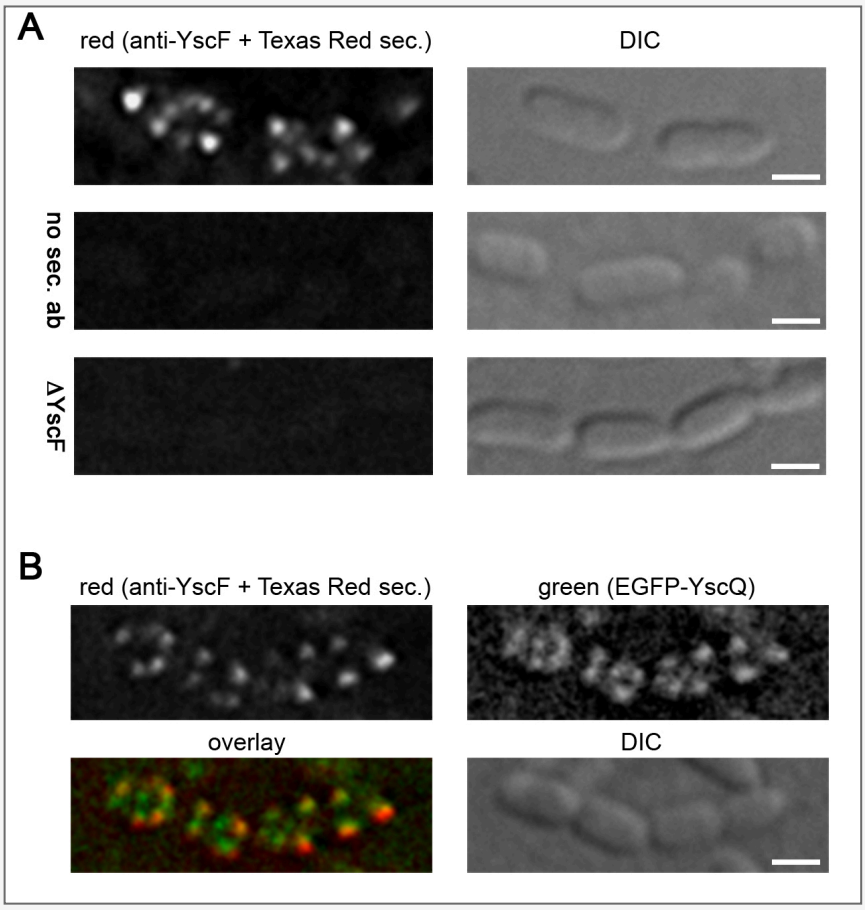

Supplementary Figure 2: Colocalization of the needle subunit YscF with the C ring component YscQ.

A: Immunofluorescence staining of the needle component YscF. First row: AD4016 bacteria [EGFP-YscQ]; second row: AD4016 bacteria, no secondary antibody; third row: AD4020 bacteria [EGFP-YscQ, ΔYscF].

B: Fluorescence deconvolution microscopy showing the co-localization of EGFP-YscQ with YscF, visualized by immunofluorescence, in AD4016 bacteria. Sharpness and intensity of the EGFP-YscQ foci are decreased due to the immunofluorescence treatment.

All strains were incubated in secretion-non-permissive medium (BHI + Ca^{2+}). Micrographs are shown in the z layer corresponding to the centre of the bacterium. Scale bars: 2 µm.

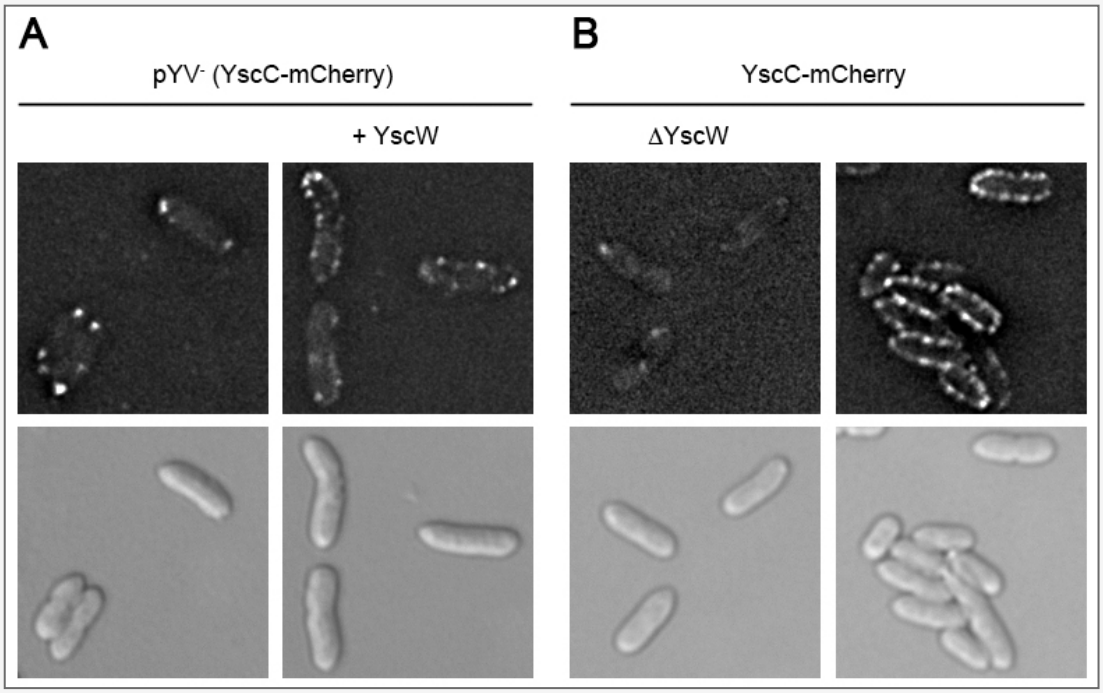

Supplementary Figure 3: YscC-mCherry aggregates in polar spots in the absence of the pilotin YscW.

Fluorescence deconvolution microscopy showing the formation of fluorescent YscC-mCherry spots at the bacterial membrane of *Y. enterocolitica* incubated in secretion-non-permissive medium (BHI + Ca^{2+}).

A: pYV^- bacteria expressing either only YscC-mCherry from expression vector pMA8 (left side) or YscC-mCherry together with YscW from expression vectors pMA8 and pRS6 (right side). Synthesis of YscC-mCherry was induced by the addition of 0.05% arabinose, while YscW was consitutively expressed.

B: Bacteria expressing the full T3S machinery with YscC-mCherry either in the absence of YscW (ADMA22784, left side) or in its presence (MAAD4006, right side).

Upper lane: mCherry fluorescence; lower lane: corresponding DIC picture.

3.10. Extended discussion

In a manuscript published after the submission of the preceding study, Schraidt *et al.* (2010) describe the topology and organization of *Salmonella* SPI-1 needle complex components. Interestingly, they present electron micrographs of needle complexes that have been purified from strain SB1171, which is mutated in the secretin InvG. The presence of NCs is surprising, and at odds with our results for the assembly of the *Yersinia* injectisome as well as with previously published results for the same strain. SB1171 carries a 500 bp frame-shift deletion after amino acid 84 of *invG* (Kaniga *et al.*, 1994), and had been shown by Sukhan *et al.* (2001) to be defective for NC base formation and needle formation. Low amounts of PrgH (YscD), but no PrgK (YscJ) could be purified from this strain in NC preparations (Sukhan *et al.*, 2001). While no obvious changes in the NC purification protocol were given that would explain the differences to the observations of Sukhan *et al.*, Schraidt *et al.* increased the culture volume for SB1171 to 18 L (as compared to 2 L for all other strains) to obtain needle complexes.

In *Yersinia*, absolutely no export of needle subunits was detected in strains lacking the secretin (own unpublished data), in agreement with the observation that the assembly of the MS ring and the interaction of its components YscD and YscJ categorically require YscC (Figure 3.2). Likewise, in *Shigella*, no interaction between the MS ring components MxiG and MxiJ could be observed in the absence of the secretin MxiD (S. Lea, personal communication). There are two possible explanations for the different behavior of the MS ring subcomplexes in *Salmonella* SB1171. On one side, it would be possible that assembly of the MS ring and subsequent needle formation are assisted by the truncated InvG that is still expressed in this strain. This would agree with the observations that (i) the remaining N terminus of InvG contains the domain that interacts with PrgH (Spreter *et al.*, 2009; Schraidt *et al.*, 2010), and (ii) only the N-terminal secretin part is required for type III secretion, as Burghout *et al.* (2004a) showed that deletions at the C terminus of YscC[7] did not abolish its function. This hypothesis could be tested by the analysis of needle formation in complete deletions of *invG* in *Salmonella* or in strains only expressing the equivalent domain of YscC in *Yersinia*.

[7] The C-terminal truncations studied in this manuscript were significantly smaller (up to 100 amino acids) than the proposed deletion described for strain SB1171.

On the other side, in all proposed assembly models, including the one presented in our study, the sequence of events is dictated by protein affinities rather than by functional requirements[8], especially as all proteins are present at the same time (see chapter 4.2). Interestingly, precisely YscD, the connector between the ring subunits, is only weakly conserved within T3S systems. The resulting different affinities between the ring-forming proteins in different systems could cause that in *Salmonella*, the secretin might not be absolutely required for formation of the somewhat stable PrgH/K MS ring. Along these lines, ring structures could be observed in the absence of secretins upon heterologous overexpression of PrgH and PrgK (Kimbrough and Miller, 2000), and the secretin ring could be mechanically removed from *Salmonella* NCs (Kimbrough and Miller, 2002), leaving structures that were similar to the ones observed for strain SB1171. In contrast, in *Yersinia* (and probably *Shigella*), the secretin is mandatory for the interaction between the MS ring proteins, as has been shown in our study, leading to a strict outside-in assembly order.

[8] The outside-in assembly order proposed in our study additionally involves a penetration of the peptidoglycan layer in the first assembly step, by the formation of the secretin ring, which could facilitate the attachment of subsequent components. Intriguingly, the *Salmonella* SPI-1 system encodes for the lytic transglycolase IagB (Miras *et al.*, 1995) that circumvents this problem, whereas the *Yersinia* Ysc system is one of the few T3S systems that has no dedicated transglycosylase (Koraimann, 2003).

Chapter 4

Supplementary results

4.1. Summary

4.1.1. Regulation of expression and function of the *Yersinia* type III secretion system

Because there was conflicting evidence in the literature, we systematically followed the expression levels of the components of the injectisome, as well as needle formation and effector secretion, over time and under different conditions.

On the level of protein expression and stability, we did not detect differential regulation, as all proteins were expressed at the same time and reacted similarly to external stimuli.

However, we discovered that after transient activation of effector secretion, the bacteria were able to efficiently shut down type III secretion upon changes in the surrounding medium. Interestingly, cessation of needle formation and of effector secretion were controlled by different pathways in this case, as the two events were influenced differently by external cues. While these novel regulation mechanisms were not yet studied in further detail, they indicate that activation and deactivation of the injectisome are controlled events *in vivo*, which allows the bacteria to modulate their response according to the specific requirements.

4.1.2. Kinetics and dynamics of the *Yersinia* type III secretion system

Beyond the determination of the assembly order of the injectisome, the functional fluorescent injectisome components were used to measure the kinetics of the assembly and the dynamics of the cytosolic subunits.

We could show that formation of the injectisome, in contrast to its function in effector translocation, is a slow process. With a combination of microscopy time courses and pre-induction experiments, we determined that attachment of YscD to the secretin ring, possibly in combination with YscC translocation to the OM, is the rate-limiting step in injectisome assembly, while all subsequent steps occur within short time.

Moreover, we demonstrated by photobleaching that the C ring is unlikely to be involved in substrate shuttling, but its subunits can be exchanged within minutes, suggesting a rather dynamic structure of the cytosolic complex.

4.1.3. Purification of subcomplexes of the injectisome

The purification of subcomplexes of the *Yersinia* injectisome required substantial changes of the protocol used in other organisms. The conditions for crosslinking, spheroplast generation and cell lysis were optimized, and the adhesin YadA was removed from all strains.

Co-immunoprecipitation of affinity-tagged injectisome components demonstrated that the membrane ring-forming proteins stably interact with each other. Both the needle subunit YscF and the inner membrane export machinery component YscV could be detected in the purified fractions in substoichiometric amounts. In contrast, the interactions between the membrane rings and the cytosolic components seem to be too weak to be detected by this approach, as has also been shown for other type III secretion systems.

4.1.4. The type III secretion “inner membrane export machinery”

YscR, S, T, U, V are five conserved essential components of type III secretion systems, which are thought to form the “export machinery” within the inner membrane. The exact localization, stoichiometry, and function of the proteins are unknown.

We found that YscV, the largest of the five proteins, harboring a 40 kDa cytosolic domain, seems to play a specific role within this protein group. It has to be induced with significantly higher arabinose levels than its partners to complement the respective mutant strains, its cytosolic domain forms multimers in solution, and it is the only component of the inner membrane export machinery for which a fluorescent variant leads to observable membrane spots.

Formation of YscV-EGFP foci at the cell periphery did not depend on the presence of the ATPase, suggesting that it is an independent event within the assembly. Interestingly, in a strain lacking the MS ring component YscJ, fluorescent spots appeared, but were highly motile within the membrane, indicating that YscV is anchored (most likely in the peptidoglycan layer) by attachment to the MS ring, directly or via another protein.

The proposed oligomer formation of YscV would further imply a localization outside the MS ring, which has consequences for the model of function of the inner membrane export machinery.

4.2. Regulation of expression and function of the *Yersinia* type III secretion system

4.2.1. Promoter activity upon induction of type III secretion

Regulation of T3S is in large parts poorly understood. Besides the immediate scientific interest in the influence of external factors on assembly and function of the injectisome, we also wanted to find out whether certain conditions or alterations in the genes encoding the regulator proteins could be used to boost the expression levels of T3S proteins. To get a solid data base for subsequent experiments, we first systematically studied promoter activity and overall protein levels of different injectisome components under various conditions.

FACS analysis of *pVir* reporter strains shows uniform upregulation of T3S promoters upon temperature shift

Most structural components of the *Yersinia* type III secretion machinery are located in three operons on the pYV virulence plasmid (see Figure 1.5): The *virB* operon contains eight genes, *yscN* to *yscU*; *virC* contains eleven genes, *yscB* to *yscM1*; and the translocator operon encodes LcrG, LcrV, LcrH, YopB, and YopD (Michiels *et al.*, 1991; Lambert de Rouvroit *et al.*, 1992). The master regulator for T3S system gene transcription, also located on the pYV plasmid, is the transcription factor VirF (Lambert de Rouvroit *et al.*, 1992).

To assay the transcriptional activation of the three main operons and *virF* itself, four reporter plasmids were designed, each of which encodes for a triple GFP under the control of the promoters for *virF*, *virB*, *virC*, or the translocator operon. The activity of these promoters upon activation of the T3S by temperature increase to 37°C under secretion-permissive conditions was monitored by fluorescence activated cell sorting (FACS) analysis of the GFP fluorescence.

Upon activation of the system by temperature shift, which leads to expression of VirF, the constructs harboring the promoter regions of the three machinery operons showed a uniform increase in fluorescence (Figure 4.1). Interestingly, *pVirF* was not influenced by the temperature increase, as the fluorescence of the *pVirF::3gfp* strain was even slightly below the start level after 4 hours at 37°C. This suggests that the remodeling of DNA structure that is thought to be responsible for the temperature dependence of VirF on the virulence plasmid did not affect the plasmid harboring the reporter construct.

In comparison to the control vector, the strains harboring the reporter constructs displayed increased fluorescence even before the temperature shift (Figure 4.1 B). While this might reflect a certain basal expression level, it could also be caused by transcriptional leakage of the reporter constructs. However, an increase in fluorescence could be observed from 30 minutes after the temperature shift on[9]. Afterwards, the GFP level steadily increased in a similar fashion for all three machinery operons, leading to a roughly three-fold higher fluorescence after 4 hours for all three strains. This shows that they are affected by VirF in a very similar manner.

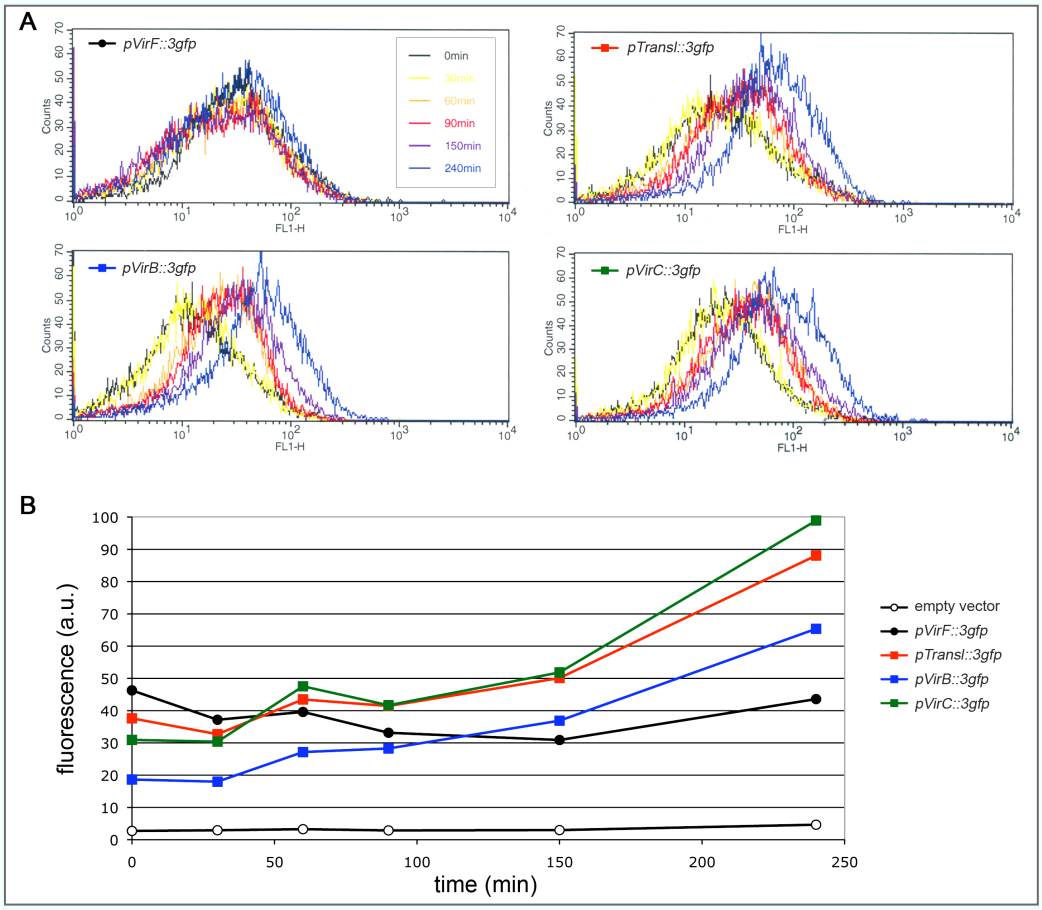

Figure 4.1: Promoter activity of the operons encoding for injectisome subunits develops similarly over time.

A: FACS analysis of strains harboring the reporter constructs pAD123, pAD124, pAD125, or pAD126 (*pVirF::3gfp*, *pTransl::3gfp*, *pVirB::3gfp*, or *pVirC::3gfp*, respectively), as indicated. Fluorescence was measured before T3S induction by temperature shift to 37° (0 min) and at the given time points afterwards. **B**: Temporal development of the mean fluorescence in the strains listed in A.

[9] GFP expression and folding requires some time, which might lead to a lag of the read-out in our experimental setup. However, other results (see chapter 3, Figure 3.6) indicate that GFP is expressed and folded within relatively short time in the *Y. enterocolitica* cytosol.

These data suggest that the assembly of the T3S injectisome is not regulated by different temporal expression profiles of the operons encoding for the components of the injectisome.

4.2.2. Effect of the transcription factor VirF, the negative regulators YscM1 and YscM2, and the extracellular calcium concentration on protein expression and needle formation

In trans induction of VirF leads to a fast increase in T3S protein expression, but does not yield higher final amounts of T3S components

To study how expression levels of the transcription factor VirF and the downstream T3S proteins evolve over time, and whether the amount of injectisome components could be increased by expression of VirF from an inducible promoter, a strain lacking VirF (AD4006) was generated and complemented for VirF expression *in trans* by plasmid pCL5, expressing *virF* under the control of the tac promoter (Lambert de Rouvroit *et al.*, 1992).

The experiment was performed under secretion-permissive conditions. While the level of plasmid-borne VirF showed a fast increase up to 60 minutes after induction, it stayed constant or even slightly decreased afterwards. In contrast, the level of endogenous VirF in the wild-type strain MRS40 showed a sigmoid increase with the steepest slope from 60 to 120 minutes after induction. The protein level of the injectisome component YscF, expressed under VirF promoter control, developed in a very similar way (Figure 4.2). The ratio YscF/VirF was significantly higher, when VirF was expressed endogenously. The reason for this is unclear.

The results show that VirF expression *in trans* leads to faster expression, but not to increased final levels of injectisome components under secretion-permissive conditions (Figure 4.2). In secretion-non-permissive conditions, it only leads to a weak increase in protein levels (data not shown). Expression of VirF *in trans* is therefore not suited to increase the amount of injectisome components under these conditions and was not applied in further experiments.

Removal of the negative regulators YscM1/M2 does not significantly influence kinetics or amount of T3S protein expression

As the negative regulators YscM1 and YscM2 have been shown to downregulate expression levels of the T3S proteins (Stainier *et al.*, 1998), we generated a strain lacking VirF and both negative regulators (AD22705) and tested it under the same conditions.

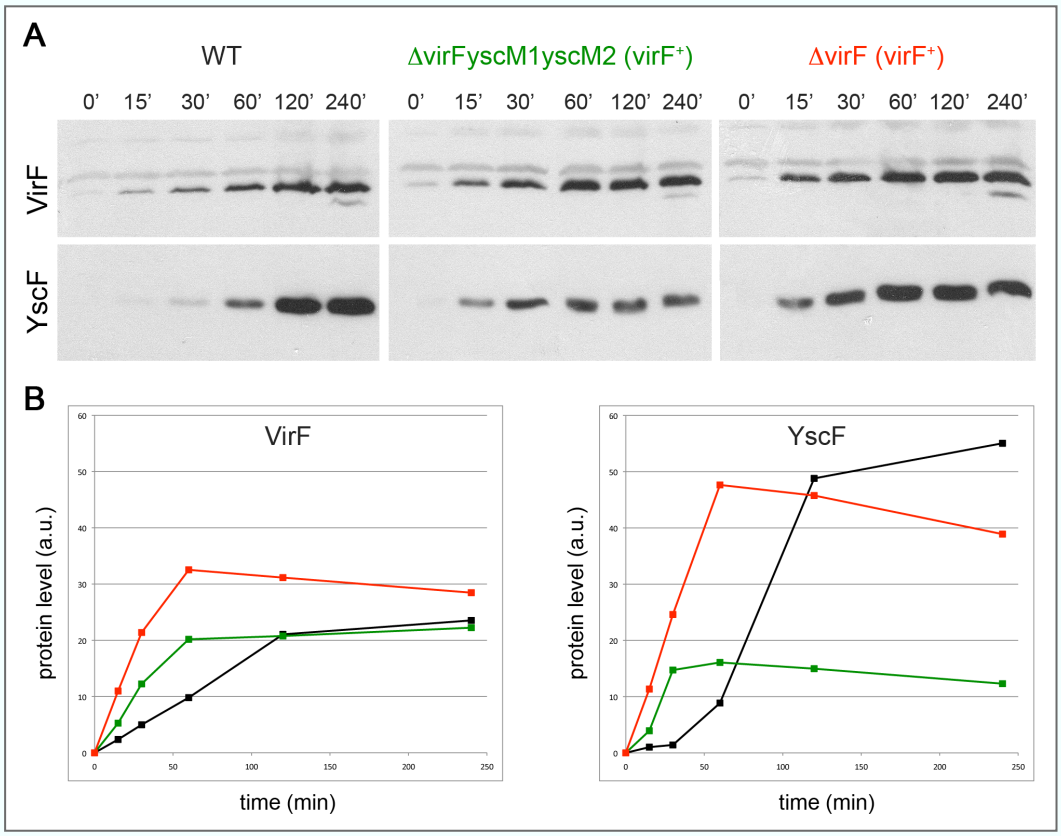

Figure 4.2: YscF is expressed faster, but not in a higher final amount, when VirF is expressed *in trans*. Lack of the negative regulators does not increase the YscF level.

A: Immunoblot analysis of the amount of the transcription factor VirF and the needle subunit YscF in secretion-permissive conditions (BHI-Ox). Samples were taken at different time points after induction of T3S and VirF in strains MRS40 (WT), AD22705(pCL5) [*ΔvirFyscM1yscM2*, *virF*$^{+}$] and AD4006(pCL5) [*ΔvirF*, *virF*$^{+}$]. **B**: Quantification of the temporal development of the protein amounts of VirF (left panel) and YscF (right panel). Black, MRS40; green, AD22705(pCL5); red, AD4006(pCL5).

It was obvious that the absence of the negative regulators YscM1 and YscM2 in strain AD22705(pCL5) did not change the expression kinetics compared to the respective control strain AD4006(pCL5), and importantly did not result in an increase in protein expression. On the contrary, the levels of VirF and YscF were even reduced (Figure 4.2). For this reason, strains lacking YscM1 and YscM2 were not used for further experiments.

Expression of different classes of T3S proteins and needle formation are similarly influenced by extracellular calcium concentrations

It has been previously reported that chelation of calcium ions in the medium at 37°C leads to a strong increase in the synthesis of effector and translocator proteins (Stainier *et al.*, 1998), as well as to an increase in the synthesis of machinery proteins (Allaoui *et al.*, 1995b). The effect of extracellular calcium concentration on the production of needles was reported to be even more pronounced (Müller *et al.*, 2005). However, despite anecdotal evidence for differential influence on different protein classes and needle formation, the impact of the external calcium level on the expression pattern of the injectisome components had never been systematically analyzed. To quantify the effect of extracellular calcium on expression levels, and to test whether different protein classes respond differently to changes in the extracellular calcium level, the protein levels of various T3S components covering different functional subunits were followed over time. Importantly, in these experiments, needle formation was monitored and quantified as well.

The results show (Figure 4.3) that the protein levels of all tested injectisome components, covering basal body proteins as well as needle components and the molecular ruler YscP, are influenced by the extracellular calcium level in a similar fashion. Three to four hours after the induction of the system by temperature increase to 37°C, cellular protein levels reached a plateau. At this time, the amount of total cellular proteins (Figure 4.3, marked in gray) in bacteria incubated in non-secretion-permissive conditions was at 40-60% of the amount in bacteria incubated in secretion-permissive conditions. Interestingly, needle formation (Figure 4.3, marked in green) also showed a two-fold increase only in secretion-permissive conditions, suggesting that the quantity of needle formation merely depends on the amount of basal body proteins. The lag of needle formation behind expression of YscF and LcrV indicates that formation of the injectisome is a relatively slow process, requiring about 60 minutes.

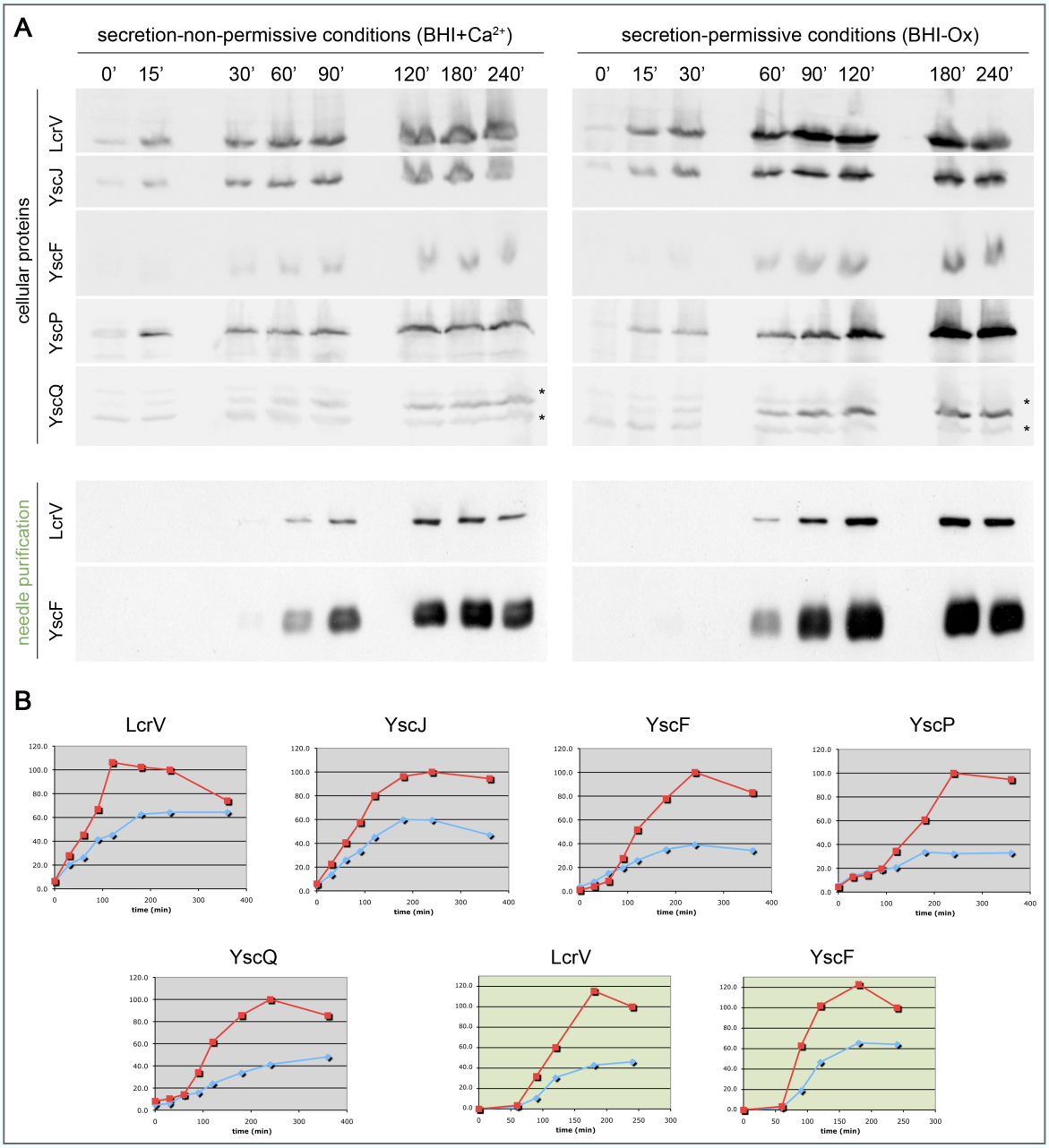

Figure 4.3: Cellular protein levels of various injectisome components and the amount of needles are similarly influenced by extracellular calcium levels and develop likewise over time.

A: Immunoblot time course analysis of protein amounts in the total cell fraction and in purified needles, under secretion-non-permissive conditions (BHI+Ca^{2+}, left side) and secretion-permissive conditions (BHI-Ox, right side). Asterisks denote unspecific bands in the immunoblot. **B**: Quantification of the immunoblot bands shown in A. The 240 min value in secretion-permissive conditions has been set as 100%. Background colours indicate cellular protein levels (gray) or purified needles (green). Blue lines, secretion-non-permissive conditions (BHI+Ca^{2+}); red lines, secretion-permissive conditions (BHI-Ox).

4.2.3. Needle formation and effector secretion are regulated differentially in response to extracellular cues

Downregulation of T3S after transient secretion is achieved by separate pathways in response to either temperature decrease for needle assembly or calcium addition for effector secretion

Experiments on the regulation of T3S mainly focus on the establishment of secretion upon changes in the environment. *In vivo*, however, the opposite case – transition to non-secretion-permissive conditions – is likely to be as important. Whether, and how, T3S is downregulated in these cases, is unknown. Therefore, in a series of experiments, the injectisome was first assembled under secretion-permissive conditions (37°C, BHI-Ox). Afterwards, the bacteria were subjected either to non-secretion-permissive conditions (BHI+Ca^{2+}), or to low temperature, and the effect on the secretion pattern was observed over time.

As Figure 4.4 A shows, bacteria that remained under secretion-permissive conditions (BHI-Ox) at 37°C continued to export effectors and translocators, even to a higher extent than before. Bacteria that remained in BHI-Ox, but were incubated at 26°C, continued to export effector proteins for at least three more hours, but seemed to stop the export of proteins required for needle formation (YscF, LcrV, YscP, YopB, YopD), suggesting that they did not assemble new needles. In contrast, bacteria that stayed at 37°C, but were incubated in non-secretion-permissive conditions (BHI+Ca^{2+}), rapidly stopped the export of effector proteins, but kept exporting the proteins required for needle formation.

To rule out that these effects were a mere consequence of the changes in cellular protein levels, immunoblot analysis of YscP, LcrV, YopE, and YscF was performed for cellular proteins (TC, Figure 4.4 B). The same was done for secreted proteins (SN, Figure 4.4 C), which allowed to verify the data of the previous experiments and to analyze the differences in export in more detail. As controls, cultures that were not pretreated ("initial cultures") were included. Samples were taken three hours after induction of the system, or change of the medium, respectively (see Material and methods for experimental details). The cellular protein levels of the tested components in the initial cultures (Figure 4.4 B, left side) showed that expression was turned on by the temperature shift to 37°C, and the extracellular calcium level had a comparably small effect (see chapter 4.2.2). Afterwards, the cellular proteins levels stayed surprisingly unaffected by changes in temperature or calcium concentration (Figure 4.4 B, right side), confirming that the cellular levels of T3S proteins are not subject to tight regulation by rapid degradation and resynthesis.

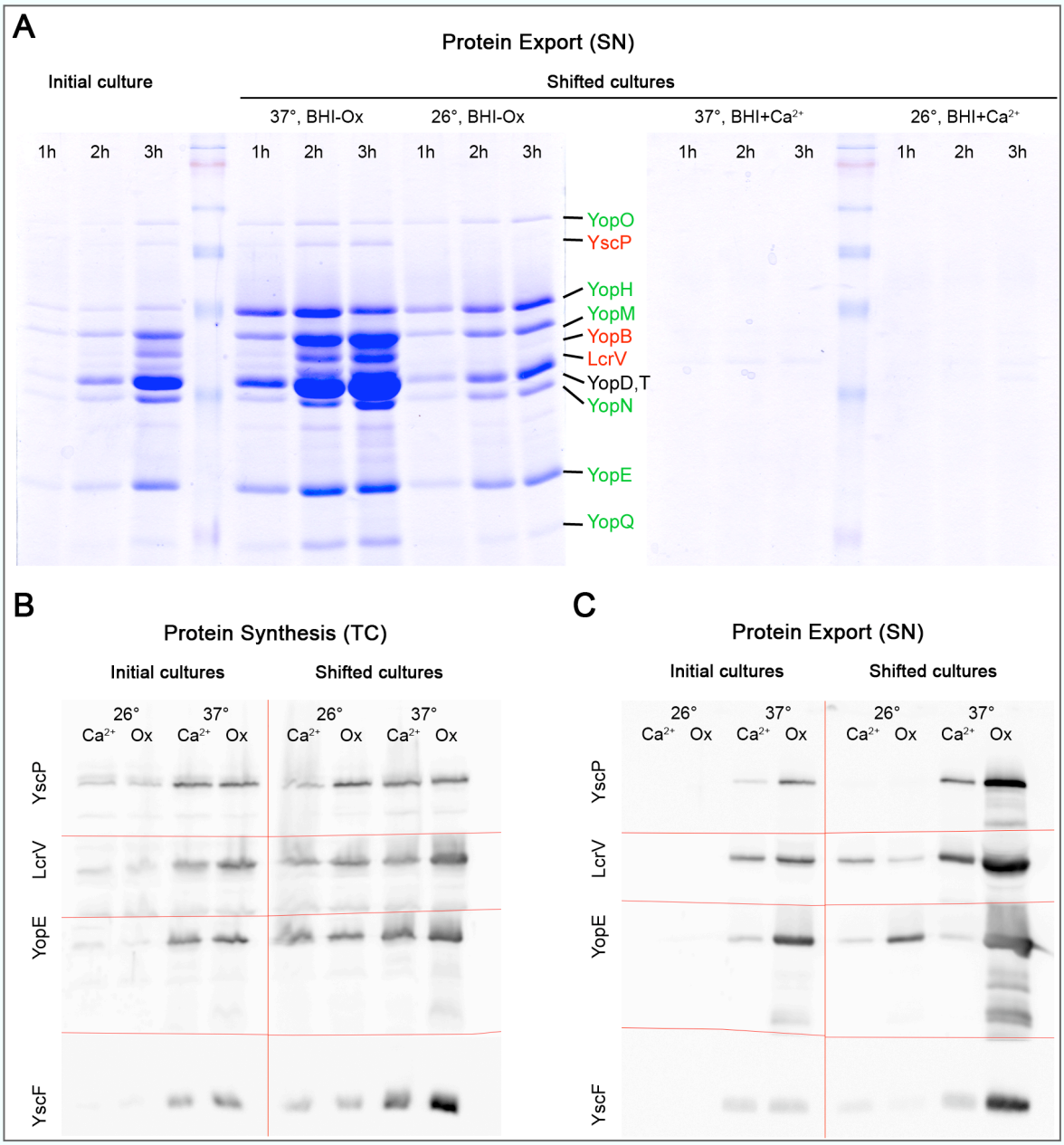

Figure 4.4: Export of proteins required for needle formation and effectors is regulated by different external stimuli, independently of the cellular protein levels

A: Time course of protein export (culture supernatant, SN) in the initial culture (37°, BHI-Ox) and the subsequently shifted cultures, as denoted. Proteins exported in BHI-Ox, irrespective of the temperature (effectors, see text) are printed in green font. Proteins exported at 37°, irrespective of the extracellular calcium level (translocators, see text) are printed in red font. The double band consisting of the translocator YopD and the effector YopT cannot be resolved in this gel and is printed in black font. **B**: Immunoblot analysis of protein synthesis (total cellular protein, TC) under the denoted conditions. **C**: Immunoblot analysis of protein export (culture supernatant, SN) under the denoted conditions. In all cases, the amount of loaded proteins has been normalized according to the OD_{600} of the culture. Red lines mark the borders of incubation with the respective antibodies.

In contrast, the export of proteins was highly dependent on extracellular conditions. The proteins required for needle formation (YscF, LcrV, YscP) were released both in BHI+Ca^{2+} and BHI-Ox (but strongly temperature dependent), whereas effectors (YopE) were released independently of the temperature, but were fully dependent on low extracellular calcium levels, after injectisomes had been functional once (Figure 4.4 A, C).

4.2.4. Discussion

Formation of the injectisome (Allaoui *et al.*, 1995b) and secretion of effector proteins (Stainier *et al.*, 1998) are the two controlled steps of type III secretion. In this study, we have systematically observed both events under various conditions.

As expected from the fact that transcription of the three main T3S operons depends on the presence of the transcription factor VirF (Michiels *et al.*, 1991; Lambert de Rouvroit *et al.*, 1992), it is induced simultaneously. Using reporter gene constructs, we could further show that afterwards, promoter activities of the operons develop in the same way (Figure 4.1). The analysis of protein levels showed that this is also directly reflected in the cellular amounts of T3S components. Injectisome subunits expressed from different operons and exerting different functions display the same temporal development. Their amount depends on the amount of VirF (Figure 4.2) and reacts similarly to external cues (two-fold increase of expression in secretion-permissive conditions, Figure 4.3). This argues against a control through differences in protein stability or specific degradation mechanisms. In conclusion, all components of the T3S system are present in a defined ratio over time. Importantly, we could show that the amount of needle formation also parallels the expression levels of T3S components (Figure 4.3). This clarifies that extracellular calcium has the same effect on the expression of all T3S components and the formation of needles (Allaoui *et al.*, 1995b; Stainier *et al.*, 1998; Müller *et al.*, 2005). The data also suggest that the number of injectisomes is similarly controlled by the extracellular calcium level, even though this could not be directly assayed.

Once expression has been turned on by temperature shift to 37°C, the protein levels for all tested T3S components stay remarkably unaffected by external influences (Figure 4.4 B). However, our results show for the first time that both the secretion of effectors and of components needed for needle assembly (YscF, LcrV, YopB, YopD, YscP) are tightly controlled and can be shut down quickly in response to changes in the environment (Figure 4.4 A, C). Importantly, effector secretion and needle assembly are regulated by two different mechanisms:

Effectors are continuously being exported once secretion has been established, as long as no Ca^{2+} is present in the medium. This finding also shows that injectisome function does not depend on temperature. However, addition of calcium blocks effector secretion within a short time, presumably through reassembly of the secretion plug. How the calcium level is sensed, how the signal is transferred, and how the fast plug assembly occurs mechanistically, remains unknown. In clear contrast to this, export of the components required for needle assembly strongly depends on the temperature, whereas the dependence on the calcium level is less pronounced. During the course of these studies, a similar differential effect of the calcium level on export has also been described for *P. aeruginosa* (Cisz *et al.*, 2008). However, our finding that export of the proteins needed for needle assembly (and, presumably, needle formation itself) only occurs at 37°C, despite the presence of the respective proteins even at lower temperatures, suggests an added regulation mechanism beyond the translational control, which prevents needle formation at low temperatures[10].

Taken together, we could show that needle formation and effector secretion are differently controlled by independent mechanisms that can be put back into function after their release. Type III secretion is therefore not a one-shot deal, but can be regulated both on the level of a single injectisome (by blocking effector secretion upon calcium addition) and on the cellular level (by halting *de novo* needle formation upon decreased temperature).

[10] If one needle is formed by each basal body, this temperature regulation mechnism could be exerted on any of the steps of injectisome assembly, not only on needle formation itself. However, as shown in the next chapter (Figure 4.11), assembly of YscC is not affected by low temperature, so that the regulation acts downstream of secretin ring formation.

4.3. Kinetics and dynamics of the *Yersinia* type III secretion system

4.3.1. Analysis of fluorescently labeled injectisome components

Choice of tags and functionality of tagged components

Fusions to fluorescent proteins are an excellent way to study protein localization and kinetics. However, fluorescent proteins are relatively large and in order to minimize the influence of the tag on protein localization and function, a suitable combination of fusion protein and site has to be found.

In the course of this study, we constructed various fusions to injectisome proteins, either with small affinity tags or with fluorescent proteins. Table III shows the fusion proteins that were tested and their influence on protein function.

Injectisome component	Function (location)	Fusion protein	Location of fusion	Strain name	Functionality
YscC	Secretin (OM)	mCherry (1)	C terminus	MA4005	+
YscD	MS ring (IM)	His_8-FLAG-X_8 (2)	N terminus	AD4049	+
		EGFP	N terminus	AD4050	(+)
YscJ	MS ring (IM)	Gly_4-FLAG-His_8	C terminus	AD40085	+
		FlAsH (3)	C terminus	AD4058	-
		EGFP	C terminus	AD40083	-
YscN	ATPase (cytosol) (4)	FLAG-His_8-X_8	N terminus	AD4136(pAD190)	+
		EGFP	N terminus	AD4136(pAD182)	+
		EGFP	C terminus	AD4136(pAD181)	-
YscQ	C ring (cytosol) (4)	His_8-FLAG-X_8	N terminus	AD4014	+
		EGFP	N terminus	AD4016	+
		mCherry	N terminus	CJC4003	+

(1): EGFP and mCherry are followed / preceded by an unspecific 6-12 amino acid linker from the multiple cloning site of the origin vector in all cases (see chapters 7.3 and 7.5 for details)
(2): The sequence of the flexible X_8 linker is GGAGGAGG
(3): The sequence of the FlAsH tetracysteine tag is FLNCCPGCCMEP (Tsien, 2005).
(4): membrane-associated

TABLE III: Fusions to proteins in the structural membrane rings and cytosolic components that were used in this study.

YscC-mCherry has been cloned and tested by M. Amstutz, mCherry-YscQ has been cloned and tested in cooperation with C. Cattin (Cattin, 2009).

All tags were introduced onto the pYV virulence plasmid by homologous recombination, leaving the hybrid genes in their original genetic environment under the native promoter. Fusions to *yscN* that were introduced this way caused a reduction in the expression of downstream genes (data not shown). Therefore, as an exception, a non-polar deletion in *yscN* was generated, which could be complemented with the fusion proteins *in trans*.

YscC has a predicted N-terminal sec signal sequence and is proposed to be anchored within the OM with its conserved C-terminal half. Most GFP derivatives do not fold properly in the periplasm due to the oxidizing conditions and subsequent non-native formation of a disulfide bridge (Feilmeier *et al.*, 2000). As the introduction of a red fluorophore additionally allowed the colocalization of components, mCherry was fused to the C terminus of YscC. To generate a non-polar mutant, the ribosome binding site of YscD had to be reinserted after the tag (M. Amstutz, unpublished data). YscC-mCherry was fully functional for secretion (see Figure 3.1).

YscD does not have a predicted signal sequence. The N terminus of YscD is predicted to be localized in the cytosol, thus allowing the fusion of EGFP. The functionality of EGFP-YscD was decreased. Most likely, this was due to steric clashes, as both the combination of EGFP-YscD with a deletion in YscJ, and the fusion of a small His_8-FLAG tag to YscD did not impede its assembly and function (Figure 3.2, see also chapter 4.4, Figure 4.17). During the course of this study, the *Shigella* homologue MxiG was shown to be functional with a small N-terminal tag as well (Zenk *et al.*, 2007).

YscJ is a mainly periplasmic lipoprotein with a predicted transmembrane helix at the extreme C terminus, which is followed by a short cytoplasmic domain of only four amino acids. As this transmembrane helix is absent in homologues of YscJ, including EscJ, we assumed that it is unlikely to be involved in protein-protein interactions, making it a suitable location for the fusion of proteins. However, large tags rendered YscJ non-functional, most likely due to steric problems, as small tags did not affect functionality (Figure 4.5). Surprisingly, introduction of a twelve amino acid tetracysteine tag (Tsien, 2005) completely abolished the function of YscJ for unknown reasons (data not shown).

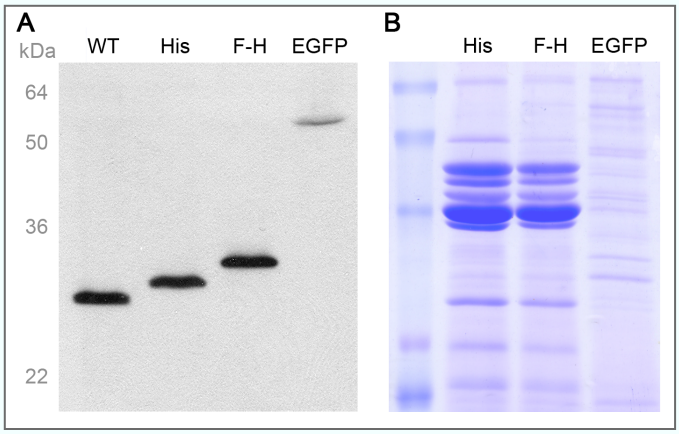

Figure 4.5: YscJ remains functional with small C-terminal tags.

A: Immunoblot with antibodies against YscJ, showing the size and expression level of WT YscJ (strain MRS40, "WT"), YscJ-Gly_4-His_8 (AD40082, "His"), YscJ-Gly_4-FLAG-His_8 (AD40085, "F-H"), and YscJ-EGFP (AD40083, "EGFP"). **B**: *In vitro* secretion of the tagged strains.

YscN, as a cytosolic protein, does not have a signal sequence. For this reason, EGFP was fused both to the N terminus and to the C terminus. The C terminal fusion was less stable and non-functional (Figure 4.6), whereas EGFP-YscN complemented the deletion and showed expression levels in the WT range (data not shown) when induced with 0.05% arabinose.

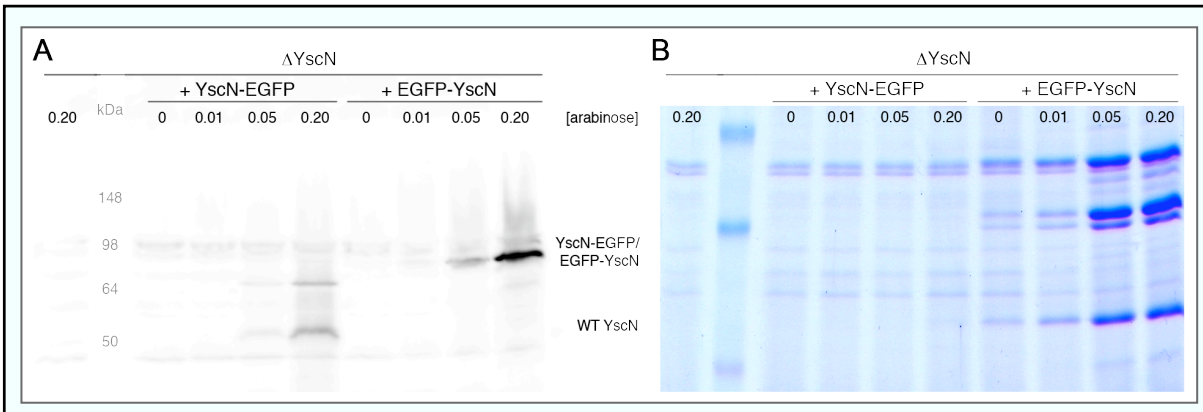

Figure 4.6: EGFP-YscN is functional, whereas YscN-EGFP is instable and non-functional.

A: Immunoblot with antibodies against YscN, showing the size and expression level of YscN-EGFP (strain AD4136(pAD181)) and EGFP-YscN (AD4136(pAD182)) at the given induction levels. **B**: *In vitro* secretion of the tagged strains.

YscQ, like YscN, does not have a signal sequence. As it had been successfully affinity-tagged for antibody production before, and remained functional with an N-terminal tag (I. Sorg, personal communication), the tags were fused to the N terminus. To facilitate colocalization with other components, both mCherry and EGFP were used as fluorophores. While all fusions of YscQ retained their functionality, mCherry-YscQ localization was less focused than EGFP-YscQ fluorescence (Cattin, 2009).

Assembly and colocalization of injectisome components are independent of temperature and extracellular calcium level and remain stable over time

As expected from the fact that the formation of EGFP-YscQ spots was not strongly influenced by extracellular calcium levels (Figure 3.1), neither the assembly of YscC-mCherry (M. Amstutz, unpublished data), nor of EGFP-YscD (Figure 4.7) showed a significant difference between secretion-permissive and non-permissive conditions.[11]

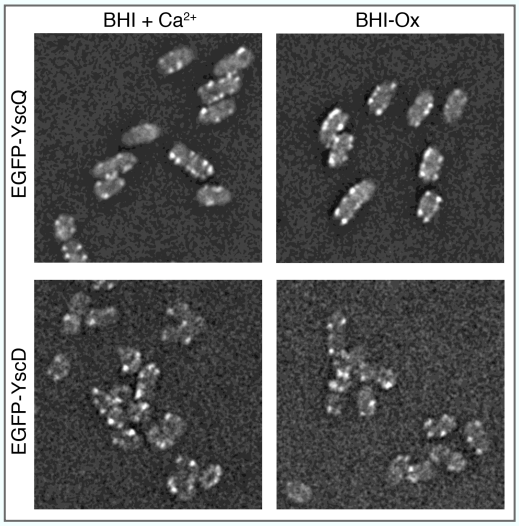

Figure 4.7: The extracellular calcium level has no detectable influence on the localization of the tested injectisome components.

Fluorescence micrographs of bacteria expressing EGFP-YscQ (AD4016, upper panels) or EGFP-YscD (AD4050, lower panels) under secretion-non-permissive and secretion-permissive conditions (BHI+Ca^{2+} and BHI-Ox, respectively). Pictures were taken three hours after T3S induction.

Irrespective of the extracellular calcium levels, EGFP-YscD fluorescence within the foci is lower than EGFP-YscQ fluorescence. Further, there is less EGFP-YscD present in the cell than EGFP-YscQ (see chapter 3.9, Supplementary Figure 1). This might display a lower stoichiometry for YscD than for YscQ. However, strains expressing EGFP-YscD are impaired in effector secretion; thus it cannot be excluded that the stoichiometry of EGFP-YscD is lower than for WT YscD.

As shown in chapter 3, the most proximal tagged injectisome component, EGFP-YscQ, colocalized with the outer membrane ring component YscC-mCherry, as well as with the needle subunit YscF in wild-type *Yersinia* under normal conditions (induction of the T3S by temperature shift to 37°C in either secretion-permissive or non-permissive conditions).

When bacteria were subjected to secretion-non-permissive conditions after transient secretion, differential downregulation of needle formation (at low temperatures) and effector secretion (upon calcium addition) was observed (chapter 4.2.3).

[11] As EGFP-YscN was expressed *in trans*, the effect of the extracellular calcium level could not be assayed with this method.

To find out whether these phenotypes are caused by, or at least reflected in, a different localization pattern of injectisome components, bacteria expressing both EGFP-YscQ and YscC-mCherry were observed under the fluorescence microscope after they had been first incubated for 3 hours at 37°C in secretion-permissive conditions and then were subjected to lower temperature (26°C) and / or calcium-containing medium (BHI+Ca^{2+}, see chapter 4.2.3 and Material and methods for details).

As shown in Figure 4.8, neither the decreased temperature (leading to a stop in export of needle subunits), nor the addition of calcium (leading to a blocking of effector secretion) or a combination of both conditions led to an observable change in the localization pattern or to dissociation of the C ring spots and the secretin spots. Therefore, these two phenotypes are neither caused by a dissociation of the cytosolic components of the injectisome, nor lead to such a dissociation.

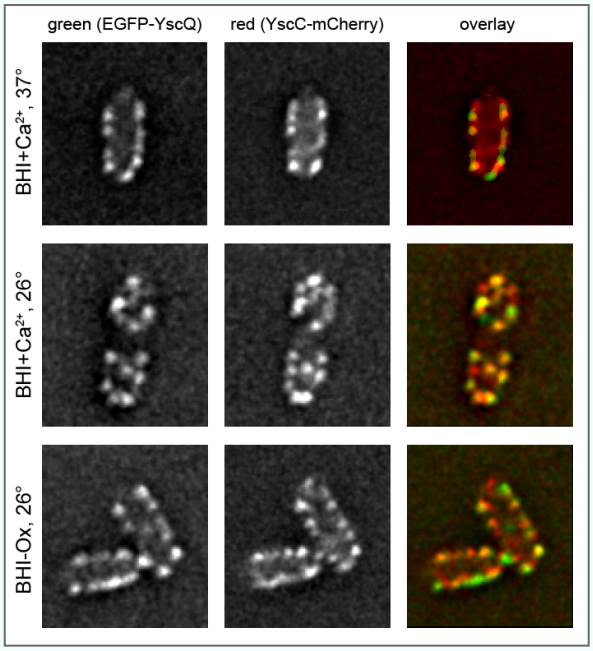

Figure 4.8: Colocalization of EGFP-YscQ and YscC-mCherry remains stable three hours after addition of calcium or decrease of temperature.

Fluorescence micrographs of bacteria expressing EGFP-YscQ and YscC-mCherry (MAAD4006) that have been incubated at 37° under secretion-permissive condition (BHI-Ox) and were subsequently incubated under secretion-non-permissive or secretion-permissive conditions (BHI+Ca^{2+} or BHI-Ox), at 26° or 37°, as denoted. Pictures were taken three hours after conditions were changed.

4.3.2. Kinetics of the assembly of the injectisome

Assembly of the MS ring can be detected 60 minutes after T3S induction; subsequent steps occur within short time.

As shown in Figure 3.6, formation of the C ring, a late step in the assembly of the injectisome, can be observed 60 minutes after induction of the T3S. To scrutinize the kinetics of the events before C ring formation, similar microscopy time course experiments using the

other fluorescent constructs were performed. Formation of the first YscC-mCherry secretin rings could not be observed, as the background in the red fluorescence channel prevented the detection of the weaker early spots (data not shown). The formation of EGFP-YscN spots was not examined as the *in trans* expression of this protein might lead to artefacts in the assembly kinetics. In contrast, formation of EGFP-YscD spots could be observed. As for EGFP-YscQ, the first spots were visible 60 min after T3S induction. As already observed in Figure 4.7, both the increase in cytoplasmic formation and the intensity of spots is less pronounced than shown for the C ring component. However, the kinetics are very similar, suggesting that formation of the ATPase – C ring complex occurs fast after establishment of the MS ring and is not the rate-limiting step.

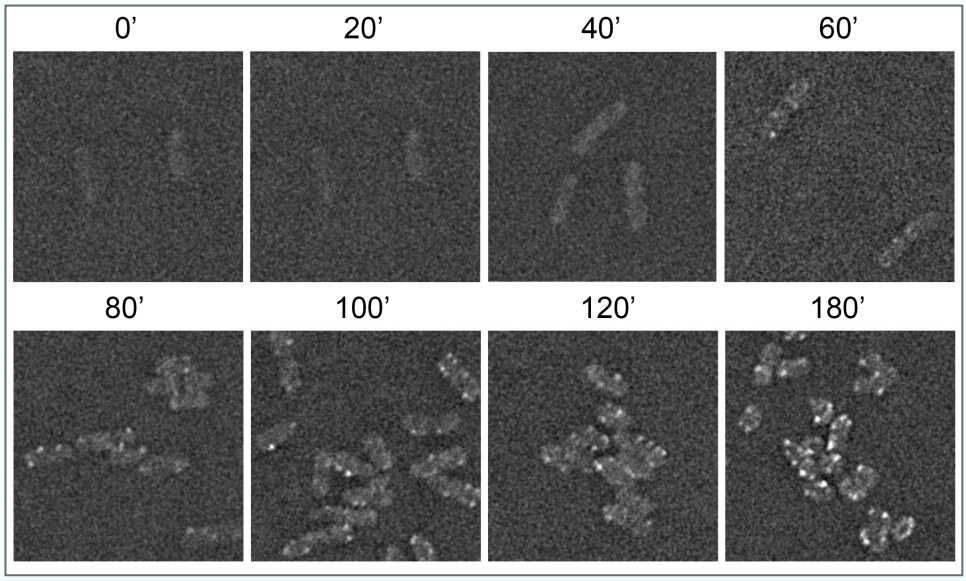

Figure 4.9: Formation of EGFP-YscD spots can be observed 60 minutes after T3S induction.

Time course of bacteria expressing EGFP-YscD (AD4050) under secretion-non-permissive conditions (BHI+Ca^{2+}), before (0'), and at different time points after induction of T3S by temperature shift to 37°.

At the same time as the formation of the first C ring spots, the first needles can be observed, and effector secretion starts (Figure 3.6). We had assumed that needle formation requires presence of the ATPase – C ring complex, but to formally show the order of these events, a needle purification was performed in strains lacking YscN or YscQ (Figure 4.10). No needles could be observed in the mutant strains, showing that indeed, the ATPase and the C ring are required for the formation of the needle. Therefore, needle formation and effector secretion take place fast *after* completion of the ATPase – C ring complex, as proposed in chapter 3.

A recent paper by Konishi *et al.* (2009) showed that the requirement of the flagellar C ring subunits FliM and FliN for the formation (but not the function) of the flagellum could be overcome by overproduction of the ATPase FliI. To test whether this also holds true for the injectisome, the homologous ATPase YscN was overproduced *in trans* in a strain lacking YscQ (Figure 4.10, right side). Even at an induction with 0.5% arabinose, ten times the amount required for a wild-type level of YscN, the amount of needle proteins was not increased compared to the uninduced control strain. This is accordance with the proposed essential function of YscQ for the assembly of the ATPase – C ring complex (chapter 3).

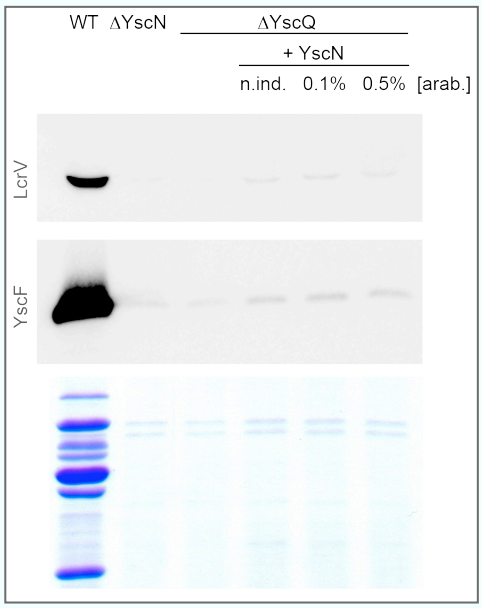

Figure 4.10: Needle formation and effector secretion requires presence of YscN and YscQ and cannot be restored by overexpression of YscN in strains lacking YscQ.

Upper panels: Immunoblot analysis using antibodies directed against the needle tip component LcrV and the needle subunit YscF in needle preparations of strains MRS40 (WT), AD4136 (ΔYscN), ISOA4015 (ΔYscQ), or ISO4015(pAD165) (ΔYscQ + pBAD-*yscN*), induced with different concentrations of arabinose. Lower panel: *In vitro* secretion assay of these strains.

Oligomerization and OM integration of YscC is not the sole rate-limiting step of the assembly of the injectisome

As the assembly steps following MS ring formation seem to occur within a short time frame after 40-60 min (Figure 3.6), and do not merely reflect the expression pattern of the respective proteins (Figure 4.3), rate-limiting steps have to exist within the early injectisome assembly.

Formation of the secretin ring is one of most complex steps in injectisome formation: It forms the first oligomer and the first ring structure of the injectisome, it has to be delivered from the IM to the OM by its pilotin YscW, and it bridges the peptidoglycan layer. Secretin formation thus was a candidate for the rate-limiting step in injectisome formation. Since YscC assembly could not be directly assayed by analysis of a fluorescent variant, pre-induction experiments were performed. As an earlier completion of a rate-limiting step would expedite all subsequent steps, effector secretion was chosen as a simple and unambiguous read-out.

Strain ADMA4098 (ΔYscC) was complemented *in trans* by pMA6 (YscC under an inducible promoter) and pRS6 (YscW under a constitutive promoter). YscC was induced with 0.05% arabinose, which complements for effector secretion (M. Amstutz, personal communication). This was done either one hour before induction of the remaining injectisome components by temperature shift to 37°C, at the same time, or one hour after induction of the remaining components. As a control, an uninduced strain was used.

As visible in Figure 4.11 A, pre-induction of YscC did not lead to earlier effector export. However, the strain in which YscC was induced one hour after the temperature shift showed a secretion pattern that resembled the patterns of the other strains 30 – 60 minutes before. As expected, the uninduced control did not show any secretion.

To rule out that the secretin ring does not assemble at temperatures below 37°C, which would prevent its formation in the pre-induction time course, YscC-mCherry was expressed together with YscW in a strain cured of the virulence plasmid (pYV$^-$(pMA8, pRS6)) at 26°C and 37°C, and formation of fluorescent spots was monitored three hours later. Figure 4.11 B shows that, even though the fluorescent spots appear brighter at 37°C (which might be a consequence of mCherry folding), formation of the secretin ring remains unaffected by the lower temperature.

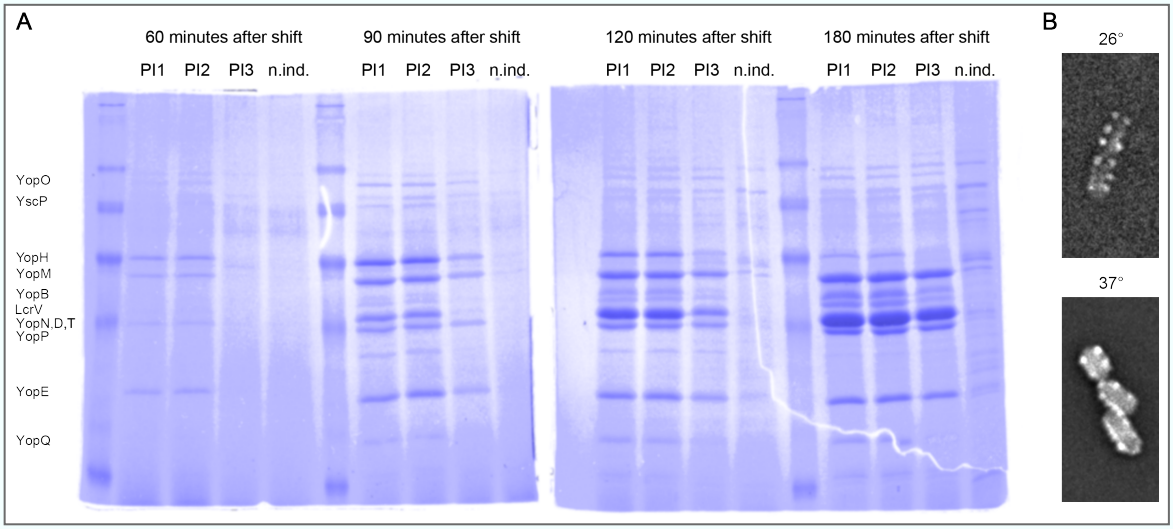

Figure 4.11: Pre-induction of YscC does not lead to earlier secretion of effectors; in contrast, later induction of YscC defers secretion.

A: *In vitro* secretion time course using strain ADMA98(pMA6, pRS6) (ΔYscC + pBAD-*yscC* + *yscW*). PI1, YscC induction 1 h before T3S induction by temperature shift; PI2, YscC induction concurrently with temperature shift; PI3, YscC induction 1 h after temperature shift; n.ind., not induced. **B**: Fluorescence micrograph pictures of pYV$^-$(pMA8, pRS6) bacteria expressing YscC-mCherry and YscW at the given temperatures.

These results confirm that the presence of YscC is a crucial prerequisite of the further events, as shown by the delay in secretion caused by the later YscC induction. However, assembly of the secretin ring alone does not expedite the following steps, which in the absence of further candidates suggests that assembly of YscD is at least part of the rate-limiting step.

4.3.3. Dynamics of the injectisome basal body

FRAP experiments indicate dynamic exchange of subunits, but no function in substrate shuttling for EGFP-YscQ

For the cytosolic subunits of the flagellum, a model has been proposed in which the ATPase is involved in the transport of substrates from the cytosol to the C ring, and from there to the export channel (Minamino *et al.*, 2008). Our results indicate that in the injectisome, the C ring and the ATPase assemble in one complex (chapter 3). As, further, the injectisome C ring is not required for the rotational switch, and has been proposed to serve as a "central hub of protein-protein interactions" in *Chlamydia* (Spaeth *et al.*, 2009), we tested the possibility that YscQ localizes dynamically to the proximal side of the injectisome, possibly participating in a shuttling mechanism.

To assay this hypothesis, we performed a fluorescence recovery after photobleaching (FRAP) experiment, in which the fluorescence of single EGFP-YscQ foci was bleached, and the recovery of the foci was observed over time. The strain used in this experiment, AD4085, expresses EGFP-YscQ in a strain that can be grown in a safety class I environment (see chapter 7.3 for details). It was functional for secretion and EGFP-YscQ localization did not differ from strain AD4016 (EGFP-YscQ in wild-type background, data not shown).

Fluorescence at the foci within the bleached area reappeared with a recovery half-time of 4.26 min (+/- 1.02 min) for EGFP-YscQ (Figure 4.12, see Table IV for details). While this indicates a faster subunit exchange than for the flagellar MS ring component FliF-YFP that was used as a control (Figure 4.12 C), it appears to be too slow to agree with a dynamic shuttling mechanism.

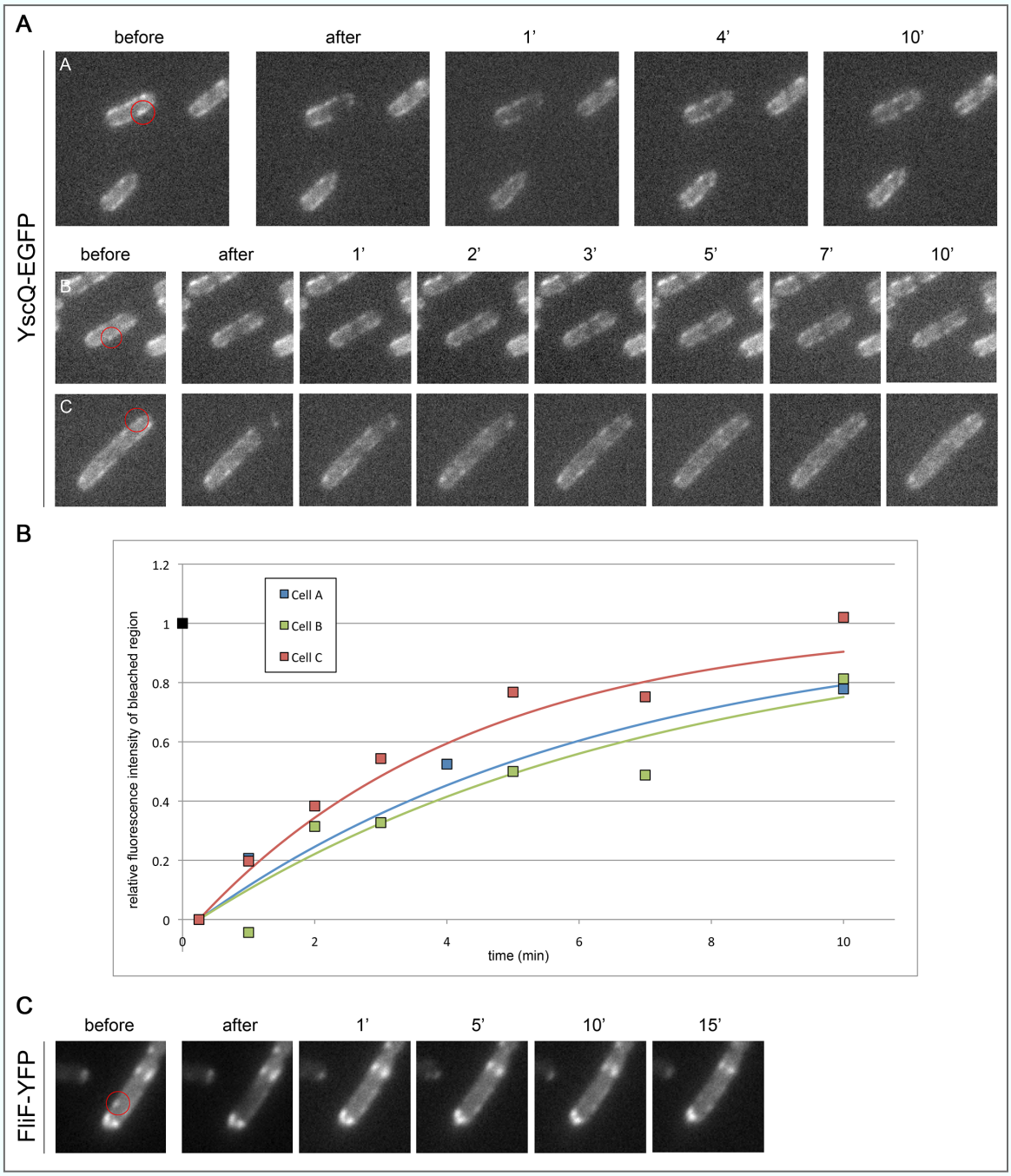

Figure 4.12: EGFP-YscQ foci recover fluorescence within minutes.

A: Fluorescence micrographs showing the bleaching and fluorescence recovery of YscQ-EGFP spots in strain AD4085. Red circles indicate the approximate borders of the bleached area. **B:** Quantification of spot fluorescence and extrapolation of recovery. See table IV for details. **C:** Fluorescence micrographs showing the bleaching and fluorescence recovery of FliF-YFP spots (courtesy of Hui Li, University of Heidelberg).

cell	time (min)	fluorescence intensities				$t_{1/2(recovery)}$ (min)	r^2 (curve fit)
		back-ground	total cell	bleached spot	normalized		
A	0	43.788	66.309	125.156	1.000	4.56	0.973
	0.25	42.629	54.446	52.899	0.000		
	1	44.079	52.002	55.452	0.206		
	4	42.694	56.219	73.915	0.525		
	10	43.212	56.727	83.829	0.779		
B	0	51.510	88.314	122.652	1.000	5.10	0.900
	0.25	47.577	73.556	76.609	0.000		
	1	43.551	68.717	70.780	-0.044		
	2	41.856	66.083	75.138	0.314		
	3	42.455	66.305	75.471	0.327		
	5	48.500	75.478	89.647	0.500		
	7	53.403	76.143	87.859	0.488		
	10	57.193	82.473	102.198	0.813		
C	0	55.251	89.781	117.364	1.000	3.13	0.956
	0.25	51.303	76.978	62.589	0.000		
	1	52.237	75.431	68.655	0.197		
	2	51.323	73.387	72.518	0.383		
	3	50.749	74.590	78.840	0.543		
	5	52.543	77.237	89.165	0.768		
	7	49.778	76.901	89.421	0.752		
	10	55.830	88.165	114.884	1.020		

Table IV: Fluorescence recovery after the photobleaching of EGFP-YscQ foci.

The average value for $t_{½(recovery)}$ is 4.26 min (+/- 1.02 min). The normalized fluorescence values were obtained by calculating the ratio of background-corrected fluorescence intensities in the area of the bleached spot and in the complete cell, which accounts for variations in total fluorescence due to bleaching effects. Subsequently, the fluorescence ratio was normalized using the pre-bleach and post-bleach fluorescence ratios as 1 and 0, respectively. The $t_{1/2}$ value was calculated by fitting the resulting curve to the exponential recovery function $y = 1 – 0.5^{(x/t_{1/2})}$, where x is the time in min after bleaching.

FRET experiments do not indicate pre-formation of the ATPase – C ring complex in the cytosol

YscQ and YscN simultaneously assemble at the proximal side of the injectisome as part of the large cytosolic ATPase - C ring complex (chapter 3). Whether this complex already forms in the cytosol, or requires the MS ring as assembly platform, is unknown. To study this question, the combination of mCherry-YscQ and EGFP-YscN was tested in FRET experiments. GFP and mCherry have been shown to be applicable as FRET pair with an efficiency similar to the widely used CFP/YFP (Tramier *et al.*, 2006; V. Sourjik, personal communication). In case of a positive FRET result for the strain lacking only YscJ, this setup would allow to study the roles of YscK and YscL in assembly and localization of the ATPase – C ring complex.

The results of the experiments are summarized in Figure 4.13. To ensure the cytoplasmic localization of the proteins, all strains used lack the MS component YscJ. The control strains for cytoplasmic fluorescence of mCherry-YscQ or EGFP-YscN alone (ADCC4148 and AD4139(pAD182), respectively) were tested for fluorescence in the red, green, and FRET channel (GFP excitation, mCherry emission, see Material and methods for details). While the green and red channel were tightly separated, both EGFP and mCherry caused a background signal in the FRET channel (12.3% +/- 1.4% and 12.6% +/- 1.4% of the respective fluorescence signal, see Figure 4.13 A, Table V), as expected from the excitation/emission spectra of the fluorophores (Figure 4.13 B). The strain expressing both fluorescently labeled proteins, ADCC4148(pAD182), showed a fluorescence level in the FRET channel that was slightly below the sum of the expected background signals caused by the two single fluorophores (see Table V for details). This indicates that there is no energy transfer between mCherry-YscQ and EGFP-YscN. Whether this is caused by large distance or sterical mismatch between the fluorophores, or shows that there is no pre-formation of the ATPase – C ring complex in the cytosol, cannot be concludingly distinguished due to the lack of structural data for the complex. A copurification approach based on the affinity tagged constructs for YscQ and YscN (see table III) is currently being performed.

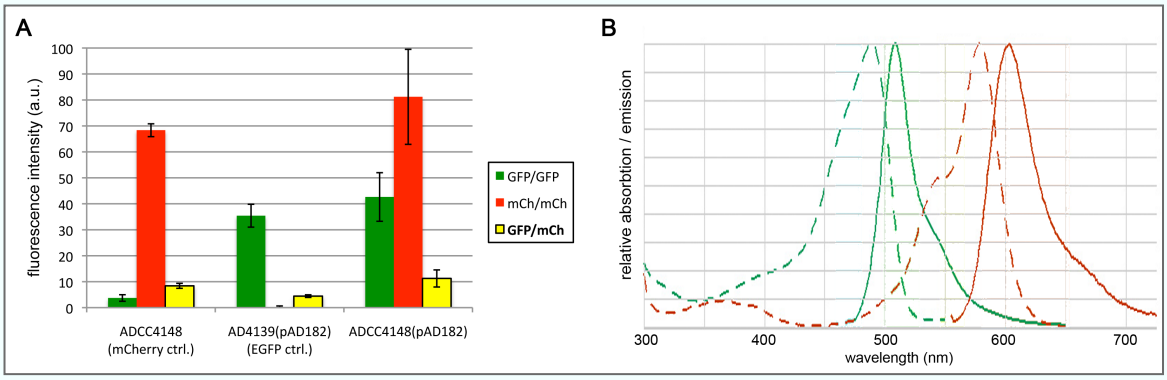

Figure 4.13: FRET measurements do not indicate energy transfer between mCherry-YscQ and YscN-EGFP.

A: FRET results for strains ADCC4148 (ΔYscJ, ΔYscN, mCherry-YscQ), AD4139(pAD182) (ΔYscJ, ΔYscN + pBAD-*yscN-egfp*), and ADCC4148(pAD182) (ΔYscJ, ΔYscN, mCherry-YscQ + pBAD-*yscN-egfp*). Green bars: GFP fluorescence; red bars: mCherry fluorescence; yellow bars: FRET signal (excitation GFP, emission mCherry). **B**: Fluorescence excitation (dashed line) and emission (continuous line) spectra for GFP (green) and mCherry (red) (adapted from Keck Microscopy Facility, University of Washington, http://depts.washington.edu/keck/DV-RT/Filtersets%20Live-Cell.html, accessed Mai 3, 2010).

strain	expression of fusion proteins		fluorescence intensity (a.u.)		
	EGFP-YscN	mCherry-YscQ	green (GFP/GFP)	red (mCh/mCh)	FRET (GFP/mCh)
ADCC4148	-	+	3.73	68.35	8.41
AD4139(pAD182)	+	-	35.41	0.23	4.45
ADCC4148(pAD182)	+	+	42.62	81.20	11.26

Table V: FRET results for EGFP-YscN and mCherry-YscQ.

4.3.4. Discussion

Formation of the injectisome after induction of the T3S system by temperature increase to 37°C is a relatively slow process. Needle formation and effector secretion can only be observed after 60 minutes (Figure 3.6 B, C). To learn about the kinetics and possible checkpoints of the assembly process, we performed a series of experiments to define the rate-limiting step in the assembly of the injectisome. We could show that, despite the earlier presence of all tested injectisome components (Figure 4.3 A), assembly of both the C ring (EGFP-YscQ, Figure 3.6 A) and the MS ring (EGFP-YscD, Figure 4.9) also only can be observed after 60 minutes. This restricts the possible rate-limiting step to one of the earliest events in assembly – the possible degradation of the peptidoglycan layer, multimerization or OM integration of the secretin YscC, or assembly of YscD. However, pre-induction of YscC in the presence of its pilotin YscW did not expedite the later events (Figure 4.11), showing that YscC assembly is not the sole rate-limiting step. This is in agreement with previous pulse-chase experiments (Burghout *et al.*, 2004a), where oligomerization of YscC was observed already after 5 – 30 minutes. The integration of YscC into the OM was not tested in this study. Therefore, it cannot be excluded that this step is rate-limiting in combination with YscD attachment. This would also agree with the fact that delayed YscC expression also led to deferral of the following steps. Effector secretion lagged by 30-60 min when YscC was expressed 60 min after T3S induction. This time is in perfect agreement with data observed for the type II secretion secretin ExeD in *Aeromonas hydrophila*, where export of the substrate aerolysin was observed 40-60 min after induction of ExeAB, which are suggested to exert the pilotin function (Ast *et al.*, 2002). To determine whether YscC integration in the OM and YscD assembly really jointly constitute the rate-limiting step in the assembly of the injectisome, a construct expressing both proteins would have to be pre-induced in the presence of YscW. This construct has been created and verified, but could not be tested in a time course experiment yet.

Moreover, we could show that for neither of the tested proteins EGFP-YscD and EGFP-YscQ, the extracellular calcium level had an influence on the localization pattern (Figure 4.7), The same could be observed for YscC-mCherry (M. Amstutz, unpublished data). Our results for the colocalization of the secretin and the C ring under different conditions, after the transient incubation of bacteria under secretion-permissive conditions, further indicate that the injectisomes are stable for hours, even at low temperature and in the presence of calcium. This agrees with the functionality of the system under these conditions (Figure 4.4), and

shows that the observed change in substrate specificity is neither caused by, nor reflected in dissociation of the cytoplasmic components.

To test whether the cytosolic components of the injectisome participate in a cargo shuttling mechanism, as has been proposed for the flagellar ATPase complex $FliH_2FliI$ (Minamino *et al.*, 2008), we tested the dynamics of EGFP-YscQ by FRAP. Despite the clear result of the experiment, the interpretation of the data is difficult. The measured recovery half-time (equivalent to the exchange of 50% of the bleached subunits of the C ring with fluorescent subunits) of several minutes (Figure 4.12 A, B) appears to be too slow to be compatible with a dynamic shuttling mechanism. The C ring component is only slightly more dynamic than the structural subunits of the flagellar MS ring (FliF, see Figure 4.12 C), and C ring, where a recent publication shows that in a rotating flagellum, the two components FliM and FliN exchange subunits "in tens of minutes", whereas FliG does not show a detectable subunit exchange (Fukuoka *et al.*, 2010). In a study examining the dynamics of the nuclear pore complex (Rabut *et al.*, 2004), an exchange rate of $t_{½}$ = 4.4 min, similar to the one we observed for YscQ, was detected for the most dynamic structural component gp210, whereas the importin, which shuttles substrates, had a recovery halftime of below 2 seconds. In conclusion, the C ring component YscQ does not seem to be involved in substrate shuttling, but shows a comparably high subunit exchange, which suggests a low structural stability for the ATPase – C ring complex, consistent with the purification data (see chapter 4.4).

4.4. Purification of subcomplexes of the injectisome

4.4.1. Effect of the pH value and the adhesin YadA on spheroplasting and solubilization

Needles can only be purified at pH values below 8.0

Needle complexes have been purified from various organisms. The protocol that has been, with slight modifications, applied in all these cases, consists in spheroplast generation by lysozyme / EDTA treatment, lysis by addition of detergent, and subsequent purification by ultracentrifugation (Kubori *et al.*, 1998; Kimbrough and Miller, 2000; Blocker *et al.*, 2001; Sekiya *et al.*, 2001; Marlovits *et al.*, 2004; Ogino *et al.*, 2006). This protocol, however, did not lead to the purification of injectisomes in *Y. enterocolitica* (S.-I. Aizawa, personal communication; own unpublished data). One possible reason for this is that needles either detach or depolymerize under the given conditions. A needle preparation screen at different pH values revealed that *Yersinia* needles could not be purified at pH above 8.0 (Figure 4.14). In order to create *Yersinia* spheroplasts in conditions under which the needles are stable, the protocol therefore had to be adapted to a lower pH of 7.8, which required a significant increase in the concentrations of lysozyme and EDTA, and a prolonged incubation time (data not shown).

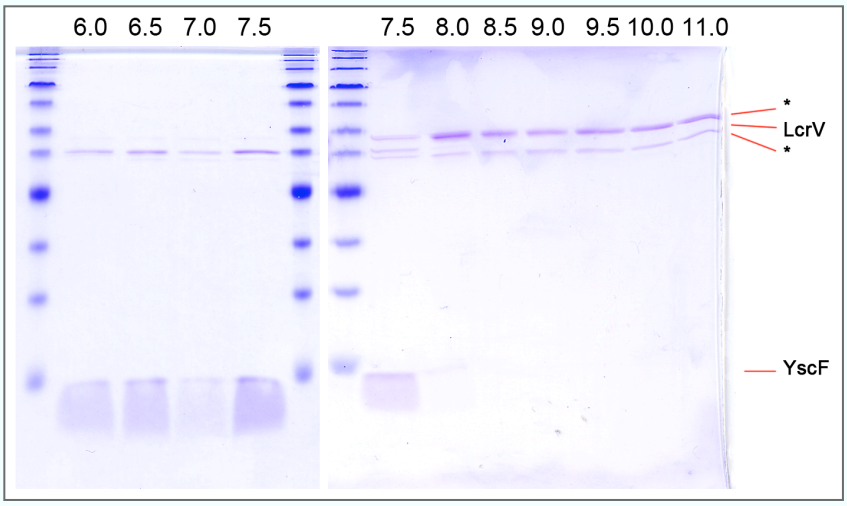

Figure 4.14: *Yersinia* injectisome needles cannot be purified at pH above 8.0.

Needle preparations were performed at different pH values (see Material and Methods for details), and the resulting fractions were analyzed an a 17.5% SDS-PAGE gel and stained with Coomassie Brilliant Blue. The size of LcrV and YscF is displayed, asterisks mark flagellar subunits present in the purification at higher pH values.

Removal of YadA improves spheroplast generation and lysis efficiency

However, the *Yersinia* spheroplasts quickly aggregated under these conditions, which led to a decreased efficiency of cell lysis and, even more pronounced, of solubilization of injectisome components. To overcome this problem, the *Yersinia* adhesin YadA was removed by integration of the mutator plasmid pLJM31 into the *yadA* gene.[12]

Surprisingly, the resulting strains showed weak growth (Figure 4.15 A) due to partial lysis (Figure 4.15 B) after induction of the T3S under standard conditions. However, this could be completely prevented when the carbon source was exchanged (0.4% glycerol instead of 0.4% glucose). It thus seems the glucose taken up from the medium was converted to sucrose, which subsequently was polymerized to toxic levels of levan, due to the presence of the levansucrase gene on the integrated *yadA* mutator plasmid. In subsequent experiments, glycerol was used as a carbon source when working with *ΔyadA* strains.

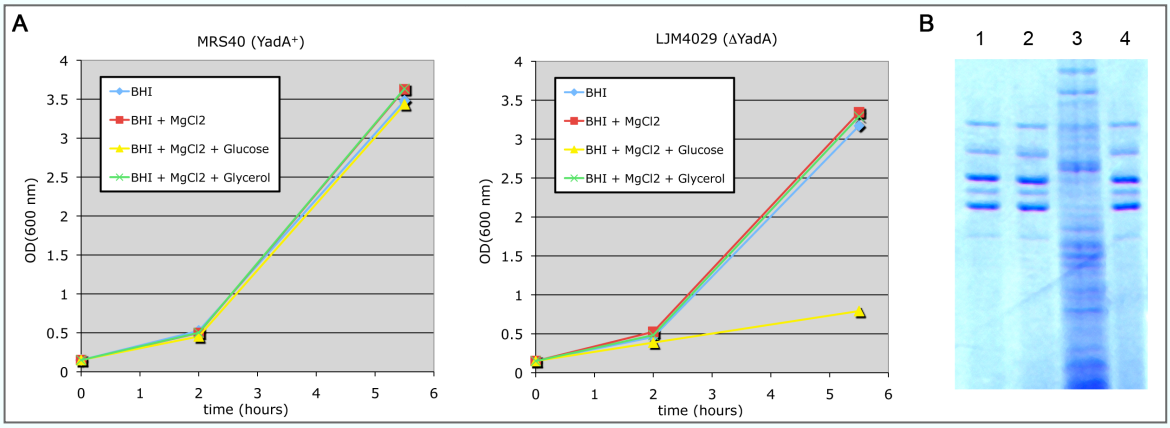

Figure 4.15: Media containing glucose lead to weak growth and cell lysis in strains carrying the YadA mutator plasmid.

A: Growth curves of strains MRS40 (WT) and LJM4029 (ΔYadA) in the given media. T3S was induced two hours after inoculation. **B**: Supernatant of strain LJM4029 (ΔYadA) in different media, three hours after induction of T3S. Medium 1, BHI; 2, BHI + $MgCl_2$; 3, BHI + $MgCl_2$ + Glucose; 4, BHI + $MgCl_2$ + Glycerol.

When incubated under these conditions, cells lacking YadA (Figure 4.16 A) did not aggregate after spheroplast formation (Figure 4.16 B), leading to complete lysis of the bacteria at a Triton X-100 concentration of 0.75% (data not shown).

[12] Unlike most other T3S components in *Yersinia*, YadA is not part of a larger operon and can therefore be removed by simple integration of a mutator plasmid without polar effects.

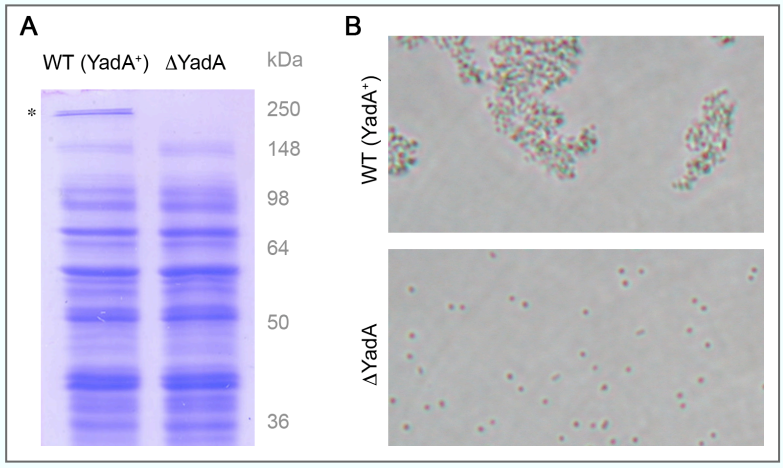

Figure 4.16: Absence of YadA abolishes the aggregation after spheroplast formation

A: Total cellular proteins in strains pIML421*asd* (WT YadA) and AD4053 (corresponding ΔYadA). The position of the YadA trimer is marked by an asterisk. **B**: Micrograph showing the aggregation behavior of the bacteria after spheroplast generation.

4.4.2. Purification and analysis of the inner membrane MS ring

Functionality of tagged MS ring components and split-TAP approach YscD / YscJ

To purify parts of the *Yersinia* injectisome basal body and examine the role of different proteins by the comparison of deletion mutants, a purification method which is not based on physicochemical properties had to be applied. To achieve a high enrichment under gentle conditions, a tandem affinity purification (TAP) tag approach (Gavin *et al.*, 2002) was applied using small affinity tags that are less likely to disturb protein function and complex formation (Yang *et al.*, 2006). During the course of these studies, a paper describing the affinity-based purification of the *Shigella* needle complex (Zenk *et al.*, 2007) confirmed the general applicability of this strategy.

In the basal body, the two proposed components of the MS ring, YscD and YscJ, were tagged with either a His_8 tag, a FLAG tag (DYKDDDDK) (Chubet and Brizzard, 1996), or a combination of both. While larger tags in the same position led to a decrease or complete abolishment of effector secretion (see Table III, Figure 3.1, Figure 4.5), the used affinity tags with a molecular weight below 3 kDa did not impair the function of the proteins (Figure 4.17).

Surprisingly, although both YscJ-His_8 and FLAG-YscD (strains AD40082, AD4047) were functional, a combination of both tagged proteins led to a complete abolishment of secretion (Figure 4.17). This suggests that the C terminus of YscJ and the N terminus of YscD are in close proximity in the cytoplasmic part of the injectisome structure. A direct steric clash of the tags is unlikely, as tags on one protein, with the length of both single tags, are still

functional (Figure 4.17). However, the proximity might lead to a non-productive interaction between the (mildly positively charged) His tag and the (negatively charged) FLAG tag which prevents injectisome function.

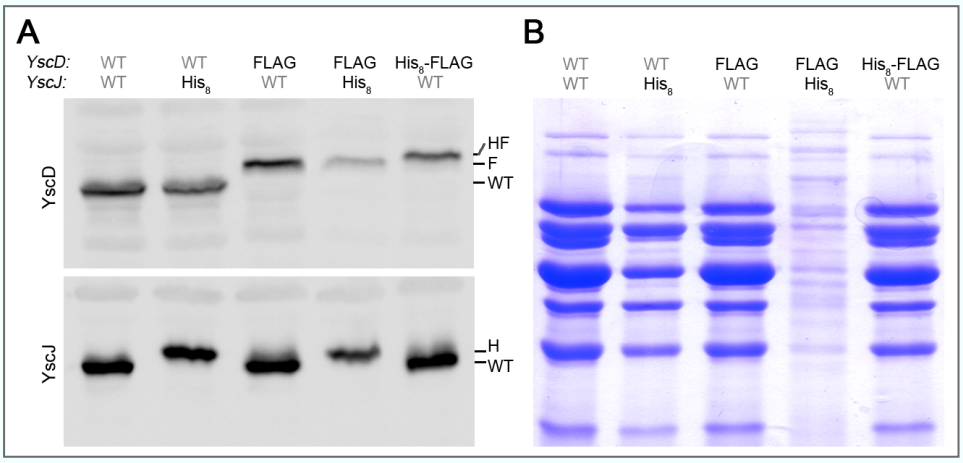

Figure 4.17: While neither tag alone interferes with injectisome function, a combination of FLAG-YscD and YscJ-His$_8$ abolishes effector secretion.

A: Immunoblot analysis of cellular proteins using antibodies directed against YscD and YscJ in strains MRS40 (WT), AD40082 (YscJ-His$_8$), AD4047 (FLAG-YscD), AD4048 (FLAG-YscD, YscJ-His$_8$), and AD4049 (FLAG-His$_8$-YscD). Expected protein sizes: H, His-tagged protein; F, FLAG-tagged protein; HF, His-FLAG-tagged protein; WT, wild-type protein. **B**: *In vitro* secretion assay of these strains.

Choice of crosslinker and its effect on spheroplast generation and cell lysis

Specific copurification of the basal body components is likely to depend on crosslinking of the proteins. As the crosslinker used for this purpose had to be membrane-permeable and preferably cleavable, para-formaldehyde (FA) and Dithiobis[succinimidyl propionate] (Lomant's reagent, DSP) were compared for their applicability.

In a comparison of different concentrations of FA and DSP for their effect on copurification of YscC and YscD with YscJ-FLAG-His$_8$, after the gentle resuspension of cells in PBS, 0.5% FA and 2.0 mM DSP yielded the best results (Figure 4.18). As DSP led to a decrease in lysis efficiency (data not shown), FA was used in the subsequent experiments.

Since crosslinking also had an obvious influence on spheroplast generation and cell lysis, the optimal FA concentration and time point of crosslinking were determined. Different concentrations of formaldehyde were used either directly in the bacterial culture, or after gentle resuspension in PBS.

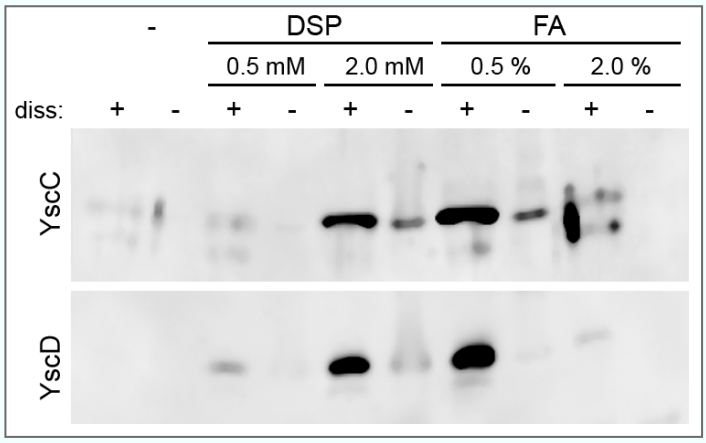

Figure 4.18: Influence of different crosslinking conditions on the copurification of the membrane ring proteins

Immunoblot analysis of the copurification of YscC and YscD with YscJ-FLAG-His in strain AD40085 after crosslinking with the given concentrations of crosslinkers Dithiobis[succinimidyl propionate] (DSP) or para-formaldehyde (FA).

+: Dissociation of crosslinking by heat treatment of the sample (5 min at 99° in sample buffer containing 5% β-mercaptoethanol (BME)); -: No dissociation of crosslinking (5 min at 65° in sample buffer without BME).

As visible in Figure 4.19, lysis efficiency (as determined by measurement of the optical density at 600 nm) varied from 37% - 99%. Overall, the washing step in PBS significantly increased lysis efficiency. Further, there was an optimum in formaldehyde concentration at 0.4% when crosslinked in the bacterial culture, and at 0.5% when crosslinked in PBS.

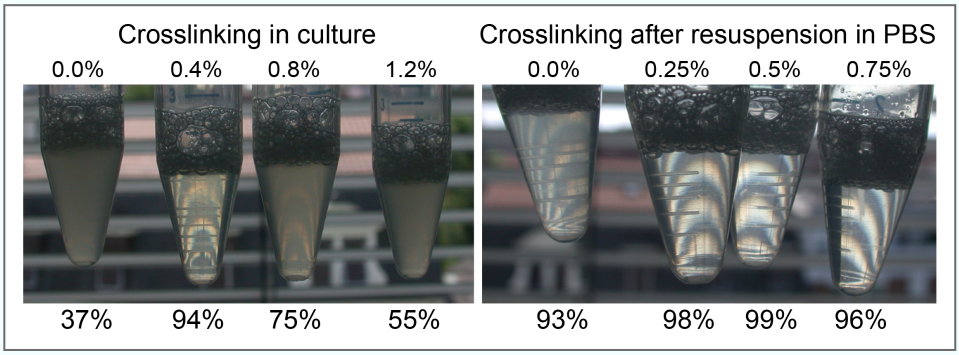

Figure 4.19: Lysis efficiency after different crosslinking treatments

Photographs of cultures pre-treated as denoted with different concentrations of para-formaldehyde, after addition of 1.0% Triton X-100. Calculated lysis efficiencies, as determined by measurement of OD_{600}, are indicated in the bottom row.

To achieve efficient crosslinking while retaining high lysis rates, the following protocol was applied in subsequent experiments: Crosslinking with 0.25% FA in the culture; gentle resuspension in PBS; crosslinking with further 0.4% FA (see Material and methods for details). This treatment consistently led to good crosslinking and high lysis efficiency.

The membrane ring proteins YscC, YscD, and YscJ can be copurified

As shown in chapter 3, the proteins forming the membrane rings within the basal body can be copurified using affinity tagged YscD or YscJ. While a one-step FLAG purification was sufficient to copurify the three membrane ring proteins and to show the requirements for this copurification, TAP decreased the unspecific background and was therefore used to assay the copurification of further injectisome components.

The result of such a two-step purification (Ni^{2+} affinity followed by FLAG affinity, see Material and methods for details) is shown in Figure 4.20. After the second purification step, the sample contained a large amount of the tagged protein YscJ-FLAG-His_8, which is visible as the most intense band on the silver stained gel. The two copurified proteins YscC and YscD (identified by comparison of band intensity and location to an immunoblot of the same samples) were visible as well, albeit in significantly lower concentrations. Several bands that could not be unambiguously assigned (marked by asterisks) were still present in this fraction. The higher intensity of the tagged YscJ, compared with the copurified proteins, indicates that monomeric cytosolic YscJ was purified with this protocol as well, besides partially or fully assembled membrane ring complexes.

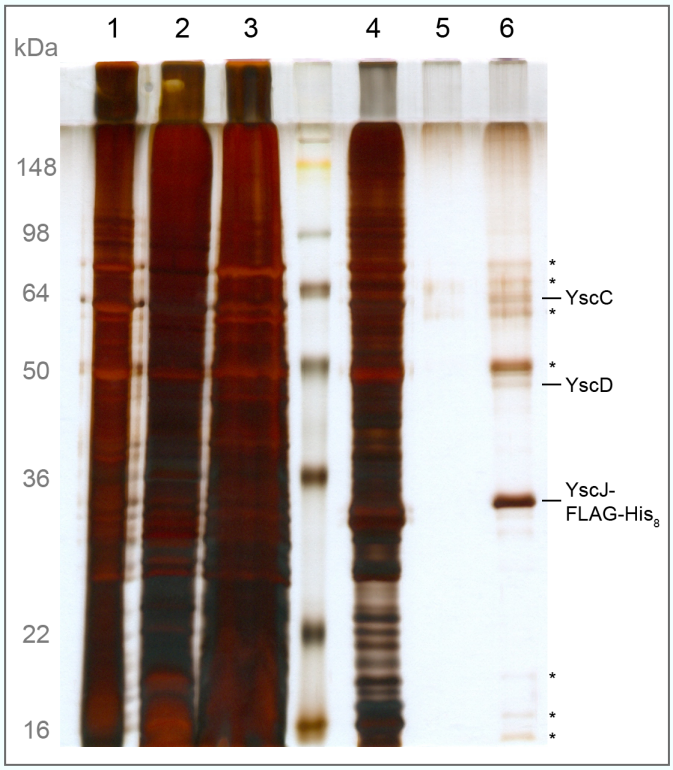

Figure 4.20: TAP purification of strain AD40085 (YscJ-FLAG-His_8).

Silver staining of a 12% SDS-PAGE gel, lanes: 1, cellular proteins before crosslinking; 2, cellular proteins after crosslinking; 3, solubilised protein after lysis; 4, eluate from Ni^{2+} affinity column; 5, wash fraction from FLAG affinity column; 6, eluate from FLAG affinity column. Asterisks mark bands in lane 6 that could not be unambiguously assigned. Note that the highest MW band marked by an asterisk corresponds to the MW of YscV.

Mass spectrometry and immunoblot indicate limited copurification of YscV and YscF with the membrane ring complex

To test whether additional injectisome components were copurified, the outcome of a TAP purification of strain AD40085 (YscJ-FLAG-His_8) was analyzed by mass spectrometry.

To decrease the risk of false positive results, all following quality criteria had to be met for a protein to be considered as specifically copurified:

- At least five different matched peptides per protein
- E value < 10^{-4} (for search of nr database) / < 10^{-7} (for search of T3S protein database)[13]
- Amongst top 50 hits from search against nr database

Table VI shows the detected proteins. The presence of the three known purified proteins YscC, YscD, and YscJ shows the specificity of the purification and detection methods. Beside these three membrane ring-forming proteins, only YscV matched the quality criteria. All of these proteins were amongst the twenty most abundant proteins (including different isoforms) detected by mass spectrometry in a search against the nr database. Contaminants that were detected were either directly linked to the purification procedure (various isoforms of lysozyme, IgG, protein A) or highly abundant proteins (keratin, pyruvate dehydrogenase). The only unspecific hit for a *Yersinia* protein was the abundant OM protein YadA (Hoiczyk *et al.*, 2000). Further T3S proteins that were detected, but did not meet the quality criteria, were YscR and YscU (data not shown).

Ranking	Protein name	E value
1	Keratin	1.00E-30
2	YadA	9.08E-07
3	Pyruvate dehydrogenase	1.05E-06
4	Lysozyme	1.01E-11
5	**YscJ**	**5.43E-09**
6	Protein A	9.87E-11
7	**YscC**	**3.42E-07**
8	**YscD**	**5.84E-09**
9	**YscV**	**2.75E-05**
10	IgG heavy chain	9.30E-07

Table VI: Mass spectrometry results of the copurification with YscJ-FLAG-His_8

The MS results for the FLAG elution fraction of a TAP of strain AD40085 (YscJ-FLAG-His_8) were manually curated for different isoforms of the same proteins. Components of the injectisome are denoted in bold. Ranking and E values were calculated by the Mascot software (Matrix Science, Boston, MA, USA).

[13] The nr (non-redundant) database includes all GenBank, RefSeq Nucleotides EMBL, DDBJ, and PDB protein sequences. The T3S protein database includes all proteins which are encoded on the pYV plasmid pYVe227 (GenBank ID AF102990.1).

Copurification of YscV with the ring proteins could not be confirmed by immunoblotting, probably due to the low specificity of the YscV antibody. However, the highest MW band in the silver stained TAP gel (Figure 4.20) matches the MW of YscV (77.9 kDa). The detection of YscV is even more plausible because data suggests that YscV is present more than once in each injectisome (see chapter 4.5).

The needle subunit YscF was not detected in the mass spectrometry experiment. However, YscF is a very small protein (9 kDa) that contains only five peptides possibly detectable by mass spectrometry, and might therefore have been missed in this analysis. To specifically test for the copurification of YscF, a FLAG purification was performed for strains tagged at YscD (AD4055) or YscJ (AD4054). As controls, an untagged strain (LJM4029), and tagged strains lacking the OM secretin YscC (ADMA4101, AD4109, tagged at YscD and YscJ, respectively) were used.

A small amount of YscF copurified with the strain tagged at YscD, a larger amount with the strain tagged at YscJ (Figure 4.21). YscF was absent in all control strains. The amount of copurified YscF in strains AD4055 and AD4054 corresponded to the amount of copurified YscC (not shown). The copurification therefore seems to be specific. However, the concentration of YscF was low, and its copurification was not observed in all experiments. By transmission electron microscopy, no needles could be visualized in the sample.

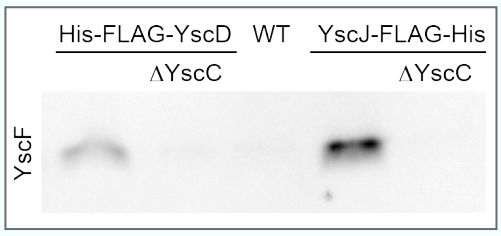

Figure 4.21: Copurification of YscF with affinity tagged YscD or YscJ

Immunoblot analysis of YscF in the FLAG elution fraction of strains AD4055 (His-FLAG-YscD), ADMA4101 (His-FLAG-YscD, ΔYscC), LJM4029 (WT), AD4054 (YscJ-FLAG-His), and AD4109 (YscJ-FLAG-His, ΔYscC).

The cytosolic components YscN and YscQ are not copurified with the membrane ring complex

The same purification samples were analyzed for copurification of the cytosolic components YscN and YscQ. Neither of both proteins could be detected (data not shown), suggesting that the cytosolic ATPase – C ring complex copurifies very poorly with the membrane rings under these conditions, if at all. This observation is in accordance with purification data from other organisms (Kubori *et al.*, 1998; Tamano *et al.*, 2000; Sekiya *et al.*, 2001).

4.4.3. Purification and analysis of the cytosolic C ring

Functionality of the tagged C ring component and split-TAP approach YscQ / YscJ

As shown in Table III and Figure 3.1, N-terminal tags do not interfere with the function of YscQ. To allow a possible purification of the basal body containing the cytosolic components, which could not be obtained with a single tag on YscJ (see previous chapter), a strain was generated that expresses both YscJ-His_8 and FLAG-YscQ (AD4015, "split-TAP"), which was functional for effector secretion, with a slightly reduced efficiency (Figure 4.22).

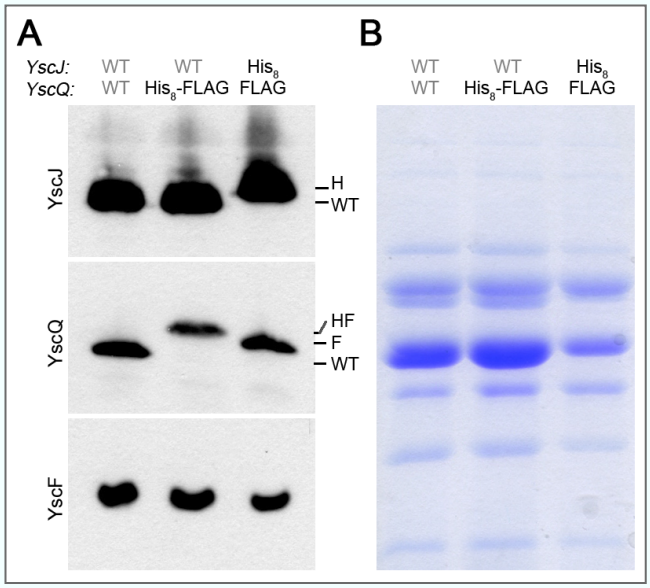

Figure 4.22: Expression and functionality of tagged YscQ variants.

A: Immunoblot analysis of cellular proteins using antibodies directed against YscJ, YscQ and YscF in strains MRS40 (WT), AD4014 (His-FLAG-YscQ), and AD4015 (YscJ-His, FLAG-YscQ). Expected protein sizes: H, His-tagged protein; F, FLAG-tagged protein; HF, His-FLAG-tagged protein; WT, wild-type protein. **B**: *In vitro* secretion assay of these strains.

No membrane ring component is purified with YscQ; size exclusion chromatography suggests the formation of YscQ tetramers

TAP was performed using the split-TAP tagged strain AD4015. As a control, strain AD40085, harboring both tags at YscJ, was used. Both strains were first purified with a Ni^{2+} affinity column (binding the His_8 tag at YscJ), and subsequently with an anti-FLAG column (binding the FLAG tag at YscQ or at YscJ, respectively).

While the first purification step yielded similar results for both strains, no proteins were eluted from the anti-FLAG column for the split-TAP strain AD4015 (Figure 4.23). This suggests that there is no stable interaction between the C ring and the MS ring under these conditions.

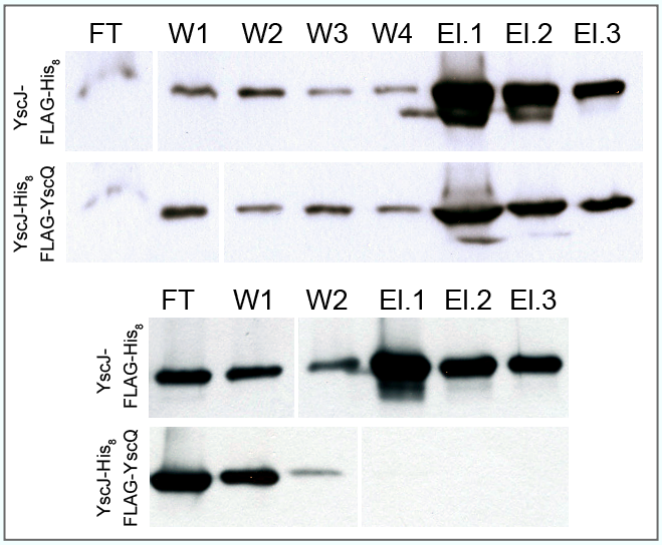

Figure 4.23:
By TAP, no copurification of YscJ and YscQ can be obtained.

Immunoblot analysis of purification fractions, using antibodies directed against YscJ. Upper panel: Ni^{2+} affinity purification. Lower panel: Subsequent FLAG affinity purification. FT, flow-through; W, wash fractions; El., elution fractions.

FLAG affinity purification of strain AD4014 expressing His_8-FLAG-tagged YscQ, after crosslinking, resulted in specific purification of YscQ without evidence for significant copurification of other T3S components (Figure 4.24 A). This result was confirmed by mass spectrometry analysis of this sample, which did not detect any T3S component except for YscQ itself.

To determine the oligomeric state of YscQ, analytic size exclusion chromatography was performed on purified YscQ obtained by FLAG purification as described above. The resulting broad peak corresponded to a molecular weight of 80 – 150 kDa (Figure 4.24 B). This suggests the formation of trimers or tetramers (MW(YscQ) = 34.4 kDa). A tetramerization property of C ring components has been observed before for HrcQ and FliN (Fadouloglou *et al.*, 2004; Brown *et al.*, 2005). As no peak corresponding to a large complex could be observed, it is unlikely that the complete C ring was purified under these conditions. This result supports the model of an instable or dynamic C ring (see chapter 4.3.3).

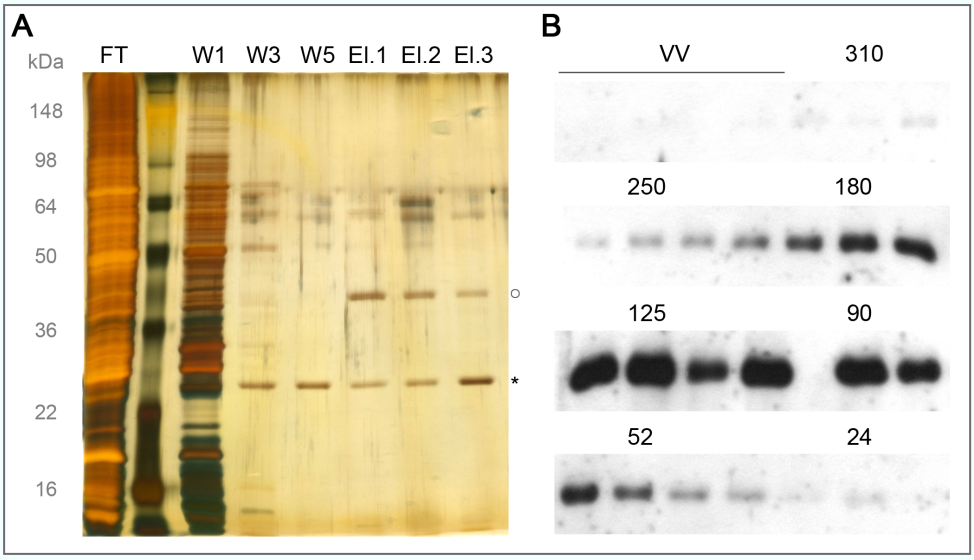

Figure 4.24: Purification of His-FLAG-YscQ shows no major copurification of other injectisome components; subsequent analysis by size exclusion chromatography indicates the formation of YscQ tetramers.

A: Silver staining of a FLAG affinity purification of strain AD4014 (His-FLAG-YscQ). FT, flow-through; W, washing steps; El., elution steps. The circle denotes the size of YscQ, the asterisk denotes a background band. **B**: Immunoblot analysis of fractions resulting from a size exclusion chromatography of the pooled elution fraction from A. Numbers denote the molecular weight in kDa corresponding to the respective fractions. VV, void volume

4.4.4. Constructs for the crystallization of injectisome components

In the framework of the Sinergia project, several constructs have been generated for crystallization and structure determination in the group of Dirk Heinz at the Helmholtz Centre for Infection Research, Braunschweig, Germany (Figure 4.25, Table VII). As the structure determination is part of the ongoing work in the Sinergia project, this chapter focuses on the biochemical properties of the corresponding protein domains.

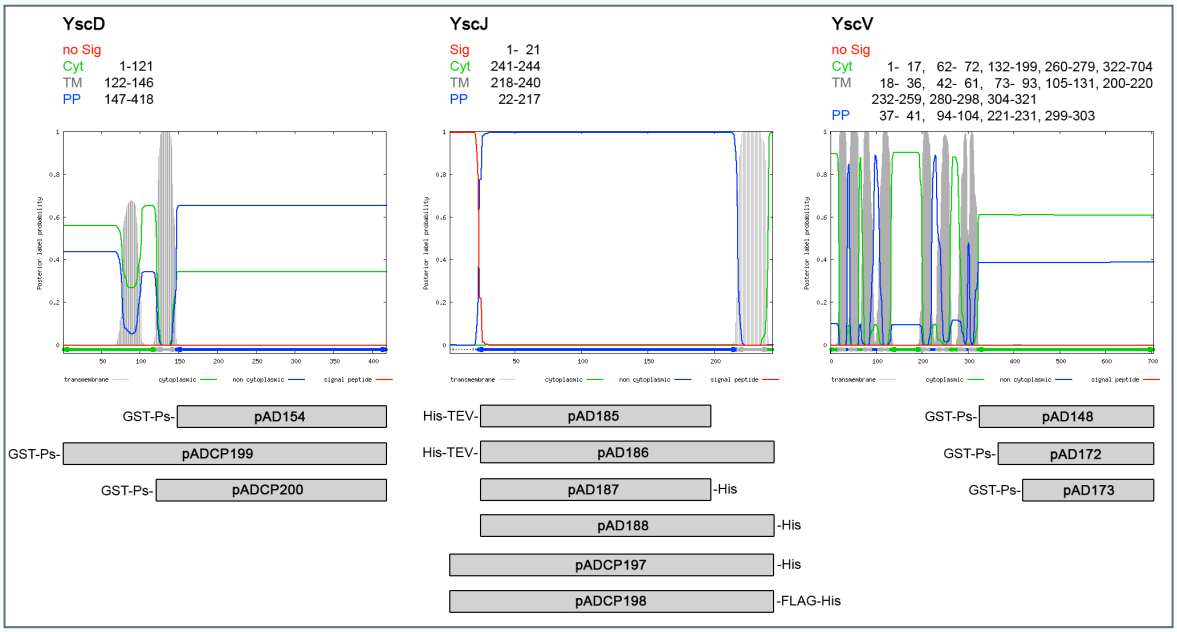

Figure 4.25: Topology of YscD, YscJ, and YscV, and schematic depiction of the proteins expressed in the denoted constructs.

Upper part: Phobius domain prediction. Numbers correspond to amino acid positions of the domains predicted to be located in the respective compartments, graphs depict the calculated probability of the prediction. Red, signal sequence (Sig); green, cytosolic domain (Cyt); gray, TM helix (TM); red, periplasmic domain (PP). Lower part: Schematic depiction of the generated constructs. Note the different scale of the x axis between the proteins.

The proposed cytosolic domain of YscV

YscV is a multi-membrane spanning protein. The transmembrane helices are clustered in the N-terminus (see Figure 4.25). The C terminus harbors the largest soluble domain among all IM export proteins YscR, S, T, U, V, which makes it an interesting candidate for regulatory functions. This domain is predicted to be located in the cytosol by most topology prediction programs. Recently, the C terminus of the homologue HrcV from *Xanthomonas campestris* pv. Vesicatoria has been shown to be localized in the cytosol (Berger *et al.*, 2010).

Name	Protein	Expressed domain	Fusion (Expression vector)
pAD148	YscV	putative cytosolic domain (aa 322-704)	N-terminal GST-PreScission (pGEX-6P-1)
pAD172	YscV	stable fragment of putative cytosolic domain (aa 356-704)	N-terminal GST-PreScission (pGEX-6P-1)
pAD173	YscV	shorter putative cytosolic domain lacking putative additional TM helices (aa 412-704)	N-terminal GST-PreScission (pGEX-6P-1)
pAD154	YscD	putative periplasmic domain (aa 150-418)	N-terminal GST-PreScission (pGEX-6P-1)
pADCP199	YscD	full-length protein (aa 1-418)	N-terminal GST-PreScission (pGEX-6P-1)
pADCP200	YscD	trans-membrane helix and putative periplasmic domain (aa 120-418)	N-terminal GST-PreScission (pGEX-6P-1)
pAD185	YscJ	putative stable periplasmic domain (20-195)	N-terminal His_6-TEV (pET-21b)
pAD186	YscJ	complete periplasmic domain (aa 20-217)	N-terminal His_6-TEV (pET-21b)
pAD187	YscJ	putative stable periplasmic domain (aa 20-195)	C-terminal His_6 (pET-21b)
pAD188	YscJ	complete periplasmic domain (aa 20-217)	C-terminal His_6 (pET-21b)
pADCP197	YscJ	full-length protein (aa 1-244)	C-terminal Gly_4-His_6 (pET-21b)
pADCP198	YscJ	full-length protein (aa 1-244)	C-terminal Gly_4-FLAG-His_8 (pET21-b)

Table VII: Constructs used for crystallization within the Sinergia project

As the most C-terminal transmembrane domain of YscV was predicted to consist of amino acids 304-321, the construct pAD148 encodes amino acids 322-704 in the bacterial expression vector pGEX-6P-1 with an N-terminal cleavable GST-PreScission tag.

E. coli harboring pAD148 were used for an expression and purification test. $YscV_{322-704}$ was overexpressed in *E. coli* Top10 upon induction with 0.2 mM IPTG. A one-step affinity purification with Glutathion Sepharose was performed, and the eluted protein was cleaved with PreScission protease. The results showed that $YscV_{322-704}$ can be produced and purified from *E. coli*. The resulting protein was soluble and ran according to its calculated MW on an SDS-PAGE gel after proteolytic cleavage (Figure 4.26).

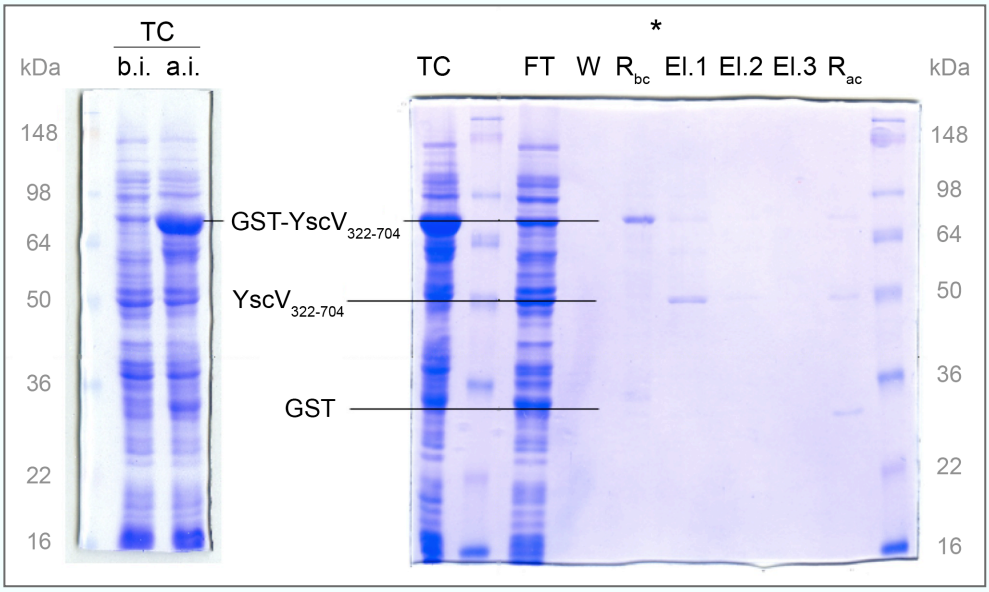

Figure 4.26: Expression, purification, and cleavage of $YscV_{322-704}$.

Asterisk denotes cleavage of the protein by addition of PreScission protease. TC, total cell; b.i., before induction; a.i., after induction; FT, flow-through; W, wash; R_{bc}, resin before cleavage; El., elution fractions; R_{ac}, resin after cleavage

YscV expressed from this construct did not yield suitable crystals (U. Wiesand, personal communication). Limited proteolysis resulted in a stable fragment lacking about 30-40 amino acids at the N terminus. Sequence analysis and comparison with the flagellar homologue FlhA suggested that the cleavage occurs at Ser354 (U. Wiesand, personal communication). Therefore, a further construct (pAD172) was cloned expressing amino acids 356-704. Last, results from *X. campestris* (Berger, 2005) showed two further putative transmembrane helices in HrcV. Alignment of the two structures predicted the most C-terminal of these helices to end at amino acid 414. Although the evidence for these additional transmembrane helices is weak, a third construct (pAD173), coding for amino acids 412-704, was constructed to exclude the possibility of transmembrane helices preventing crystallization of the construct.

At present, only two of the constructs, pAD148 and pAD172, could be studied in detail. Both proteins were well expressed and soluble. After purification, 5-10 mg protein per liter solution could be obtained for pAD148 (Wiesand, 2010). Both constructs unexpectedly showed oligomerization properties. While pAD148 led to the formation of various oligomeric species, the stable fragment encoded for by pAD172 showed a distinct peak at a M_r of 480 kDa, corresponding to a dodecamer of $YscV_{356-704}$ (MW = 40.2 kDa), assuming a globular shape (Wiesand, 2010).

The periplasmic domain and full-length protein of YscD

YscD is a bitopic protein predicted to have a shorter N-terminal cytosolic domain (amino acids 1-121) and a larger C-terminal periplasmic domain (amino acids 147-418) (Figure 4.25). It is less conserved among species than most other basal body components; its role has been unclear for a long time. The results of the assembly determination (chapter 3) suggested that it might link the two membrane rings. This view is in accordance with recent models based on structure determination (Spreter *et al.*, 2009).

The linking domain in the periplasm would be the C terminus of YscD. To determine the structure of this domain, pAD154 was created, which encodes amino acids 150-418 in the bacterial expression vector pGEX-6P-1 with an N-terminal cleavable GST-PreScission tag. *E. coli* harboring pAD154 were used for an expression test. YscD was strongly overexpressed upon induction with 0.2 mM IPTG and soluble (Figure 4.27). Further purification and characterization was performed in the lab of Dirk Heinz.

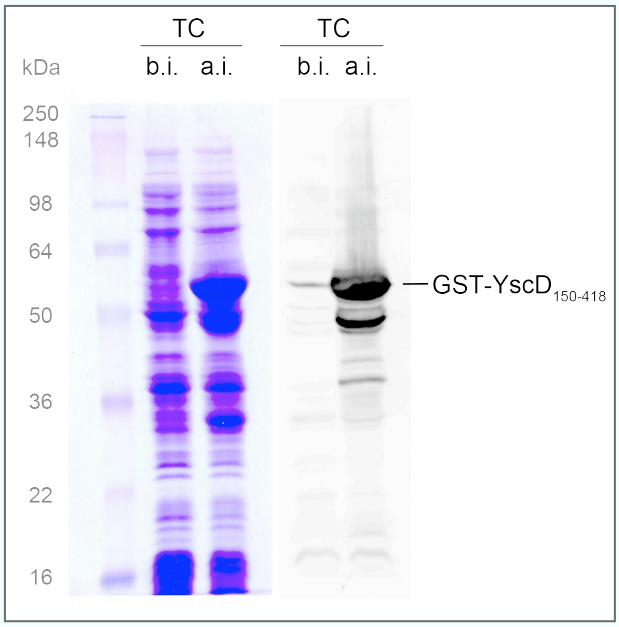

Figure 4.27: Expression of $YscD_{150-418}$. Left side: Coomassie staining; right side: immunoblot anti-YscD. TC, total cellular proteins; b.i., before induction; a.i., after induction

YscD could be purified in large amounts from plasmid pAD154, was soluble and monomeric (U. Wiesand, personal communication). It is being studied in Dirk Heinz' lab at the moment.

For a new approach based on the co-crystallization of the membrane ring structures, two further YscD constructs were generated, expressing the full-length protein (pADCP199), and the putative periplasmic domain including the transmembrane helix (amino acids 120-418, pADCP200).

The periplasmic domain of YscJ

YscJ is a bitopic protein that has been suggested to form the MS ring in the IM (Yip *et al.*, 2005). It has a predicted N-terminal sec signal sequence, a lipid anchor at position Cys-19 and a TM helix at the very C-terminus, which is not present in all homologues (Michiels *et al.*, 1991; Burghout, 2004; Silva-Herzog *et al.*, 2008).

To determine the structure of the strongly conserved periplasmic domain, several constructs have been cloned (Table VII). These constructs cover either the complete periplasmic domain or the equivalent of the stable periplasmic domain crystallized in EPEC (Yip *et al.*, 2005) and have been fused to either an N-terminal or a C-terminal His tag.

All four proteins were expressed well and soluble (U. Wiesand, personal communication). They are being studied in Dirk Heinz' lab at the moment.

For a new approach based on the co-crystallization of the membrane ring structures, two further YscJ constructs were generated based on the functional proteins used for the copurification of the ring structures in *Yersinia* (chapter 3). They encode for the full-length protein including the signal sequence, fused either to a C-terminal Gly_4-His_6 tag (pADCP197, based on AD40082), or to a C-terminal Gly_4-FLAG-His_8 tag (pADCP198, based on AD40085).

4.4.5. Discussion

Substructures of the injectisome have been purified from various organisms, using similar protocols that include spheroplast generation, lysis, and differential centrifugation (Kubori *et al.*, 1998; Tamano *et al.*, 2000; Sekiya *et al.*, 2001). To obtain copurification of the membrane ring proteins of the *Y. enterocolitica* injectisome, the protocol had to be adapted, and the adhesin YadA, which led to aggregation of the spheroplasts, was removed. The resulting protocol, which led to consistently good spheroplast generation and lysis, was combined with a one-step affinity purification or TAP in strains expressing functional tagged components. During the course of this work, the purification of *Shigella* NCs using a His tag at the YscD homologue MxiG (Zenk *et al.*, 2007), illustrated the principal applicability of this approach. Surprisingly, a strain co-expressing His-YscD and YscJ-FLAG was non-functional, in contrast to strains expressing either of both proteins or even larger tags at the respective positions. This finding suggests a close proximity of the N-terminus of YscD and the C-terminus of YscJ, both located in the cytosol. Recently, this was demonstrated for the *S. enterica* SPI-1 homologues; by crosslinking and mass spectrometry, Schraidt *et al.* (2010) could show that the extreme N-terminus of PrgH (Met-1 and Lys-4) and the extreme C-terminus of PrgK (Lys-246 and Lys-248) are in close proximity.

Using tags on either YscD or YscJ, the membrane-ring forming proteins YscC, YscD, and YscJ could be copurified, which allowed to determine the assembly order of these components (chapter 3). This purification could be slightly improved by adding a second purification step. In a more detailed analysis, the copurification of two more proteins could be shown: The needle subunit YscF (by immunoblot), and the IM export machinery component YscV (by mass spectrometry). The high proportion of the respective tagged component in relation to the copurified components, especially YscF, suggests that the purification at least to some extent yields monomeric proteins and partially assembled complexes. Especially the contact between needle and basal body seems to be fragile. In the few cases, in which purification samples were analyzed by electron microscopy, no needle complexes were observed. Like it is the case for other bacteria, there was no copurification of cytosolic components. This was further confirmed by purification of the tagged C ring component YscQ, which yielded tetramers, but no copurification of the membrane ring proteins, in agreement with the data obtained for the dynamics of YscQ (chapter 4.3).

In summary, the modified purification procedure developed in this study can be used for the purification of subcomplexes of the injectisome. The limited copurification of the needle subunit and an IM component shows that, in principle, the purification of larger parts of the injectisome is possible with this protocol. However, for this task, the purity and the ratio of fully assembled complexes to monomers have to be increased.

The preliminary results of the characterization of the cytosolic domain of YscV are discussed in the context of the IM export machinery (chapter 4.5).

4.5. The type III secretion "inner membrane export machinery"

4.5.1. An improved method to generate non-secreting mutant strains of *Yersinia*

Genetic alterations in *Yersinia enterocolitica*, either on the virulence plasmid pYV, or on the chromosome, are usually achieved by a two-step homologous recombination. A mutator plasmid carrying the altered gene sequence flanked by two homologous regions is first integrated into the native genetic environment and subsequently removed (Kaniga *et al.*, 1991). The second step occurs spontaneously at a low rate, while the strain is propagated for 36 to 72 hours in non-selective medium, and is selected for sucrose tolerance.[14] After removal of the mutator plasmid, the resulting clones carry either the wild-type gene or the altered gene. If the recombination event would occur randomly in both flanking regions, the ratio of clones carrying the mutated gene would be 50%. However, even if the length of the flanking regions is identical, the actual mutant ratio is significantly lower in most cases, ranging between 10^{-1} and 10^{-3}. As this makes the generation of mutants a labor- and resource-demanding task, a method was devised to increase the fraction of mutant strains.

Yersinia that carry a functional T3S system are impaired in growth in the absence of calcium at 37°C (Straley, 1991). Thus, the propagation of the strains after the first recombination event was performed in secretion-permissive medium (BHI-Ox) at 37°C (see Material and methods for details). Since T3S mutant strains are able to replicate faster under these conditions, this approach should increase their ratio.

By design, this method can only be applied to generate mutant strains that are non-functional for type III secretion, such as mutants in the IM export machinery proteins YscR, S, T, U, V.

Table VIII shows the outcome of the revised protocol in comparison to the traditional method to generate such mutants (Kaniga *et al.*, 1991). Ten different clones (five different strains, two clones per strain) that had undergone the first recombination event were propagated as described above. After three twelve-hour propagation steps, the cultures were plated on agar containing sucrose to select for the second recombination event. Colonies were then tested for the presence of the wild-type or mutated gene by colony PCR. Using the traditional method, only one of 144 tested colonies carried a mutated gene, whereas the improved method yielded

[14] The mutator plasmid pKNG101 carries the levansucrase gene that confers lethality in the presence of sucrose.

22 mutants out of 120 tested colonies, covering all five strains. The efficiency of the method was increased from 0.7% to 18.3%.

	Traditional method	Revised method
Colonies tested	144	120
Mutant colonies	1	22
Wild-type colonies	143	98
Ratio of mutant colonies	0.7%	18.3%
Generated mutant strains	1 / 5	5 / 5

Table VIII: The revised method to generate non-secreting mutant strains of *Yersinia* significantly increases the ratio of mutant colonies

Comparison of the efficiency of the traditional method (Kaniga *et al.*, 1991) and the revised method in generating non-secreting mutant strains.

4.5.2. Analysis of the IM export machinery YscRSTUV

Analysis and complementation of single and complete mutants in YscR, YscS, YscT, YscU, and YscV

Mutant strains were generated for each of the single proteins YscR, S, T, U, V, as well as for all five proteins (see table IX for details). As *yscRSTU* are located adjacently in the *virB* operon, while *yscV* is located in another operon, complete deletions were generated by deleting *yscRSTU* in strains already lacking *yscV*.

Strain names*	Genotype	Secretion	Complementation	C ring formation
AD4031 / AD4032	*ΔyscR*	-	+	decreased
AD4033 / AD4034	*ΔyscS*	-	+	decreased
AD4035 / AD4036	*ΔyscT*	-	+	wild-type
LY4001 / AD4026	*ΔyscU*	-	+	wild-type
AD4037 / AD4038	*ΔyscV*	-	+	decreased
AD4107 / AD4108	*ΔyscRSTUV*	-	+	decreased

*: Name of the strain carrying the mutated gene / the mutated gene in combination with *egfp-yscQ*.
In the case of the complete deletion *ΔyscRSTUV*, the strains additionally are *yscJ-flag-his*.

Table IX: Overview of the strains lacking the IM export machinery proteins YscR, S, T, U, V, and their phenotypes.

As expected, all strains were unable to secrete effector proteins, and could be complemented *in trans* by plasmids expressing the removed protein (pMA19, pMA22, pAD152, pLY7, pAD153, pAD189 for YscR, S, T, U, V, and the complete deletion, respectively) (Figure 4.28).[15]

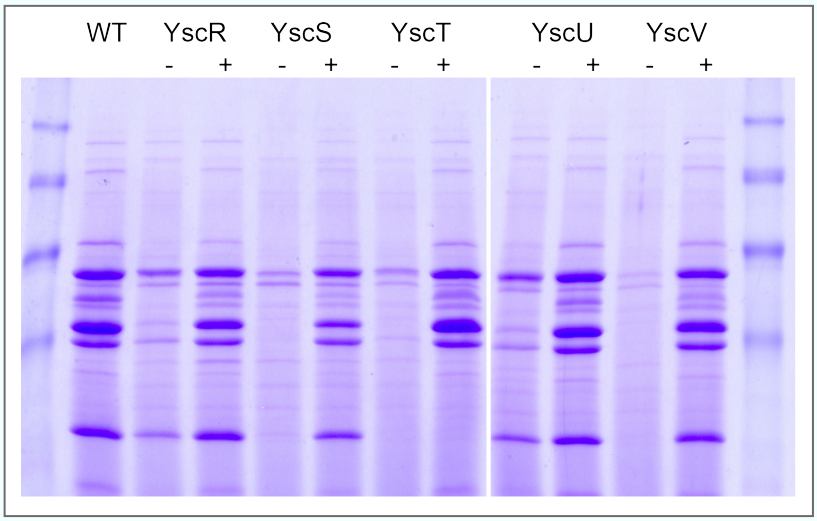

Figure 4.28: Mutants in the IM export machinery proteins are defective in effector secretion and can be complemented *in trans*.

Coomassie staining of *in vitro* secreted proteins in strains lacking the denoted proteins that were complemented *in trans*: MRS40 (WT); AD4031(pMA19) (ΔYscR + pBAD-*yscR*); AD4033(pMA22) (ΔYscS + pBAD-*yscS*); AD4035(pAD152) (ΔYscT + pBAD-*yscT*); LY4001(pLY7) (ΔYscU + pBAD-*yscU*); AD4037(pAD153) (ΔYscV + pBAD-*yscV*). -: plasmid not induced; +: induction with 0.2% arabinose.

The proteins of the IM export machinery have been proposed to localize to a membrane ring within the MS ring, where they would exert their role in substrate recognition (Sorg *et al.*, 2007) and export; only one copy of each protein would fit into this position. Therefore, it is crucial to establish the stoichiometry of the proteins; for this reason, we determined the induction level that was required for *in trans* complementation of each protein.

Interestingly, strong induction (0.3% arabinose) of YscR, but no other protein, led to cell lysis (Figure 4.29) and a low final OD (data not shown). More importantly, the required arabinose concentration for an induction level that completely restores effector secretion was about 0.03% for YscR and YscS. The same concentration of 0.03% was required for YscT and

[15] Plasmids pMA19 and pLY7 have a basal expression level even without arabinose induction under the used conditions. Uncomplemented mutant strains did not show any effector secretion (data not shown).

YscU (not shown). However, YscV required an induction level of 0.3% to be expressed at a concentration that completely restores secretion (Figure 4.29).

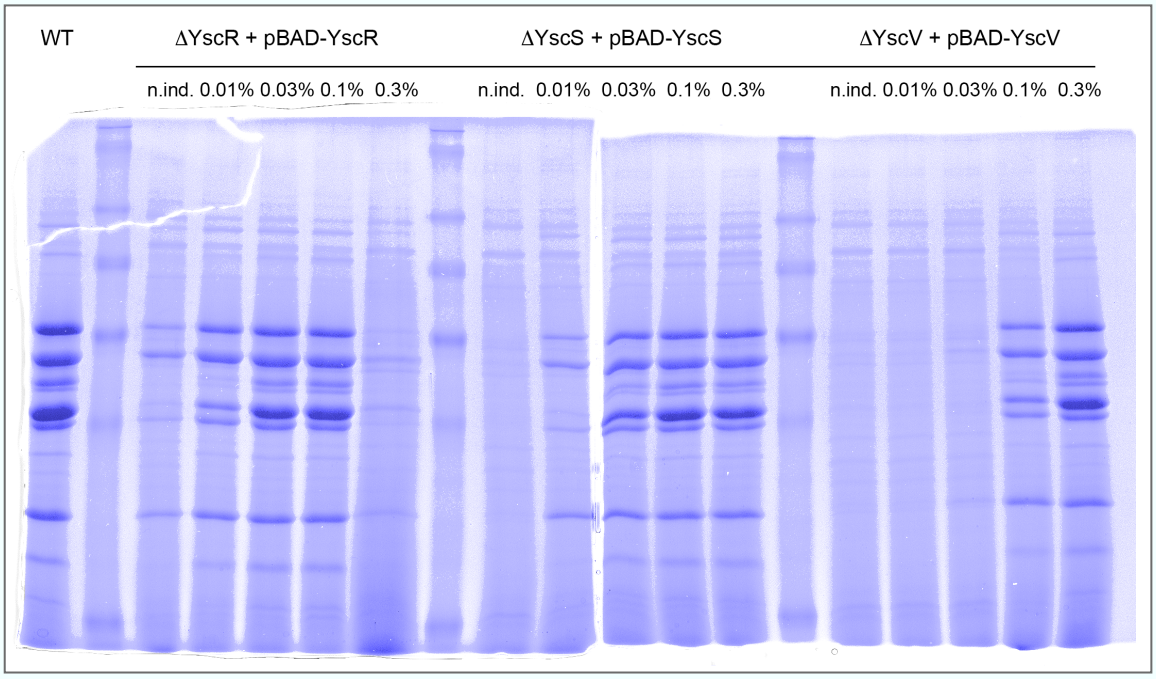

Figure 4.29: YscV has to be induced by a significantly higher arabinose concentration than YscR or YscS to complement for effector secretion.

Coomassie staining of secreted proteins in strains: MRS40 (WT); AD4031(pMA19) (ΔYscR + pBAD-*yscR*); AD4033(pMA22) (ΔYscS + pBAD-*yscS*); AD4037(pAD153) (ΔYscV + pBAD-*yscV*). Induction by different arabinose concentrations, n.ind.: not induced.

Even though all proteins were cloned in the same way, with the start codon at the identical position of the same vector, protein expression does not necessarily directly correlate with the arabinose concentration used for induction. Although this experiment therefore only allows qualitative statements, the result indicates a higher stoichiometry for YscV than for the other members of the IM export machinery.

Functionality and dominant negative effect of fluorescently tagged protein variants

As the study of fluorescent fusions can help to gain insight into both stoichiometry and assembly order, several fusions to the IM export machinery proteins were tested for functionality and analyzed under the fluorescence microscope.

Transmembrane helix predictions in combination with knowledge about the existing fusion proteins YscRS (in *Y. pestis* FV-1; Touchman *et al.*, 2007) and YscTU (in the *Chlostridium* flagellar homologues, also functional in *Salmonella*; Van Arnam *et al.*, 2004), suggested that the C-termini of all five proteins are localized in the cytosol, making them suitable for fusions to EGFP, which allows the easier visualization of weak spots in our experimental settings (own unpublished data)[16]. As N-terminal fusions could interfere with the sec signal sequence predicted for some of the proteins, all proteins were fused to EGFP at their C terminus. YscT and YscV, which have no predicted N-terminal sec signal sequence, were additionally cloned as N-terminal EGFP fusions.

As shown in Figure 4.30 A, the two N-terminal fusions as well as the C-terminal fusions of YscR, YscS, and YscV did not restore secretion in the respective mutant strains and were therefore considered non-functional. In contrast, YscT-EGFP and YscU-EGFP did complement for secretion.

As non-functional mutants of cooperatively acting multimeric proteins can show a dominant negative effect when coexpressed with functional wild-type variants of the proteins, the functionality of injectisomes was tested in wild-type strains coexpressing the non-functional proteins YscR-EGFP, YscS-EGFP, or YscV-EGFP. However, even at an induction level far above the levels required for complementation, no negative effect of any of these fusion proteins could be observed (Figure 4.30 B). This implies that the fusion proteins are not or less efficiently integrated into injectisomes than the wild-type proteins.

[16] Recently, a study investigating the topology of the *Xanthomonas campestris* homologues (Berger *et al.*, 2010) suggested different topologies for YscR, YscS, and YscT. However, the presented results are at odds with the derivations from the fusion proteins and most *in silico* predictions. At the present stage, the topologies of the three small IM export machinery proteins YscR, YscS, and YscT remain unclear.

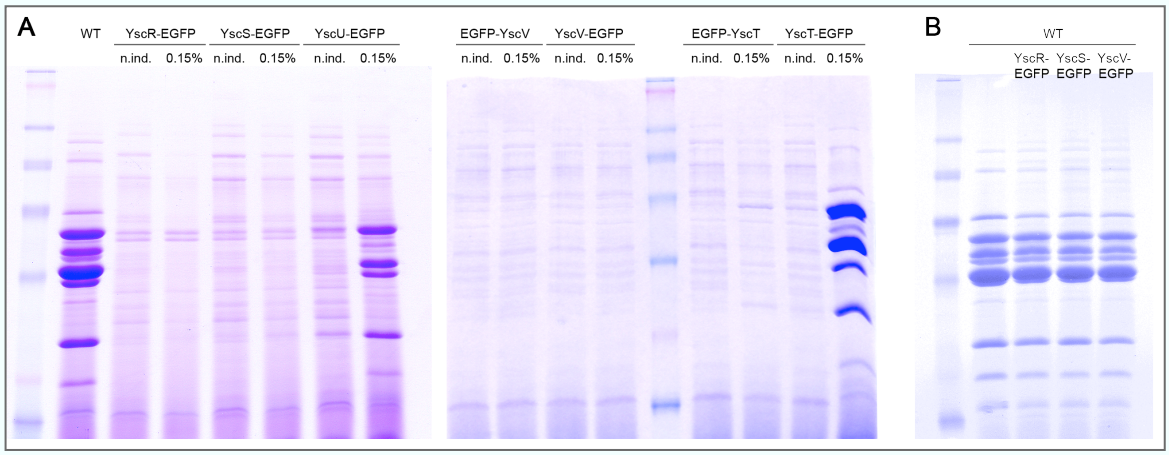

Figure 4.30: YscT-EGFP and YscU-EGFP are the only tested fusion proteins that are functional. The non-functional EGFP fusions do not show a dominant negative effect.

A: Complementation of effector secretion in the corresponding mutant strains by expression of fluorescent fusion proteins. Strains: MRS40 (WT); AD4031(pAD192) (ΔYscR + pBAD-*yscR-egfp*); AD4033(pAD194) (ΔYscS + pBAD-*yscS-egfp*); LY4001(pAD195) (ΔYscU + pBAD-*yscU-egfp*); AD4037(pAD159) (ΔYscV + pBAD-*egfp-yscV*); AD4037(pAD155) (ΔYscV + pBAD–*yscV-egfp*); AD4035(pAD160) (ΔYscT + pBAD-*egfp-yscT*); AD4035(pAD161) (ΔYscT + pBAD-*yscT-egfp*). *In trans* expression of the fusion proteins was either not induced (n.ind.) or induced by 0.15% arabinose (0.15%). **B**: Coexpression of the non-functional fusion proteins YscR-EGFP (from pAD192), YscS-EGFP (pAD194), or YscV-EGFP (pAD155) with the WT protein in strain MRS40. Plasmids were induced twice with 0.3% arabinose.

EGFP-YscV assembles in the membrane independently of YscN, but requires YscJ for stable localization

All C-terminal EGFP fusions were tested under the fluorescence microscope. Neither the non-functional fusions to YscR and YscS, nor the functional fluorescent variants of YscT and YscU showed the appearance of fluorescent membrane spots when induced at the level required for complementation of secretion (0.03% arabinose) or stronger (0.3%) (data not shown). In the case of the functional proteins YscT-EGFP and YscU-EGFP, this indicates a stoichiometry within the functional injectisome, which is below the detection limit.[17]

In contrast, YscV-EGFP showed the appearance of membrane spots (Figure 4.31), indicating a higher stoichiometry of YscV.

To test for the significance of the YscV-EGFP foci, they were colocalized with YscC-mCherry. As visible in Figure 4.31 A, there are fewer YscV spots than YscC spots, but YscV spots do largely colocalize with YscC spots, suggesting that they can be used as a read-out for YscV assembly.

Further, YscV-EGFP localization was tested in strains lacking either the MS ring component YscJ or the ATPase YscN. Lack of YscN did not influence the localization of YscV-EGFP (Figure 4.31 B). As, *vice versa*, lack of YscV does not prevent assembly of YscN (chapter 3), this suggests that assembly of YscV occurs independently from the assembly of the ATPase – C ring complex.

Removal of YscJ caused a unique phenotype for YscV-EGFP localization: While fluorescent foci were detectable under the microscope, they were highly motile. Figure 4.31 C shows series of images taken at the same position in intervals of five seconds. Whereas YscV-EGFP spots normally displayed a stable localization, the spots in a strain lacking YscJ quickly changed their positions within the bacterial membrane. This suggests that the presence of the MS ring is not required for the oligomerization of YscV-EGFP, but for its localization to the machinery (which is itself anchored within the peptidoglycan layer, most likely through YscC).

[17] As the fusion proteins could not be detected by immunoblot due to low protein levels and lack of specific antibodies, proteolytic cleavage of the fluorophores cannot be excluded at the present stage.

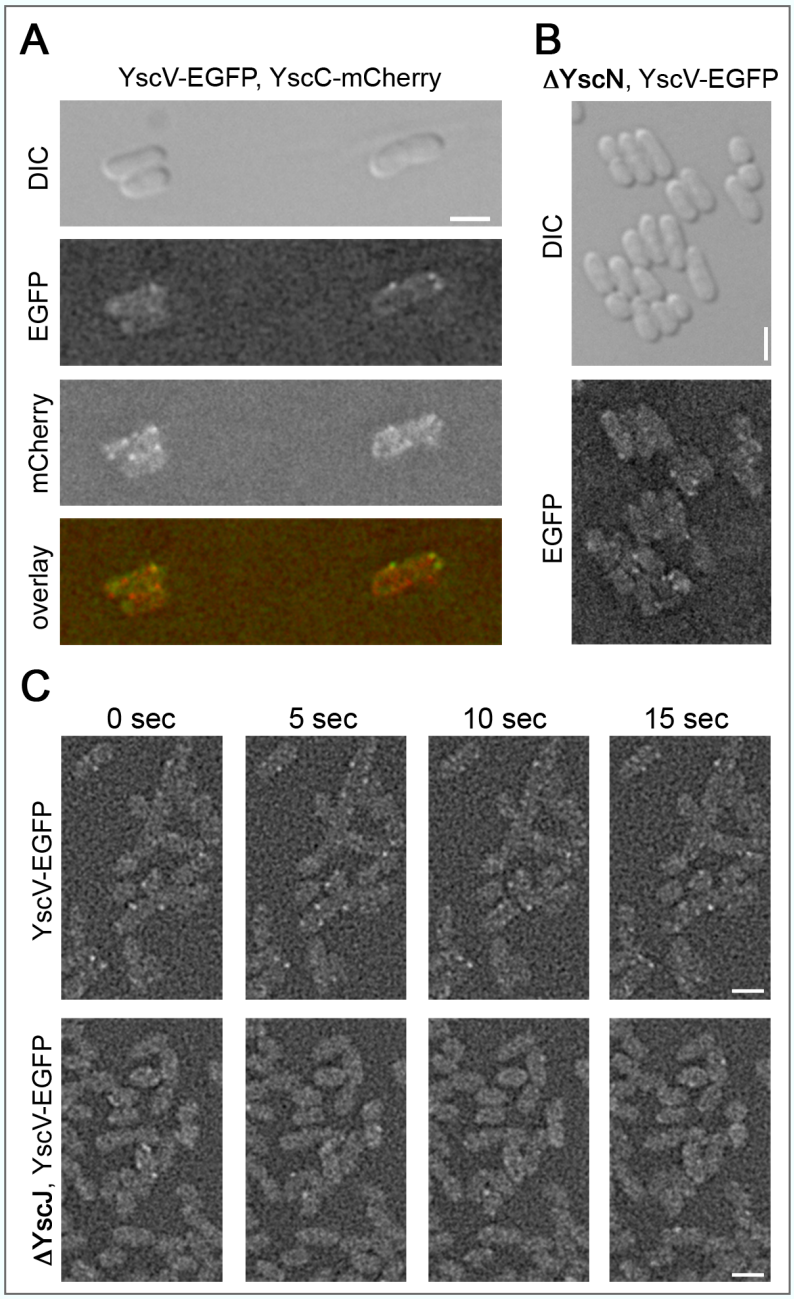

Figure 4.31: YscV-EGFP forms membrane foci in the absence of YscN, but requires YscJ for stable localization.

A: Fluorescence micrograph showing the partial colocalization of YscV-EGFP and YscC-mCherry in strain ADMA4158(pAD155) (YscC-mCherry, ΔYscV + pBAD-*yscV-egfp*). **B**: Fluorescence micrograph showing YscV-EGFP spot formation in strain AD4161(pAD155) (ΔYscN, ΔYscV + pBAD-*yscV-egfp*). **C**: Fluorescence micrograph showing pattern of YscV-EGFP localization over time for strains ADMA4158(pAD155) (YscC-mCherry, ΔYscV + pBAD-*yscV-egfp*) and AD4160(pAD155) (ΔYscJ, ΔYscV + pBAD-*yscV-egfp*). Note that the z level slightly changes with time due to shrinking of the agar layer used in microscopy, which may influence the fluorescence pattern or intensity. Scale bars: 2 µm.

4.5.3. Discussion

The IM export machinery consists of the five proteins YscR, S, T, U, V. In the determination of the assembly order, we found that, while deletion of some of these proteins reduced the number of EGFP-YscQ foci, none of them was required for the assembly of the cytosolic components. This result was unexpected, considering the proposed localization of the proteins within the MS ring. There are three possible explanations for this: (i) YscR, S, T, U, V assemble prior to the MS ring *in vivo*, but there is no checkpoint for their incorporation; (ii) they can diffuse laterally into the MS ring; (iii) at least some of the subunits are localized outside of the MS ring. All of these explanations have consequences for the function of the IM export machinery and the complete injectisome.

For this reason, we studied the function and localization of these proteins in more detail. As expected, all five proteins were essential for secretion, and the deletion strains could be complemented by expression of the respective protein *in trans*. Subsequently, we checked the required induction level and the functionality and localization of EGFP fusions to the C termini of the proteins. We found that in both cases, YscV displayed a unique behavior within the protein family[18]. It did not only require a substantially higher induction level to complement a mutant for effector secretion, but also was the only protein that could be detected in spots at the bacterial membrane (even though YscV-EGFP was, as the fusions to YscR and YscS, non-functional).

We thus focused our studies on the role of YscV, the protein with the most TM helices (eight; Plano *et al.*, 1991) and the largest soluble domain (> 40 kDa) within the IM export apparatus. The flagellar homologue FlhA has been shown to interact with FlhB (YscU), the MS ring component FliF (YscJ) and the components of the ATPase complex FliH and FliI (YscL, N) (McMurry *et al.*, 2004), but the interactions between these proteins and wild-type FlhA are weak (Minamino *et al.*, 2010). Interestingly, a mutation in the cytosolic domain of FlhA restored flagellar protein export in a FliH (YscL) deletion mutant (Minamino *et al.*, 2003).

Our data showing the visibility of YscV-EGFP foci at the membrane and the higher induction level required for complementation suggest that YscV is present at a higher stoichiometry than the other components of the IM export machinery. Stoichiometry of YscV is a critical

[18] Notably, while FlhB and FlhA are in the same operon in most flagellar systems, YscV is in a separate operon in all non-flagellar T3S, except for *Chlamydia* (Hefty and Stephens, 2007). However, the *Chlamydia* T3S represents an own lineage, that is closely related to the flagellar T3S. Some flagellar genes, including FlhA, even interact with injectisome components, including the YscU homologue, in this bacterium (Stone *et al.*, 2010).

question, as the presence of multiple copies would exclude the proposed localization within the MS ring. In agreement with our results, the analysis of the soluble cytosolic domain indicated the formation of a dodecamer (Wiesand, 2010), which intriguingly matches the rotational symmetry for the MS ring (Hodgkinson *et al.*, 2009).

In the flagellum, various FlhA mutants show a strong dominant negative effect (McMurry *et al.*, 2004; Saijo-Hamano *et al.*, 2004), suggesting a higher stoichiometry. Multimerization was demonstrated for the soluble domain of FlhA (Zhu *et al.*, 2002). However, there is conflicting evidence; in another publication, a similar part of FlhA was found to be monomeric by analytic gel filtration (Saijo-Hamano *et al.*, 2004).

In a recent publication, the structure of the C-terminal cytosolic domain of the *Salmonella* YscV homologue InvA has been solved (Worrall *et al.*, 2010). It displays a compact structure with one of the subunits resembling the E subunit of the peripheral stalk of the archeal A_0A_1 ATPase, which shows a possible mode of interaction with YscN. Importantly, this study showed that InvA contains a structural "ring building domain", as has been found in all membrane ring-forming injectisome subunits (Spreter *et al.*, 2009), even though no stable multimers could be detected in solution (Worrall *et al.*, 2010).[19]

We analyzed the localization and function of YscV-EGFP in various strain backgrounds. YscV-EGFP did not complement a deletion in YscV, but also displayed no dominant negative effect. This suggests that it is less efficiently integrated into assembling injectisomes than the WT YscV. As we could not study the stability of the fusion protein so far, the results based on localization of YscV-EGFP have to be treated with care. An antibody against YscV is currently being produced, which will help to overcome some of these problems.

YscV-EGFP largely colocalized with YscC-mCherry, indicating that the protein can be used for localization studies. Spot formation did not depend on YscN. This suggests an independent assembly of YscV and the ATPase – C ring complex (which does not exclude subsequent interaction and stabilization, as indicated by the lower number of C ring foci in a strain lacking YscV). Strikingly, in a strain lacking the MS ring component YscJ, YscV-EGFP foci appeared, but were highly motile within the membrane. This is a unique phenotype, as all other observed fusion proteins (as well as YscV-EGFP in the presence of YscJ) stably localize, indicating that they are anchored within the peptidoglycan layer. Our

[19] Two recent reports on the crystal structure of the cytosolic domain of the flagellar homologue FlhA (Moore and Jia, 2010; Saijo-Hamano *et al.*, 2010) show that the overall structure is similar to the one of InvA. Neither of these studies reports indicates whether the domains were monomeric or multimeric in solution.

data therefore suggest that YscV-EGFP multimerization does not depend on the presence of the MS ring, but that it binds to YscJ, or a protein which depends on YscJ for its localization, in wild-type conditions. The copurification of YscV with the MS ring (chapter 4.4) gives further evidence for this hypothesis.

Taken together, our data support a specific role for YscV in the function of the IM export apparatus and indicate a higher stoichiometry compared to other members of this subfamily. However, in the absence of further data, this interpretation remains highly speculative. The localization of the fluorescent YscV might help to pinpoint its localization and the requirements therefore. Based on the crystal structure of the homologue InvA, an EGFP fusion site less likely to disturb the interactions of YscV with other proteins, and subsequently injectisome function in the hybrid strain, might be found. To test for the role of the TM helices of YscV, a strain overexpressing only the soluble domain of YscV in a *ΔyscV* background could be assayed for complementation of secretion.

Obviously, more work is required to uncover the mechanism of the IM export apparatus. While the nature of these proteins makes them difficult study objects, rewarding information about a central, but so far surprisingly uncharacterized mechanism – recognition and export of T3S substrates – is to be gained.

Chapter 5

Conclusions and Outlook

The principal goal of my PhD thesis was to determine the assembly order of the *Yersinia* injectisome. We analyzed the requirements for the oligomerization and localization of various functional fluorescent injectisome components, covering major substructures of the type III secretion system, and combined the findings with data from co-immunoprecipitation experiments. Our results show that the assembly of the injectisome is initiated by formation of the secretin ring in the outer membrane, and proceeds via stepwise attachment of the MS ring components YscD and YscJ in the inner membrane. While assembly of the membrane rings is a slow process, the subsequent steps occur within short time. Here we could, for the first time, study the assembly of the cytosolic subunits of the injectisome. After completion of the membrane rings, the ATPase YscN and the C ring component YscQ can attach, requiring each other – but not the ATPase function – and the two interacting proteins YscK and YscL. The inner membrane export machinery is not required for these formation steps, and the time point of its assembly *in vivo* is so far unknown. Our results, however, indicate an independent assembly, at least for YscV, that depends on the membrane rings, but not on the cytosolic components.

These finding have structural implications, as they show that YscD connects the ring structures in the outer and inner membrane formed by YscC and YscJ. This has been recently confirmed by integration of crystal structures into medium-resolution overall structures and crosslinking analysis (Spreter *et al.*, 2009; Schraidt *et al.*, 2010). However, the exact position of the proteins within the basal body differed between these studies. In the light of these new findings, insinuating a different architecture of the membrane rings between species, it seems worthwhile to apply the copurification procedure presented in this work to determine the interactions within the membrane ring proteins by the analysis of crosslinked peptides, in order to obtain a detailed structure of the *Yersinia* injectisome basal body.

Irrespective of the recent progress in the determination of injectisome structure and assembly, the role of the inner membrane export machinery remains the enigma of type III secretion. Our data suggest that YscV plays a unique role within this protein family, as it is required in larger amounts and possibly forms oligomers. This, however, would be in conflict with its proposed site of function within the MS ring. Further studies about the localization and assembly of the IM export machinery might present an important step to reveal the mechanism of substrate selection and export, the “core process” of type III secretion.

Chapter 6

Material and methods

Bacterial strains

The strains used in this study are listed and described in Chapter 7.3.

Genetic constructions

The plasmids used in this study are listed and described in Chapter 7.4.

E. coli Top10 used for plasmid purification and cloning and *E. coli* Sm10 λpir used for conjugation were routinely grown on LB agar plates and in LB broth. Ampicillin was used at a concentration of 200 µg/ml to select for expression vectors, Streptomycin was used at a concentration of 100 µg/ml to select for suicide vectors. Plasmids were generated using either Phusion polymerase (Finnzymes, Espoo, Finland) or Vent DNA polymerase (New England Biolabs, Frankfurt, Germany). All constructs were confirmed by sequencing using a 3100-Avant genetic analyzer (Applied Biosystems, Rotkreuz, Switzerland). The oligonucleotides used for genetic constructions are listed in Chapter 7.5.

Mutators for modification or deletion of genes in the pYV plasmids were constructed by overlapping PCR using purified pYV40 plasmid as template, leading to 200 – 250 bp of flanking sequences on both sides of the deleted or modified part of the respective gene. For the mutator strains introducing EGFP, a precursor mutator vector was created as described above. Subsequently, the EGFP gene was inserted in frame from plasmid pEGFP-C1 into the digested precursor vectors. The respective regions containing the flanking sequences were subcloned into the pKNG101 suicide vector. The allelic exchange was selected by plating diploid bacteria on sucrose as described previously (1991), with the following modifications: After the integration of the mutator plasmid, 5 ml cultures of BHI-Ox were inoculated with 20 µl of pre-culture and propagated for 12 h at 37°C. This was repeated two more times, before plating 0.5 µl of the last culture on LB agar plates containing 5% sucrose.

Vectors for protein expression in *Yersinia* or for overexpression in *E. coli* were constructed according to standard cloning procedures. Affinity tags, unless stated otherwise, and the FlAsH tag were introduced with the used oligonucleotides. For vectors harboring hybrid genes for fluorescent fusion proteins, precursor vectors were generated and EGFP was introduced from pEGFP-C1, as described above. pAD166 expressing $YscN_{K175E}$ was generated by overlapping PCR using internal primers encoding for the modified protein sequence, and selected by colony PCR and sequencing. For the reporter constructs expressing 3xGFP under the control of various *Yersinia* promoters, the regions upstream of the first gene in the respective operon (250 – 350 bp) were amplified by PCR and restricted. The resulting

promoter sequence fragments were ligated with corresponding restricted fragments of pCDFduet-1 (vector backbone) and pOM-3GFP (3xGFP). The resulting clones were for their identity by colony PCR and sequencing.

Y. enterocolitica cultures for secretion and microscopy analysis

Induction of the *yop* regulon was performed by shifting the culture to 37°C, either in BHI-Ox (secretion-permissive conditions) or in BHI + 5 mM $CaCl_2$ (secretion-non-permissive conditions) (Cornelis *et al.*, 1987). Expression of the inducible constructs was induced by adding 0.05% L-arabinose to the culture just before the shift to 37°C, unless stated otherwise. The carbon source was glycerol (4 mg/ml) when expressing genes from the pBAD promoter and for *ΔyadA* strains harboring the YadA mutator pLJM31, and glucose (4 mg/ml) in the other cases.

Yop secretion

Total cell and supernatant fractions were separated by centrifugation at 20,800 g for 10 min at 4°C. The cell pellet was taken as total cell fraction. Proteins in the supernatant were precipitated with trichloroacetic acid 10% (w/v) final for 1 h at 4°C.

Secreted proteins were analyzed by SDS–PAGE; in each case, proteins secreted by 3 x 10^8 bacteria were loaded per lane. Total secreted proteins were analyzed by Coomassie staining of 12% SDS-PAGE gels. Detection of specific secreted proteins by immunoblotting was done using 15% SDS-PAGE gels. For detection of proteins in total cells, proteins from 1 x 10^8 or 2 x 10^8 bacteria were loaded per lane, if not stated otherwise, and proteins were separated on 15% SDS-PAGE gels before detection by immunoblotting.

Membranes were blocked in 5% milk powder (Coop, Basel, Switzerland) in PBS for 1 h at RT or 12 h at 4°. Immunoblotting was carried out using rabbit polyclonal antibodies (see chapter 7.6) with 5% milk powder in PBS, for 1h at RT. Detection was performed with secondary antibodies directed against rabbit Ig and conjugated to horseradish peroxidase (1:5000 with 5% milk powder in PBS; Dako), before development with ECL chemiluminescent substrate (Pierce).

For the analysis of protein expression and secretion after transient incubation in secretion-permissive conditions, bacteria were inoculated and T3S was induced as described above. After 3 h at 37°C, the OD_{600} was determined, cells were gently pelleted (2000 g, 2 min), and

resuspended in fresh medium (BHI+Ca^{2+} or BHI-Ox, at 26°C or 37°C) to a final OD_{600} of 0.4. To completely exchange the medium, cells were pelleted and resuspended a second time immediately afterwards in the same way. Afterwards, cells were incubated for 3 h in the new conditions, and proteins were analyzed as described above.

Needle purification

Needles were purified from cultures incubated under secretion-permissive conditions, essentially as described by Müller *et al.* (2005). For time course experiments, 48 ml bacteria were removed from the 500 ml culture at the given time points. For end point experiments, a 100 ml culture was used. In both cases, bacteria were harvested by centrifugation (5 min at 4000 g) and resuspended in 1 ml 20 mM Tris–HCl, pH 7.5. Needle detachment was increased by repeated pipetting through a 1 ml pipet tip. Cells were pelleted by centrifugation (5 min at 4000 g), and the supernatant containing the needles was passed through a 0.45 µm mesh filter (cellulose acetate membrane) and then centrifuged for 60 min at 20,800 g. The resulting pellet was resuspended in 20 µl or 40 µl (for time course or end-point experiments, respectively) of Lämmli buffer, 15 µl of which were analyzed by SDS-PAGE followed by immunoblotting.

Fluorescence microscopy

For fluorescence imaging, cells were placed on a microscope slide layered with a pad of 2 % agarose dissolved in water or PBS. A Deltavision Spectris optical sectioning microscope (Applied Precision, Issaquah, WA, United States) equipped with an UPlanSApo 100x/1.40 oil objective (Olympus, Tokyo, Japan) and a coolSNAP HQ CCD camera (Photometrics, Tucson, AZ, United States) was used to take differential interference contrast (DIC) and fluorescence photomicrographs. To visualize GFP and mCherry fluorescence, GFP filter sets (Ex 490/20 nm, Em 525/30 nm) and mRFP filter sets (Ex 560/40 nm, EM 632/60 nm), respectively, were used. DIC frames were taken with 0.3 s and fluorescence frames with 1.0 s exposure time. Per image, a Z-stack containing 20 frames per wavelength with a spacing of 150 nm was acquired. The stacks were deconvoluted using softWoRx v3.3.6 with standard settings (Applied Precision, WA). The DIC frame at the centre of the bacterium and the corresponding fluorescence frame were selected and further processed with ImageJ software.

Immunofluorescence

Three hours after the induction of the T3S system by temperature shift to 37°C, bacteria were attached to poly-D-lysine coated cover slips and fixed with 4% para-formaldehyde for 15 min at 25°C. Subsequent steps were performed at 4°C: Cells were blocked with 2% BSA in PBS for 60 min, incubated with primary antibody for 90 min, and subsequently incubated for 60 min either with secondary antibody, or with 2% BSA in PBS, where indicated (no sec. ab). Microscopy slides were covered with cover slips using Vectashield mounting medium and subsequently analyzed. The primary polyclonal rabbit anti-YscF antibody (MIPA 80) was first affinity-purified on YscF from purified needles (Müller *et al.*, 2005) from 900 ml culture, and subsequently preabsorbed with bacteria lacking YscF. The remaining solution was used undiluted with 2% BSA in PBS. The secondary antibody (Texas Red coupled swine anti-rabbit, Southern Biotech) was diluted 1:150 in 2% BSA in PBS. Further image analysis was performed as described above.

Fluorescence recovery after photobleaching (FRAP)

FRAP experiments were performed as described in Schulmeister *et al.* (2008). The laser for bleaching of the GFP spots emitted light at a wavelength of 488 nm. The laser was focused on the smallest possible area and fluorescence was bleached at 10% of the maximal intensity for 0.3 s. Directly afterwards, a picture was taken, which was used to determine the zero value for fluorescence normalization.

Co-immunoprecipitation

Y. enterocolitica cultures were grown in secretion-non-permissive conditions to an OD_{600} of 1.5-2.2. Protein complexes were then stabilized by crosslinking with 0.25% formaldehyde for 15 min at 37°C. Cells were harvested by centrifugation (15 min at 1500 g, 25°C) and resuspended in 1/5 volume of PBS. After a second crosslinking step (0.4% formaldehyde, 15 min, 25°C) and harvesting as before, spheroplast generation and lysis was performed as described by Kubori *et al.* (1997) and Blocker *et al.* (2001), with the modifications listed below. In short, cells were resuspended in 1/5 original volume of ice-cold spheroplasting buffer (0.75 M Sucrose, 50 mM Tris, pH adjusted with HCl to 7.8, 0.6 mg/ml Lysozyme, 6 mM EDTA), and incubated at 25°C up to 90 min, until complete spheroplast formation could be observed. Cells were lysed by addition of 1% Triton X-100 and subsequent incubation at 4°C for 15 min. After addition of 15 mM $MgCl_2$, unlysed cells were removed by

centrifugation (20 min at 6000 g, 4°C). 300 µl of anti-FLAG M2 affinity gel (Sigma-Aldrich, Buchs, Switzerland) were added to the supernatant, and the proteins were purified in batch according to the manufacturer's protocol. The elution fractions were recentrifuged to completely remove resin, and separated on 12% SDS-PAGE gels or 4-12% gradient SDS-PAGE gels (Serva, Heidelberg, Germany). Silver Staining was performed as described by Blum *et al.* (1987). Immunoblotting was carried out using rabbit polyclonal antibodies (see chapter 7.6), as described above.

Ni^{2+} affinity purification

If not indicated otherwise, the Ni^{2+} affinity purification step in a TAP experiment was performed after cell lysis and before FLAG affinity purification. 1 M imidazole (pH 8.0) solution was added to the lysate to a final concentration of 30 mM. 1/120 original culture volume of Ni^{2+}-loaded Chelating Sepharose FF slurry (GE Healthcare, Amersham, UK) was added and the mixture was incubated for 12 h at 4°C in the presence of protease inhibitor (Complete EDTA-free, Roche, Basel, Switzerland). The washing and elution steps were performed in batch according to manufacturer's protocol. Proteins binding to the Ni^{2+} column were eluted with buffer containing 500 mM imidazole and the elution fractions wee recentrifuged to completely remove resin.

Glutathion affinity purification

Cell pellets were frozen in liquid nitrogen and stored at -80°C. Before lysis, they were thawed on ice, and resuspended in 1/30 original culture volume of resuspension buffer (PBS, 0.2% Triton X-100, 1 tablet / 20 ml Complete EDTA-free protease inhibitor). Cells were lysed on ice by sonication (70% intensity, 30 intervals à 5 sec, followed by 10 sec intermissions) and centrifuged (15,500 x g, 30 min, 4°C). The centrifugation supernatant was filtered through a 0.45 µm mesh and purified according to manufacturer's conditions (GE Healthcare). On-bead digestion was performed using 15 µl PreScission Protease (GE Healthcare) in 1 ml of cleavage buffer (50 mM Tris-HCl pH 7, 150 mM NaCl, 1 mM EDTA, 1 mM DTT) and incubating the resin in this buffer for 2 hours at 4°C.

Size exclusion chromatography

Size exclusion chromatography was performed on a Tricorn 10/600 column hand-packed with Sepharose CL-2B resin (GE Healthcare) in SEC running buffer (20 mM Tris-HCl pH 8, 150 mM NaCl, 0.1% Triton X-100) according to manufacturer's protocols. The column was calibrated for MW determination in the same buffer using the Gel Filtration LMW Calibration Kit (GE Healthcare).

Mass spectrometry analysis

Purification samples for mass spectrometry analysis were reduced by addition of 15 mM DTT and incubation at 37°C for 45 min. Afterwards, samples were alkylated by addition of 80 mM iodoacetamid at 25°C for 15 min in the dark. To increase protein concentration, a TCA-Precipitation was performed for (10% v/v final concentration, 4°C, >1 h). The resulting pellet was washed twice with ice-cold aceton and resuspended in 10 µl denaturing buffer (100 mM Tris pH 8.0, 6 M Urea). The first digest was performed by addition of 1 µl endoproteinase Lys C (1h, 37°C). Afterwards, 100 mM Tris-HCl pH 8.0 was added to decrease to urea concentration to 2 M. The second digest was performed by addition of 200 ng trypsin and incubation at 37°C for 1 h, followed by addition of further 200 ng trypsin and another incubation at 37°C for 12 h.

The samples were analyzed in the lab of Paul Jenö by tandem MS using a LTQ Orbitrap mass spectrometer (Thermo Scientific, Waltham, MA, USA). Data processing was done using Mascot (Matrix Science, Boston, MA, USA).

Chapter 7

Appendix

7.1. Abbreviations

aa ..... Amino acid
BSA ..... Bovine serum albumin
CV ..... Column volume
DMSO ..... Dimethylsulfoxide
DNA ..... Desoxyribonucleic acid
DSP ..... Dithiobis[succinimidyl propionate]
DTT ..... Dithiothreitol
E. coli ..... *Escherichia coli*
ECL ..... Enhanced chemoluminescence
EDTA ..... Ethylenediaminetetraacetic acid
EHEC ..... Enterohemorrhagic *Escherichia coli*
EGFP ..... Enhanced green fluorescent protein
EM ..... Electron microscopy
EPEC ..... Enteropathogenic *Escherichia coli*
FA ..... Para-formaldehyde
FACS ..... Fluorescence activated cell sorting
FITC ..... Fluoresceine-isothiocyanate
FRAP ..... Fluorescence recovery after photobleaching
FRET ..... Förster resonance energy transfer
g ..... Gravitational acceleration constant
GFP ..... Green fluorescent protein
h ..... Hour(s)
HBB ..... Hook-basal body
IF ..... Immunofluorescence
Ig ..... Immunoglobulin
IM ..... Inner membrane
IP ..... Immunoprecipitation
kDa ..... Kilodalton
min ..... Minute(s)

mRNA ..... Messenger RNA
MS ..... Mass spectrometry
MS ring ..... Membrane/supramembrane ring
MW ..... Molecular weight
NC ..... Needle complex
Ni-NTA ..... Nickel-nitrilo tetra-acetic acid agarose
nr ..... non-redundant
o/n ..... Over night
OD_{600} ..... Optical density at 600 nm
OM ..... Outer membrane
ORF ..... Open reading frame
P. aeruginosa ..... *Pseudomonas aeruginosa*
P. syringae ..... *Pseudomonas syringae*
PAGE ..... Polyacrylamide gel electrophoresis
PBS ..... Phosphate buffered saline
PCR ..... Polymerase chain reaction
PMF ..... Proton-motive force
PP ..... Periplasm
pYV ..... Plasmid of *Yersinia* virulence
RNA ..... Ribonucleic acid
rpm ..... Revolutions per minute
RT ..... Room temperature
S. enterica ..... *Salmonella enterica*
S. flexneri ..... *Shigella flexneri*
SDS ..... Sodium dodecyl sulfate
sec ..... Second(s)
SPI-1 ..... *Salmonella* pathogenicity island 1
SPI-2 ..... *Salmonella* pathogenicity island 2
T3S ..... Type III secretion
TAP ..... Tandem-affinity purification

TCA..... Trichloro acetic acid

TEM ..... Transmission electron microscopy

TM..... Transmembrane

Tris ..... Tris(hydroxymethylaminomethane)

WT ..... Wild-type

Y. enterocolitica ..... *Yersinia enterocolitica*

Y. pestis ..... *Yersinia pestis*

Y. pseudotuberculosis ..... *Yersinia pseudotuberculosis*

According to the suggestions of the IUPAC-IUB Joint Commission on Biochemical Nomenclature (JCBN, 1983), the One-Letter or the Three-Letter code were used for amino acids.

7.2. Software

Genetic analyzes

Sequence homology searches were performed with BLAST (Altschul *et al.*, 1990).
Primers were designed using Primer3 (Rozen and Skaletsky, 2000).

Protein analyzes

Protein parameters were analyzed with the ExPASy ProtParam tool (Wilkins *et al.*, 1999).
Topology predictions were done with Phobius (Kall *et al.*, 2004).

Image processing

Stacks of fluorescence micrographs were deconvoluted using softWoRx v3.3.6 with standard settings (Applied Precision, Issaquah, WA, USA).
Image analysis and processing was done using ImageJ (US National Institutes of Health, Bethesda, MD, USA) and Photoshop CS4 (Adobe, San Jose, CA, USA).

Mass spectrometry

Mass spectrometry data were analyzed and filtered using Mascot (Matrix Science, Boston, MA, USA) and Phenix (Genebio, Geneva, Switzerland).

7.3. Bacterial strains

pYV plasmids based on pYV227 were used in KNG22703 (Kaniga *et al.*, 1991), which is an ampicillin sensitive derivate of strain W22703 (Cornelis and Colson, 1975).

pYV plasmids based on pYV40 were used in MRS40, which is an ampicillin sensitive derivate of strain E40 (Sory *et al.*, 1995).

Yersinia strain names correspond to the name of the pYV plasmid (AD4016 = MRS40(pAD4016)).

Chapter 3 – Deciphering the assembly of the *Yersinia* type III secretion injectisome

pYV plasmid	Relevant characteristics	References
pAA207	pYV227 *yscH::aphA-3* (does not encode YscH)	(Allaoui *et al.*, 1995b)
pAA210	pYV227 *yscK::aphA-3* (does not encode YscK)	(Allaoui *et al.*, 1995b)
pAD4016	pYV40 *egfp-yscQ* (pYV40 mutated with pAD118)	this work
pAD4020	pYV40 *egfp-yscQ* $yscF_{\Delta 1\text{-}74}$ (pISO4006 mutated with pAD118)	this work
pAD4022	pYV40 *egfp-yscQ ΔyscI* (pKEM4001 mutated with pAD118)	this work
pAD4024	pYV40 *egfp-yscQ* $yscO_{\Delta 4\text{-}149}$ (pISO4008 mutated with pAD118)	this work
pAD4026	pYV40 *egfp-yscQ ΔyscU* (pLY4001 mutated with pAD118)	this work
pAD4027	pYV40 *egfp-yscQ* $yscX_{\Delta 42\text{-}75}$ (pIM405 mutated with pAD118)	this work
pAD4032	pYV40 *egfp-yscQ* $yscR_{\Delta 2\text{-}207}$ (pAD4016 mutated with pAD128)	this work
pAD4034	pYV40 *egfp-yscQ ΔyscS* (pAD4016 mutated with pAD130)	this work
pAD4036	pYV40 *egfp-yscQ* $yscT_{\Delta 2\text{-}250}$ (pAD4016 mutated with pAD132)	this work
pAD4037	pYV40 $yscV_{\Delta 5\text{-}680}$ (pYV40 mutated with pAD134)	this work
pAD4038	pYV40 *egfp-yscQ* $yscV_{\Delta 5\text{-}680}$ (pAD4016 mutated with pAD134)	this work
pAD4039	pYV40 *egfp-yscQ ΔyscL* (pSI4006 mutated with pAD118)	this work
pAD4040	pYV40 *egfp-yscQ* $yscY_{\Delta 21\text{-}51}$ (pIM406 mutated with pAD118)	this work
pAD4041	pYV40 *egfp-yscQ* $lcrG_{\Delta 8\text{-}57}$ (pMRS4043 mutated with pAD118)	this work
pAD4042	pYV40 *egfp-yscQ* $lcrV_{\Delta 3\text{-}324}$ (pMRS4071 mutated with pAD118)	this work
pAD4043	pYV40 *egfp-yscQ* $yopN_{45}$ (pIM41 mutated with pAD118)	this work
pAD4049	pYV40 his_8*-flag-yscD* (pYV40 mutated with pAD138)	this work
pAD4050	pYV40 *egfp-yscD* (pYV40 mutated with pAD140)	this work
pAD4051	pYV40 $yscD_{\Delta 2\text{-}404}$ (pYV40 mutated with pAD164)	this work
pAD4052	pYV40 *egfp-yscQ* $yscD_{\Delta 2\text{-}404}$ (pAD4016 mutated with pAD164)	this work
pAD4054	pYV40 *yscJ-flag-*his_8 *yadA::pLJM31* (pAD40085 mutated with pLJM31)	this work
pAD4055	pYV40 his_8*-flag-yscD yadA::pLJM31* (pAD4049 mutated with pLJM31)	this work

pAD4061	pYV40 *egfp-yscD yscQ$_{\Delta 2\text{-}295}$* (pISOA4015 mutated with pAD140)	this work
pAD4078	pYV40 Δ*yscJ* (pYV40 mutated with pAD158)	this work
pAD4080	pYV40 *egfp-yscD* Δ*yscJ* (pAD4050 mutated with pAD158)	this work
pAD4082	pYV40 *egfp-yscQ* Δ*yscJ* (pAD4016 mutated with pAD158)	this work
pAD4088	pYV40 *his$_8$-flag-yscD* Δ*yscJ* (pAD4078 mutated with pAD138)	this work
pAD4089	pYV40 *his$_8$-flag-yscD* Δ*yscJ yadA::pLJM31* (pAD4088 mutated with pLJM31)	this work
pAD4091	pYV40 *yscJ-flag-his$_8$ yscC$_{\Delta 2\text{-}598}$* (pAD40085 mutated with pMA26)	this work
pAD4092	pYV40 *yscJ-flag-his$_8$ yscD$_{\Delta 2\text{-}404}$* (pAD40085 mutated with pAD164)	this work
pAD4104	pYV40 *egfp-yscQ yscN$_{\Delta 2\text{-}427}$* (pAD4016 mutated with pAD168)	this work
pAD4106	pYV40 *yscJ-flag-his$_8$ yscQ$_{\Delta 2\text{-}295}$* (pAD40085 mutated with pISOA131)	this work
pAD4107	pYV40 Δ*yscRSTU yscV*Δ$_{5\text{-}680}$ (pYV40 mutated with pAD170)	this work
pAD4108	pYV40 *egfp-yscQ* Δ*yscRSTU yscV*Δ$_{5\text{-}680}$ (pAD4038 mutated with pAD170)	this work
pAD4109	pYV40 *yscJ-flag-his$_8$ yscC$_{\Delta 2\text{-}598}$ yadA::pLJM31* (pAD4091 mutated with pLJM31)	this work
pAD4110	pYV40 yscJ-flag-his$_8$ yscD$_{\Delta 2\text{-}404}$ yadA::pLJM31 (pAD4092 mutated with pLJM31)	this work
pAD4111	pYV40 yscJ-flag-his$_8$ yscQ$_{\Delta 2\text{-}295}$ yadA::pLJM31 (pAD4106 mutated with pLJM31)	this work
pAD4136	pYV40 *yscN$_{\Delta 2\text{-}427}$* (pYV40 mutated with pAD168)	this work
pAD4139	pYV40 *yscN$_{\Delta 2\text{-}427}$* Δ*yscJ* (pAD4078 mutated with pAD168)	this work
pAD4141	pYV40 *yscN$_{\Delta 2\text{-}427}$* Δ*yscL* (pSI4006 mutated with pAD168)	this work
pAD4142	pYV40 *yscN$_{\Delta 2\text{-}427}$ yscQ*Δ$_{2\text{-}295}$ (pISOA4015 mutated with pAD168)	this work
pAD4143	pYV40 *yscN$_{\Delta 2\text{-}427}$* Δ*yscRSTU yscV*Δ$_{5\text{-}680}$ (pAD4107 mutated with pAD168)	this work
pAD4157	pYV40 *yscF$_{\Delta 1\text{-}74}$ yscN$_{\Delta 2\text{-}427}$* (pISO4006 mutated with pAD168)	this work
pAD22723	pYV227 *egfp-yscQ* Δ*yscK* (pAA210 mutated with pAD118)	this work
pAD22729	pYV227 *egfp-yscQ* (pYV227 mutated with pAD118)	this work
pAD22769	pYV227 *egfp-yscQ* Δ*yscH* (pAA207 mutated with pAD118)	this work
pAD22840	pYV227 *yscN$_{\Delta 2\text{-}427}$* Δ*yscK* (pAA210 mutated with pAD168)	this work
pAD40082	pYV40 *yscJ-his$_8$* (pYV40 mutated with pAD104)	this work
pAD40085	pYV40 *yscJ-flag-his$_8$* (pYV40 mutated with pAD110)	this work
pADMA4099	pYV40 *his$_8$-flag-yscD yscC$_{\Delta 2\text{-}598}$* (pYV40 mutated with pMA27)	this work
pADMA4101	pYV40 *his$_8$-flag-yscD yscC$_{\Delta 2\text{-}598}$ yadA::pLJM31* (pADMA4099 mutated with pLJM31)	this work
pADMA4137	pYV40 *yscC-mCherry yscN$_{\Delta 2\text{-}427}$* (pMA4005 mutated with pAD168)	this work
pADMA4151	pYV40 *egfp-yscQ yscC$_{\Delta 2\text{-}598}$* (pAD4016 mutated with pMA26)	this work
pADMA4156	pYV40 *yscC$_{\Delta 2\text{-}598}$ yscN$_{\Delta 2\text{-}427}$* (pMA4005 mutated with pAD168)	this work
pADMA22784	pYV227 *egfp-yscQ yscC-mCherry yscW::aphA-3* (pMA22708 mutated with pAD118)	this work
pIM405	pYV40 yscX$_{\Delta 42\text{-}75}$	(Iriarte and Cornelis, 1999)

pIM406	pYV40 yscY$_{\Delta 21\text{-}45}$	(Iriarte and Cornelis, 1999)
pIM41	pYV40 *yopN$_{45}$* (does not encode YopN)	(Boland *et al.*, 1996)
pISO4006	pYV40 *yscF$_{\Delta 1\text{-}74}$* (pYV40 mutated with pISO85)	this work
pISO4008	pYV40 *yscO$_{\Delta 4\text{-}149}$* (pYV40 mutated with pISO110)	this work
pISOA4015	pYV40 *yscQ$_{\Delta 2\text{-}295}$* (pYV40 mutated with pISO131)	this work
pKEM4001	pYV40 Δ*yscI* (pYV40 mutated with pKEM5)	this work
pLJM4029	pYV40 *yadA::pLJM31* (does not encode YadA)	(Mota and Cornelis, 2005)
pLY4001	pYV40 *ΔyscU*	(Sorg *et al.*, 2007)
pMA22708	pYV227 *yscC-mCherry yscW::aphA-3* (pRS227 mutated with pMA12)	this work
pMA4005	pYV40 *yscC-mCherry* (pYV40 mutated with pMA12)	this work
pMA4007	pYV40 *yscC-mCherry yscQ$_{\Delta 2\text{-}295}$* (pISO4015 mutated with pMA12)	this work
pMA4011	pYV40 *yscC-mCherry yscV$_{\Delta 5\text{-}680}$* (pAD4037 mutated with pMA12)	this work
pMA4015	pYV40 *yscC-mCherry yscF$_{\Delta 1\text{-}74}$* (pISO4006 mutated with pMA12)	this work
pMAAD4006	pYV40 *egfp-yscQ yscC-mCherry* (pAD4016 mutated with pMA12)	this work
pMAAD4018	pYV40 *yscC$_{\Delta 2\text{-}598}$ egfp-yscD* (pYV40 mutated with pMA28)	this work
pMRS4043	pYV40 lcrG$_{\Delta 8\text{-}57}$	(Sarker *et al.*, 1998b)
pMRS4071	pYV40 lcrV$_{\Delta 3\text{-}324}$	(Sarker *et al.*, 1998a)
pRS227	pYV227 *yscW::aphA-3* (does not encode YscW)	(Allaoui *et al.*, 1995a)
pSI4006	pYV40 Δ*yscL* (pYV40 mutated with pSI51)	this work
pYV227	wild-type pYV plasmid of *Y. enterocolitica* W22703	(Cornelis and Colson, 1975)
pYV40	wild-type pYV plasmid of *Y. enterocolitica* E40	(Sory *et al.*, 1995)

Chapter 4.2 – Regulation of expression and function of the *Yersinia* type III secretion system

pYV plasmid	Relevant characteristics	References
pAD4006	pYV40 *ΔvirF* (pYV40 mutated with pAD3)	this work
pAD22705	pYV227 *yscM1$_{\Delta 310}$ yscM2::aphA-3 ΔvirF* (pSI2273 mutated with pAD3)	this work
pSI2273	pYV227 *yscM1$_{\Delta 310}$ yscM2::aphA-3* (does not encode YscM2)	(Stainier *et al.*, 1998)
pYV40	wild-type pYV plasmid of *Y. enterocolitica* E40	(Sory *et al.*, 1995)

Chapter 4.3 – Kinetics and dynamics of the *Yersinia* type III secretion system

pYV plasmid	Relevant characteristics	References
pAD4014	pYV40 *his$_8$-flag-yscQ* (pYV40 mutated with pAD116)	this work
pAD4016	pYV40 *egfp-yscQ* (pYV40 mutated with pAD118)	this work
pAD4049	pYV40 *his$_8$-flag-yscD* (pYV40 mutated with pAD138)	this work
pAD4050	pYV40 *egfp-yscD* (pYV40 mutated with pAD140)	this work
pAD4058	pYV40 *yscJ-flash* (pYV40 mutated with pAD157)	this work
pAD4085	pYV40 egfp-yscQ yopO$_{\Delta 2\text{-}427}$ yopE$_{21}$ yopH$_{\Delta 1\text{-}352}$ yopM$_{23}$ yopP$_{23}$ yopT$_{135}$ Δasd (pIML421*asd* mutated with pAD118)	this work
pAD4136	pYV40 *yscN$_{\Delta 2\text{-}427}$* (pYV40 mutated with pAD168)	this work
pAD4139	pYV40 *yscN$_{\Delta 2\text{-}427}$ ΔyscJ* (pAD4078 mutated with pAD168)	this work
pAD40082	pYV40 *yscJ-his$_8$* (pYV40 mutated with pAD104)	this work
pAD40083	pYV40 *yscJ-egfp* (pYV40 mutated with pAD106)	this work
pAD40085	pYV40 *yscJ-flag-his$_8$* (pYV40 mutated with pAD110)	this work
pADCC4138	pYV40 *mCherry-yscQ yscN$_{\Delta 2\text{-}427}$* (pCJC4003 mutated with pAD168)	this work
pADCC4148	pYV40 *mCherry-yscQ yscN$_{\Delta 2\text{-}427}$ ΔyscJ* (pADCC4138 mutated with pAD158)	this work
pADMA4098	pYV40 *yscC$_{\Delta 2\text{-}598}$* (pYV40 mutated with pMA26)	this work
pCJC4003	pYV40 *mCherry-yscQ*	(Cattin, 2009)
pIML421	pYV40 *yopO$_{\Delta 2\text{-}427}$ yopE$_{21}$ yopH$_{\Delta 1\text{-}352}$ yopM$_{23}$ yopP$_{23}$ yopT$_{135}$*	(Iriarte and Cornelis, 1998)
pIML421*asd*	pYV40 *yopO$_{\Delta 2\text{-}427}$ yopE$_{21}$ yopH$_{\Delta 1\text{-}352}$ yopM$_{23}$ yopP$_{23}$ yopT$_{135}$ Δasd*	Kuhn, unpublished
pISOA4015	pYV40 *yscQ$_{\Delta 2\text{-}295}$* (pYV40 mutated with pISO131)	this work
pMAAD4006	pYV40 *egfp-yscQ yscC-mCherry* (pAD4016 mutated with pMA12)	this work
pYV40	wild-type pYV plasmid of *Y. enterocolitica* E40	(Sory *et al.*, 1995)

Chapter 4.4 – Purification of subcomplexes of the injectisome

pYV plasmid	Relevant characteristics	References
pAD4014	pYV40 *his$_8$-flag-yscQ* (pYV40 mutated with pAD116)	this work
pAD4015	pYV40 *flag-yscQ yscJ-his$_8$* (pAD40082 mutated with pAD114)	this work
pAD4047	pYV40 *flag-yscD* (pYV40 mutated with pAD136)	this work
pAD4048	pYV40 *flag-yscD yscJ-his$_8$* (pAD40082 mutated with pAD136)	this work
pAD4049	pYV40 *his$_8$-flag-yscD* (pYV40 mutated with pAD138)	this work
pAD4053	pYV40 yopO$_{\Delta 2\text{-}427}$ yopE$_{21}$ yopH$_{\Delta 1\text{-}352}$ yopM$_{23}$ yopP$_{23}$ yopT$_{135}$ Δasd ΔyadA (pIML421asd mutated with pLJM31)	this work
pAD4054	pYV40 *yscJ-flag-his$_8$ yadA::pLJM31* (pAD40085 mutated with pLJM31)	this work
pAD4055	pYV40 *his$_8$-flag-yscD yadA::pLJM31* (pAD4049 mutated with pLJM31)	this work
pAD4109	pYV40 *yscJ-flag-his$_8$ yscC$_{\Delta 2\text{-}598}$ yadA::pLJM31* (pAD4091 mutated with pLJM31)	this work

pAD40082	pYV40 *yscJ-his$_8$* (pYV40 mutated with pAD104)	this work
pAD40085	pYV40 *yscJ-flag-his$_8$* (pYV40 mutated with pAD110)	this work
pADMA4101	pYV40 *his$_8$-flag-yscD yscC$_{\Delta 2\text{-}598}$ yadA::pLJM31* (pADMA4099 mutated with pLJM31)	this work
pIML421*asd*	pYV40 yopO$_{\Delta 2\text{-}427}$ yopE$_{21}$ yopH$_{\Delta 1\text{-}352}$ yopM$_{23}$ yopP$_{23}$ yopT$_{135}$ Δasd	Kuhn, unpublished
pLJM4029	pYV40 *yadA::pLJM31* (does not encode YadA)	(Mota and Cornelis, 2005)
pYV40	wild-type pYV plasmid of *Y. enterocolitica* E40	(Sory *et al.*, 1995)

Chapter 4.5 – The type III secretion "IM export machinery"

pYV plasmid	Relevant characteristics	References
pAD4026	pYV40 *egfp-yscQ ΔyscU* (pLY4001 mutated with pAD118)	this work
pAD4031	pYV40 *yscR$_{\Delta 2\text{-}207}$* (pYV40 mutated with pAD128	this work
pAD4032	pYV40 *egfp-yscQ yscR$_{\Delta 2\text{-}207}$* (pAD4016 mutated with pAD128)	this work
pAD4033	pYV40 *ΔyscS* (pYV40 mutated with pAD130)	this work
pAD4034	pYV40 *egfp-yscQ ΔyscS* (pAD4016 mutated with pAD130)	this work
pAD4035	pYV40 *yscT$_{\Delta 2\text{-}250}$* (pYV40 mutated with pAD132)	this work
pAD4036	pYV40 *egfp-yscQ yscT$_{\Delta 2\text{-}250}$* (pAD4016 mutated with pAD132)	this work
pAD4037	pYV40 *yscV$_{\Delta 5\text{-}680}$* (pYV40 mutated with pAD134)	this work
pAD4038	pYV40 *egfp-yscQ yscV$_{\Delta 5\text{-}680}$* (pAD4016 mutated with pAD134)	this work
pAD4107	pYV40 *ΔyscRSTU yscVΔ$_{5\text{-}680}$* (pYV40 mutated with pAD170)	this work
pAD4108	pYV40 *egfp-yscQ ΔyscRSTU yscVΔ$_{5\text{-}680}$* (pAD4038 mutated with pAD170)	this work
pAD4160	pYV40 *ΔyscJ yscV$_{\Delta 5\text{-}680}$* (pAD4037 mutated with pAD158)	this work
pAD4161	pYV40 *yscN$_{\Delta 2\text{-}427}$ yscV$_{\Delta 5\text{-}680}$* (pAD4037 mutated with pAD168)	this work
pADMA4158	pYV40 *yscC-mCherry yscV$_{\Delta 5\text{-}680}$* (pAD4037 mutated with pMA12)	this work
pLY4001	pYV40 *ΔyscU*	(Sorg *et al.*, 2007)
pYV40	wild-type pYV plasmid of *Y. enterocolitica* E40	(Sory *et al.*, 1995)

7.4. Plasmids

Chapter 3 – Deciphering the assembly of the *Yersinia* type III secretion injectisome

Suicide vectors and mutators

Plasmid	Relevant characteristics	References
pAD104	pKNG101 *yscJ-his*$_8^+$ (*his*$_8$ cloned in-frame at the C-terminus of *yscJ*)	this work
pAD110	pKNG101 *yscJ-flag-his*$_8^+$ (*flag-his*$_8$ cloned in-frame at the C-terminus of *yscJ*)	this work
pAD118	pKNG101 *egfp-yscQ*$^+$ (*egfp* cloned in-frame at the N-terminus of *yscQ*)	this work
pAD128	pKNG101 *yscR*$_{\Delta 2\text{-}207}^+$	this work
pAD130	pKNG101 *ΔyscS*$^+$	this work
pAD132	pKNG101 *yscT*$_{\Delta 2\text{-}250}^+$	this work
pAD134	pKNG101 *yscV*$_{\Delta 5\text{-}680}^+$	this work
pAD138	pKNG101 *his*$_8$*-flag-yscD*$^+$ (*his*$_8$*-flag* cloned in-frame at the N-terminus of *yscD*)	this work
pAD140	pKNG101 *egfp-yscD*$^+$ (*egfp* cloned in-frame at the N-terminus of *yscD*)	this work
pAD158	pKNG101 *ΔyscJ*$^+$	this work
pAD164	pKNG101 *yscD*$_{\Delta 2\text{-}404}^+$	this work
pAD168	pKNG101 *yscN*$_{\Delta 2\text{-}427}^+$	this work
pAD170	pKNG101 *ΔyscRSTU*$^+$	this work
pISO85	pKNG101 *yscF*$_{\Delta 1\text{-}74}^+$	this work
pISO110	pKNG101 *yscO*$_{\Delta 4\text{-}149}^+$	this work
pISOA131	pKNG101 *yscQ*$_{\Delta 2\text{-}295}^+$	this work
pKEM5	pKNG101 *ΔyscI*$^+$	this work
pKNG101	ori$_{R6K}$ *sacBR*$^+$ oriT$_{RK2}$ *strAB*$^+$ (suicide vector)	(Kaniga *et al.*, 1991)
pLJM31	pKNG101 *yadA*	(Mota and Cornelis, 2005)
pMA12	pKNG101 *yscC-mCherry*$^+$ (*mCherry* cloned in-frame at the C-terminus of *yscC*)	this work
pMA26	pKNG101 *yscC*$_{\Delta 2\text{-}598}^+$	this work
pMA27	pKNG101 *yscC*$_{\Delta 2\text{-}598}^+$ *his*$_8$*-flag-yscD*$^+$	this work
pMA28	pKNG101 *yscC*$_{\Delta 2\text{-}598}^+$*egfp-yscD*$^+$	this work
pSI51	pKNG101 *ΔyscL*$^+$	this work

Clones and vectors

Plasmid	Relevant characteristics	References
pAD165	pBAD::*yscN*$_{WT}$ (complete *yscN* gene)	this work
pAD166	pBAD::*yscN*$_{K175E}$ (complete *yscN* gene with Lys to Glu mutation in pos. 175)	this work
pAD182	pBAD::*egfp-yscN*$_{WT}$ (complete *yscN* gene with N-terminal *egfp*)	this work
pBAD::*his*/B	pBR322-derived expression vector	Invitrogen
pEGFP-C1	contains *egfp* gene	BD Biosciences Clontech
pISO101	pBAD::*egfp*	this work
pISOA129	pBAD::*his*$_6$*-yscQ* (complete *yscQ* gene with N-terminal *his*$_6$)	this work
pMA8	pBAD::*yscC-mCherry* (complete *yscC* gene with C-terminal *mCherry*)	this work
pRVCHYN-5	contains *mCherry* gene	(Thanbichler *et al.*, 2007)
pRS6	contains *yscW* (*virG*)	(Allaoui *et al.*, 1995a)

Chapter 4.2 – Regulation of expression and function of the Yersinia type III secretion system

Suicide vectors and mutators

Plasmid	Relevant characteristics	References
pAD3	pKNG101 *ΔvirF*$^+$	this work
pKNG101	ori$_{R6K}$ *sacBR*$^+$ oriT$_{RK2}$ *strAB*$^+$ (suicide vector)	(Kaniga *et al.*, 1991)

Clones and vectors

Plasmid	Relevant characteristics	References
pAD123	pCDFduet-1::*pVirF-3xGFP* (3xGFP downstream of the virF promoter region)	this work
pAD124	pCDFduet-1::*pTransl-3xGFP* (3xGFP downstream of the promoter region of the translocator operon)	this work
pAD125	pCDFduet-1::*pVirB-3xGFP* (3xGFP downstream of the virB promoter region)	this work
pAD126	pCDFduet-1::*pVirC-3xGFP* (3xGFP downstream of the virC promoter region)	this work
pCDFduet-1	pBR322-compatible medium copy expression vector suitable for the coexpression of two genes	Novagen
pOM-3GFP	contains 3 fused *gfp* genes	(Sturgill *et al.*, 2008)

Chapter 4.3 – Kinetics and dynamics of the Yersinia type III secretion system

Suicide vectors and mutators

Plasmid	Relevant characteristics	References
pAD104	pKNG101 *yscJ-his$_8^+$* (*his$_8$* cloned in-frame at the C-terminus of *yscJ*)	this work
pAD106	pKNG101 *yscJ-egfp$^+$* (*egfp* cloned in-frame at the C-terminus of *yscJ*)	this work
pAD110	pKNG101 *yscJ-flag-his$_8^+$* (*flag-his$_8$* cloned in-frame at the C-terminus of *yscJ*)	this work
pAD116	pKNG101 *his$_8$-flag-yscQ$^+$* (*his$_8$-flag* cloned in-frame at the N-terminus of *yscQ*)	this work
pAD138	pKNG101 *his$_8$-flag-yscD$^+$* (*his$_8$-flag* cloned in-frame at the N-terminus of *yscD*)	this work
pAD140	pKNG101 *egfp-yscD$^+$* (*egfp* cloned in-frame at the N-terminus of *yscD*)	this work
pAD157	pKNG101 *yscJ-flash$^+$*	this work
pAD158	pKNG101 *ΔyscJ$^+$*	this work
pAD168	pKNG101 *yscN$_{Δ2-427}^+$*	this work
pKNG101	ori$_{R6K}$ *sacBR$^+$* oriT$_{RK2}$ *strAB$^+$* (suicide vector)	(Kaniga *et al.*, 1991)
pLJM31	pKNG101 *yadA*	(Mota and Cornelis, 2005)
pISO131	pKNG101 *yscQ$_{Δ2-295}^+$*	this work
pMA26	pKNG101 *yscC$_{Δ2-598}^+$*	this work

Clones and vectors

Plasmid	Relevant characteristics	References
pAD142	pBAD::*yscJ-flash* (complete *yscJ* gene with C-terminal FlAsH tag FLNCCPGCCMEP)	this work
pAD148	pGEX-6P-1::*yscV$_{322-704}$* (GST-PreScission-YscV$_{cytosolic}$)	this work
pAD154	pGEX-6P-1::yscD$_{150-418}$ (GST-PreScission-YscD$_{periplasmic}$)	this work
pAD165	pBAD::*yscN$_{WT}$* (complete *yscN* gene)	this work
pAD172	pGEX-6P-1::*yscV$_{356-704}$* (GST-PreScission-YscV$_{cytosolic}$)	this work
pAD173	pGEX-6P-1::*yscV$_{412-704}$* (GST-PreScission-YscV$_{cytosolic}$)	this work
pAD181	pBAD::*yscN$_{WT}$-egfp* (complete *yscN* gene with C-terminal *egfp*)	this work
pAD182	pBAD::*egfp-yscN$_{WT}$* (complete *yscN* gene with N-terminal *egfp*)	this work
pAD185	pET-21b::*yscJ$_{20-195}$* (His$_6$-TEV-YscJ$_{periplasmic}$)	this work
pAD186	pET-21b::*yscJ$_{20-217}$* (His$_6$-TEV-YscJ$_{periplasmic}$)	this work
pAD187	pET-21b::*yscJ$_{20-195}$* (YscJ$_{periplasmic}$-His$_6$)	this work
pAD188	pET-21b::*yscJ$_{20-217}$* (YscJ$_{periplasmic}$-His$_6$)	this work
pAD190	pBAD::*flag-his$_8$-yscN$_{WT}$* (complete *yscN* gene with N-terminal *flag-his$_8$*)	this work
pADCP197	pET-21b::*yscJ* (YscJ$_{complete}$-His$_6$)	this work

pADCP198	pET-21b::*yscJ* ($YscJ_{complete}$-FLAG-His_6)	this work
pADCP199	pGEX-6P-1::*yscD* (GST-PreScission-$YscD_{complete}$)	this work
pADCP200	pGEX-6P-1::$yscD_{120-418}$ (GST-PreScission-$YscD_{TM+periplasmic}$)	this work
pBAD::his/B	pBR322-derived expression vector	Invitrogen
pEGFP-C1	contains *egfp* gene	BD Biosciences Clontech
pET-21b	high-copy expression vector	EMD Biosciences
pGEX-6P-1	high-copy expression vector for N-terminal GST-PreScission fusions	GE Healthcare
pISOA129	pBAD::his_6-*yscQ* (complete *yscQ* gene with N-terminal his_6)	this work
pMA6	pBAD::*yscC* (complete *yscC*)	this work
pMA8	pBAD::*yscC-mCherry* (complete *yscC* gene with C-terminal *mCherry*)	this work
pRS6	contains *yscW* (*virG*)	(Allaoui *et al.*, 1995a)

Chapter 4.4 – Purification of subcomplexes of the injectisome

Suicide vectors and mutators

Plasmid	Relevant characteristics	References
pAD104	pKNG101 *yscJ-*his_8^+ (*his*$_8$ cloned in-frame at the C-terminus of *yscJ*)	this work
pAD110	pKNG101 *yscJ-flag-*his_8^+ (*flag-his*$_8$ cloned in-frame at the C-terminus of *yscJ*)	this work
pAD114	pKNG101 *flag-*$yscQ^+$ (*flag* cloned in-frame at the N-terminus of *yscQ*)	this work
pAD116	pKNG101 his_8-*flag-*$yscQ^+$ (his_8-*flag* cloned in-frame at the N-terminus of *yscQ*)	this work
pAD136	pKNG101 *flag-*$yscD^+$ (*flag* cloned in-frame at the N-terminus of *yscD*)	this work
pAD138	pKNG101 his_8-*flag-*$yscD^+$ (his_8-*flag* cloned in-frame at the N-terminus of *yscD*)	this work
pKNG101	ori_{R6K} $sacBR^+$ $oriT_{RK2}$ $strAB^+$ (suicide vector)	(Kaniga *et al.*, 1991)
pLJM31	pKNG101 *yadA*	(Mota and Cornelis, 2005)

Chapter 4.5 – The type III secretion "IM export machinery"

Suicide vectors and mutators

Plasmid	Relevant characteristics	References
pAD118	pKNG101 *egfp-yscQ*$^{+}$ (*egfp* cloned in-frame at the N-terminus of *yscQ*)	this work
pAD128	pKNG101 *yscR*$_{\Delta 2\text{-}207}^{+}$	this work
pAD130	pKNG101 *ΔyscS*$^{+}$	this work
pAD132	pKNG101 *yscT*$_{\Delta 2\text{-}250}^{+}$	this work
pAD134	pKNG101 *yscV*$_{\Delta 5\text{-}680}^{+}$	this work
pAD158	pKNG101 *ΔyscJ*$^{+}$	this work
pAD168	pKNG101 *yscN*$_{\Delta 2\text{-}427}^{+}$	this work
pAD170	pKNG101 *ΔyscRSTU*$^{+}$	this work
pKNG101	ori$_{R6K}$ *sacBR*$^{+}$ oriT$_{RK2}$ *strAB*$^{+}$ (suicide vector)	(Kaniga *et al.*, 1991)
pMA12	pKNG101 *yscC-mCherry*$^{+}$ (*mCherry* cloned in-frame at the C-terminus of *yscC*)	this work

Clones and vectors

Plasmid	Relevant characteristics	References
pAD152	pBAD::*yscT* (complete *yscT* gene)	this work
pAD153	pBAD::*yscV* (complete *yscV* gene)	this work
pAD155	pBAD::*yscV-egfp* (complete *yscV* gene with C-terminal *egfp*)	this work
pAD159	pBAD::*egfp-yscV* (complete *yscV* gene with N-terminal *egfp*)	this work
pAD160	pBAD::*egfp-yscT* (complete *yscT* gene with N-terminal *egfp*)	this work
pAD161	pBAD::*yscT-egfp* (complete *yscT* gene with C-terminal *egfp*)	this work
pAD192	pBAD::*yscR-egfp* (complete *yscR* gene with C-terminal *egfp*)	this work
pAD194	pBAD::*yscS-egfp* (complete *yscS* gene with C-terminal *egfp*)	this work
pAD195	pBAD::*yscU-egfp* (complete *yscU* gene with C-terminal *egfp*)	this work
pMA19	pBAD::*yscR* (complete *yscR* gene)	this work
pMA22	pBAD::*yscS* (complete *yscS* gene)	this work
pLY7	pBAD::*yscU* (complete *yscU* gene)	(Sorg *et al.*, 2007)

7.5. Oligonucleotides

No.	Sequence	Features	Used for cloning of	Template
4462	catggtcgacaaaactgaatccagctcaacg	SalI site	pAD3, ext. fwd. primer	pYV40
4463	agtaattggtgagcatgagttattatgcgtgcgatg		pAD3, int. rev. primer	pYV40
4464	acgcataataactcatgctcaccaattacttcttaatgg		pAD3, int. fwd. primer	pYV40
4465	catgtctagatggctcatcccattgaatct	XbaI site	pAD3, ext. rev. primer	pYV40
4523	gatcgggcccttcagtttgacacctacataccctca	ApaI site	pAD104, pAD106, pAD110, ext. fwd. primer	pYV40
4527	gatctctagaacagttcgagctgtgattgg	XbaI site	pAD104, pAD106, pAD110, ext. rev. primer	pYV40
4532	gtgatggtgatggtgatggtggtgaccaccgccacctttcttcctctggagccaaaaatattgagcaagattgg	introduces gly_4-his_8	pAD104, int. rev. primer	pYV40
4533	caccaccatcaccatcaccatcactgaggttacaacgcaagaagtgatg	introduces gly_4-his_8	pAD104, int. fwd. primer	pYV40
4524	gtcgacctgcagcgtacgaccaccgccaccttttcttcctctggagccaaaaatattgagcaagattgg		pAD106, int. rev. primer	pYV40
4525	ccagcgacatggaggcccaggttacaacgcaagaagtgatg		pAD106, int. fwd. primer	pYV40
4534	ccttgtagtcaccaccgccacctttcttcctctggagccaaaaatattgagcaagattgg	introduces part of gly_4-*flag*-his_8	pAD110, int. fwd. primer 1	pYV40
4535	gtgatggtgatggtgatggtggtgcttatcatcgtcgtccttgtagtcaccaccgcca	introduces part of gly_4-*flag*-his_8	pAD110, int. fwd. primer 2	pYV40
4762	gatcgggccctgaattgggggctattatg	ApaI site	pAD114, pAD116, pAD118, ext. fwd. primer	pYV40
4763	gatctctagaaatggagcccctagtaagtcg	XbaI site	pAD114, pAD116, pAD118, ext. rev. primer	pYV40
4766	gactacaaggacgacgatgataagggtggagcaggtggtgccggaggtagtttgttaaccttgccacaagc	introduces part of *ggaggagg-flag*	pAD114 and pAD116, int. fwd. primer	pYV40
4764	cttatcatcgtcgtccttgtagtcactcattcttcagcctcccac	introduces part of *flag*	pAD114, int. rev. primer	pYV40
4765	cttatcatcgtcgtccttgtagtcgtgatggtgatggtgatggtggtgactcattcttcagcctcccac	introduces part of his_8-*flag*	pAD116, int. rev. primer	pYV40
4767	ctgctccaccggatccatacggcaaccggtctcattcttcagcctcccac	AgeI and BamHI sites for *egfp* insertion	pAD118, int. rev. primer	pYV40
4768	tatggatccggtggagcaggtggtgccggaggtagtttgttaaccttgccacaagc		pAD118, int. fwd. primer	pYV40
4641	gactaagcttggtcaaccctctcttttcca	HindIII site	pAD123	pYV40
4675	gatcggatccataaatgttatactgtcctaaaaatctaa	SacI site		pYV40
4643	gactaagctttggcaatgtcgatgtactgg	HindIII site	pAD124	pYV40
4676	gatcggatccataatctacctcctattttattacgttattt	SacI site		pYV40
4645	gactaagcttactggcaatctctggatgct	HindIII site	pAD125	pYV40
4677	gatcggatccataaatccataatggttgaaatattaa	SacI site		pYV40
4647	gactaagcttggataagcgagcgacgtatt	HindIII site	pAD126	pYV40

4678	gatcggatccatcccattgaatcttcaaaatc	SacI site		pYV40
4929	gatcgggcccgaaccaacttccggttcaag	ApaI site	pAD128 and pAD170, ext. fwd. primer	pYV40
4930	ccagcccatgcgtcatgaaatcgtaacctctg tca		pAD128, int. rev. primer	pYV40
4931	ttacgatttcatgacgcatgggctggtgatta		pAD128, int. fwd. primer	pYV40
4932	gatctctagaagcaaacagtgtgaccacca	XbaI site	pAD128, ext. rev. primer	pYV40
4933	gatcgggcccctgcgtttacggtgagtgag	ApaI site	pAD130, ext. fwd. primer	pYV40
4934	aagccacgaggcgtcaccctccgtaactaatc acc		pAD130, int. rev. primer	pYV40
4935	tacggagggtgacgcctcgtggcttggtaatg		pAD130, int. fwd. primer	pYV40
4936	gatctctagaagacataaagagccaatgaaca gac	XbaI site	pAD130, ext. rev. primer	pYV40
4937	gatcgggccctggctggtgctagtcctttc	ApaI site	pAD132, ext. fwd. primer	pYV40
4938	cagtaaacttatagtcatcttatgccttgtat cttcatc		pAD132, int. rev. primer	pYV40
4939	aaggcataagatgactataagtttactgatcc ctgttttgg		pAD132, int. fwd. primer	pYV40
4940	gatctctagactctgctctgcggggatta	XbaI site	pAD132, ext. rev. primer	pYV40
4941	gatcgggcccgctgacgttaaatcctgagca	ApaI site	pAD134, ext. fwd. primer	pYV40
4942	agtaccggcaagtcatggggattcattatgat cttt		pAD134, int. rev. primer	pYV40
4943	tgaatccccatgacttgccggtactttcatac ca		pAD134, int. fwd. primer	pYV40
4944	gatctctagaggataagcacgatccaaacc	XbaI site	pAD134, ext. rev. primer	pYV40
4858	gatcgggccctggtcaggatctacgtactggt	ApaI site	pAD136, pAD138, pAD140, ext. fwd. primer	pYV40
4859	gatctctagaaccctacttccagacaagtgc	XbaI site	pAD136, pAD138, pAD140, ext. rev. primer	pYV40
4862	gactacaaggacgacgatgataagggtggagc aggtggtgccggaggtagttgggtctgtcgtt tttatca	introduces part of *ggaggagg-flag*	pAD136 and pAD138, int. fwd. primer	pYV40
4860	cttatcatcgtcgtccttgtagtctctcacaa tacgccacgctta	introduces part of *flag*	pAD136, int. rev. primer	pYV40
4861	cttatcatcgtcgtccttgtagtcgtgatggt gatggtgatggtggtgtctcacaatacgccac gctta	introduces part of *his$_8$-flag*	pAD138, int. rev. primer	pYV40
4863	ctgctccaccagaattcatacggcaaccggtc tcacaatacgccacgctta	AgeI and EcoRI sites for *egfp* insertion	pAD140, int. rev. primer	pYV40
4864	tatgaattctggtggagcaggtggtgccggag gtagttgggtctgtcgtttttatca		pAD140, int. fwd. primer	pYV40
5151	gactgaattccgtaagcagagtcgtaatgacg	EcoRI site	pAD148	pYV40
5152	gactctcgagcatcataagcaaactcgtccaa	XhoI site	pAD148, pAD172, pAD173	pYV40
5168	gactccatggggatagcggatttaatccaaag ac	NcoI site	pAD152 and pAD161	pYV40
5169	gactaagcttctccgctcattacttctcca	HindIII site	pAD152 and pAD160	pYV40
5170	gactccatggggaatccccatgatcttgagtg	NcoI site	pAD153 and pAD155	pYV40
5171	gactaagcttagggtcttccatcataagcaaa	HindIII site	pAD153 and pAD159	pYV40
5174	gactggatccaaccaggatggacaacttgtt	BamHI site	pAD154	pYV40
5175	gactctcgagaattgtgtcatcgaggtttacc	XhoI site	pAD154	pYV40

5176	gactaagcttaagaattcgactgctagccataagcaaactcgtccaagtg	HindIII site	pAD155	pYV40
4528	gatcgggccctgcggcaatgtcagaagata	ApaI site	pAD158, ext. fwd. primer	pYV40
5079	ttgcgttgtaacctagttctcacccccccttc		pAD158, int. rev. primer	pYV40
5080	gggtgagaactaggttacaacgcaagaagtgatg		pAD158, int. fwd. primer	pYV40
4527	gatctctagaacagttcgagctgtgattgg	XbaI site	pAD158, ext. rev. primer	pYV40
5195	gactccatggagctagcgactgaattcgaatcccatgatcttgagtg	NcoI site	pAD159	pYV40
5196	gactccatggagctagcgactgaattcgatagcggatttaatccaaagac	NcoI site	pAD160	pYV40
5197	gactaagcttaagaattcgactgctagcttctccaaaacagggatcagt	Hind III site	pAD161	pYV40
4925	gatcgggcccgatgaaatatctaatcaaagcactacc	ApaI site	pAD164, ext. fwd. primer	pYV40
4926	cacaaattcccgtttcacaatacgccacgcttag		pAD164, int. rev. primer	pYV40
4927	tggcgtattgtgaaacgggaatttgtgatccag		pAD164, int. fwd. primer	pYV40
4928	gatctctagatcctgctacataatgaataatggcta	XbaI site	pAD164, ext. rev. primer	pYV40
5275	gactacatgttgtcactagatcagatacctcatcatattcgt	PciI site	pAD165 and pAD166, ext. fwd. primer	pYV40
5278	gactctcgagtatcattgggtcagcgtctc	XhoI site	pAD165 and pAD166, ext. rev. primer	pYV40
5276	aagcagtgtactttcaccaccaccggcggccgcgaagat	mutated *yscN* sequence encoding $GGGE_{175}$	pAD166, int. rev. primer	pYV40
5277	ggtggtggtgaaagtacactgcttgcttcgc	mutated *yscN* sequence encoding $GGGE_{175}$	pAD166, int. fwd. primer	pYV40
5271	gactgggcccagcggggtattgccataag	ApaI site	pAD168, ext. fwd. primer	pYV40
5272	ctcattgaaatggagcataaatccataatggttgaaat		pAD168, int. rev. primer	pYV40
5273	atggatttatgctccatttcaatgagacgctga		pAD168, int. fwd. primer	pYV40
5274	gacttctagactttacaattcagtgtggtgttttt	XbaI site	pAD168, ext. rev. primer	pYV40
5297	ttttgcctttctatcatgaaatcgtaacctctgtca		pAD170, int. rev. primer	pYV40
5298	gttacgatttcatgatagaaaggcaaaatatcgagaaaca		pAD170, int. fwd. primer	pYV40
5299	gatctctagatcctaatataagtgaacctcttgttgg	XbaI site	pAD170, ext. rev. primer	pYV40
5310	gactgaattcgcaaacaagggccgacta	EcoRI site	pAD172	pYV40
5311	gactgaattcatccatctgcgttttaatgagg	EcoRI site	pAD173	pYV40
5475	gactacatgttgctagcatcagggccctatgctctcactagatcagatacctc	PciI site, NheI and ApaI sites for *egfp* insertion	pAD182	pYV40
5278	gactctcgagtatcattgggtcagcgtctc	XhoI site	pAD182	pYV40
5623	gactcatatgcatcatcaccatcaccatgaaaacttgtactttcagggcaaagttgatctttataccggaatt	NdeI site	pAD185 and pAD186	pYV40
5625	gactgagctcattgacgaacatctaccgatgg	SacI site	pAD185	pYV40

5626	gactgagctcaacgccttttgactcttcac	SacI site	pAD186	pYV40
5624	gactcatatgaaagttgatctttataccggaattag	NdeI site	pAD187 and pAD188	pYV40
5627	gactgagctcaatggtgatggtgatgatgttgacgaacatctaccgatgg	SacI site	pAD187	pYV40
5628	gactgagctcaatggtgatggtgatgatgacgccctttgactcttcac	SacI site	pAD188	pYV40
5709	catcaccatcaccatcacggtggagcaggtggtgccggaggtatgctctcactagatcagatacctc		pAD190	pYV40
5710	gactacatgtccgactacaaggacgacgatgataagcaccaccatcaccatcaccatcacgg	PciI site	pAD190	pYV40
5629	gactccatggtccagttaccggatgaaatta	NcoI site	pAD192	pYV40
5751	gactctgcaggcggccgcatcagagctcccctccgtaactaatcaccag	SacI site	pAD192	pYV40
5752	gactccatgggtcaaggtgacataattcacttcac	NcoI site	pAD194	pYV40
5754	gactctgcaggcggccgcatcagagctctcttatgccttgtatcttcatcatgg	SacI site	pAD194	pYV40
3724	gatcccatggccagcggagaaaagacagag	NcoI site	pAD195	pYV40
5755	gactctgcaggcggccgcatcagagctctaacatttcggaatgctgtttc	SacI site	pAD195	pYV40
5965	gactcatatgaaagttaagacttcactgtcaaca	NdeI site	pADCP197 and pADCP198	pAD40082, pAD40085
5966	gactgagctccctcagtgatggtgatggtg	SacI site	pADCP197 and pADCP198	pAD40082, pAD40085
5967	gactggatccatgagttgggtctgtcgttttt	BamHI site	pADCP199	pYV40
5969	gactctcgagtgctcctctaattgtgtcatcg	XhoI site	pADCP199 and pADCP200	pYV40
5968	gactggatcctcacgacttggggttggg	BamHI site	pADCP200	pYV40

7.6. Antibodies

No.	Specificity	Donor organism	Dilution	Source
57	anti-YscP (polyclonal)	rabbit	1:3000	(1)
66	anti-YscJ (polyclonal)	rabbit	1:5000	(1)
73	anti-YopE	rabbit	1:1000	(1)
80	anti-YscF aa 1-21 (polyclonal) (2)	rabbit	(3)	(1)
163	Texas red anti-rabbit Ig	swine	1:150	(4)
168	HRP anti-rabbit Ig	swine	1:5000	(5)
189	anti-YscN (polyclonal)	rabbit	1:1000	(1)
220	anti-LcrV (polyclonal)	rabbit	1:2000	(1)
221	anti-YscU (polyclonal)	rabbit	1:1000	(1)
223	anti-YscF (polyclonal) (6)	rabbit	1:1000	(1)
227	anti-YscV aa 133-200 (polyclonal)	rabbit	1:2000	(1)
231	anti-GFP	rabbit	1:800	(7)
232	anti-YscD (polyclonal)	rabbit	1:1000	(1)
250	anti-YscC (polyclonal)	rabbit	1:1000	(1)

(1): Centre d'économie rurale, Laboratoire d'hormonologie, Marloie, Belgium
(2): Used for immunofluorescence
(3): Used undiluted after positive and negative purification (see Material and methods)
(4): Southern Biotech, Birmingham, AL, USA
(5): DAKO, Glostrup, Denmark
(6): Used for immunoblot analysis
(7): Invitrogen, Carlsbad, CA, USA

7.7. Original publication

The EMBO Journal (2010), 1–13 | © 2010 European Molecular Biology Organization | All Rights Reserved 0261-4189/10
www.embojournal.org

THE EMBO JOURNAL

Deciphering the assembly of the *Yersinia* type III secretion injectisome

Andreas Diepold, Marlise Amstutz, Sören Abel, Isabel Sorg, Urs Jenal and Guy R Cornelis*

Infection Biology, Biozentrum der Universität Basel, Basel, Switzerland

The assembly of the *Yersinia enterocolitica* type III secretion injectisome was investigated by grafting fluorescent proteins onto several components, YscC (outer-membrane (OM) ring), YscD (forms the inner-membrane (IM) ring together with YscJ), YscN (ATPase), and YscQ (putative C ring). The recombinant injectisomes were functional and appeared as fluorescent spots at the cell periphery. Epistasis experiments with the hybrid alleles in an array of injectisome mutants revealed a novel outside-in assembly order: whereas YscC formed spots in the absence of any other structural protein, formation of YscD foci required YscC, but not YscJ. We therefore propose that the assembly starts with YscC and proceeds through the connector YscD to YscJ, which was further corroborated by co-immunoprecipitation experiments. Completion of the membrane rings allowed the subsequent assembly of cytosolic components. YscN and YscQ attached synchronously, requiring each other, the interacting proteins YscK and YscL, but no further injectisome component for their assembly. These results show that assembly is initiated by the formation of the OM ring and progresses inwards to the IM ring and, finally, to a large cytosolic complex.

The EMBO Journal advance online publication, 7 May 2010; doi:10.1038/emboj.2010.84
Subject Categories: microbiology & pathogens
Keywords: microbial pathogenesis; nanomachine; protein complex assembly; protein transport

Introduction

The type III secretion (T3S) apparatus, also called injectisome, allows bacteria to export effector proteins on contact with eukaryotic cell membranes (Cornelis and Wolf-Watz, 1997; Galan and Collmer, 1999; Cornelis and Van Gijsegem, 2000). Effectors (called Yops in *Yersinia*) display a large repertoire of biochemical activities and modulate the function of crucial host regulatory molecules to the benefit of the bacterium (Alfano and Collmer, 2004; Mota and Cornelis, 2005; Grant *et al*, 2006). In *Yersinia spp.*, the injectisome is built when temperature reaches 37°C and export of the Yops can be artificially triggered, in the absence of cell contact, by Ca^{2+} chelation (Cornelis, 2006).

About 25 proteins (called Ysc in *Yersinia*) are needed to build the injectisome. Most of these are structural components, but some are ancillary components that are only involved during the assembly process and are either shed afterwards (e.g. the molecular ruler) or kept in the cytosol (e.g. chaperones). In contrast to the large diversity observed among effectors, the core proteins forming the injectisome (YscC, J, N, Q, R, S, T, U, V, and, to a lesser extent, YscD in *Yersinia*) are well conserved (Van Gijsegem *et al*, 1995; Cornelis, 2006).

A number of injectisome proteins copurify as a complex cylindrical structure, resembling the flagellar basal body. This structure, called the needle complex, consists of two pairs of rings that span the inner membrane (IM) and outer membrane (OM) of bacteria, joined together by a narrower cylinder and terminated by a needle, a filament, or a pilus (Kubori *et al*, 1998; Blocker *et al*, 1999; Kimbrough and Miller, 2000; Daniell *et al*, 2001; Jin and He, 2001; Sekiya *et al*, 2001; Morita-Ishihara *et al*, 2006; Sani *et al*, 2007; Hodgkinson *et al*, 2009; Schraidt *et al*, 2010). The needle is a hollow tube assembled through helical polymerization of a small protein (around 150 copies of YscF in *Yersinia*) (Cordes *et al*, 2003; Deane *et al*, 2006). It terminates with a tip structure serving as a scaffold for the formation of a pore in the host cell membrane (Mueller *et al*, 2005). The ring spanning the OM (hereafter called OM ring) and protruding into the periplasm consists of a 12–14mer of a protein from the YscC family of secretins (Koster *et al*, 1997; Kubori *et al*, 2000; Tamano *et al*, 2000; Blocker *et al*, 2001; Marlovits *et al*, 2004; Burghout *et al*, 2004b; Spreter *et al*, 2009). The lower ring spanning the IM is called MS ring and made of a lipoprotein (YscJ in *Yersinia*, MxiJ in *Shigella*, PrgK in *Salmonella enterica* SPI-1) proposed to form a 24-subunit ring (Kimbrough and Miller, 2000; Crepin *et al*, 2005; Yip *et al*, 2005; Silva-Herzog *et al*, 2008; Hodgkinson *et al*, 2009). A protein from the less-conserved YscD family (MxiG in *Shigella*, PrgH in *S. enterica* SPI-1), which has the same general fold as the components of the two rings, is proposed to participate in MS ring formation and possibly connect the rings in the two membranes (Spreter *et al*, 2009).

Besides these proteins forming a rigid scaffold, the injectisome contains five essential integral membrane proteins (YscR, S, T, U, V), which are believed to recognize export substrates (Sorg *et al*, 2007) and form the export channel across the IM. Some of them, if not all, are likely to be inserted in a patch of membrane enclosed within the MS ring, but this could not be shown so far. We will refer to these proteins as to the 'export apparatus'. At the cytosolic side of the injectisome, an ATPase of the AAA^+ family (YscN) forms a hexameric ring that is activated by oligomerization (Woestyn *et al*, 1994; Pozidis *et al*, 2003; Muller *et al*, 2006; Zarivach *et al*, 2007) and resembles the flagellar ATPase FliI

*Corresponding author. Biozentrum der Universität Basel, Universität Basel, Infection Biology, Klingelbergstrasse 50-70, Basel CH 4056, Switzerland. Tel.: +41 61 267 2110; Fax: +41 61 267 2118; E-mail: guy.cornelis@unibas.ch

Received: 12 January 2010; accepted: 13 April 2010

(Abrahams *et al*, 1994; Imada *et al*, 2007). The ATPase is associated with two proteins (YscK, L) (Jackson and Plano, 2000; Blaylock *et al*, 2006), one of them (YscL) probably exerting a control on the ATPase activity as was shown for FliH in the flagellum (Minamino and MacNab, 2000; Gonzalez-Pedrajo *et al*, 2002; McMurry *et al*, 2006). The ATPase is strikingly similar to the α and β subunits of the stator of the F_0F_1 ATP synthase (Abrahams *et al*, 1994), suggesting an evolutionary relation. This assumption is reinforced by the sequence similarity observed between $YscL_{N\text{-}term}$ and the b subunit of the F-type ATPase, and between $YscL_{C\text{-}term}$ and the δ subunit of the same ATPase (Pallen *et al*, 2006). A function of the ATPase, characterized in *S. enterica* Typhimurium SPI-1, is to detach some T3S substrates from their cytoplasmic chaperone before their export and to unfold the exported proteins in an ATP-dependent manner (Akeda and Galan, 2005). It is likely that the ATPase also directly energizes export, but the proton motive force is also involved (Wilharm *et al*, 2004; Minamino and Namba, 2008; Paul *et al*, 2008).

In the flagellum, the most proximal part of the basal body is the 45–50 nm C ring (for cytosolic) made of FliM and FliN (Driks and DeRosier, 1990; Khan *et al*, 1992; Kubori *et al*, 1997; Young *et al*, 2003; Thomas *et al*, 2006). Together with FliG, it forms the switch complex reversing the rotation of the motor, but in its absence, no filament appears, indicating that it is also involved in the export of distal constituents (Macnab, 2003). However, recent reports (Konishi *et al*, 2009; Erhardt and Hughes, 2010) showed that in C ring mutants, the export function can be partially restored by overexpression of the ATPase or the master regulator. No such C ring could be visualized so far by electron microscopy in a needle complex, but proteins of the YscQ family, which are essential components of all injectisomes, have a significant similarity to FliN and FliM. In *Pseudomonas syringae*, the orthologue of YscQ even appears as two products called $HrcQ_A$ and $HrcQ_B$, which interact with each other, and the overall fold of $HrcQ_B$ is remarkably similar to that of FliN (Fadouloglou *et al*, 2004). This suggests that injectisomes do have a C ring, although they have not been reported to rotate. YscQ and its homologues have been shown to bind the ATPase complex (Jackson and Plano, 2000) as well as substrate–chaperone complexes (Morita-Ishihara *et al*, 2006). The C ring would, therefore, form a platform at the cytoplasm/IM interface for the recruitment of other proteins. In agreement with this assumption, immunogold-labelling experiments have shown that the *Shigella* orthologue of YscQ (Spa33) localizes to a lower portion of the injectisome (Morita-Ishihara *et al*, 2006). A list of homologues in the flagellum and the various archetypal T3S systems is given in Supplementary Table 3.

The assembly of the flagellum is for the most part linear and sequential, proceeding from more proximal structures to more distal ones. The proposed scenario is that the plasma membrane ring (called the MS ring) formed by FliF assembles first, followed by periplasmic components, OM components, and finally components that lie in the cell exterior (Kubori *et al*, 1992; Macnab, 2003). The C ring (FliG, FliM, FliN) is thought to appear immediately after the MS ring, because it forms spontaneously when its components are overexpressed in the presence of FliF even in the absence of any other component (Kubori *et al*, 1997; Lux *et al*, 2000; Young *et al*, 2003).

Less is known about the assembly steps of the injectisome. The heterologous overexpression of the *S. enterica* SPI-1 MS ring components PrgH and PrgK in *Escherichia coli* leads to stable ring structures (Kimbrough and Miller, 2000). The same is true for the *Yersinia* secretin YscC together with its pilotin YscW (Koster *et al*, 1997). This suggests that the transmembrane rings might form independently. It has thus been proposed (Kimbrough and Miller, 2000) that the first step consists in the assembly of the MS ring, possibly along with the recruitment of the transmembrane proteins forming the export apparatus. In parallel, the secretin ring would form in the OM. Afterwards, the two rings would join by an unknown mechanism, allowing the assembly of the remaining machinery, which then exports the distal components, including the needle and the needle tip. The exact order of these later steps of the injectisome assembly remains largely unknown. A similar model was put forward based on the genetic analysis of the requirements for needle complex formation in *S. enterica* SPI-1 (Sukhan *et al*, 2001).

In this paper, we systematically investigate the whole assembly process of the *Yersinia* injectisome by combining four functional fluorescent hybrid proteins covering different parts of the machinery with an array of deletions. We conclude that the assembly starts from the secretin, the outermost and most stable ring, and sequentially proceeds inwards through YscD and YscJ. After completion of the membrane rings, an ATPase–C ring complex formed by YscK, YscL, YscN, and YscQ joins the machinery. All of the four participating proteins, but not the ATPase activity of YscN are required for the formation of this structure.

Results

Various substructures of the Yersinia injectisome including the C ring can be monitored using functional fluorescent fusion proteins

To visualize the injectisome and its subunits, the wild-type alleles of *yscC*, *yscD*, and *yscQ* on the virulence plasmid of *Y. enterocolitica* E40 were replaced by hybrid genes encoding the fluorescent proteins YscC–mCherry, EGFP–YscD, and EGFP–YscQ. Further, a non-polar complete deletion of *yscN* was constructed and complemented *in trans* with a plasmid encoding EGFP–YscN. The fusion proteins were expressed at near wild-type levels; no proteolytic release of the fluorophore was detected (Supplementary Figure 1).

To test the functionality of the fusion proteins, the pattern of proteins secreted into the supernatant in secretion-permissive medium (BHI-Ox) was analysed 3 h after induction of the system. YscC–mCherry, EGFP–YscN, and EGFP–YscQ were fully functional, whereas the strain expressing EGFP–YscD secreted a lower amount of effector proteins (Figure 1B). All fusion proteins allowed the formation of needles, which could be visualized by transmission electron microscopy (data not shown).

The localization of the hybrid proteins was analysed by fluorescence microscopy. Three hours after induction of synthesis of the injectisome, fluorescent spots were observed at the cell periphery for all labelled proteins (Figure 1A, three-dimensional view in Supplementary data). The formation of these spots was independent of the Ca^{2+} concentration in the medium, showing that their appearance was not directly

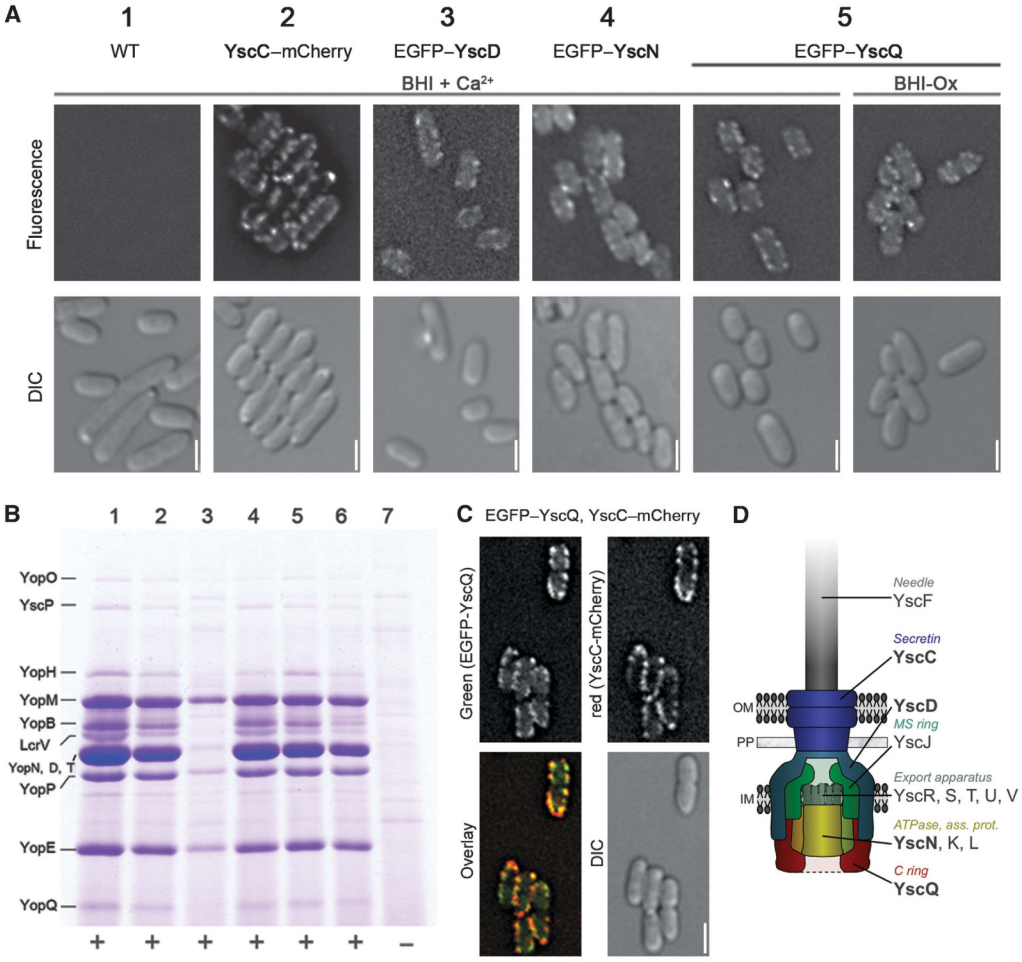

Figure 1 Fluorescently labelled Ysc proteins are functional and allow visualization of the injectisome. (**A**) Fluorescence deconvolution microscopy showing the formation of fluorescent spots at the bacterial membrane of *Y. enterocolitica* bacteria grown in secretion-non-permissive (BHI + Ca^{2+}) and secretion-permissive medium (BHI-Ox): 1—E40(pYV40) [wild type], 2—E40(pMA4005) [YscC–mCherry], 3—E40(pAD4050) [EGFP–YscD], 4—E40(pAD4136)(pAD182) [ΔYscN + pBAD-*egfp–yscN*], 5—E40(pAD4016) [EGFP–YscQ]. All fusion proteins except for EGFP–YscN are encoded under their native promoter on the pYV virulence plasmid. Upper lane: mCherry fluorescence for strain 2, EGFP fluorescence for other strains; lower lane: corresponding DIC picture. All fluorescence pictures were taken 3 h after the induction of the T3S system by temperature shift to 37°C. Scale bars: 2 μm. (**B**) Analysis of the Yop proteins secreted in secretion-permissive conditions. The tagged strains are fully functional for effector secretion, except for the strain expressing EGFP–YscD (lane 3), which shows reduced secretion. Culture supernatants were separated on a 12% SDS–PAGE gel and stained with Coomassie Brilliant Blue. Strains as listed in (**A**), 6—E40(pMAAD4006) [EGFP–YscQ, YscC–mCherry], 7—E40(pAD4051) [ΔYscD, negative control]. Bottom line: Needle formation (+/−) in the tested strains (data not shown). (**C**) Fluorescence microscopy showing the colocalization of EGFP–YscQ with YscC–mCherry in E40(pMAAD4006) bacteria. Fluorescent pictures were obtained as described in (**A**). (**D**) Model of the *Yersinia* Ysc injectisome. Fluorescently labelled proteins are shown in bold print. OM, outer membrane; PP, periplasm; IM, inner membrane.

linked to the secretion of Yop proteins by the T3S system (Figure 1A).

To ascertain that the membrane spots correspond to assembled basal bodies, we constructed a strain expressing both YscC–mCherry and EGFP–YscQ, and monitored the localization of the green fluorescence from EGFP–YscQ and the red fluorescence from YscC–mCherry. As visible in Figure 1C, the green and red spots largely colocalized, with small deviations because of chromatic aberrations of the microscope. We thus assumed that the fluorescent spots correspond to assembled basal bodies. In a minority of cells, a polarily localized YscC–mCherry spot without EGFP–YscQ equivalent could be observed in addition to the colocalizing spots. We assumed that these polar spots consist of misassembled YscC–mCherry proteins. Colocalization of spots was also observed for EGFP–YscD and EGFP–YscN with YscC–mCherry (data not shown). To test for colocalization of the needle with the basal body components, bacteria producing EGFP–YscQ were analysed by immunofluorescence with purified antibodies directed against the needle subunit. Overlays of the resulting pictures with the EGFP–YscQ fluorescence revealed that the majority of spots for YscF and YscQ colocalized (Supplementary Figure 2). A fraction of YscQ spots did not correspond to YscF spots.

Most likely, the needles of these basal bodies were detached during the immunofluorescence procedure. We conclude from all these experiments that the fluorescent spots correspond to functional injectisomes.

Assembly of the injectisome starts from the secretin ring in the OM and proceeds inwards through stepwise assembly of YscD and YscJ

As earlier work has shown that secretins can insert in the OM provided they are assisted by their pilotin (Burghout *et al*, 2004a; Guilvout *et al*, 2006), the fluorescent YscC–mCherry and its pilotin YscW were expressed *in trans* in *Y. enterocolitica* E40 (pMA8)(pRS6), in the absence of the pYV virulence plasmid encoding the T3S components. YscC–mCherry localized in membrane spots (Figure 2A), as observed before for PulD, the secretin involved in a type II secretion pathway (Buddelmeijer *et al*, 2009). These data thus confirm earlier results showing that YscC only requires its pilotin for assembly in the OM (Burghout *et al*, 2004a). In the absence of YscW, the majority of YscC–mCherry clustered in spots at the bacterial pole (Supplementary Figure 3). This phenotype was clearly distinguishable from the membrane spot formation in the presence of YscW, and confirmed the function of YscW in proper localization and oligomerization of YscC (Burghout *et al*, 2004a).

Not surprisingly, mutants lacking any of the structural ring proteins YscC, YscD, or YscJ failed to assemble the cytosolic injectisome components YscN and YscQ (Table I), showing that establishment of the membrane-spanning structure formed by YscC, YscD, and YscJ is at the beginning of injectisome formation. To test for the assembly order of these proteins, we combined the *egfp–yscD* allele on the pYV plasmid with non-polar deletions in *yscC* and *yscJ*. Although the absence of YscC clearly abolished the formation of EGFP–YscD spots at the bacterial membrane, the absence of YscJ did not affect this assembly (Figure 2B). This implies that YscC assembles first, followed by YscD, and finally YscJ.

To confirm this order of assembly, we performed co-immunoprecipitation assays using strains in which the wild-type alleles of *yscD* or *yscJ* on the virulence plasmid were replaced by *his-flag-yscD* or *yscJ-flag-his*, respectively. The affinity tagged proteins were functional for effector secretion (data not shown) and hence assumed to assemble in the same way as wild type. They were further combined

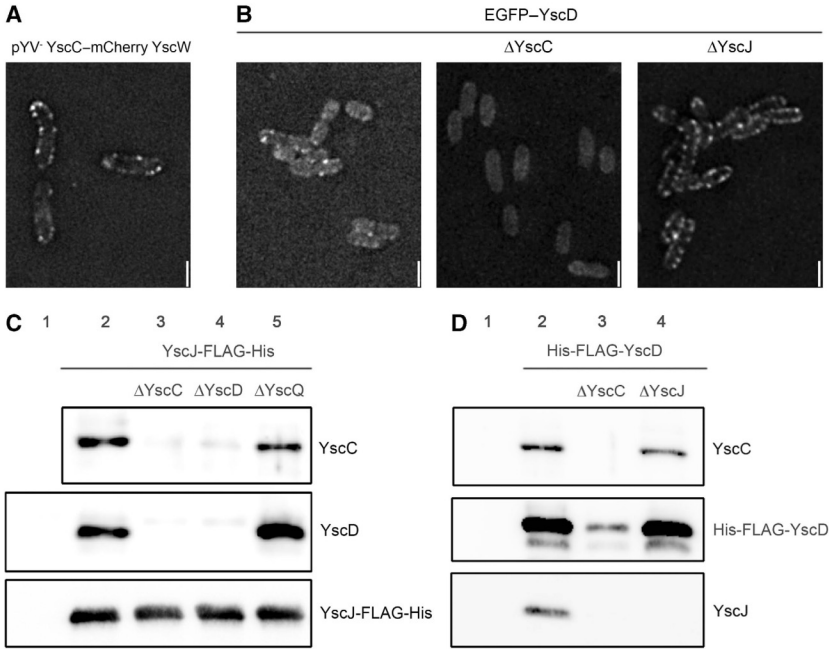

Figure 2 YscC assembly only requires its pilotin; YscD assembly requires the presence of YscC, but not of YscJ. Copurification of the three structural ring proteins suggests the stepwise assembly order YscC–YscD–YscJ. (**A**) Fluorescence microscopy showing the formation of secretin spots [YscC–mCherry] at the bacterial membrane in a strain lacking the virulence plasmid pYV, after *in trans* expression of YscC–mCherry and YscW (plasmids pMA8, pRS6) for 3 h at 37°C. Scale bars: 2 μm. (**B**) Fluorescence microscopy showing the formation of YscD spots at the bacterial membrane in strains E40(pAD4050) [EGFP–YscD], E40(pMAAD4018) [EGFP–YscD, ΔYscC], and E40(pAD4080) [EGFP–YscD, ΔYscJ]. YscD remains cytosolic in the absence of YscC, whereas it assembles in membrane spots in the absence of YscJ. (**C**) Analysis of the copurification of YscC and YscD after affinity purification of YscJ. Deletion of either YscC or YscD abolishes the copurification of the respective other protein with YscJ-FLAG-His. Bacteria were incubated for 3 h at 37°C, spheroplasted, and lysed. Proteins were purified by FLAG affinity, separated on 4–12% gradient SDS–PAGE, and analysed by immunoblot with the respective anti-YscC, -YscD, or -YscJ antibodies. All strains were ΔYadA to facilitate cell lysis: 1—E40(pLJM4029) [WT], 2—E40(pAD4054) [YscJ-FLAG-His], 3—E40(pAD4109) [YscJ-FLAG-His, ΔYscC], 4—E40(pAD4110) [YscJ-FLAG-His, ΔYscD], 5—E40(pAD4112) [YscJ-FLAG-His, ΔYscQ]. (**D**) Analysis of the copurification of YscC and YscJ after affinity purification of YscD. Whereas deletion of YscC abolishes copurification of YscJ with His-FLAG-YscD, YscJ is not required for the interaction between YscC and YscD. Samples were obtained as described for (**C**). All strains were ΔYadA to facilitate cell lysis: 1—E40(pLJM4029) [WT], 2—E40(pAD4055) [His-FLAG-YscD], 3—E40(pADMA4101) [His-FLAG-YscD, ΔYscC], 4—E40(pAD4089) [His-FLAG-YscD, ΔYscJ].

Table I Formation of fluorescent spots in various injectisome mutants

Protein missing	Family/function	Localization	YscC–mCherry fluorescence	EGFP–YscD fluorescence	EGFP–YscN fluorescence	EGFP–YscQ fluorescence
All (pYV$^-$)			+ (pMA8 + pRS6)	ND	ND	ND
YscC	Secretin	OM		− (pMAAD4018)	− (pADMA4156)	− (pADMA4151)
YscD	MS ring	IM	ND		ND	− (pAD4052)
YscJ	MS ring	IM	+ (pADMA4082)	+ (pAD4080)	− (pAD4139)	− (pADMA4082)
YscN	ATPase	Cytoplasmic, IM associated	+ (pADMA4137)	ND		− (pAD4104)
YscK	ATPase associated	Cytoplasmic, IM associated	ND	ND	− (pAD22840)	− (pAD22723)
YscL	ATPase associated	Cytoplasmic, IM associated	ND	ND	− (pAD4141)	− (pAD4039)
YscQ	C ring	Cytoplasmic, IM associated	+ (pMA4007)	+ (pAD4061)	− (pAD4142)	
YscR	Export machinery	IM	ND	ND	ND	+ (pAD4032)
YscS	Export machinery	IM	ND	ND	ND	+ (pAD4034)
YscT	Export machinery	IM	ND	ND	ND	+ (pAD4036)
YscU	Export machinery[a]	IM	ND	ND	ND	+ (pAD4026)
YscV(LcrD)	Export machinery	IM	+ (pMA4011)	ND	ND	+ (pAD4038)
YscRSTUV	Export machinery	IM	ND	ND	+ (pAD4143)	+ (pAD4108)
YscF	Needle subunit	Extracellular	+ (pMA4015)	ND	+ (pAD4157)	+ (pAD4020)
LcrV	Needle tip	Extracellular	ND	ND	ND	+ (pAD4042)
YscH	Unknown	Exported	ND	ND	ND	+ (pAD22769)
YscI	Unknown[b]	Exported	ND	ND	ND	+ (pAD4022)
YscO	Unknown	Exported	ND	ND	ND	+ (pAD4024)
YscX	Unknown	Exported	ND	ND	ND	+ (pAD4027)
YscY	Chaperone of YscX	Cytoplasmic	ND	ND	ND	+ (pAD4040)
YopN	Ca^{2+} plug	Cytoplasmic, IM associated	ND	ND	ND	+ (pAD4043)
LcrG	Ca^{2+} plug	Cytoplasmic, IM associated	ND	ND	ND	+ (pAD4041)

The formation of fluorescent spots was checked for YscC–mCherry, EGFP–YscD, EGFP–YscN, and EGFP–YscQ in combination with deletions of different proteins. +: Spot formation at the bacterial membrane; −: diffuse cytosolic fluorescence. The virulence plasmids of the corresponding strains are given in brackets (see Supplementary Table I for strain details). ND: not determined.
[a]Substrate specificity switch.
[b]Proposed inner rod.

with non-polar deletions in *yscC*, *yscD*, or *yscJ*. In each of the strains, the adhesin YadA was removed to facilitate cell lysis. Synthesis of the injectisome in these strains was induced under secretion-non-permissive conditions. Mild crosslinking was performed, spheroplasts were created, and the bacteria were lysed by the addition of detergent (see Material and methods). Afterwards, a one-step affinity purification was performed, and the (co-)purification of YscC, YscD, and YscJ was tested. YscJ-FLAG-His copurified YscC and YscD from complete injectisomes, and removal of YscQ, a protein thought to act further downstream in the assembly process, did not affect this copurification. In contrast, removal of YscC prevented copurification of YscD with YscJ-FLAG-His, and removal of YscD prevented copurification of YscC (Figure 2C). Likewise, His-FLAG-YscD copurified YscC and YscJ from complete injectisomes. However, although removal of YscC prevented copurification of YscJ with His-FLAG-YscD, removal of YscJ still allowed the copurification of YscC (Figure 2D). The amount of purified His-FLAG-YscD was reduced in the absence of YscC, most likely as a consequence of decreased cellular YscD levels, either because of its mislocalization in the absence of YscC or because of a lower expression level. Taken together, these data indicate (i) that the insertion of the secretin ring in the OM is required for the subsequent association of YscD and YscJ and (ii) that YscD makes the link between YscC and YscJ. Hence, the OM ring is the first ring of the injectisome to be assembled. This assembly step is followed by the attachment of YscD, which then allows the completion of the MS ring by YscJ.

The C ring only assembles in the presence of the membrane rings, YscN, YscK, and YscL

To determine at which stage the C ring forms during the assembly process, we combined the *egfp–yscQ* allele with an array of deletions in most injectisome genes (Table I; Supplementary Table 1 for details of strains). Deletion of any of the membrane ring proteins (YscC, YscD, or YscJ) completely abolished the formation of membrane spots and led to an increased diffuse cytoplasmic fluorescence (Figure 3). This indicates that the C ring forms after the YscCDJ ring structure. Removal of the ATPase YscN or any of its two interacting proteins YscK and YscL (Jackson and Plano, 2000; Blaylock *et al*, 2006) also fully prevented C ring formation (Figure 3), indicating that assembly of the C ring additionally requires YscN as well as YscK and YscL.

Removal of individual proteins YscR, S, T, U, or V from the export apparatus as well as a complete deletion of all these proteins did not completely abolish the formation of the C ring. However, in the absence of YscR, YscS, or YscV, the number of spots was reduced, indicating that these proteins are either beneficial (but not absolutely required) for C ring formation, or have a stabilizing effect on fully assembled injectisomes.

As expected from the fact that YscF, YscI, YscO, YscX, and YopN are substrate proteins exported by the injectisome

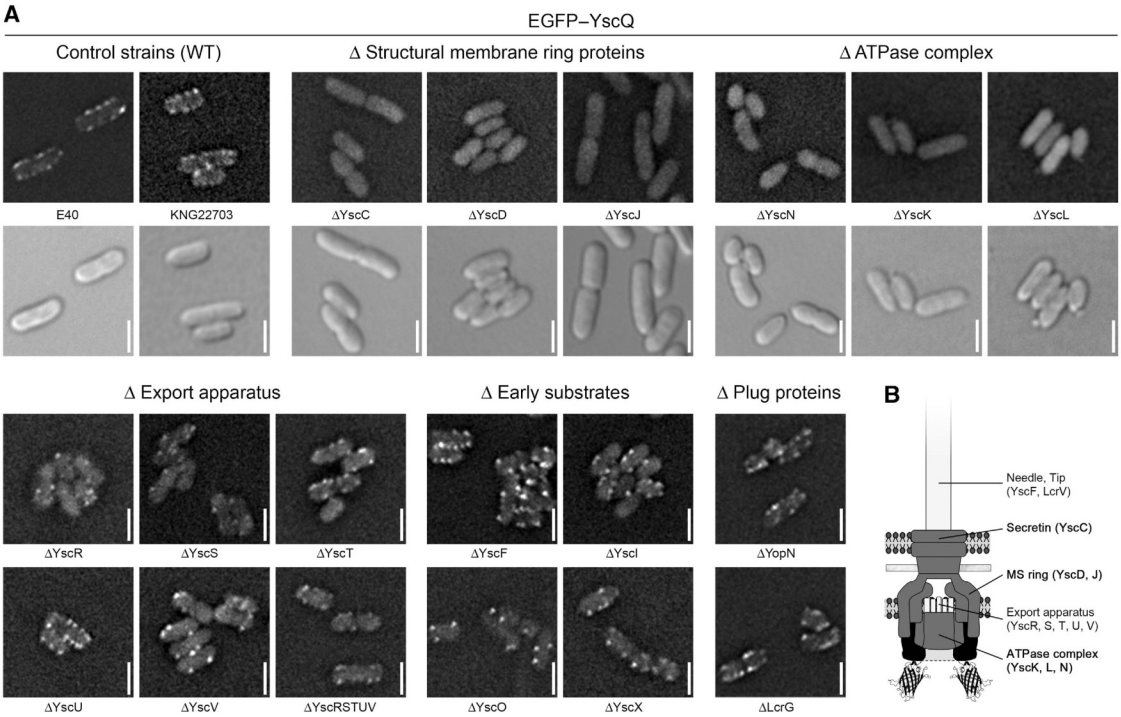

Figure 3 C ring formation requires both transmembrane rings and the ATPase complex, but not the export apparatus or any secreted substrate. (**A**) Fluorescence microscopy pictures of bacteria expressing EGFP–YscQ combined with deletions of different genes. Micrographs were taken 3 h after induction of the T3S system. (For the control strains and the strains with deletions in the proteins required for C ring formation—upper lane: EGFP fluorescence, lower lane: corresponding DIC picture). Scale bars: 2 μm. (**B**) Schematic representation of the injectisome showing the components required (bold, dark) and not required (normal, light) for C ring formation. For information about the used strains, refer to Table I.

itself, their absence also did not prevent the formation of the C ring. Likewise, deletion of LcrG, a regulatory protein (Nilles *et al*, 1997; Torruellas *et al*, 2005), had no effect on assembly of the C ring (Figure 3; see Table I for additional strains).

ATPase assembly not only requires the presence of the YscCDJ platform, but also needs YscK, YscL, and YscQ

Finally, assembly of the ATPase YscN was tested. As replacement of the wild-type allele on the virulence plasmid by a gene encoding a fluorescent fusion protein decreased the expression of downstream genes in the *virB* operon, whereas a complete deletion of *yscN* was non-polar (Figure 1B), *egfp–yscN* was cloned in a pBAD vector and used to complement *in trans* double deletions in *yscN* and several other genes. Induction of synthesis of EGFP–YscN with 0.05% arabinose led to YscN protein levels similar to the native level (Supplementary Figure 1), and to effector secretion at wild-type levels (data not shown). As shown in Figure 4, YscN assembly required the presence of YscC (secretin), YscJ (MS ring), YscK and YscL (two proteins known to interact with the ATPase), and YscQ (the C ring). In contrast, even the complete deletion of the IM export proteins YscR, S, T, U, V still allowed formation of YscN spots, albeit again in a reduced number (Figure 4).

These data suggest that the cytosolic components of the injectisome form a single large ATPase–C ring complex, requiring all of its components YscK, L, N, Q to assemble.

In agreement with the essential function of YscQ for the ATPase assembly, we did not observe any needle formation in strains that lack YscQ, but overexpress YscN, in contrast to recent results obtained with the flagellum (Konishi *et al*, 2009) (data not shown).

ATPase activity of YscN is not required for the assembly of the ATPase–C ring complex at the injectisome

To determine whether assembly of the C ring requires YscN for its ATPase activity or as a structural component, a deletion of *yscN* in an *egfp–yscQ* background was examined. As expected, the resulting strain secreted neither Yops nor the ruler and needle subunits. Secretion could be complemented *in trans* by a wild-type *yscN* allele, but not by an *yscN* allele encoding $YscN_{K175E}$ altered in the Walker box (Figure 5B and C). Interestingly, however, although $YscN_{K175E}$ was not functional, it did restore the formation of the C ring spots (Figure 5A), implying that the YscN requirement for the formation of the ATPase–C ring complex is exclusively structural.

After assembly of the ATPase–C ring complex, needle formation and effector secretion take place rapidly

The kinetics of C ring formation in a strain expressing EGFP–YscQ was followed in a time-course experiment. Pictures were taken every 20 min up to 2 h after induction of the *ysc-yop* regulon (Cornelis *et al*, 1989) in a Ca^{2+}-depleted medium. Weak diffuse cytoplasmic fluorescence could be observed 20 and 40 min after the temperature shift, suggest-

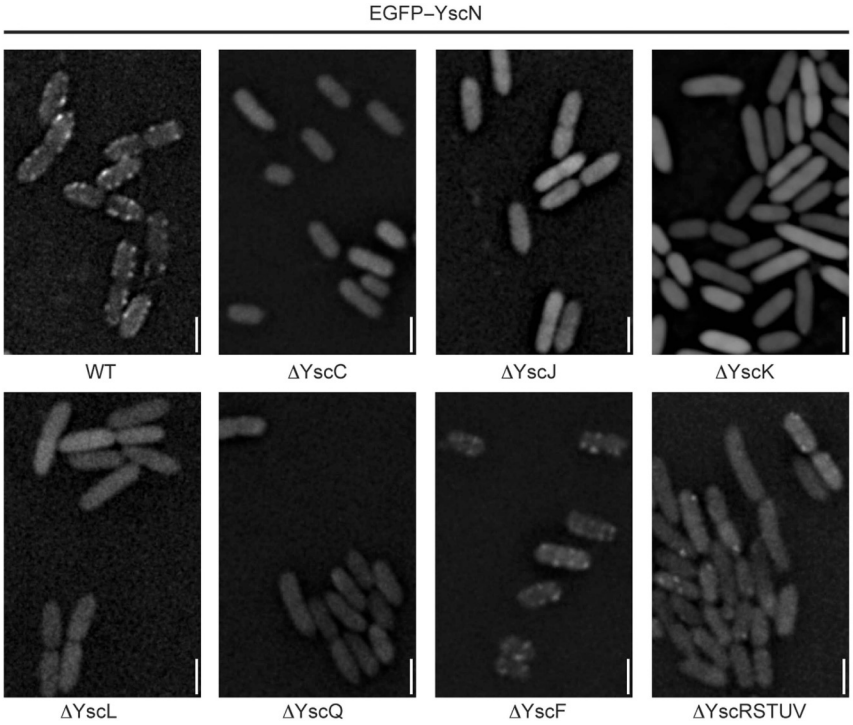

Figure 4 The assembly of the ATPase requires both transmembrane rings, YscK, YscL, and YscQ, but not the export apparatus. Fluorescence microscopy pictures of YscN null mutants complemented with EGFP–YscN combined with deletions of different genes. Wild-type protein levels were established by EGFP–YscN induction with 0.05% arabinose. Micrographs were taken 3 h after induction of EGFP–YscN and the T3S system. Scale bars: 2 μm. For information about the used strains, refer to Table I.

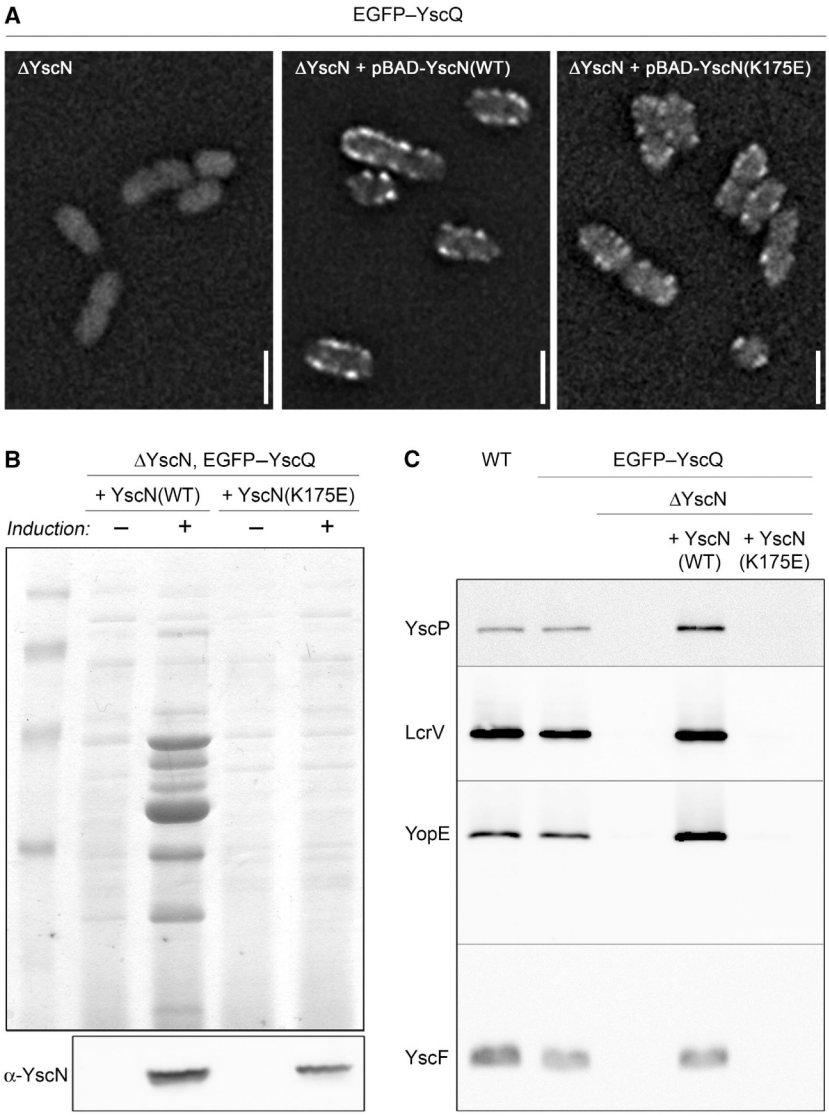

Figure 5 The structure, but not the ATPase activity of YscN, is required for the formation of the C ring. (**A**) Fluorescence microscopy showing the formation of C ring spots in E40(pAD4104) [EGFP–YscQ, ΔYscN], complemented with plasmids encoding wild-type YscN or the catalytically inactive YscN(K175E), 3 h after induction of the type III secretion system. Scale bars: 2 μm. (**B**) Upper part: Analysis of Yop protein secretion in strain E40(pAD4104) complemented with wild type, or catalytically inactive YscN. Expression of YscN was either not induced (−) or induced with 0.05% arabinose (+). Culture supernatants were separated on a 12% SDS–PAGE gel and stained with Coomassie Brilliant Blue. Lower part: Expression of YscN in the corresponding strains. Cell pellets were separated on a 12% SDS–PAGE gel and analysed by immunoblot with anti-YscN antibodies. (**C**) Export of different classes of substrates in strains expressing EGFP–YscQ, and the different YscN variants. Culture supernatants were separated on a 15% SDS–PAGE gel and analysed by immunoblot with the respective antibodies.

ing that synthesis of YscQ was turned on directly after the shift, and that EGFP folds rapidly in the *Yersinia* cytosol (Figure 6A). The rapid synthesis of YscQ was also confirmed by immunoblotting (data not shown). The first membrane spots could, however, only be observed 60 min after induction. Although the fluorescence intensity of single spots seemed to increase over time, the number of spots stayed roughly constant up to 3 h after induction (Figure 6A). Interestingly, the timeframe of appearance of the C ring was approximately the same as the timeframe of appearance of the needles (Figure 6B) and secretion of the effector proteins (Figure 6C), suggesting that needle formation and effector secretion occur within a short time after establishment of the ATPase–C ring complex. A model of injectisome assembly that incorporates the above mentioned results is depicted in Figure 7.

Discussion

The assembly of the T3S injectisome is a complex process that engages >20 different proteins, and results in the

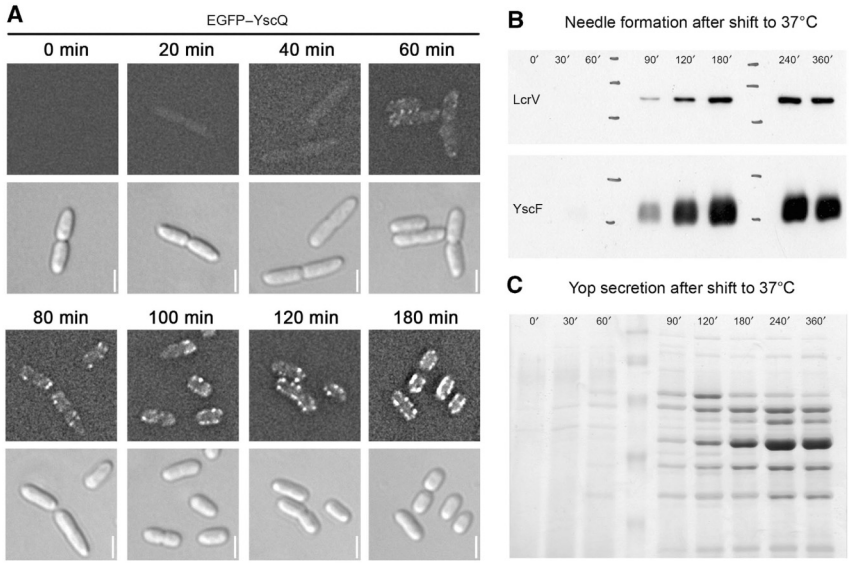

Figure 6 Formation of the C ring occurs about 60 min after induction of the T3S system. It directly precedes needle formation and effector secretion. (**A**) Fluorescence microscopy showing the formation of C ring spots [EGFP–YscQ] in strain E40(pAD4016) at various time points after induction of the synthesis of the T3S system by temperature shift to 37°C (upper lane: EGFP fluorescence; lower lane: corresponding DIC picture). Scale bars: 2 μm. (**B**) Time course of needle formation in wild-type strain E40(pYV40). Needle formation was monitored by SDS–PAGE analysis of purified needles. The needle pellet was separated on a 15% gel and analysed by immunoblot with anti-LcrV and anti-YscF antibodies, respectively. (**C**) Time course of Yop protein secretion by wild-type strain E40(pYV40). Culture supernatants were separated on a 12% SDS–PAGE gel and stained with Coomassie Brilliant Blue. All time-course experiments were performed in secretion-permissive conditions (Ca^{2+}-depleted medium).

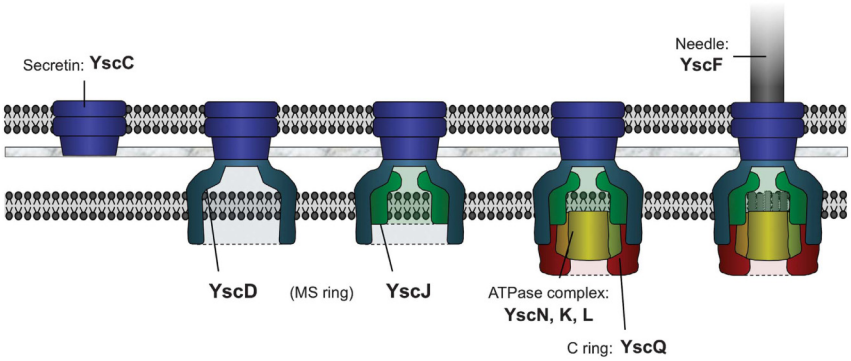

Figure 7 Model of assembly of the *Yersinia* injectisome. Formation of the injectisome is initiated by formation of the secretin ring in the outer membrane. Next, YscD attaches to YscC, which allows the subsequent completion of the MS ring by attachment of YscJ. After the formation of the membrane ring structures, the ATPase–C ring complex, consisting of YscN, K, L, and Q assembles at the cytoplasmic side of the injectisome. The exact time point of the integration of the IM proteins YscR, S, T, U, and V is unclear. Afterwards, the needle consisting of YscF and LcrV can be assembled. Bold font denotes protein names, normal font denotes functional subunits. The global structure of YscC, D, J is derived from Spreter *et al* (2009).

formation of a nanomachine spanning both bacterial membranes and protruding outside the bacterium. So far, little is known about this process. On the basis of the observation that heterologously overexpressed *S. enterica* MS ring components PrgH and PrgK form large rings in the absence of any other T3S component, a model was proposed (Kimbrough and Miller, 2002) in which the IM ring assembles first, and then fuses with the secretin ring in the OM. This model suggests the same general assembly scheme as the one that has been proposed for the flagellum (Kubori *et al*, 1997; Macnab, 2003), but does not explain how the two membrane rings find each other. The subsequent steps of assembly could not be examined so far.

To gain better insight into the assembly process and the functional relations between the proteins, we constructed strains in which a number of injectisome constituents were fused to fluorescent proteins. To minimize artefacts because of non-native expression levels or timing of the fusion proteins, we replaced the wild-type allele on the pYV virulence plasmid by the hybrid allele in the case of *yscC*, *yscD*, and *yscQ*. The hybrid *yscN* was plasmid borne, but it was expressed at wild-type level.

All recombinant injectisomes were functional, and in all cases, fluorescent spots appeared at the bacterial membrane, distributed all over the bacterial body. Colocalization of the fluorophores confirmed that the fluorescent spots correspond to injectisomes. The brightness of the spots likely results from the multimeric nature of the tagged proteins, although at this stage, one cannot conclude that each spot corresponds to only one injectisome. A fluorescence quantification based on external standards, presently in progress, will address this question.

We observed that the membrane ring-forming proteins YscC, YscD, and YscJ are required for assembly of any cytosolic structure. Importantly, by monitoring the formation of YscC–mCherry and EGFP–YscD spots, we observed that YscC assembles independently of YscD and YscJ and that YscD assembles independently of YscJ, but not of YscC. Co-immunoprecipitation assays confirmed that YscJ requires YscD to become attached to YscC. All this implies that the assembly of the injectisome is initiated by formation of the secretin ring in the OM and proceeds inwards through stepwise assembly of YscD and YscJ. These data contradict the earlier report that PrgH and PrgK, the *Salmonella* homologues of YscD and YscJ, can form a ring alone (Kimbrough and Miller, 2000). The discrepancy might result from the fact that the earlier study was based on heterologously overexpressed proteins, whereas this study is based on functional proteins produced in their natural environment at native expression levels. These data are also at odd with the report indicating that MxiD and MxiJ, the *Shigella* homologues of YscC and YscJ, interact even in the absence of the connector (Schuch and Maurelli, 2001). However, this interaction was observed in the absence of the pilot protein. In this case, the majority of secretin proteins are mislocalized to the IM (Koster *et al*, 1997), which might lead to non-native interaction with MxiJ. Interestingly, it was shown recently that the assembly of two ring-forming IM components of the *Vibrio cholerae* type II secretion complex also depends on the presence of the OM secretin (Lybarger *et al*, 2009), suggesting conservation or convergent evolution of the formation process in these two prokaryotic export systems. Taken together, our results show that the order of assembly of the OM and IM rings differs between the injectisome and the flagellum. We do not see any obvious reason for this, but this observation indicates that the two nanomachines differ more than is often thought. The flagellum is indeed significantly more complex than the injectisome because it rotates, which implies not only a motor but also bushings in the peptidoglycan and the OM. The P and L rings, having this function, are precisely replaced by a very stable secretin ring in the injectisome. This basic structural difference might explain the different order of assembly of the two nanomachines.

The outside-in assembly order consistently shown by co-immunprecipitation and fluorescence microscopy further implies that YscD is the connector between the two membrane rings, which is coherent with recent crystal structure and modelling data (Spreter *et al*, 2009). Our biochemical data allow to assess the recent models to integrate the crystal structures of the membrane ring proteins into the overall shape generated by electron microscopy averaging of purified injectisomes (Hodgkinson *et al*, 2009; Spreter *et al*, 2009). The electron density between the membranes would be generated by YscD. This in turn places YscJ in the IM, as proposed by manual fits (Moraes *et al*, 2008; Hodgkinson *et al*, 2009; Spreter *et al*, 2009), but not by the best automated fit (Hodgkinson *et al*, 2009).

After assembly of the OM and IM membrane rings, cytosolic components can assemble onto the structure. The observation that the proposed C ring component YscQ assembles in membrane spots colocalizing with the other components shows that the C ring is an integral component of the injectisome, confirming an assumption so far mainly based on immunogold-labelling experiments (Morita-Ishihara *et al*, 2006). Our data indicate that a large cytosolic complex consisting of the ATPase YscN, the two interacting proteins YscK and YscL, and the C ring component YscQ is formed, requiring all of its components, but not the ATPase activity of YscN for assembly. This differs again from the situation in the flagellum. There, FliM, FliN, and FliG (together forming the C ring) appear in significant amount in the membrane fraction in the presence of FliF (MS ring), but in the absence of FliI (ATPase) or FliH (homologue to YscL). This suggests that the flagellar C ring forms in the absence of the ATPase complex (Kubori *et al*, 1997), in agreement with the observation that it forms on overexpression of FliM, FliN, and FliG together with FliF (Lux *et al*, 2000; Young *et al*, 2003). Although the heterologous overexpression of the proteins in these studies might account for the different observations, these results can also be the consequence of functional differences between the two nanomachines. As the constraint of rotation and spatial separation of the C ring and ATPase does not exist for the injectisome, the apparatus could be optimized for secretion. A tighter contact between the ATPase complex and the C ring might be a consequence of this optimization. The fact that we could not overcome the requirement of YscQ for secretion by overexpression of the ATPase is consistent with the essential function of YscQ for assembly of the complete ATPase–C ring complex.

Our results are also in perfect agreement with earlier results showing interactions between YscK, YscL, YscN, and YscQ (Jackson and Plano, 2000). However, the hypothesis that YscQ recruits the ATPase should be revised: YscK, L, N, and Q would rather assemble in one step. The proposed function of YscL as a negative regulator of ATPase activity (Blaylock *et al*, 2006) as well as its direct interaction with YscN and YscQ (Jackson and Plano, 2000) is consistent with the presence of YscL in this complex. Less is known about the function of YscK. As it interacts with YscQ, but not with YscN and weakly at the most with YscL (Jackson and Plano, 2000; Blaylock *et al*, 2006), it might act at the interface of the ATPase–C ring complex.

Formation and assembly of the ATPase–C ring complex did not depend on any of the five proteins forming the export apparatus, even though the number of membrane spots was reduced when YscR, YscS, YscV, or the five proteins YscRSTUV were missing. This implies that a YscKLNQ complex docks onto the IM ring rather than onto the export apparatus, which agrees with the observations made with the flagellum (Kubori *et al*, 1997). As currently, little is known about stoichiometry, localization, and function of the export apparatus, its function in the assembly process remains unclear.

In conclusion, this work shows that the assembly of the injectisome starts with the formation of the stable secretin ring in the OM, and proceeds inwards through discrete attachment steps of YscD and YscJ at the IM. Afterwards,

the components of the cytosolic ATPase–C ring complex assemble at the cytosolic side of the injectisome in one step, which allows the subsequent fast steps leading to needle formation and effector secretion.

Materials and methods

Bacterial strains, plasmids, and genetic constructions

Y. enterocolitica strains and plasmids are listed in Supplementary Table 1.

E. coli Top10, used for plasmid purification and cloning, and *E. coli* Sm10 λ pir, used for conjugation, were routinely grown on LB agar plates and in LB broth. Ampicillin was used at a concentration of 200 μg/ml to select for expression vectors. Streptomycin was used at a concentration of 100 μg/ml to select for suicide vectors. Plasmids were generated using either Phusion polymerase (Finnzymes, Espoo, Finland) or Vent DNA polymerase (New England Biolabs, Frankfurt, Germany). The oligonucleotides used for genetic constructions are listed in Supplementary Table 2. Mutators for modification or deletion of genes in the pYV plasmids were constructed by overlapping PCR using purified pYV40 plasmid as template, leading to 200–250 bp of flanking sequences on both sides of the deleted or modified part of the respective gene. As an exception, pKEM5 was constructed by introduction of the deletion through religation of the 5′ phoshorylated internal oligonucleotides. For the mutator strains introducing EGFP, a precursor mutator vector was created as described above. Subsequently, the EGFP gene was inserted in frame from plasmid pEGFP-C1 into the digested precursor vectors. The respective regions containing the flanking sequences were subcloned into the pKNG101 suicide vector. For pMA12, insert 2 was created by overlapping PCR using oligos 5017 and 5087 to amplify mCherry from vector pRVCHYC-5 (Thanbichler *et al*, 2007), and oligos 5088 and 5068 to amplify the downstream flanking region from the pYV plasmid. Afterwards, ligation of *Sal*I/*Xho*I digested insert 1, containing the upstream flanking region, *Xho*I/*Xba*I digested insert 2, and *Sal*I/*Xba*I digested pKNG101 suicide vector lead to the mutator pMA12. All constructs were confirmed by sequencing using a 3100-Avant genetic analyser (Applied Biosystems, Rotkreuz, Switzerland). The allelic exchange was selected by plating diploid bacteria on sucrose (Kaniga *et al*, 1991). pAD166 expressing $YscN_{K175E}$ was generated by overlapping PCR using internal primers encoding for the modified protein sequence, and selected by colony PCR and sequencing. For pAD182 expressing EGFP–YscN, a precursor vector was generated and EGFP was introduced from pEGFP-C1, as described above.

Y. enterocolitica cultures for secretion and microscopy analysis

Induction of the *yop* regulon was performed by shifting the culture to 37°C, either in BHI-Ox (secretion-permissive conditions) or in BHI + 5 mM $CaCl_2$ (secretion-non-permissive conditions) (Cornelis *et al*, 1987). Expression of the inducible YscN constructs was induced by adding 0.05% L-arabinose to the culture just before the shift to 37°C. The carbon source was glycerol (4 mg/ml) when expressing genes from the pBAD promoter, and glucose (4 mg/ml) in the other cases.

Yop secretion

Total cell and supernatant fractions were separated by centrifugation at 20 800 *g* for 10 min at 4°C. The cell pellet was taken as total cell fraction. Proteins in the supernatant were precipitated with trichloroacetic acid 10% (w/v) final for 1 h at 4°C.

Secreted proteins were analysed by SDS–PAGE; in each case, proteins secreted by 3×10^8 bacteria were loaded per lane. Total secreted proteins were analysed by Coomassie staining of 12% SDS–PAGE gels. Detection of specific secreted proteins by immunoblotting was performed using 15% SDS–PAGE gels. For detection of proteins in total cells, 2×10^8 bacteria were loaded per lane, if not stated otherwise, and proteins were separated on 15% SDS–PAGE gels before detection by immunoblotting.

Immunoblotting was carried out using rabbit polyclonal antibodies against LcrV (MIPA220; 1:2000), YscF (MIPA223; 1:1000), YscN (MIPA189; 1:1000), YscP (MIPA57; 1:3000), or YopE (MIPA73; 1:1000). Detection was performed with secondary antibodies directed against rabbit antibodies and conjugated to horseradish peroxidase (1:5000; Dako), before development with ECL chemiluminescent substrate (Pierce).

Needle purification

Needles were purified from cultures incubated under secretion-permissive conditions. At the given time points, 48 ml bacteria were removed from the 500 ml culture, harvested by centrifugation (5 min at 4000 *g*) and resuspended in 1 ml 20 mM Tris–HCl, pH 7.5. Needle detachment was increased by repeated pipetting through a 1 ml pipet tip. Cells were pelleted by centrifugation (5 min at 4000 *g*), and the supernatant containing the needles was passed through a 0.45 μm mesh filter (cellulose acetate membrane) and then centrifuged for 60 min at 20 800 *g*. The resulting pellet was resuspended in 20 μl Laemmli buffer, 15 μl of which were analysed by SDS–PAGE followed by immunoblotting (Mueller *et al*, 2005).

Fluorescence microscopy

For fluorescence imaging, cells were placed on a microscope slide layered with a pad of 2% agarose dissolved in water or PBS. A Deltavision Spectris optical sectioning microscope (Applied Precision, Issaquah, WA) equipped with an UPlanSApo 100 × /1.40 oil objective (Olympus, Tokyo, Japan) and a coolSNAP HQ CCD camera (Photometrics, Tucson, AZ) was used to take differential interference contrast (DIC) and fluorescence photomicrographs. To visualize GFP and mCherry fluorescence, GFP filter sets (Ex 490/20 nm, Em 525/30 nm) and mRFP filter sets (Ex 560/40 nm, EM 632/60 nm), respectively, were used. DIC frames were taken with 0.3 s and fluorescence frames with 1.0 s exposure time. Per image, a Z-stack containing 20 frames per wavelength with a spacing of 150 nm was acquired. The stacks were deconvoluted using softWoRx v3.3.6 with standard settings (Applied Precision, WA). The DIC frame at the centre of the bacterium and the corresponding fluorescence frame were selected and further processed with ImageJ software.

Co-immunoprecipitation of YscC, YscD, and YscJ

Y. enterocolitica cultures were grown in secretion-non-permissive conditions to an OD_{600} of 1.5–2.2. Protein complexes were then stabilized by crosslinking with 0.25% formaldehyde for 15 min at 37°C. Cells were harvested by centrifugation (15 min at 1500 *g*, 25°) and resuspended in 1/5 volume of PBS. After a second crosslinking step (0.4% formaldehyde, 15 min, 25°C) and harvesting as before, spheroplast generation and lysis was performed as described by Kubori *et al* (1997) and Blocker *et al* (2001). In short, cells were resuspended in 1/5 original volume of ice-cold spheroplasting buffer (0.75 M sucrose, 50 mM Tris, pH adjusted with HCl to 7.8, 0.6 mg/ml lysozyme, 6 mM EDTA), and incubated at 25°C up to 90 min, until complete spheroplast formation could be observed. Cells were lysed by addition of 1% Triton X-100 and subsequent incubation at 4°C for 15 min. After addition of 15 mM $MgCl_2$, unlysed cells were removed by centrifugation (20 min at 6000 *g*, 4°C); 300 μl of anti-FLAG M2 affinity gel (Sigma-Aldrich, Buchs, Switzerland) were added to the supernatant, and the proteins were purified in batch according to the manufacturer's protocol. The elution fractions were recentrifuged to completely remove resin, and separated on 12% SDS–PAGE gels or 4–12% gradient SDS–PAGE gels (Serva, Heidelberg, Germany). Immunoblotting was carried out using rabbit polyclonal antibodies against YscC (MIPA250, 1:1000), YscD (MIPA232, 1:1000), and YscJ (MIPA66, 1:5000), as described above.

Supplementary data

Supplementary data are available at *The EMBO Journal* Online (http://www.embojournal.org).

Acknowledgements

We thank K Maylandt and I Stainier for providing strains pKEM5, pKEM4001, pSI51, and pSI4006. This work was supported by the Swiss National Science Foundation (grant 310000-113333/1) to GC.

Conflict of interest

The authors declare that they have no conflict of interest.

References

Abrahams JP, Leslie AG, Lutter R, Walker JE (1994) Structure at 2.8 A resolution of F1-ATPase from bovine heart mitochondria. *Nature* **370:** 621–628

Akeda Y, Galan JE (2005) Chaperone release and unfolding of substrates in type III secretion. *Nature* **437:** 911–915

Alfano JR, Collmer A (2004) Type III secretion system effector proteins: double agents in bacterial disease and plant defense. *Annu Rev Phytopathol* **42:** 385–414

Blaylock B, Riordan KE, Missiakas DM, Schneewind O (2006) Characterization of the Yersinia enterocolitica type III secretion ATPase YscN and its regulator, YscL. *J Bacteriol* **188:** 3525–3534

Blocker A, Gounon P, Larquet E, Niebuhr K, Cabiaux V, Parsot C, Sansonetti P (1999) The tripartite type III secreton of Shigella flexneri inserts IpaB and IpaC into host membranes. *J Cell Biol* **147:** 683–693

Blocker A, Jouihri N, Larquet E, Gounon P, Ebel F, Parsot C, Sansonetti P, Allaoui A (2001) Structure and composition of the Shigella flexneri 'needle complex', a part of its type III secreton. *Mol Microbiol* **39:** 652–663

Buddelmeijer N, Krehenbrink M, Pecorari F, Pugsley AP (2009) Type II secretion system secretin PulD localizes in clusters in the Escherichia coli outer membrane. *J Bacteriol* **191:** 161–168

Burghout P, Beckers F, de Wit E, van Boxtel R, Cornelis GR, Tommassen J, Koster M (2004a) Role of the pilot protein YscW in the biogenesis of the YscC secretin in Yersinia enterocolitica. *J Bacteriol* **186:** 5366–5375

Burghout P, van Boxtel R, Van Gelder P, Ringler P, Muller SA, Tommassen J, Koster M (2004b) Structure and electrophysiological properties of the YscC secretin from the type III secretion system of Yersinia enterocolitica. *J Bacteriol* **186:** 4645–4654

Cordes FS, Komoriya K, Larquet E, Yang S, Egelman EH, Blocker A, Lea SM (2003) Helical structure of the needle of the type III secretion system of Shigella flexneri. *J Biol Chem* **278:** 17103–17107

Cornelis G, Vanootegem JC, Sluiters C (1987) Transcription of the yop regulon from Y. enterocolitica requires trans acting pYV and chromosomal genes. *Microb Pathog* **2:** 367–379

Cornelis GR (2006) The type III secretion injectisome. *Nat Rev Microbiol* **4:** 811–825

Cornelis GR, Biot T, Lambert de Rouvroit C, Michiels T, Mulder B, Sluiters C, Sory MP, Van Bouchaute M, Vanooteghem JC (1989) The Yersinia yop regulon. *Mol Microbiol* **3:** 1455–1459

Cornelis GR, Van Gijsegem F (2000) Assembly and function of type III secretory systems. *Annu Rev Microbiol* **54:** 735–774

Cornelis GR, Wolf-Watz H (1997) The Yersinia Yop virulon: a bacterial system for subverting eukaryotic cells. *Mol Microbiol* **23:** 861–867

Crepin VF, Prasannan S, Shaw RK, Wilson RK, Creasey E, Abe CM, Knutton S, Frankel G, Matthews S (2005) Structural and functional studies of the enteropathogenic Escherichia coli type III needle complex protein EscJ. *Mol Microbiol* **55:** 1658–1670

Daniell SJ, Takahashi N, Wilson R, Friedberg D, Rosenshine I, Booy FP, Shaw RK, Knutton S, Frankel G, Aizawa S (2001) The filamentous type III secretion translocon of enteropathogenic Escherichia coli. *Cell Microbiol* **3:** 865–871

Deane JE, Roversi P, Cordes FS, Johnson S, Kenjale R, Daniell S, Booy F, Picking WD, Picking WL, Blocker AJ, Lea SM (2006) Molecular model of a type III secretion system needle: implications for host-cell sensing. *Proc Natl Acad Sci USA* **103:** 12529–12533

Driks A, DeRosier DJ (1990) Additional structures associated with bacterial flagellar basal body. *J Mol Biol* **211:** 669–672

Erhardt M, Hughes KT (2010) C-ring requirement in flagellar type III secretion is bypassed by FlhDC upregulation. *Mol Microbiol* **75:** 376–393

Fadouloglou VE, Tampakaki AP, Glykos NM, Bastaki MN, Hadden JM, Phillips SE, Panopoulos NJ, Kokkinidis M (2004) Structure of HrcQB-C, a conserved component of the bacterial type III secretion systems. *Proc Natl Acad Sci USA* **101:** 70–75

Galan JE, Collmer A (1999) Type III secretion machines: bacterial devices for protein delivery into host cells. *Science* **284:** 1322–1328

Gonzalez-Pedrajo B, Fraser GM, Minamino T, Macnab RM (2002) Molecular dissection of Salmonella FliH, a regulator of the ATPase FliI and the type III flagellar protein export pathway. *Mol Microbiol* **45:** 967–982

Grant SR, Fisher EJ, Chang JH, Mole BM, Dangl JL (2006) Subterfuge and manipulation: type III effector proteins of phytopathogenic bacteria. *Annu Rev Microbiol* **60:** 425–449

Guilvout I, Chami M, Engel A, Pugsley AP, Bayan N (2006) Bacterial outer membrane secretin PulD assembles and inserts into the inner membrane in the absence of its pilotin. *EMBO J* **25:** 5241–5249

Hodgkinson JL, Horsley A, Stabat D, Simon M, Johnson S, da Fonseca PC, Morris EP, Wall JS, Lea SM, Blocker AJ (2009) Three-dimensional reconstruction of the Shigella T3SS transmembrane regions reveals 12-fold symmetry and novel features throughout. *Nat Struct Mol Biol* **16:** 477–485

Imada K, Minamino T, Tahara A, Namba K (2007) Structural similarity between the flagellar type III ATPase FliI and F1-ATPase subunits. *Proc Natl Acad Sci USA* **104:** 485–490

Jackson MW, Plano GV (2000) Interactions between type III secretion apparatus components from Yersinia pestis detected using the yeast two-hybrid system. *FEMS Microbiol Lett* **186:** 85–90

Jin Q, He SY (2001) Role of the Hrp pilus in type III protein secretion in Pseudomonas syringae. *Science* **294:** 2556–2558

Kaniga K, Delor I, Cornelis GR (1991) A wide-host-range suicide vector for improving reverse genetics in gram-negative bacteria: inactivation of the blaA gene of Yersinia enterocolitica. *Gene* **109:** 137–141

Khan IH, Reese TS, Khan S (1992) The cytoplasmic component of the bacterial flagellar motor. *Proc Natl Acad Sci USA* **89:** 5956–5960

Kimbrough TG, Miller SI (2000) Contribution of Salmonella typhimurium type III secretion components to needle complex formation. *Proc Natl Acad Sci USA* **97:** 11008–11013

Kimbrough TG, Miller SI (2002) Assembly of the type III secretion needle complex of Salmonella typhimurium. *Microbes Infect/ Institut Pasteur* **4:** 75–82

Konishi M, Kanbe M, McMurry JL, Aizawa S (2009) Flagellar formation in C-ring-defective mutants by overproduction of FliI, the ATPase specific for flagellar type III secretion. *J Bacteriol* **191:** 6186–6191

Koster M, Bitter W, de Cock H, Allaoui A, Cornelis GR, Tommassen J (1997) The outer membrane component, YscC, of the Yop secretion machinery of Yersinia enterocolitica forms a ring-shaped multimeric complex. *Mol Microbiol* **26:** 789–797

Kubori T, Matsushima Y, Nakamura D, Uralil J, Lara-Tejero M, Sukhan A, Galan JE, Aizawa SI (1998) Supramolecular structure of the Salmonella typhimurium type III protein secretion system. *Science* **280:** 602–605

Kubori T, Shimamoto N, Yamaguchi S, Namba K, Aizawa S (1992) Morphological pathway of flagellar assembly in Salmonella typhimurium. *J Mol Biol* **226:** 433–446

Kubori T, Sukhan A, Aizawa SI, Galan JE (2000) Molecular characterization and assembly of the needle complex of the Salmonella typhimurium type III protein secretion system. *Proc Natl Acad Sci USA* **97:** 10225–10230

Kubori T, Yamaguchi S, Aizawa S (1997) Assembly of the switch complex onto the MS ring complex of Salmonella typhimurium does not require any other flagellar proteins. *J Bacteriol* **179:** 813–817

Lux R, Kar N, Khan S (2000) Overproduced Salmonella typhimurium flagellar motor switch complexes. *J Mol Biol* **298:** 577–583

Lybarger SR, Johnson TL, Gray MD, Sikora AE, Sandkvist M (2009) Docking and assembly of the type II secretion complex of Vibrio cholerae. *J Bacteriol* **191:** 3149–3161

Macnab RM (2003) How bacteria assemble flagella. *Annu Rev Microbiol* **57:** 77–100

Marlovits TC, Kubori T, Sukhan A, Thomas DR, Galan JE, Unger VM (2004) Structural insights into the assembly of the type III secretion needle complex. *Science* **306:** 1040–1042

McMurry JL, Murphy JW, Gonzalez-Pedrajo B (2006) The FliN-FliH interaction mediates localization of flagellar export ATPase FliI to the C ring complex. *Biochemistry* **45:** 11790–11798

Minamino T, MacNab RM (2000) FliH, a soluble component of the type III flagellar export apparatus of Salmonella, forms a complex with FliI and inhibits its ATPase activity. *Mol Microbiol* **37:** 1494–1503

Minamino T, Namba K (2008) Distinct roles of the FliI ATPase and proton motive force in bacterial flagellar protein export. *Nature* **451:** 485–488

Moraes TF, Spreter T, Strynadka NC (2008) Piecing together the type III injectisome of bacterial pathogens. *Curr Opin Struct Biol* **18:** 258–266

Morita-Ishihara T, Ogawa M, Sagara H, Yoshida M, Katayama E, Sasakawa C (2006) Shigella Spa33 is an essential C-ring component of type III secretion machinery. *J Biol Chem* **281:** 599–607

Mota LJ, Cornelis GR (2005) The bacterial injection kit: type III secretion systems. *Ann Med* **37:** 234–249

Mueller CA, Broz P, Muller SA, Ringler P, Erne-Brand F, Sorg I, Kuhn M, Engel A, Cornelis GR (2005) The V-antigen of Yersinia forms a distinct structure at the tip of injectisome needles. *Science* **310:** 674–676

Muller SA, Pozidis C, Stone R, Meesters C, Chami M, Engel A, Economou A, Stahlberg H (2006) Double hexameric ring assembly of the type III protein translocase ATPase HrcN. *Mol Microbiol* **61:** 119–125

Nilles ML, Williams AW, Skrzypek E, Straley SC (1997) Yersinia pestis LcrV forms a stable complex with LcrG and may have a secretion-related regulatory role in the low-Ca2 + response. *J Bacteriol* **179:** 1307–1316

Pallen MJ, Bailey CM, Beatson SA (2006) Evolutionary links between FliH/YscL-like proteins from bacterial type III secretion systems and second-stalk components of the FoF1 and vacuolar ATPases. *Protein Sci* **15:** 935–941

Paul K, Erhardt M, Hirano T, Blair DF, Hughes KT (2008) Energy source of flagellar type III secretion. *Nature* **451:** 489–492

Pozidis C, Chalkiadaki A, Gomez-Serrano A, Stahlberg H, Brown I, Tampakaki AP, Lustig A, Sianidis G, Politou AS, Engel A, Panopoulos NJ, Mansfield J, Pugsley AP, Karamanou S, Economou A (2003) Type III protein translocase: HrcN is a peripheral ATPase that is activated by oligomerization. *J Biol Chem* **278:** 25816–25824

Sani M, Allaoui A, Fusetti F, Oostergetel GT, Keegstra W, Boekema EJ (2007) Structural organization of the needle complex of the type III secretion apparatus of Shigella flexneri. *Micron* **38:** 291–301

Schraidt O, Lefebre MD, Brunner MJ, Schmied WH, Schmidt A, Radics J, Mechtler K, Galan JE, Marlovits TC (2010) Topology and organization of the Salmonella typhimurium type III secretion needle complex components. *PLoS Pathog* **6:** e1000824

Schuch R, Maurelli AT (2001) MxiM and MxiJ, base elements of the Mxi-Spa type III secretion system of Shigella, interact with and stabilize the MxiD secretin in the cell envelope. *J Bacteriol* **183:** 6991–6998

Sekiya K, Ohishi M, Ogino T, Tamano K, Sasakawa C, Abe A (2001) Supermolecular structure of the enteropathogenic Escherichia coli type III secretion system and its direct interaction with the EspA-sheath- like structure. *Proc Natl Acad Sci USA* **98:** 11638–11643

Silva-Herzog E, Ferracci F, Jackson MW, Joseph SS, Plano GV (2008) Membrane localization and topology of the Yersinia pestis YscJ lipoprotein. *Microbiology (Reading, England)* **154:** 593–607

Sorg I, Wagner S, Amstutz M, Muller SA, Broz P, Lussi Y, Engel A, Cornelis GR (2007) YscU recognizes translocators as export substrates of the Yersinia injectisome. *EMBO J* **26:** 3015–3024

Spreter T, Yip CK, Sanowar S, Andre I, Kimbrough TG, Vuckovic M, Pfuetzner RA, Deng W, Yu AC, Finlay BB, Baker D, Miller SI, Strynadka NC (2009) A conserved structural motif mediates formation of the periplasmic rings in the type III secretion system. *Nat Struct Mol Biol* **16:** 468–476

Sukhan A, Kubori T, Wilson J, Galan JE (2001) Genetic analysis of assembly of the Salmonella enterica serovar Typhimurium type III secretion-associated needle complex. *J Bacteriol* **183:** 1159–1167

Tamano K, Aizawa S, Katayama E, Nonaka T, Imajoh-Ohmi S, Kuwae A, Nagai S, Sasakawa C (2000) Supramolecular structure of the Shigella type III secretion machinery: the needle part is changeable in length and essential for delivery of effectors. *EMBO J* **19:** 3876–3887

Thanbichler M, Iniesta AA, Shapiro L (2007) A comprehensive set of plasmids for vanillate- and xylose-inducible gene expression in Caulobacter crescentus. *Nucleic Acids Res* **35:** e137

Thomas DR, Francis NR, Xu C, DeRosier DJ (2006) The three-dimensional structure of the flagellar rotor from a clockwise-locked mutant of Salmonella enterica serovar Typhimurium. *J Bacteriol* **188:** 7039–7048

Torruellas J, Jackson MW, Pennock JW, Plano GV (2005) The Yersinia pestis type III secretion needle plays a role in the regulation of Yop secretion. *Mol Microbiol* **57:** 1719–1733

Van Gijsegem F, Gough C, Zischek C, Niqueux E, Arlat M, Genin S, Barberis P, German S, Castello P, Boucher C (1995) The hrp gene locus of Pseudomonas solanacearum, which controls the production of a type III secretion system, encodes eight proteins related to components of the bacterial flagellar biogenesis complex. *Mol Microbiol* **15:** 1095–1114

Wilharm G, Lehmann V, Krauss K, Lehnert B, Richter S, Ruckdeschel K, Heesemann J, Trulzsch K (2004) Yersinia enterocolitica type III secretion depends on the proton motive force but not on the flagellar motor components MotA and MotB. *Infect Immun* **72:** 4004–4009

Woestyn S, Allaoui A, Wattiau P, Cornelis GR (1994) YscN, the putative energizer of the Yersinia Yop secretion machinery. *J Bacteriol* **176:** 1561–1569

Yip CK, Kimbrough TG, Felise HB, Vuckovic M, Thomas NA, Pfuetzner RA, Frey EA, Finlay BB, Miller SI, Strynadka NC (2005) Structural characterization of the molecular platform for type III secretion system assembly. *Nature* **435:** 702–707

Young HS, Dang H, Lai Y, DeRosier DJ, Khan S (2003) Variable symmetry in Salmonella typhimurium flagellar motors. *Biophys J* **84:** 571–577

Zarivach R, Vuckovic M, Deng W, Finlay BB, Strynadka NC (2007) Structural analysis of a prototypical ATPase from the type III secretion system. *Nat Struct Mol Biol* **14:** 131–137

Chapter 8

References

Adams SR, Campbell RE, Gross LA, Martin BR, Walkup GK, Yao Y, Llopis J and Tsien RY (2002). "New biarsenical ligands and tetracysteine motifs for protein labeling in vitro and in vivo: synthesis and biological applications." *J Am Chem Soc* **124**(21): 6063-6076.

Agrain C, Callebaut I, Journet L, Sorg I, Paroz C, Mota LJ and Cornelis GR (2005). "Characterization of a Type III secretion substrate specificity switch (T3S4) domain in YscP from Yersinia enterocolitica." *Mol. Microbiol.* **56**(1): 54-67.

Aizawa SI (1996). "Flagellar assembly in Salmonella typhimurium." *Mol. Microbiol.* **19**(1): 1-5.

Aizawa SI (2001). "Bacterial flagella and type III secretion systems." *FEMS Microbiol. Lett.* **202**(2): 157-164.

Akeda Y and Galán JE (2005). "Chaperone release and unfolding of substrates in type III secretion." *Nature* **437**(7060): 911-915.

Aldridge P and Hughes KT (2002). "Regulation of flagellar assembly." *Curr. Opin. Microbiol.* **5**(2): 160-165.

Allaoui A, Scheen R, Lambert de Rouvroit C and Cornelis GR (1995a). "VirG, a Yersinia enterocolitica lipoprotein involved in Ca2+ dependency, is related to exsB of Pseudomonas aeruginosa." *J. Bacteriol.* **177**(15): 4230-4237.

Allaoui A, Schulte R and Cornelis GR (1995b). "Mutational analysis of the Yersinia enterocolitica virC operon: characterization of yscE, F, G, I, J, K required for Yop secretion and yscH encoding YopR." *Mol. Microbiol.* **18**(2): 343-355.

Allaoui A, Woestyn S, Sluiters C and Cornelis GR (1994). "YscU, a Yersinia enterocolitica inner membrane protein involved in Yop secretion." *J. Bacteriol.* **176**(15): 4534-4542.

Althage M, Bizouarn T, Kindlund B, Mullins J, Alander J and Rydstrom J (2004). "Cross-linking of transmembrane helices in proton-translocating nicotinamide nucleotide transhydrogenase from Escherichia coli: implications for the structure and function of the membrane domain." *Biochim Biophys Acta* **1659**(1): 73-82.

Altschul SF, Gish W, Miller W, Myers EW and Lipman DJ (1990). "Basic local alignment search tool." *J Mol Biol* **215**(3): 403-410.

Andresen M, Schmitz-Salue R and Jakobs S (2004). "Short tetracysteine tags to beta-tubulin demonstrate the significance of small labels for live cell imaging." *Mol Biol Cell* **15**(12): 5616-5622.

Apel D and Surette MG (2008). "Bringing order to a complex molecular machine: the assembly of the bacterial flagella." *Biochim. Biophys. Acta* **1778**(9): 1851-1858.

Ast V, Schoenhofen I, Langen G, Stratilo C, Chamberlain M and Howard S (2002). "Expression of the ExeAB complex of Aeromonas hydrophila is required for the localization and assembly of the ExeD secretion port multimer." *Mol. Microbiol.* **44**(1): 217-231.

Berger C (2005). "Molekulare Charakterisierung des Typ III-Sekretionssystems von Xanthomonas campestris pv. vesicatoria." **Dissertation** Martin-Luther-Universität Halle-Wittenberg.

Berger C, Robin GP, Bonas U and Koebnik R (2010). "Membrane topology of conserved components of the type III secretion system from the plant pathogen Xanthomonas campestris pv. vesicatoria." *Microbiology (Reading, Engl)*. Epub ahead of print, April 8, DOI 10.1099/mic.0.039248-0

Blaylock B, Riordan KE, Missiakas DM and Schneewind O (2006). "Characterization of the Yersinia enterocolitica type III secretion ATPase YscN and its regulator, YscL." *J. Bacteriol.* **188**(10): 3525-3534.

Blocker A, Gounon P, Larquet E, Niebuhr K, Cabiaux V, Parsot C and Sansonetti P (1999). "The tripartite type III secreton of Shigella flexneri inserts IpaB and IpaC into host membranes." *J Cell Biol* **147**(3): 683-693.

Blocker A, Jouihri N, Larquet E, Gounon P, Ebel F, Parsot C, Sansonetti P and Allaoui A (2001). "Structure and composition of the Shigella flexneri "needle complex", a part of its type III secreton." *Mol. Microbiol.* **39**(3): 652-663.

Blum H, Beier H and Gross H (1987). "Improved silver staining of plant proteins, RNA and DNA in polyacrylamide gel." *Electrophoresis* **8**(2): 93-99.

Boland A, Sory MP, Iriarte M, Kerbourch C, Wattiau P and Cornelis GR (1996). "Status of YopM and YopN in the Yersinia Yop virulon: YopM of Y.enterocolitica is internalized inside the cytosol of PU5-1.8 macrophages by the YopB, D, N delivery apparatus." *EMBO J* **15**(19): 5191-5201.

Botteaux A, Sory MP, Biskri L, Parsot C and Allaoui A (2009). "MxiC is secreted by and controls the substrate specificity of the Shigella flexneri type III secretion apparatus." *Molecular Microbiology* **71**(2): 449-460.

Brown PN, Mathews MAA, Joss LA, Hill CP and Blair DF (2005). "Crystal structure of the flagellar rotor protein FliN from Thermotoga maritima." *J. Bacteriol.* **187**(8): 2890-2902.

Broz P, Mueller CA, Müller SA, Philippsen A, Sorg I, Engel A and Cornelis GR (2007). "Function and molecular architecture of the Yersinia injectisome tip complex." *Mol. Microbiol.* **65**(5): 1311-1320.

Buddelmeijer N, Krehenbrink M, Pecorari F and Pugsley A (2009). "Type II secretion system secretin PulD localizes in clusters in the Escherichia coli outer membrane." *J. Bacteriol.* **191**(1): 161-168

Bumann D (2002). "Examination of Salmonella gene expression in an infected mammalian host using the green fluorescent protein and two-colour flow cytometry." *Molecular Microbiology* **43**(5): 1269-1283.

Burghout P (2004). "Structure and biogenesis of YscC and YscJ. two major components of the Yersinia enterocolitica type III protein secretion system." **Dissertation** Universiteit Utrecht.

Burghout P, Beckers F, de Wit E, van Boxtel R, Cornelis GR, Tommassen J and Koster M (2004a). "Role of the pilot protein YscW in the biogenesis of the YscC secretin in Yersinia enterocolitica." *J. Bacteriol.* **186**(16): 5366-5375.

Burghout P, van Boxtel R, Van Gelder P, Ringler P, Müller SA, Tommassen J and Koster M (2004b). "Structure and electrophysiological properties of the YscC secretin from the type III secretion system of Yersinia enterocolitica." *J. Bacteriol.* **186**(14): 4645-4654.

Cascales E and Christie PJ (2003). "The versatile bacterial type IV secretion systems." *Nat Rev Microbiol* **1**(2): 137-149.

Cattin C (2009). "Stoichiometry Analysis of Type III Secretion Components by Fluorescent Labeling." **Master thesis**

Chandran V, Fronzes R, Duquerroy S, Cronin N, Navaza J and Waksman G (2009). "Structure of the outer membrane complex of a type IV secretion system." *Nature* **462**(7276): 1011-1015.

Chevance FFV and Hughes KT (2008). "Coordinating assembly of a bacterial macromolecular machine." *Nat Rev Microbiol* **6**(6): 455-465.

Chilcott GS and Hughes KT (2000). "Coupling of flagellar gene expression to flagellar assembly in Salmonella enterica serovar typhimurium and Escherichia coli." *Microbiol. Mol. Biol. Rev.* **64**(4): 694-708.

Chubet RG and Brizzard BL (1996). "Vectors for expression and secretion of FLAG epitope-tagged proteins in mammalian cells." *BioTechniques* **20**(1): 136-141.

Cisz M, Lee P-C and Rietsch A (2008). "ExoS Controls the Cell Contact-Mediated Switch to Effector Secretion in Pseudomonas aeruginosa." *J. Bacteriol.* **190**(8): 2726-2738.

Cordes FS, Komoriya K, Larquet E, Yang S, Egelman EH, Blocker A and Lea SM (2003). "Helical structure of the needle of the type III secretion system of Shigella flexneri." *J Biol Chem* **278**(19): 17103-17107.

Cornelis G and Colson C (1975). "Restriction of DNA in Yersinia enterocolitica detected by recipient ability for a derepressed R factor from Escherichia coli." *J Gen Microbiol* **87**(2): 285-291.

Cornelis G, Vanootegem JC and Sluiters C (1987). "Transcription of the yop regulon from Y. enterocolitica requires trans acting pYV and chromosomal genes." *Microb Pathog* **2**(5): 367-379.

Cornelis GR (2006). "The type III secretion injectisome." *Nat. Rev. Microbiol.* **4**(11): 811-825.

Cornelis GR, Agrain C and Sorg I (2006). "Length control of extended protein structures in bacteria and bacteriophages." *Curr. Opin. Microbiol.* **9**(2): 201-206.

Cornelis GR, Biot T, Lambert de Rouvroit C, Michiels T, Mulder B, Sluiters C, Sory MP, Van Bouchaute M and Vanooteghem JC (1989). "The Yersinia yop regulon." *Mol Microbiol* **3**(10): 1455-1459.

Cornelis GR and Van Gijsegem F (2000). "Assembly and function of type III secretory systems." *Annu Rev Microbiol* **54**: 735-774.

Cornelis GR and Wolf-Watz H (1997). "The Yersinia Yop virulon: a bacterial system for subverting eukaryotic cells." *Mol. Microbiol.* **23**(5): 861-867.

Crepin VF, Prasannan S, Shaw RK, Wilson RK, Creasey E, Abe CM, Knutton S, Frankel G and Matthews S (2005). "Structural and functional studies of the enteropathogenic Escherichia coli type III needle complex protein EscJ." *Mol. Microbiol.* **55**(6): 1658-1670.

D'Enfert C and Pugsley AP (1989). "Klebsiella pneumoniae pulS gene encodes an outer membrane lipoprotein required for pullulanase secretion." *J. Bacteriol.* **171**(7): 3673-3679.

Daniell SJ, Takahashi N, Wilson R, Friedberg D, Rosenshine I, Booy FP, Shaw RK, Knutton S, Frankel G and Aizawa S (2001). "The filamentous type III secretion translocon of enteropathogenic Escherichia coli." *Cell. Microbiol.* **3**(12): 865-871.

Deane JE, Abrusci P, Johnson S and Lea SM (2010). "Timing is everything: the regulation of type III secretion." *Cell. Mol. Life Sci.* **67**(7): 1065-1075

Deane JE, Roversi P, Cordes FS, Johnson S, Kenjale R, Daniell S, Booy F, Picking WD, Picking WL, Blocker AJ and Lea SM (2006). "Molecular model of a type III secretion system needle: Implications for host-cell sensing." *Proc. Natl. Acad. Sci. U.S.A.* **103**(33): 12529-12533.

Diepold A, Amstutz M, Abel S, Sorg I, Jenal U and Cornelis GR (2010). "Deciphering the assembly of the Yersinia type III secretion injectisome." *EMBO J*. Epub ahead of print, May 11, DOI 10.1038/emboj.2010.84

Driks A and DeRosier DJ (1990). "Additional structures associated with bacterial flagellar basal body." *J. Mol. Biol.* **211**(4): 669-672.

Durand JM, Dagberg B, Uhlin BE and Björk GR (2000). "Transfer RNA modification, temperature and DNA superhelicity have a common target in the regulatory network of the virulence of Shigella flexneri: the expression of the virF gene." *Mol. Microbiol.* **35**(4): 924-935.

Enninga J, Mounier J, Sansonetti P and Tran Van Nhieu G (2005). "Secretion of type III effectors into host cells in real time." *Nat. Methods* **2**(12): 959-965.

Enninga J and Rosenshine I (2009). "Imaging the assembly, structure and activity of type III secretion systems." *Cell. Microbiol.* **11**(10): 1462-1470.

Erhardt M and Hughes KT (2010). "C-ring requirement in flagellar type III secretion is bypassed by FlhDC upregulation." *Mol. Microbiol*. **75**(2): 376-393

Fadouloglou VE, Tampakaki AP, Glykos NM, Bastaki MN, Hadden JM, Phillips SE, Panopoulos NJ and Kokkinidis M (2004). "Structure of HrcQB-C, a conserved component of the bacterial type III secretion systems." *Proc. Natl. Acad. Sci. U.S.A.* **101**(1): 70-75.

Feilmeier BJ, Iseminger G, Schroeder D, Webber H and Phillips GJ (2000). "Green fluorescent protein functions as a reporter for protein localization in Escherichia coli." *J Bacteriol* **182**(14): 4068-4076.

Ferracci F, Schubot FD, Waugh DS and Plano GV (2005). "Selection and characterization of Yersinia pestis YopN mutants that constitutively block Yop secretion." *Mol. Microbiol.* **57**(4): 970-987.

Fields KA, Plano GV and Straley SC (1994). "A low-Ca2+ response (LCR) secretion (ysc) locus lies within the lcrB region of the LCR plasmid in Yersinia pestis." *J. Bacteriol.* **176**(3): 569-579.

Forsberg A and Wolf-Watz H (1988). "The virulence protein Yop5 of Yersinia pseudotuberculosis is regulated at transcriptional level by plasmid-plB1-encoded trans-acting elements controlled by temperature and calcium." *Mol Microbiol* **2**(1): 121-133.

Fronzes R, Christie PJ and Waksman G (2009a). "The structural biology of type IV secretion systems." *Nat Rev Microbiol* **7**(10): 703-714.

Fronzes R, Schäfer E, Wang L, Saibil HR, Orlova EV and Waksman G (2009b). "Structure of a type IV secretion system core complex." *Science* **323**(5911): 266-268.

Fukuoka H, Inoue Y, Terasawa S, Takahashi H and Ishijima A (2010). "Exchange of rotor components in functioning bacterial flagellar motor." *Biochem Biophys Res Commun* **394**(1): 130-135.

Galán JE and Collmer A (1999). "Type III secretion machines: bacterial devices for protein delivery into host cells." *Science* **284**(5418): 1322-1328.

Gavin A-C, Aloy P, Grandi P, Krause R, Boesche M, Marzioch M, Rau C, Jensen LJ, Bastuck S, Dümpelfeld B, Edelmann A, Heurtier M-A, Hoffman V, Hoefert C, Klein K, Hudak M, Michon A-M, Schelder M, Schirle M, Remor M, Rudi T, Hooper S, Bauer A, Bouwmeester T, Casari G, Drewes G, Neubauer G, Rick JM, Kuster B, Bork P, Russell RB and Superti-Furga G (2006). "Proteome survey reveals modularity of the yeast cell machinery." *Nature* **440**(7084): 631-636.

Gavin A-C, Bösche M, Krause R, Grandi P, Marzioch M, Bauer A, Schultz J, Rick JM, Michon A-M, Cruciat C-M, Remor M, Höfert C, Schelder M, Brajenovic M, Ruffner H, Merino A, Klein K, Hudak M, Dickson D, Rudi T, Gnau V, Bauch A, Bastuck S, Huhse B, Leutwein C, Heurtier M-A, Copley RR, Edelmann A, Querfurth E, Rybin V, Drewes G, Raida M, Bouwmeester T, Bork P, Seraphin B, Kuster B, Neubauer G and Superti-Furga G (2002). "Functional organization of the yeast proteome by systematic analysis of protein complexes." *Nature* **415**(6868): 141-147.

Ghosh P (2004). "Process of protein transport by the type III secretion system." *Microbiol. Mol. Biol. Rev.* **68**(4): 771-795.

González-Pedrajo B, Fraser GM, Minamino T and Macnab RM (2002). "Molecular dissection of Salmonella FliH, a regulator of the ATPase FliI and the type III flagellar protein export pathway." *Mol. Microbiol.* **45**(4): 967-982.

Gophna U, Ron EZ and Graur D (2003). "Bacterial type III secretion systems are ancient and evolved by multiple horizontal-transfer events." *Gene* **312**: 151-163.

Guilvout I, Chami M, Engel A, Pugsley AP and Bayan N (2006). "Bacterial outer membrane secretin PulD assembles and inserts into the inner membrane in the absence of its pilotin." *EMBO J* **25**(22): 5241-5249.

Håkansson S, Schesser, Persson C, Galyov EE, Rosqvist R, Homblé F and Wolf-Watz H (1996). "The YopB protein of Yersinia pseudotuberculosis is essential for the translocation of Yop effector proteins across the target cell plasma membrane and displays a contact-dependent membrane disrupting activity." *EMBO J.* **15**(21): 5812-5823.

Hansen-Wester I and Hensel M (2001). "Salmonella pathogenicity islands encoding type III secretion systems." *Microbes Infect* **3**(7): 549-559.

Hefty PS and Stephens RS (2007). "Chlamydial type III secretion system is encoded on ten operons preceded by sigma 70-like promoter elements." *J. Bacteriol.* **189**(1): 198-206.

Helms V (2002). "Attraction within the membrane. Forces behind transmembrane protein folding and supramolecular complex assembly." *EMBO Rep.* **3**(12): 1133-1138.

Hodgkinson J, Horsley A, Stabat D, Simon M, Johnson S, da Fonseca P, Morris E, Wall J, Lea S and Blocker A (2009). "Three-dimensional reconstruction of the Shigella T3SS transmembrane regions reveals 12-fold symmetry and novel features throughout." *Nat Struct Mol Biol*. **16**(5): 477-485

Hoe NP and Goguen JD (1993). "Temperature sensing in Yersinia pestis: translation of the LcrF activator protein is thermally regulated." *J. Bacteriol.* **175**(24): 7901-7909.

Hoiczyk E, Roggenkamp A, Reichenbecher M, Lupas A and Heesemann J (2000). "Structure and sequence analysis of Yersinia YadA and Moraxella UspAs reveal a novel class of adhesins." *EMBO J.* **19**(22): 5989-5999.

Ibarra JA, Knodler LA, Sturdevant DE, Virtaneva K, Carmody AB, Fischer ER, Porcella SF and Steele-Mortimer O (2010). "Induction of Salmonella pathogenicity island 1 under different growth conditions can affect Salmonella-host cell interactions in vitro." *Microbiology (Reading, Engl)* **156**(Pt 4): 1120-1133.

Ikeda T, Asakura S and Kamiya R (1985). ""Cap" on the tip of Salmonella flagella." *J. Mol. Biol.* **184**(4): 735-737.

Iriarte M and Cornelis GR (1998). "YopT, a new Yersinia Yop effector protein, affects the cytoskeleton of host cells." *Mol Microbiol* **29**(3): 915-929.

Iriarte M and Cornelis GR (1999). "Identification of SycN, YscX, and YscY, three new elements of the Yersinia yop virulon." *J Bacteriol* **181**(2): 675-680.

Jackson MW and Plano GV (2000). "Interactions between type III secretion apparatus components from Yersinia pestis detected using the yeast two-hybrid system." *FEMS Microbiol. Lett.* **186**(1): 85-90.

James B. Kaper JH (1999). Pathogenicity Islands and Other Mobile Virulence Elements, ASM Press.

Jin Q and He SY (2001). "Role of the Hrp pilus in type III protein secretion in Pseudomonas syringae." *Science* **294**(5551): 2556-2558.

Journet L, Agrain C, Broz P and Cornelis GR (2003). "The needle length of bacterial injectisomes is determined by a molecular ruler." *Science* **302**(5651): 1757-1760.

Kall L, Krogh A and Sonnhammer EL (2004). "A combined transmembrane topology and signal peptide prediction method." *J Mol Biol* **338**(5): 1027-1036.

Kaniga K, Bossio JC and Galán JE (1994). "The Salmonella typhimurium invasion genes invF and invG encode homologues of the AraC and PulD family of proteins." *Molecular Microbiology* **13**(4): 555-568.

Kaniga K, Delor I and Cornelis GR (1991). "A wide-host-range suicide vector for improving reverse genetics in gram-negative bacteria: inactivation of the blaA gene of Yersinia enterocolitica." *Gene* **109**(1): 137-141.

Kashino Y (2003). "Separation methods in the analysis of protein membrane complexes." *J. Chromatogr. B Analyt. Technol. Biomed. Life Sci.* **797**(1-2): 191-216.

Khan IH, Reese TS and Khan S (1992). "The cytoplasmic component of the bacterial flagellar motor." *Proc. Natl. Acad. Sci. U.S.A.* **89**(13): 5956-5960.

Kimbrough TG and Miller SI (2000). "Contribution of Salmonella typhimurium type III secretion components to needle complex formation." *Proc. Natl. Acad. Sci. U.S.A.* **97**(20): 11008-11013.

Kimbrough TG and Miller SI (2002). "Assembly of the type III secretion needle complex of Salmonella typhimurium." *Microbes Infect.* **4**(1): 75-82.

Knutton S, Rosenshine I, Pallen MJ, Nisan I, Neves BC, Bain C, Wolff C, Dougan G and Frankel G (1998). "A novel EspA-associated surface organelle of enteropathogenic Escherichia coli involved in protein translocation into epithelial cells." *EMBO J.* **17**(8): 2166-2176.

Komeda Y (1986). "Transcriptional control of flagellar genes in Escherichia coli K-12." *J. Bacteriol.* **168**(3): 1315-1318.

Konishi M, Kanbe M, McMurry J and Aizawa S (2009). "Flagellar formation in C-ring defective mutants by overproduction of FliI, the ATPase specific for the flagellar type III secretion." *J. Bacteriol.* **191**(19): 6186-6191

Koraimann G (2003). "Lytic transglycosylases in macromolecular transport systems of Gram-negative bacteria." *Cell Mol Life Sci* **60**(11): 2371-2388.

Koster M, Bitter W, de Cock H and Allaoui A (1997). "The outer membrane component, YscC, of the Yop secretion machinery of Yersinia enterocolitica forms a ring-shaped multimeric complex." *Mol. Microbiol*. **26**(4): 789-797

Kubori T, Matsushima Y, Nakamura D, Uralil J, Lara-Tejero M, Sukhan A, Galán JE and Aizawa SI (1998). "Supramolecular structure of the Salmonella typhimurium type III protein secretion system." *Science* **280**(5363): 602-605.

Kubori T, Shimamoto N, Yamaguchi S, Namba K and Aizawa S (1992). "Morphological pathway of flagellar assembly in Salmonella typhimurium." *J. Mol. Biol.* **226**(2): 433-446.

Kubori T, Yamaguchi S and Aizawa S (1997). "Assembly of the switch complex onto the MS ring complex of Salmonella typhimurium does not require any other flagellar proteins." *J. Bacteriol.* **179**(3): 813-817.

Kutsukake K, Ohya Y and Iino T (1990). "Transcriptional analysis of the flagellar regulon of Salmonella typhimurium." *J. Bacteriol.* **172**(2): 741-747.

Lambert de Rouvroit C, Sluiters C and Cornelis GR (1992). "Role of the transcriptional activator, VirF, and temperature in the expression of the pYV plasmid genes of Yersinia enterocolitica." *Mol. Microbiol.* **6**(3): 395-409.

Lux R, Kar N and Khan S (2000). "Overproduced Salmonella typhimurium flagellar motor switch complexes." *J. Mol. Biol.* **298**(4): 577-583.

Lybarger SR, Johnson TL, Gray MD, Sikora AE and Sandkvist M (2009). "Docking and assembly of the type II secretion complex of Vibrio cholerae." *J. Bacteriol.* **191**(9): 3149-3161.

Macnab RM (2003). "How bacteria assemble flagella." *Annu Rev Microbiol* **57**: 77-100.

Macnab RM (2004). "Type III flagellar protein export and flagellar assembly." *Biochim. Biophys. Acta* **1694**(1-3): 207-217.

Marlovits TC, Kubori T, Lara-Tejero M, Thomas D, Unger VM and Galán JE (2006). "Assembly of the inner rod determines needle length in the type III secretion injectisome." *Nature* **441**(7093): 637-640.

Marlovits TC, Kubori T, Sukhan A, Thomas DR, Galán JE and Unger VM (2004). "Structural insights into the assembly of the type III secretion needle complex." *Science* **306**(5698): 1040-1042.

Marteyn B, West NP, Browning DF, Cole JA, Shaw JG, Palm F, Mounier J, Prévost M-C, Sansonetti P and Tang CM (2010). "Modulation of Shigella virulence in response to available oxygen in vivo." *Nature* **465**(7296): 355-358

McMurry JL, Van Arnam JS, Kihara M and Macnab RM (2004). "Analysis of the cytoplasmic domains of Salmonella FlhA and interactions with components of the flagellar export machinery." *J. Bacteriol.* **186**(22): 7586-7592.

Michiels T, Vanooteghem JC, Lambert de Rouvroit C, China B, Gustin A, Boudry P and Cornelis GR (1991). "Analysis of virC, an operon involved in the secretion of Yop proteins by Yersinia enterocolitica." *J. Bacteriol.* **173**(16): 4994-5009.

Minamino T, Gonzalez-Pedrajo B, Kihara M, Namba K and Macnab RM (2003). "The ATPase FliI can interact with the type III flagellar protein export apparatus in the absence of its regulator, FliH." *J Bacteriol* **185**(13): 3983-3988.

Minamino T, Imada K and Namba K (2008). "Mechanisms of type III protein export for bacterial flagellar assembly." *Mol Biosyst* **4**(11): 1105-1115.

Minamino T and Macnab RM (2000). "Interactions among components of the Salmonella flagellar export apparatus and its substrates." *Mol. Microbiol.* **35**(5): 1052-1064.

Minamino T and Namba K (2008). "Distinct roles of the FliI ATPase and proton motive force in bacterial flagellar protein export." *Nature* **451**(7177): 485-488.

Minamino T, Shimada M, Okabe M, Saijo-Hamano Y, Imada K, Kihara M and Namba K (2010). "Role of the C-terminal cytoplasmic domain of FlhA in bacterial flagellar type III protein export." *J Bacteriol* **192**(7): 1929-1936.

Minamino T, Yoshimura SDJ, Morimoto YV, González-Pedrajo B, Kami-Ike N and Namba K (2009). "Roles of the extreme N-terminal region of FliH for efficient localization of the FliH-FliI complex to the bacterial flagellar type III export apparatus." *Mol. Microbiol.* **74**(6): 1471-1483.

Miras I, Hermant D, Arricau N and Popoff MY (1995). "Nucleotide sequence of iagA and iagB genes involved in invasion of HeLa cells by Salmonella enterica subsp. enterica ser. Typhi." *Res Microbiol* **146**(1): 17-20.

Moore SA and Jia Y (2010). "Structure of the cytoplasmic domain of the flagellar secretion apparatus component Flha from Helicobacter pylori." *J. Biol. Chem.* Epub ahead of print, May 4, DOI 10.1074/jbc.M110.119412

Moraes TF, Spreter T and Strynadka NC (2008). "Piecing together the type III injectisome of bacterial pathogens." *Curr. Opin. Struct. Biol.* **18**(2): 258-266.

Morita-Ishihara T, Ogawa M, Sagara H, Yoshida M, Katayama E and Sasakawa C (2005). "Shigella Spa33 is an essential C-ring component of type III secretion machinery." *J. Biol. Chem.* **281**(1): 599-607.

Morrow MR, Huschilt JC and Davis JH (1985). "Simultaneous modeling of phase and calorimetric behavior in an amphiphilic peptide/phospholipid model membrane." *Biochemistry* **24**(20): 5396-5406.

Mota LJ and Cornelis GR (2005). "The bacterial injection kit: type III secretion systems." *Ann Med* **37**(4): 234-249.

Müller CA (2004). "Identification of Minor Components Associated with the Yersinia enterocolitica Injectisome Needle." **Master thesis**

Müller CA, Broz P, Müller SA, Ringler P, Erne-Brand F, Sorg I, Kuhn M, Engel A and Cornelis GR (2005). "The V-antigen of Yersinia forms a distinct structure at the tip of injectisome needles." *Science* **310**(5748): 674-676.

Müller SA, Pozidis C, Stone R, Meesters C, Chami M, Engel A, Economou A and Stahlberg H (2006). "Double hexameric ring assembly of the type III protein translocase ATPase HrcN." *Mol. Microbiol.* **61**(1): 119-125.

Nilles ML, Williams AW, Skrzypek E and Straley SC (1997). "Yersinia pestis LcrV forms a stable complex with LcrG and may have a secretion-related regulatory role in the low-Ca2+ response." *J. Bacteriol.* **179**(4): 1307-1316.

Ogino T, Ohno R, Sekiya K, Kuwae A, Matsuzawa T, Nonaka T, Fukuda H, Imajoh-Ohmi S and Abe A (2006). "Assembly of the type III secretion apparatus of enteropathogenic Escherichia coli." *J. Bacteriol.* **188**(8): 2801-2811.

Ohnishi K, Fan F, Schoenhals GJ, Kihara M and Macnab RM (1997). "The FliO, FliP, FliQ, and FliR proteins of Salmonella typhimurium: putative components for flagellar assembly." *J. Bacteriol.* **179**(19): 6092-6099.

Pallen MJ, Bailey CM and Beatson SA (2006). "Evolutionary links between FliH/YscL-like proteins from bacterial type III secretion systems and second-stalk components of the FoF1 and vacuolar ATPases." *Protein Sci.* **15**(4): 935-941.

Paul K, Erhardt M, Hirano T, Blair DF and Hughes KT (2008). "Energy source of flagellar type III secretion." *Nature* **451**(7177): 489-492.

Plano GV, Barve SS and Straley SC (1991). "LcrD, a membrane-bound regulator of the Yersinia pestis low-calcium response." *J. Bacteriol.* **173**(22): 7293-7303.

Pozidis C, Chalkiadaki A, Gomez-Serrano A, Stahlberg H, Brown I, Tampakaki AP, Lustig A, Sianidis G, Politou AS, Engel A, Panopoulos NJ, Mansfield J, Pugsley AP, Karamanou S and Economou A (2003). "Type III protein translocase: HrcN is a peripheral ATPase that is activated by oligomerization." *J. Biol. Chem.* **278**(28): 25816-25824.

Rabut G, Doye V and Ellenberg J (2004). "Mapping the dynamic organization of the nuclear pore complex inside single living cells." *Nat Cell Biol* **6**(11): 1114-1121.

Rigaut G, Shevchenko A, Rutz B, Wilm M, Mann M and Séraphin B (1999). "A generic protein purification method for protein complex characterization and proteome exploration." *Nat. Biotechnol.* **17**(10): 1030-1032.

Roine E, Wei W, Yuan J, Nurmiaho-Lassila EL, Kalkkinen N, Romantschuk M and He SY (1997). "Hrp pilus: an hrp-dependent bacterial surface appendage produced by Pseudomonas syringae pv. tomato DC3000." *Proc. Natl. Acad. Sci. U.S.A.* **94**(7): 3459-3464.

Rosqvist R, Magnusson KE and Wolf-Watz H (1994). "Target cell contact triggers expression and polarized transfer of Yersinia YopE cytotoxin into mammalian cells." *EMBO J* **13**(4): 964-972.

Rozen S and Skaletsky H (2000). "Primer3 on the WWW for general users and for biologist programmers." *Methods Mol Biol* **132**: 365-386.

Saijo-Hamano Y, Imada K, Minamino T, Kihara M, Shimada M, Kitao A and Namba K (2010). "Structure of the cytoplasmic domain of FlhA and implication for flagellar type III protein export." *Mol. Microbiol.* **76**(1): 260-268

Saijo-Hamano Y, Minamino T, Macnab RM and Namba K (2004). "Structural and functional analysis of the C-terminal cytoplasmic domain of FlhA, an integral membrane component of the type III flagellar protein export apparatus in Salmonella." *J. Mol. Biol.* **343**(2): 457-466.

Sani M, Allaoui A, Fusetti F, Oostergetel GT, Keegstra W and Boekema EJ (2006). "Structural organization of the needle complex of the type III secretion apparatus of Shigella flexneri." *Micron* **38**(3): 291-301.

Sarker MR, Neyt C, Stainier I and Cornelis GR (1998a). "The Yersinia Yop virulon: LcrV is required for extrusion of the translocators YopB and YopD." *J. Bacteriol.* **180**(5): 1207-1214.

Sarker MR, Sory MP, Boyd AP, Iriarte M and Cornelis GR (1998b). "LcrG is required for efficient translocation of Yersinia Yop effector proteins into eukaryotic cells." *Infect. Immun.* **66**(6): 2976-2979.

Schlumberger MC, Müller AJ, Ehrbar K, Winnen B, Duss I, Stecher B and Hardt W-D (2005). "Real-time imaging of type III secretion: Salmonella SipA injection into host cells." *Proc. Natl. Acad. Sci. U.S.A.* **102**(35): 12548-12553.

Schneider D, Finger C, Prodöhl A and Volkmer T (2007). "From interactions of single transmembrane helices to folding of alpha-helical membrane proteins: analyzing transmembrane helix-helix interactions in bacteria." *Curr Protein Pept Sci* **8**(1): 45-61.

Schraidt O, Lefebre MD, Brunner MJ, Schmied WH, Schmidt A, Radics J, Mechtler K, Galán JE and Marlovits TC (2010). "Topology and organization of the Salmonella typhimurium type III secretion needle complex components." *PLoS Pathog* **6**(4): e1000824.

Schuch R and Maurelli AT (2001). "MxiM and MxiJ, base elements of the Mxi-Spa type III secretion system of Shigella, interact with and stabilize the MxiD secretin in the cell envelope." *J. Bacteriol.* **183**(24): 6991-6998.

Schüller S and Phillips AD (2010). "Microaerobic conditions enhance type III secretion and adherence of enterohaemorrhagic Escherichia coli to polarized human intestinal epithelial cells." *Environ. microbiol.* Epub ahead of print, April 7, DOI 10.1111/j.1462-2920.2010.02216.x

Schulmeister S, Ruttorf M, Thiem S, Kentner D, Lebiedz D and Sourjik V (2008). "Protein exchange dynamics at chemoreceptor clusters in Escherichia coli." *Proc. Natl. Acad. Sci. U.S.A.* **105**(17): 6403-6408.

Sekiya K, Ohishi M, Ogino T, Tamano K, Sasakawa C and Abe A (2001). "Supermolecular structure of the enteropathogenic Escherichia coli type III secretion system and its direct interaction with the EspA-sheath-like structure." *Proc. Natl. Acad. Sci. U.S.A.* **98**(20): 11638-11643.

Shaner NC, Steinbach PA and Tsien RY (2005). "A guide to choosing fluorescent proteins." *Nat. Methods* **2**(12): 905-909.

Silva-Herzog E, Ferracci F, Jackson MW, Joseph SS and Plano GV (2008). "Membrane localization and topology of the Yersinia pestis YscJ lipoprotein." *Microbiology (Reading, Engl)* **154**(Pt 2): 593-607.

Sivanesan D, Hancock MA, Villamil Giraldo AMa and Baron C (2010). "Quantitative Analysis of VirB8-VirB9-VirB10 Interactions Provides a Dynamic Model of Type IV Secretion System Core Complex Assembly." *Biochemistry* **49**(21): 4483-4493

Skurnik M, Bölin I, Heikkinen H, Piha S and Wolf-Watz H (1984). "Virulence plasmid-associated autoagglutination in Yersinia spp." *J. Bacteriol.* **158**(3): 1033-1036.

Sorg I, Wagner S, Amstutz M, Müller SA, Broz P, Lussi Y, Engel A and Cornelis GR (2007). "YscU recognizes translocators as export substrates of the Yersinia injectisome." *EMBO J.* **26**(12): 3015-3024.

Sory MP, Boland A, Lambermont I and Cornelis GR (1995). "Identification of the YopE and YopH domains required for secretion and internalization into the cytosol of macrophages, using the cyaA gene fusion approach." *Proc. Natl. Acad. Sci. U.S.A.* **92**(26): 11998-12002.

Spaeth KE, Chen Y-S and Valdivia RH (2009). "The Chlamydia type III secretion system C-ring engages a chaperone-effector protein complex." *PLoS Pathog* **5**(9): e1000579.

Spreter T, Yip C, Sanowar S, André, Kimbrough T, Vuckovic M, Pfuetzner R, Deng W, Yu A, Finlay B, Baker D, Miller S and Strynadka N (2009). "A conserved structural motif mediates formation of the periplasmic rings in the type III secretion system." *Nat Struct Mol Biol*. **16**(5): 468-476

Stainier I, Iriarte M and Cornelis GR (1998). "YscM1 and YscM2, two Yersinia enterocolitica proteins causing downregulation of yop transcription." *Mol. Microbiol.* **26**(4): 833-843.

Stone CB, Bulir DC, Gilchrist JD, Toor RK and Mahony JB (2010). "Interactions between flagellar and type III secretion proteins in Chlamydia pneumoniae." *BMC Microbiol.* **10**: 18.

Straley SC (1991). "The low-Ca2+ response virulence regulon of human-pathogenic Yersiniae." *Microb Pathog* **10**(2): 87-91.

Sturgill TW, Cohen A, Diefenbacher M, Trautwein M, Martin DE and Hall MN (2008). "TOR1 and TOR2 have distinct locations in live cells." *Eukaryotic Cell* **7**(10): 1819-1830.

Sukhan A, Kubori T, Wilson J and Galán JE (2001). "Genetic analysis of assembly of the Salmonella enterica serovar Typhimurium type III secretion-associated needle complex." *J. Bacteriol.* **183**(4): 1159-1167.

Tamano K, Aizawa S, Katayama E, Nonaka T, Imajoh-Ohmi S, Kuwae A, Nagai S and Sasakawa C (2000). "Supramolecular structure of the Shigella type III secretion machinery: the needle part is changeable in length and essential for delivery of effectors." *EMBO J.* **19**(15): 3876-3887.

Tampakaki AP, Fadouloglou VE, Gazi AD, Panopoulos NJ and Kokkinidis M (2004). "Conserved features of type III secretion." *Cell. Microbiol.* **6**(9): 805-816.

Thanbichler M, Iniesta AA and Shapiro L (2007). "A comprehensive set of plasmids for vanillate- and xylose-inducible gene expression in Caulobacter crescentus." *Nucleic Acids Res* **35**(20): e137.

Torruellas J, Jackson MW, Pennock JW and Plano GV (2005). "The Yersinia pestis type III secretion needle plays a role in the regulation of Yop secretion." *Mol. Microbiol.* **57**(6): 1719-1733.

Touchman JW, Wagner DM, Hao J, Mastrian SD, Shah MK, Vogler AJ, Allender CJ, Clark EA, Benitez DS, Youngkin DJ, Girard JM, Auerbach RK, Beckstrom-Sternberg SM and Keim P (2007). "A North American Yersinia pestis draft genome sequence: SNPs and phylogenetic analysis." *PLoS One* **2**(2): e220.

Tramier M, Zahid M, Mevel JC, Masse MJ and Coppey-Moisan M (2006). "Sensitivity of CFP/YFP and GFP/mCherry pairs to donor photobleaching on FRET determination by fluorescence lifetime imaging microscopy in living cells." *Microsc Res Tech* **69**(11): 933-939.

Tseng T-T, Tyler BM and Setubal JC (2009). "Protein secretion systems in bacterial-host associations, and their description in the Gene Ontology." *BMC Microbiol.* **9 Suppl 1**: S2.

Tsien RY (2005). "Building and breeding molecules to spy on cells and tumors." *FEBS Lett* **579**(4): 927-932.

Van Arnam JS, McMurry JL, Kihara M and Macnab RM (2004). "Analysis of an engineered Salmonella flagellar fusion protein, FliR-FlhB." *J Bacteriol* **186**(8): 2495-2498.

Van Gijsegem F, Gough C, Zischek C, Niqueux E, Arlat M, Genin S, Barberis P, German S, Castello P and Boucher C (1995). "The hrp gene locus of Pseudomonas solanacearum, which controls the production of a type III secretion system, encodes eight proteins related to components of the bacterial flagellar biogenesis complex." *Molecular Microbiology* **15**(6): 1095-1114.

Wagner S, Sorg I, Degiacomi M, Journet L, Dal Peraro M and Cornelis GR (2009). "The helical content of the YscP molecular ruler determines the length of the Yersinia injectisome." *Molecular Microbiology* **71**(3): 692-701.

Wiesand U (2010). "Structural and Biochemical Investigation of the Yersinia enterocolitica Type III secretion export apparatus." **Dissertation** Technische Universität Braunschweig.

Wiesand U, Sorg I, Amstutz M, Wagner S, van den Heuvel J, Lührs T, Cornelis GR and Heinz DW (2009). "Structure of the type III secretion recognition protein YscU from Yersinia enterocolitica." *J. Mol. Biol.* **385**(3): 854-866.

Wilharm G, Lehmann V, Krauss K, Lehnert B, Richter S, Ruckdeschel K, Heesemann J and Trülzsch K (2004). "Yersinia enterocolitica type III secretion depends on the proton motive force but not on the flagellar motor components MotA and MotB." *Infect. Immun.* **72**(7): 4004-4009.

Wilkins MR, Gasteiger E, Bairoch A, Sanchez JC, Williams KL, Appel RD and Hochstrasser DF (1999). "Protein identification and analysis tools in the ExPASy server." *Methods Mol Biol* **112**: 531-552.

Woestyn S, Allaoui A, Wattiau P and Cornelis GR (1994). "YscN, the putative energizer of the Yersinia Yop secretion machinery." *J. Bacteriol.* **176**(6): 1561-1569.

Worrall LJ, Vuckovic M and Strynadka NCJ (2010). "Crystal structure of the C-terminal domain of the Salmonella type III secretion system export apparatus protein InvA." *Protein Sci.* **19**(5): 1091-1096.

Yang P, Sampson HM and Krause HM (2006). "A modified tandem affinity purification strategy identifies cofactors of the Drosophila nuclear receptor dHNF4." *Proteomics* **6**(3): 927-935.

Yip CK, Kimbrough TG, Felise HB, Vuckovic M, Thomas NA, Pfuetzner RA, Frey EA, Finlay BB, Miller SI and Strynadka NCJ (2005). "Structural characterization of the molecular platform for type III secretion system assembly." *Nature* **435**(7042): 702-707.

Yonekura K, Maki S, Morgan DG, DeRosier DJ, Vonderviszt F, Imada K and Namba K (2000). "The bacterial flagellar cap as the rotary promoter of flagellin self-assembly." *Science* **290**(5499): 2148-2152.

Yother J and Goguen JD (1985). "Isolation and characterization of Ca2+-blind mutants of Yersinia pestis." *J Bacteriol* **164**(2): 704-711.

Young HS, Dang H, Lai Y, DeRosier DJ and Khan S (2003). "Variable symmetry in Salmonella typhimurium flagellar motors." *Biophys. J.* **84**(1): 571-577.

Yu X-J, McGourty K, Liu M, Unsworth KE and Holden DW (2010). "pH Sensing by Intracellular Salmonella Induces Effector Translocation." *Science* **328**(5981): 1040-1043

Zarivach, Vuckovic, Deng, Finlay and Strynadka (2007). "Structural analysis of a prototypical ATPase from the type III secretion system." *Nat Struct Mol Biol*. **14**(2): 131-137

Zarivach R, Deng W, Vuckovic M, Felise HB, Nguyen HV, Miller SI, Finlay BB and Strynadka NCJ (2008). "Structural analysis of the essential self-cleaving type III secretion proteins EscU and SpaS." *Nature* **453**(7191): 124-127.

Zenk SF, Stabat D, Hodgkinson JL, Veenendaal AKJ, Johnson S and Blocker AJ (2007). "Identification of minor inner-membrane components of the Shigella type III secretion system 'needle complex'." *Microbiology (Reading, Engl)* **153**(Pt 8): 2405-2415.

Zhu K, González-Pedrajo B and Macnab RM (2002). "Interactions among membrane and soluble components of the flagellar export apparatus of Salmonella." *Biochemistry* **41**(30): 9516-9524.